

MICROBIAL NITROGEN CYCLING IN SEDIMENTS OF AN AGRICULTURAL STREAM AS IMPACTED BY STREAM-GROUNDWATER EXCHANGE

Zhe Wang

Vollständiger Abdruck der von der TUM School of Life Sciences der Technischen Universität
München zur Erlangung eines

Doktors der Naturwissenschaften (Dr. rer. nat.)

genehmigten Dissertation.

Vorsitz: Prof. Dr. Wolfgang Liebl

Prüfer*innen der Dissertation:

1. Prof. Dr. Tillmann Lüders
2. Prof. Dr. Michael Schloter

Die Dissertation wurde am 04.04.2023 bei der Technischen Universität München eingereicht
und durch die TUM School of Life Sciences am 05.06.2023 angenommen.

**MICROBIAL NITROGEN CYCLING IN SEDIMENTS OF AN
AGRICULTURAL STREAM AS IMPACTED BY
STREAM-GROUNDWATER EXCHANGE**

Zhe Wang

ABSTRACT

Zhe Wang: Microbial nitrogen cycling in sediments of an agricultural stream as impacted by stream-groundwater exchange

Channelized streams and ditches are widespread in agricultural areas. These small, lower-order streams can constitute a significant portion of the total length of fluvial networks and exert a notable impact on the water quality of downstream rivers. Such anthropogenically modified hydrologic systems are meant to efficiently remove excess water from agricultural fields and reduce the risks of flooding. In spite of their uncontested importance for agricultural production, these small streams are also receivers of immoderate livestock manure and surplus nutrients due to the application of synthetic fertilizers. As a result, an excessive amount of nitrate often ends up in these streams, which can become a major concern as nitrate has the potential to accumulate and persist for extended periods within sediment and groundwater. Different nitrogen transformations mediated by microbes play a crucial role in regulating the overall nitrogen turnover in catchments. Therefore, investigating subsurface microbial ecology is pivotal in managing the fate of nitrate in catchments. Previous studies have had a primary focus on exploring the distribution and diversity of microbes in larger, higher-order rivers and fluvial systems under the impact of anthropogenic disturbance. However, these works have mostly ignored microbiota in lower-order streams, especially those under agricultural impact. Additionally, it has not been elucidated, how stream microbiota react to small-scale in-stream hydrological heterogeneities, despite their potential significant contribution to the turnover of nitrate and other agricultural pollutants. This dissertation aims to generate novel insights into the controls of reductive and oxidative microbial nitrogen cycling in the streambed, at the interface of surface- and groundwater in an first-order agricultural stream.

The first part of the dissertation focuses on streambed microbial nitrate reduction as controlled by in-stream bidirectional water exchange. I examined the distribution and

diversity of microbiota, and community assembly of a representative first-order agricultural stream near the city of Tübingen, Germany. Lower-order streams mostly lack the streambed complexity necessary for extensive hyporheic exchange, a process that is important for the removal of pollutants in higher-order streams. Reactive hot spots in the streambed of lower-order streams can be hypothesized as a function of hydrology, which controls the local gaining (groundwater exfiltration) or losing (infiltration) of stream water. Along with a hydraulic dissection of distinct gaining and losing reaches of the stream, community composition and the abundance of bacterial communities in the streambed were investigated using long-read sequencing of bacterial 16S rRNA gene amplicons, and qPCR of bacterial 16S rRNA and denitrification genes (*nirK* and *nirS*). Bidirectional water exchange between groundwater and the stream was shown as an important control for sediment microbiota, especially for nitrate-reducing microbes. Typical heterotrophic denitrifiers were most abundant in a midstream net losing section, while up- and downstream net gaining sections were associated with an enrichment of potential chemolithoautotrophic sulfur-oxidizing nitrate reducers. These results reveal a coupling of chemolithoautotrophic sulfur and nitrogen cycling processes in the streambed, and a prominent control of microbiology by hydrology and hydrochemistry *in situ*. Such detailed local heterogeneities in exchange fluxes and streambed microbiomes have not been reported to date.

The second part of the dissertation focuses on nitrification, as key oxidative nitrogen transformation process in the same streambed, potentially contributing to the production of secondary nitrate from ammonia *in situ*. In this part of the dissertation, the capacity of ammonia-oxidizing microbial populations in the streambed was investigated. Streambed microbiomes host both bacterial and archaeal ammonia oxidizers (AOB and AOA, respectively), but their respective contributions to oxidative N-cycling in the streambed remain unclear. My experiment employed a multidisciplinary approach, encompassing a

collection of *in situ* geochemical data, 16S rRNA gene metabarcoding, functional gene sequencing, quantitative PCR, and the assessment of potential nitrification rates in microcosms treated with disparate chemical inhibitors. Ultimately, a population-based reaction modeling was conducted by the project consortium. It confirms that AOB, rather than the much more abundant AOA drive nitrification activities, and are more responsive to incoming fluxes of ammonium *in situ*. Both *Nitrosomonas* and *Nitrospira* spp. appeared to be relevant for ammonia oxidation in the streambed. Results of this study also shed light on the importance of cautiously interpreting *in-situ amoA* abundances as indicators of reactive potentials in the environment, and the strength of combining *in-situ* observation, bench-scale microcosms and modeling to better understand nitrogen transformation in natural systems.

In the third part of the dissertation, the metabolic potential underpinning the link between nitrogen and sulfur cycling were further interrogated via a metagenomic approach. Through long-read bacterial 16S rRNA gene amplicons and a hybrid long-read assisted metagenomic approach, results from this study provide further insights into the diverse archaea and bacteria that are genetically capable of nitrogen and/or sulfur cycling in the Schönbrunn streambed. An assessment of the distribution of pertinent metabolic pathways and the contributing species to key functional gene pools was conducted. The results provided important insights on the metabolic potentials of some of the most abundant streambed microbiota via 70 complete or partially reconstructed metagenome-assembled genomes (MAGs). The MAGs described represented more than 13 bacterial phyla, not only expanding the perspective of potentially relevant nitrate-reducing lineages into canonical sulfate reducers, but also highlighting the importance of one uncharacterized lineage (B1-7BS) within the *Gammaproteobacteria*, a core constituent of the streambed community, with the genetic potential to oxidize reduced sulfur. Findings in this study further support the intricate links between nitrogen and sulfur cycling amongst the core microbiome of the streambed,

with a diverse set of taxa involved in complete and/or partial nitrate reduction processes along the stream transect.

Overall, this dissertation provides detailed quantitative and spatially resolved information on microbial communities in the streambed of a representative first-order agricultural stream, and on the important controls of hydrology on microbiology in this reactive system. Especially, the distribution and diversity of functional groups of microbes involved in nitrate reduction was clearly impacted by local stream water infiltration and groundwater exfiltration fluxes. This dissertation provides evidence for a strong connection between chemolithoautotrophic nitrogen and sulfur cycling in the streambed. This emphasizes the importance of considering the reactive capacity of agricultural lower-order streams in attempts of managing catchment-level nutrient fluxes. Better understanding of microbial communities and hydrological conditions in these streams should be critical for the development of optimized agricultural land use and management schemes.

ZUSAMMENFASSUNG

Zhe Wang: Mikrobieller Stickstoffkreislauf in Sedimenten eines landwirtschaftlich geprägten Baches unter Einfluss des Oberflächenwasser-Grundwasser-Austauschs

Kleine Bäche und Wassergräben sind weit verbreitet in landwirtschaftlichen Gebieten.

Diese Fließgewässer niederer Ordnung können einen wesentlichen Anteil eines Wassereinzugsgebietes ausmachen und haben einen erheblichen Einfluss auf die Wasserqualität. Solche oft anthropogen begründeten Bäche sollen Wasser effizient aus landwirtschaftlichen Flächen ableiten und die Gefahr von Überschwemmungen verringern. Trotz ihrer unbestrittenen Bedeutung für die landwirtschaftliche Produktion sind diese Gewässer auch oft Empfänger von Gülle und synthetischer Düngemittel. Dadurch gelangt häufig eine überhöhte Menge an Nitrat in diese Gewässer, was zu einem großen Problem werden kann, da sich Nitrat in Sedimenten und im Grundwasser ansammelt. Verschiedene mikrobielle Stickstoffumwandlungen spielen eine entscheidende Rolle in der Regulierung des Stickstoffumsatzes in solchen Einzugsgebieten. Daher ist die Untersuchung der mikrobiellen Ökologie dieser Bachsedimente von Bedeutung für das Verständnis des Verbleibs von Nitrat im Einzugsgebiet. Bisherige Studien haben sich aber meist auf die Verbreitung und Vielfalt von Mikroorganismen in Fließgewässern höherer Ordnung, auch unter anthropogenem Einfluss konzentriert. Fließgewässer niederer Ordnung, insbesondere in landwirtschaftlich geprägten Landschaften, wurden dagegen bislang kaum untersucht. Darüber hinaus wurde bisher noch nicht untersucht, wie die Mikroben im Bachbett auf kleinskalige hydrologische Heterogenität reagieren, obwohl dies für die Bewertung ihres Beitrags zum Umsatz von Nitrat und anderer landwirtschaftlicher Schadstoffe von großer Bedeutung sein könnte. Ziel dieser Dissertation ist es deshalb, neue Einblicke in die Steuerung des mikrobiellen Stickstoffkreislaufs im Bachbett, direkt an der Schnittstelle zwischen Oberflächenwasser und Grundwasser in einem landwirtschaftlich geprägten Bache zu gewinnen.

Der erste Teil der Dissertation befasst sich mit der mikrobiellen Nitratreduktion im Bachsediment und wie sie durch den bidirektionalen Wasseraustausch zwischen Oberflächen- und Grundwasser beeinflusst wird. Ich untersuchte die Verteilung und Diversität der Mikrobiota im Bachbett eines Gewässers erster Ordnung. Solchen Bächen mangelt es meist an morphologischer Komplexität des Bachbetts und an umfassendem hyporheischen Austausch, welcher für die Eliminierung von Schadstoffen in Fließgewässern höherer Ordnung entscheidend ist. Hot-Spots der Reaktivität können in Sedimenten von Fließgewässern niedrigerer Ordnung dennoch als Funktion der Hydrologie vermutet werden, welche den lokalen Zu- (Grundwasserexfiltration) oder Abfluss (Infiltration) von Oberflächenwasser steuert. Nach entsprechender hydraulischer Kartierung des untersuchten Baches wurden die Zusammensetzung und die Abundanz der Mikrobengemeinschaften im Bachbett analysiert. Neben Long-Read-Amplikonsequenzen, und qPCR bakterieller 16S rRNA-Gene wurden dabei auch Marker Gene der Nitrifikation (*nirK* und *nirS*) abgebildet. Der bidirektionale Wasseraustausch erwies sich tatsächlich als ein kontrollierender Faktor der Mikrobiome im Bachbett, insbesondere für Nitrat-reduzierende Populationen. Typische heterotrophe Denitrifikanten waren am häufigsten in einem mittleren, durch Infiltration gekennzeichneten Bachabschnitt lokalisiert. Dagegen waren in stromaufwärts und -abwärts gelegenen Exfiltrationszonen vorrangig chemolithoautotrophe Schwefel-oxidierenden Nitratreduzierer zu finden. Diese Ergebnisse deuten auf eine enge Kopplung der Stickstoff- und Schwefelkreisläufe im Bachbett hin, sowie auf eine Prägung der Mikrobiologie durch die Hydrologie und Wasserchemie *in situ*. Vergleichbare Heterogenität in der Mikrobiologie und Hydrologie eines Bachbetts wurden bislang noch nicht beschrieben.

Der zweite Teil der Dissertation befasst sich mit der Nitrifikation, also der oxidativen Transformation von Ammonium zu Nitrat im Bachbett. Hier wurde die Relevanz verschiedener Ammoniak-oxidierenden Populationen im Bachbett untersucht. Dieses

beherbergt sowohl bakterielle als auch archaeelle Ammoniakoxidierer (AOB bzw. AOA), deren jeweiliger Beitrag zum oxidativen N-Kreislauf im Bachbett jedoch noch nicht verstanden ist. Hier verwendete ich einen polyphasischen Ansatz, welche die Erhebung geochemischer Daten *in situ*, 16S rRNA-Gen-Metabarcoding, die Sequenzierung und qPCR funktioneller Genmarker, sowie die Bestimmung potenzieller Nitrifikationsraten in Mikrokosmen mit unterschiedlichen Inhibitoren umfasste. Schließlich wurde mit den experimentellen Daten noch eine Populations-basierte Reaktionsmodellierung durch das Projekt-Konsortium vorgenommen. Die Ergebnisse zeigen, dass tatsächlich die AOB und nicht die weitaus häufigeren AOA die Nitrifikations-Aktivität im Sediment bestimmen. Sowohl *Nitrosomonas* als auch *Nitrosospira* spp. waren für die Ammoniakoxidation im Bachbett von großer Bedeutung. Diese Ergebnisse zeigen ebenso, dass die Abundanz von *amoA*-Genen kein zuverlässiger Indikator für reaktive Potenziale *in situ* ist. Stattdessen ist eine Kombination von *in-situ*-Beobachtungen, Mikrokosmen-Inkubationen und Modellierung durchaus sinnvoll, um Prozesse der Stickstofftransformation in natürlichen Systemen besser zu verstehen.

Im dritten Teil der Dissertation wurde die metabolische Verbindung zwischen Stickstoff- und Schwefelkreislauf im Bachbett mittels eines metagenomischen Ansatzes weiter untersucht. Mithilfe von Long-Read-Amplikons des bakteriellen 16S rRNA-Gens, sowie einem hybriden Long-Read-gestützten metagenomischen Ansatz wurden weitere Einblicke in die Vielfalt der Archaeen und Bakterien, welche am Stickstoff- und/oder Schwefelkreislauf im Bachbett des Schönbrunnens beteiligt sind, generiert. Dazu wurde eine Erfassung der relevanten Stoffwechselwege und der mikrobiellen Arten, die zu den wichtigsten funktionellen Genpools beitragen, durchgeführt. Die Ergebnisse lieferten weitere wichtige Erkenntnisse über das metabolische Potenzial einiger der häufigsten Mikroorganismen im Bachbett. Nicht weniger als 70 vollständig oder teilweise rekonstruierte

Metagenom-assemblierte Genome (MAGs) wurden generiert. Diese repräsentieren mehr als 13 bakterielle Phyla. Dadurch wurde nicht nur die Gruppe potenziell relevanter Nitratreduzierer um kanonische Sulfatreduzierer erweitert, sondern auch die Bedeutung einer bislang nicht weiter charakterisierten Linie (B1-7BS) innerhalb der *Gammaproteobakterien* in der Nitrat-abhängigen Schwefeloxidation hervorgehoben. Dies unterstützt weiter die komplexen Verbindungen zwischen Stickstoff- und Schwefelkreislauf im Mikrobiom des Bachbetts, mit einer Vielzahl von Taxa, die an der vollständigen und/oder partiellen Nitratreduktion beteiligt sind.

Zusammenfassend liefert diese Dissertation äußerst detaillierte quantitative und räumlich aufgelöste Daten über die mikrobiellen Gemeinschaften des Bachbetts eines landwirtschaftlichen geprägten Fließgewässers erster Ordnung, sowie über den wichtigen Einfluss der Hydrologie auf die Mikrobiologie in diesem reaktiven System. Insbesondere die Verteilung und Diversität funktioneller Gruppen der Nitratreduktion wurde eindeutig durch lokale hydrologische Austauschprozesse im Bach beeinflusst. Diese Dissertation liefert zudem den Beweis für einen engen Zusammenhang zwischen den chemolithoautotrophen Stickstoff- und Schwefelkreisläufen im Bachbett. Dies unterstreicht, wie wichtig es ist, die reaktive Kapazität von Fließgewässern niederer Ordnung in der Kontrolle von Nährstoffeinträgen auf Einzugsgebietsebene zu berücksichtigen. Ein besseres Verständnis der mikrobiellen Gemeinschaften und der hydrologischen Rahmenbedingungen in solchen Bächen könnte für die Entwicklung nachhaltiger landwirtschaftlicher Flächennutzungs- und Bewirtschaftungspläne von großer Bedeutung sein.

DEDICATION

To my dear Mom and Dad.

Thank you for your unconditional love and unwavering support that you have provided at every pivotal stage of my life. It is a true privilege to be your son.

In addition, to those who never stop finding individual happiness.

“It's not what you look at that matters, it's what you see.”

- *Henry David Thoreau*

ACKNOWLEDGEMENTS

"Is doing a Ph.D. the best option for me?" I asked with hesitancy. "Well, doing a Ph.D. may not be the best decision, but you can easily make thousands of decisions worse than this one..." He replied. Thank you, Dr. Aitken. I left the Appalachians and embarked on my new scientific adventure near Bavarian Alps in Germany with courage, motivation, and unwavering faith that I am ready for any future challenges. More importantly, thank you for showing me a formidable attitude both from your outside optimism and inside calmness in the face of the impending destiny arrangement.

My experience in Germany is meaningful and unforgettable. It was really a great pleasure for me to meet and work with a group of incredible supportive individuals. I would like to express my sincere gratitude to my dissertation advisor Dr. Lüders, for his generous guidance and unreserved support for my research and future endeavors over the last few years. His sharp visions for defining the scope of the research questions, and insightful considerations for experiment design and manuscript drafting, pushed me forward steadily. Despite the unexpected relocation of the whole research group, I never felt disorientate or left behind. When motivation meets unconfined space for your own piece of mind, working in such a group helped me gain scientific independence. It also helped me better manage and enact my own sometimes crazy plans. I was also able to learn management and scientific communication skills in the group, which are valuable for my future career development. Moreover, I joined this subsurface microbiology project with little prior fieldwork experience on wet sediment samples. I could not manage fieldwork myself without instructions and substantial assistance from Dr. Lüders. Thank you so much for your help, trust, and encouragement, which have empowered me to embrace uncertainties and challenges in the next step of my life.

In addition, the work I have done would not be possible without the support and guidance from members of the Lüders Lab in Munich, including Baoli, Dheeraj, Lu, Anna, Lauren, and Gabi. I have learnt a lot from you. Thank you for your willingness to assist me and mentor me. Without your assistance, I will not be able to set up any experiments

efficiently during my first three months in the group, and present exciting results at the international conference. What's more, I would like to thank other members of the IGOE for creating the comfortable working environment and helping me regardless of circumstances, especially Lucas, He, Fengchao, and Sviatlana. During my time at the HMGU, labs of COMI were literally my second frequently visited place. I particularly want to thank Susanne, Silvia, and Akane for providing me technical support and grant me access to the powerful computing resource. Then I also want thank Lüder's Lab in Bayreuth. I am so lucky to meet and work with Melanie, Ralf, Anita, Aileen, and Dan. Thank you for making the lab so cozy and comfortable for me. I have gained plenty of valuable experience from all of you.

I am also grateful for the opportunity to be part of the CAMPOS project, and for the support I received from amazing fellow PhD students and PIs of the CAMPOS project, especially Oscar, Natalia, David, Simon, Dr. Schwientek, and Dr. Cirpka. I cherish every piece of memory of our symposiums, retreats, and dinners together. Spending with all of you never made me feel pressured or uncomfortable. Instead, we supported each other, filled each other with more excitement after each collaboration. I will not forget all of moments I spent in the city of Tübingen.

I also want to extend my genuine gratitude to my committee members. Dr. Schloter, Dr. Elsner, and Dr. Liebl for your continuously positive academic support. I would not have reached this stage without your professional guidance and generosity. Thank you for offering precious opportunities to learn from you.

Again, thank you all for your unwavering support. Your help means a lot to me and I truly appreciate it!

Finally, I would like thank my parents for everything you have done for me. I would have given up countless times on my journey without your understanding and encouragement. No words here can accurately describe my heartfelt gratitude to you.

December 7, 2022

Giesing, München

TABLE OF CONTENTS

LIST OF FIGURES	xvi
LIST OF TABLES	xvii
LIST OF ABBREVIATIONS	xviii
1 INTRODUCTION	1
1.1 Climate change and the global water issue	1
1.2 Agriculture and the nitrate issue	1
1.3 Streams in agricultural catchments	4
1.4 Microbial nitrogen cycling	6
1.4.1 Denitrification and DNRA	6
1.4.2 Nitrification	9
1.5 Links between microbial nitrogen and sulfur cycling in the streambed	11
1.5.1 Sulfide oxidation as driver of nitrate reduction	11
1.5.2 Sulfide production by sulfate reducing bacteria	13
1.6 The Ammer catchment and the Schönbrunnen subcatchment	14
1.7 Processes of hydrologic turnover	17
1.8 Assembly of streambed microbial communities	19
1.9 Molecular approaches to dissect streambed microbiomes	22
Aims of the dissertation	27
2 MATERIALS AND METHODS	30
2.1 Methods for nitrate-reducing microbial populations in the Schönbrunnen streambed as impacted by bidirectional water exchange	30
2.1.1 Site description.....	30
2.1.2 Sediment sampling	33
2.1.3 Hydrological description and water chemistry.....	34
2.1.4 Nucleic acid extraction and 16S rRNA gene amplicon sequencing	37
2.1.5 Sequencing data analysis.....	38
2.1.6 Quantitative PCR (qPCR) of bacterial 16S rRNA and nitrite reduction genes	41
2.2 Methods for nitrification in the Schönbrunnen streambed	43
2.2.1 Study site and sample collection	43
2.2.2 Sediment sample processing and microcosm setup.....	44
2.2.3 DNA isolation and amplicon sequencing	47
2.2.4 qPCR measurements	47
2.2.5 Sequencing data analysis.....	49
2.2.6 Bacteria <i>amoA</i> gene amplicon sequences analysis	50
2.3 Methods for metagenomics of the Schönbrunnen streambed microbiome	52

2.3.1 Sample collection and sulfide measurement	52
2.3.2 DNA extraction and sequencing.....	53
2.3.3 16S rRNA gene amplicon data processing and analysis	54
2.3.4 Metagenome assembly and binning	54
3 RESULTS	57
3.1 Nitrate-reducing microbial populations in the Schönbrunnen streambed as impacted by bidirectional water exchange	57
3.1.1 Hydrology and hydrochemistry of the Schönbrunnen stream	57
3.1.2 Bacterial communities in streambed sediments.....	58
3.1.3 Streambed microbial community assembly.....	68
3.1.4 Quantification of denitrifying communities	69
3.2 Nitrification in the Schönbrunnen streambed.....	71
3.2.1 <i>In-situ</i> community composition of streambed microbiomes	71
3.2.2 Microcosm incubation experiments	75
3.2.3 Diversity and composition of AOB gene pools in microcosms.....	80
3.3 Metagenomics of the Schönbrunnen streambed microbiome.....	85
3.3.1 The streambed microbiome compared via amplicon and shotgun metagenomic sequencing	85
3.3.2 Linking microbial nitrogen and sulfur cycling	88
3.3.3 Metabolic capacity of the streambed microbiome	90
3.3.4 Metabolic potentials of key populations of the streambed as revealed by metagenome assembled genomes (MAGs)	94
3.3.5 Core bacterial populations of the Schönbrunnen streambed over three years	97
4 DISCUSSION	100
4.1 Nitrate-reducing microbial populations in the Schönbrunnen streambed as impacted by bidirectional water exchange	101
4.1.1 Bidirectional water exchange as a control of water chemistry and streambed bacterial communities	101
4.1.2 Hydrological impact on microbial communities potentially involved in nitrate reduction	104
4.2 Nitrification in the Schönbrunnen streambed.....	107
4.2.1 Simulated ammonia oxidation dynamics.....	107
4.2.2 Release of ammonium from the sediment	108
4.2.3 Incomplete Inhibition of AOB by 1-Octyne.....	109
4.2.4 Contributions of AOA and AOB to ammonia oxidation	110
4.2.5 Diversity and composition of AOB gene pools.....	112
4.3 Metagenomics of the Schönbrunnen streambed microbiome.....	114
4.3.1 Diverse of microbes from the streambed revealed by amplicon and metagenomics sequencing	114
4.3.2 Linking microbial nitrogen and sulfur cycling	116
4.3.3 Long-read sequencing to dissect sediment microbial communities at high resolution.....	120
5 CONCLUSIONS AND OUTLOOK.....	123
APPENDIX: SUPPORTING INFORMATION.....	127

SI.1 Streambed microbial communities in the transition zone between groundwater and a first-order stream as impacted by bidirectional water exchange.....	127
SI.2 Linking abundance and activity of ammonia-oxidizing bacteria and archaea in an agriculturally impacted first-order stream	131
Process-based modeling of nitrification	131
Parameter Estimation & Numerical Methods.....	134
Bayesian Parameter Estimation for the Reaction Model	135
SI.3 Deciphering microbial nitrogen and sulfur cycling in lower-order agricultural stream sediments using genome-resolved long-read metagenomics	142
REFERENCES.....	157
PUBLICATIONS AND AUTHORSHIP CLARIFICATION.....	189

LIST OF FIGURES

Fig. 1.1: Scheme of major microbial nitrogen cycling processes in agriculturally impacted lower-order streams.	2
Fig. 1.2: Conceptual illustration of hyporheic flow as controlled by the complex streambed morphology of higher-order streams	5
Fig. 1.3: Scheme of microbial nitrogen-cycling processes.	7
Fig. 1.4: Conceptual illustration of the impact of bidirectional water exchange on nitrogen transformations in the streambed.	18
Fig. 1.5: Schematic illustration of microbial community assembly processes	20
Fig. 1.6: Conceptual overview of PacBio long-read amplicon sequencing	24
Fig. 2.1.1: Location of the first-order stream Schönbrunnen.....	32
Fig. 2.1.2: Stream-groundwater exchange fluxes, and maps of nitrate and sulfate concentration.....	36
Fig. 2.2.1: Location of the Schönbrunnen stream and schematic description of the microcosm setup.	44
Fig. 3.1.1: Alpha diversity of sediment bacterial communities	59
Fig. 3.1.2: Heatmap of the most abundant family-level microbial taxa	60
Fig. 3.1.3: Intersection of streambed ASVs.....	62
Fig. 3.1.4: Bray-Curtis distance-based non-metric multidimensional scaling (NMDS) plot of dissimilarities between streambed microbial communities	64
Fig. 3.1.5: Relative abundance of members within the <i>Rhodocyclaceae</i>	64
Fig. 3.1.6: Relative abundance of potential sulfur-oxidizing bacterial populations	66
Fig. 3.1.7: Maximum likelihood tree of <i>Sulfuricurvum</i> and <i>Thiobacillus</i> ASVs.....	67
Fig. 3.1.8: Heatmap for the β -NTI values	69
Fig. 3.1.9: Abundances of streambed denitrification communities.	70
Fig. 3.2.1: <i>In-situ</i> Shannon diversity index.....	72
Fig. 3.2.2: Relative abundance of top 20 most abundant microbial communities.....	73
Fig. 3.2.3: Relative abundances of taxa affiliated with well-known nitrifiers.....	74
Fig. 3.2.4: Relative abundance of <i>Nitrosomonadaceae</i> -affiliated ASVs.....	74
Fig. 3.2.5: Measured and simulated microcosm experiment results (upstream)	76
Fig. 3.2.6: Measured and simulated microcosm experiment results (Midstream).....	76
Fig. 3.2.7: Measured and simulated microcosm experiment results (downstream).....	77
Fig. 3.2.8: Alpha diversity and PCA plots of bacterial <i>amoA</i> OTUs.....	81
Fig. 3.2.9: Shift of bacterial <i>amoA</i> diversity before and after incubation.	82
Fig. 3.2.10: Maximum likelihood phylogenetic tree generated from a nucleotide-based alignment of all bacterial <i>amoA</i> OTU sequences.....	83
Fig. 3.3.1: Top 30 most abundant streambed microbial lineages	87
Fig. 3.3.2: Archaeal communities at the family level detected by shotgun metagenomic sequencing.....	88
Fig. 3.3.3: Links between nitrate reduction and reduced sulfur oxidation genes	89
Fig. 3.3.4: Differential abundance of pathways	90
Fig. 3.3.5: Relative abundance of key nitrate reduction gene families	91
Fig. 3.3.6: Relative abundance of key sulfate reduction and reduced sulfur oxidation gene families.....	93
Fig. 3.3.7: Quality of metagenome-assembled genomes (MAGs).....	96
Fig. 3.3.8: Functional features within selected MAGs of the streambed microbiota.	97
Fig. 3.3.9: Number of unique and shared ASVs based on the by sampling year.	98
Fig. 3.3.10: Core microbiome in the Schönbrunnen streambed sediments	99

LIST OF TABLES

Table 2.1.1: Water chemistry and hydrology of Schönbrunnen stream water and adjacent groundwater.	31
Table 2.1.2: Sediment sample codes according to the standardized Schönbrunnen project database.	32
Table 2.1.3: Universal primer set used for amplifying the full-length 16S rRNA gene from each sediment sample.	37
Table 2.1.4: Primer sets and annealing temperatures used for gene abundance measurements through qPCR.	42
Table 2.2.1: Simulated stream water medium modified from a previous study.	45
Table 2.2.2: Primers for qPCR amplification of bacterial and archaeal 16S rRNA genes and <i>amoA</i> genes.	49

LIST OF ABBREVIATIONS

United Nations Environment Programme (UNEP)
European Union (EU)
United Nations (UN)
World Health Organization (WHO)
CAMPOS – Catchments as Reactors: Metabolism of Pollutants on the Landscape Scale
Dissolved organic nitrogen (DON)
Dissimilatory nitrate reduction to ammonium (DNRA)
Molar ratios of carbon to nitrogen (C/N)
Ammonia-oxidizing bacteria (AOB) and ammonia-oxidizing archaea (AOA)
Complete ammonia oxidation (comammox)
Sulfur-oxidizing bacteria (SOB)
Dissimilatory sulfate-reducing bacteria (SRB)
Elemental sulfur (S)
Candidate Phyla Radiation (CPR)
Deoxyribonucleic acid (DNA)
Ribonucleic acid (RNA)
Persistent organic chemicals (POPs)
Pharmaceuticals and personal care products (PPCPs)
Denaturing gradient gel electrophoresis (DGGE)
Terminal-restriction fragment length polymorphism (T-RFLP)
Pacific Biosciences (PacBio)
Single-molecule real-time (SMRT)
Circular Consensus Sequence (CCS)
Polymerase chain reaction (PCR)
Quantitative PCR (qPCR)
Non-metric multi-dimensional scaling (NMDS)
Similarity percentage analysis (SIMPER)
 β -mean nearest taxa distance (β -MNTD)
 β -nearest taxon index (β -NTI)
Metagenome-assembled genomes (MAGs)

1 INTRODUCTION

1.1 Climate change and the global water issue

Population growth and climate change are increasingly challenging global water quality and quantity, further worsening food supply and global agricultural sector losses (Damania 2020). Declining water quality is not only a major aspect of water availability, but also harming human and ecosystem health. Sustaining water quality has been particularly emphasized in the UN 2030 Agenda for Sustainable Development (Lee et al. 2016; Colglazier 2015). Within the water sector, public perception is often more focused on water quantity issues (e.g., flood, drought), while water quality issues often remain disregarded, especially under the impact of global warming (Hannah et al. 2022).

As global warming can lead to reduced availability of irrigation water and soil fertility, agricultural regions in Europe are likely to be more limited, with the yield of the crop production subjected to slow increase (Tittonell and Giller 2013; Holman et al. 2017). Therefore, further agricultural expansion and intensification are expected to maintain the crop and livestock production following current food consumption patterns (Foley et al. 2011; Rööös et al. 2017). Excessive agricultural practices can further degrade water quality, exacerbating the already limited availability of irrigation water due to climate change (Foley et al. 2011). Scientific insights and solutions, especially those that harness potentials of natural attenuation to tackle water pollution, are particularly important as they can inform strategies for improved climate change adaptation.

1.2 Agriculture and the nitrate issue

The application of manure and agricultural fertilizers containing nitrate and phosphate contributes to agricultural nonpoint-source pollution, which is a major cause of freshwater pollution in many regions (David and Gentry 2000; Shortle and Braden 2013). Nitrate loading (Fig. 1.1), mainly stemming from agricultural fertilizer inputs and also nitrification of

ammonia arising from livestock manure, poses a significant threat to the stream water and groundwater quality (Peterson et al. 2001; Starry, Valett, and Schreiber 2005).

In addition, decreasing precipitation and river discharge, as consequences of climate change, can result in elevated and seasonally varying concentrations of nitrate and phosphate in the surrounding catchments (Badrzadeh et al. 2022). Nitrate has the potential to leach deeper into the as it is mobile and negatively charged, and even accumulate as dissolved organic nitrogen (DON) in groundwater (Basu et al. 2010; Grose et al. 2022). Accumulated nitrate can persist in groundwater for decades, continuously exerting adverse impacts on water quality, even after changes have been made to regional agricultural nitrate inputs (Basu et al. 2022). The hysteresis effects of legacy nitrogen release demonstrate that nitrogen management must consider nitrogen fluxes in both surface and subsurface environment (Basu et al. 2022).

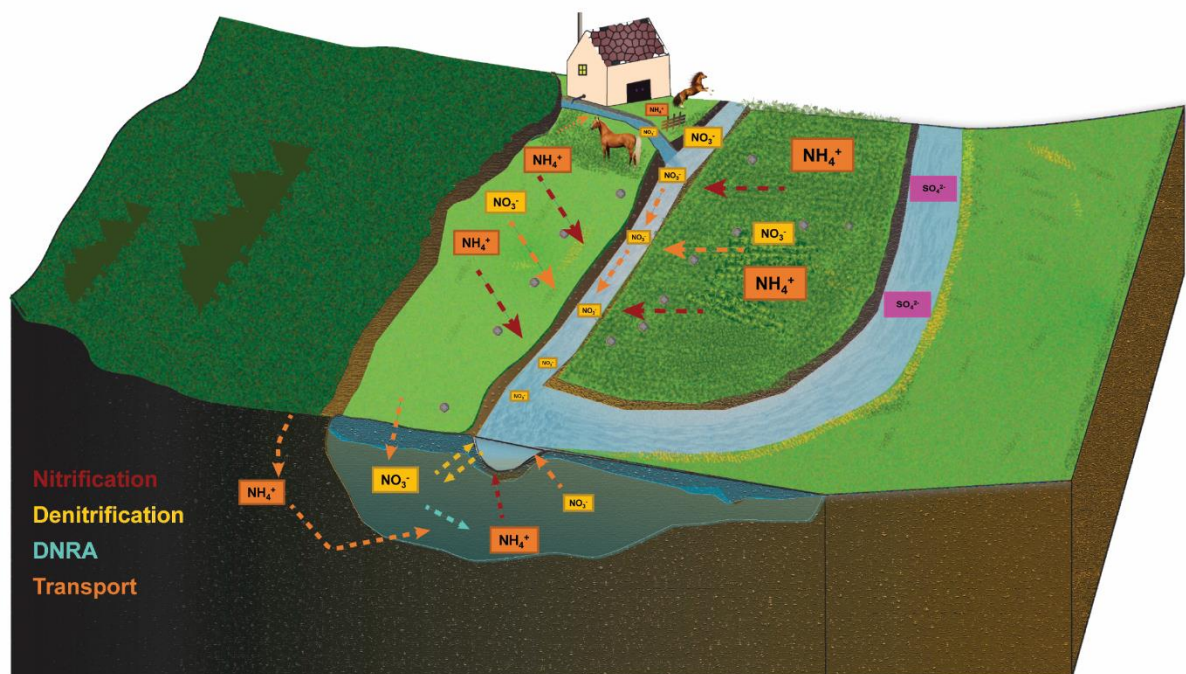


Fig. 1.1: Scheme of major microbial nitrogen cycling processes in agriculturally impacted lower-order streams. Scheme is inspired by fluxes and processes in the Schönbrunnen subcatchment, as investigated in this project.

Increasing nitrogen inputs and nitrate pollutions have been listed as one of the most pressing emergent issues of environmental concern by the United Nations Environment Programme (UNEP) (Sutton, Raghuram Nandula, and Adhya 2019). Besides this, the European Union (EU), for example, has implemented a series of directives to prevent nitrate pollution from agricultural practices, including the Nitrate Directive in 1991, followed by the Water Framework Directive in 2000, and the Groundwater Directive in 2006 (Biernat et al. 2020). Nevertheless, as per the EU nitrate measure network, approximately 25%-30% of groundwater in within the EU, and 20 % within Germany, exhibited average concentrations greater than 50 mg/L nitrate (Nitratbericht Deutschland 2020). The reductive transformation of nitrate results in the production of the greenhouse gas nitrous oxide (N₂O), thereby contributing to the issue of climate change (Beaulieu et al. 2011). Small rivers and streams (lower than fourth-order streams) are responsible for over 80% riverine N₂O emissions (Yao et al. 2020). Additionally, elevated levels of nitrate have been reported to be the major cause of eutrophication in connected water bodies, resulting in algal blooms (Singh et al. 2022), toxicity to aquatic animals (Camargo, Alonso, and Salamanca 2005), and increased risks of methemoglobinemia in infants who consume nitrate-contaminated drinking water (Fossen Johnson 2019). Although the World Health Organization (WHO) explicitly regulates nitrate levels in drinking water at 50 mg/L (Instead, maximum conc. of 10 mg/L nitrogen-N as regulated by the US Environmental Protection Agency), many countries that rely on groundwater as their primary source of drinking water face increasing nitrate-related issues (Van Grinsven et al. 2006; WHO 2016; Katsanou and Karapanagioti 2019; Guppy et al. 2018). Even drinking water with nitrate levels below regulatory thresholds (e.g., below 10 mg/L) is still often associated with an increased risk of preterm birth, and/or chronic health outcomes, such as colorectal cancer (Schullehner et al. 2018; Temkin et al. 2019). Therefore, water quality should not be disregarded, when agricultural development is primarily aimed at producing more food to meet the demands of a growing population.

1.3 Streams in agricultural catchments

The reactive potentials of different riverine compartments (e.g., streams, rivers, and interconnected wetlands) towards agricultural pollutants is not yet well understood. The morphology and connectivity of river systems is typically classified via stream/river orders (Scheidegger 1965). In general, first-order streams are the smallest streams in a river system which have no upstream tributaries (Scheidegger 1965). The confluence of two or more first-order streams can form a second-order stream. The focus of my dissertation is primarily on lower-order streams, specifically first- and second-order streams. Pristine lower-order streams in forested, upper or middle mountainous areas are often classified as headwater streams, whereas lower-order streams in lowlands and agricultural areas would not typically be termed as headwaters. Up to 85 % of the total stream length in a river system consists of lower-order streams (Peterson et al. 2001; Scheidegger 1965; Horton 1945). Lower-order streams act as the fountainhead of fluvial networks and have a substantial imprint on the water chemistry downstream (Peterson et al. 2001). However, their functioning and reactivity towards incoming pollutants, in particular from diffuse agricultural sources, have been much less frequently investigated than that of higher-order streams.

Higher-order streams are typically connected to extensive hyporheic and parafluvial flow paths, in which stream water moves through streambed and/or riparian sediments to subsequently return to the stream due to the complex streambed and/or riparian sediments morphology (Fig. 1.2) (McClain et al. 2003; Boano et al. 2014; Gomez-Velez et al. 2015; S. Krause et al. 2011). The concept of the hyporheic zone, originally described as a subsurface habitat of fauna distinct to those discovered in the water body, first appeared in the literature in 1946, authored by Chappuis in French (Herzog, Howell, and Ward 2020). The term hyporheic, derived from the Greek neologism hypo- (meaning “under”) and -rheos (meaning “flow”), was originally suggested in 1955 by Orghidan (in Romanian language) to describe

the unique biological habitat located in the streambed where stream water and groundwater approach each other in a physicochemical transition zone (Tr Orghidan 1955; Traian Orghidan 2010; Lewandowski et al. 2019). Water passage through the hyporheic zone can significantly stimulate biogeochemical turnover of pollutants and nutrient elimination, because of elongated transit times (compared to instream residence time) and increased biogeochemical and physical heterogeneity (Boano et al. 2014; McClain et al. 2003). A previous study on a third-order stream has suggested that up to 17% of nitrate in the stream was removed owing to hyporheic exchange (around 32% total reach denitrification) (Zarnetske, Haggerty, and Wondzell 2015).

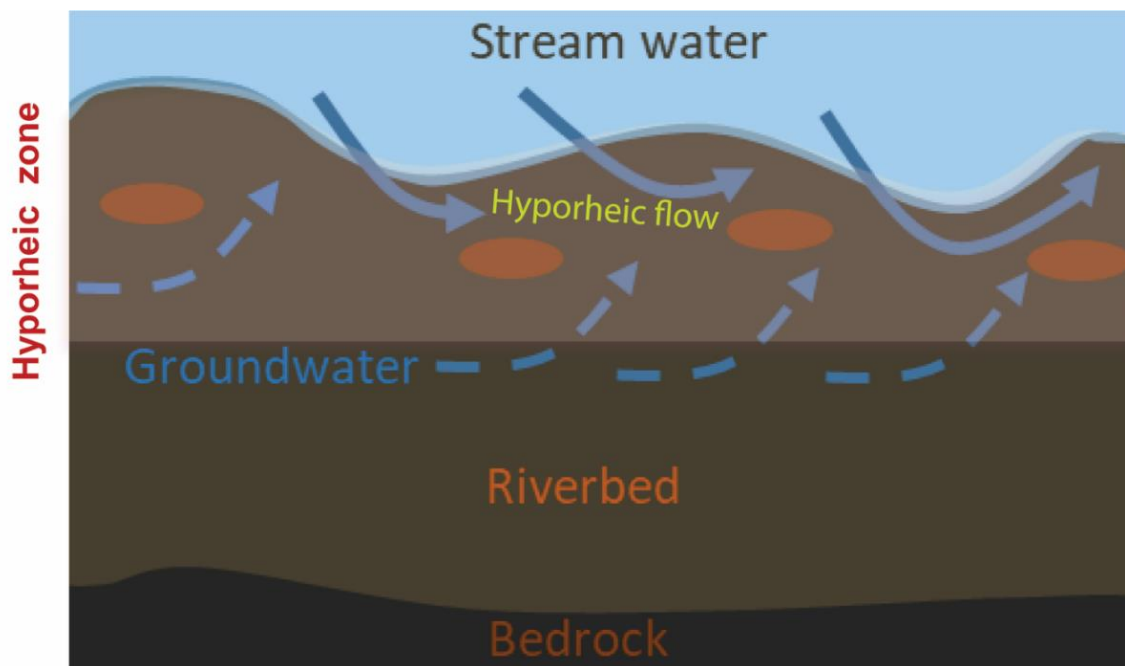


Fig. 1.2: Conceptual illustration of hyporheic flow as controlled by the complex streambed morphology of higher-order streams.

In contrast, lower-order agricultural streams are often strongly modified through dredging and straightening to more efficiently drain excess water from agricultural fields and to benefit crop production (Blann et al. 2009; Hanrahan et al. 2018). These modified streams are typically of low streambed morphological complexity, thus minimizing the potential for hyporheic exchange. Therefore, such streams have often been considered to act predominantly

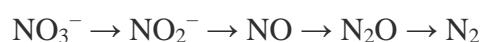
as drainage systems, largely receiving water from the surrounding landscape (Needelman et al. 2007; Yu et al. 2018; Kaandorp et al. 2018). This currently limits the perspective of how hydrology and biogeochemistry can interact to control oxidative and reductive pollutant transformation in lower-order agricultural streams.

1.4 Microbial nitrogen cycling

1.4.1 Denitrification and DNRA

Once excess nitrate enters the stream through direct runoff and/or groundwater exfiltration (Fig. 1.1), streambed sediments have a significant impact on nitrogen transformation (Newbold 1992; Butturini, Battin, and Sabater 2000). Anionic nitrate has a higher mobility than the cationic ammonium, which makes it more impactful on downstream water quality (Stuart, Rich, and Bishop 1995; Peterson et al. 2001). The transformation of nitrate can occur more rapidly in lower-order streams (i.e. first- and second-order streams) in comparison to higher-order rivers, due to their smaller channel size, shallower water depths, and therefore greater surface-to-volume ratios (Peterson et al. 2001).

Capacities for the assimilative transformation of nitrate in the stream itself mostly involve algal or macrophyte growth, as nitrate is one of the major growth limitation factors for phototrophs, along with phosphate (Gooseff et al. 2004; L. K. Smith et al. 2006). More importantly, other nitrogen transformation processes are thought to be mainly catalyzed by microbes (Doane 2017). Nitrate can be transformed by microbial communities in anoxic streambed sediments, through heterotrophic denitrification (Fig. 1.3):



and/or dissimilatory nitrate reduction to ammonium (DNRA) (Fig. 1.3):



(Tiedje 1988; Kuypers, Marchant, and Kartal 2018; Storey, Williams, and Fulthorpe 2004; Mulholland et al. 2008). However, as all of these processes require microoxic or anoxic

conditions, the local hydrologic pattern can therefore become a decisive parameter of control (Zarnetske et al. 2011; Seitzinger et al. 2002).

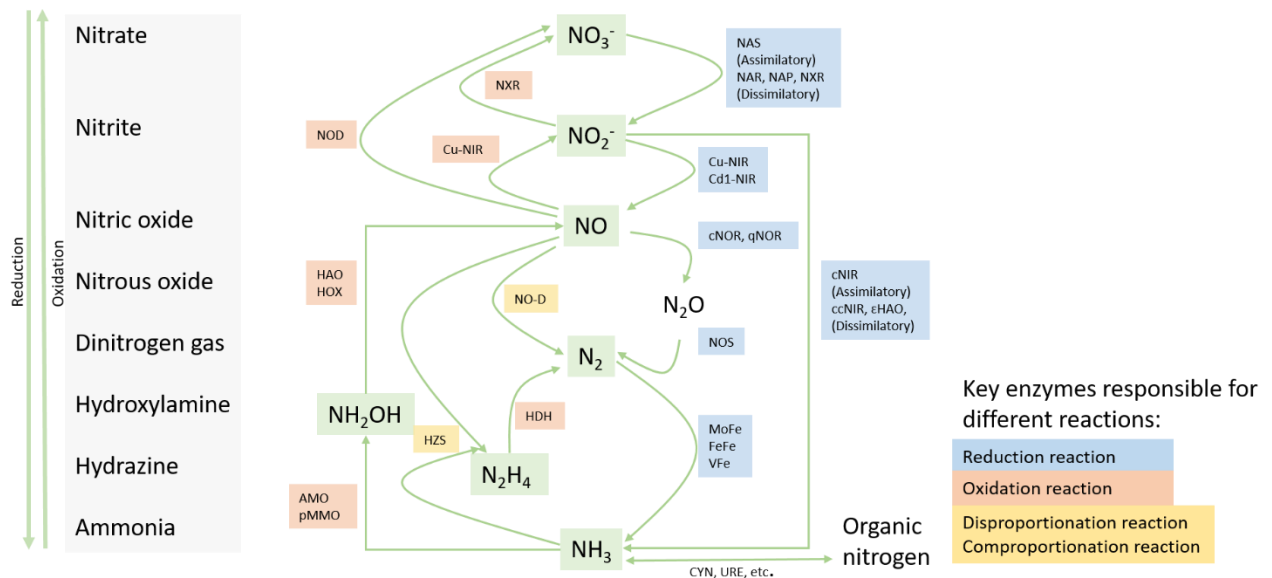


Fig. 1.3: Scheme of microbial nitrogen-cycling processes. Adapted from a previous study (Kuypers, Marchant, and Kartal 2018). Selected enzymes involved in the nitrogen transformations shown in the scheme: assimilatory nitrate reductase (NAS, *nasA* and *nirA*); membrane-bound (NAR, *narGH*) and periplasmic (NAP, *napA*) dissimilatory nitrate reductases; nitrite oxidoreductase (NXR, *nxrAB*); nitric oxide oxidase (NOD, *hmp*); copper-containing (Cu-NIR, *nirK*) and haem-containing (cd₁-NIR, *nirS*) and nitrite reductases; cytochrome c-dependent (cNOR, *cnorB*), quinol-dependent (qNOR, *norZ*); hydroxylamine oxidoreductase (HAO, *hao*); hydroxylamine oxidase (HOX; *hox*); nitrous oxide reductase (NOS, *nosZ*); nitric oxide dismutase (NO-D, *norZ*); assimilatory nitrite reductase (cNIR; *nasB* and *nirB*); dissimilatory periplasmic cytochrome c nitrite reductase (ccNIR, *nrfAH*); ϵ -hydroxylamine oxidoreductase (ϵ HAO; *haoA*); molybdenum-iron (MoFe, *nifHDK*), iron-iron (FeFe, *anfHGDK*) and vanadium-iron (VFe, *vnfHGDK*) nitrogenases; hydrazine dehydrogenase (HDH, *hdh*); hydrazine synthase (HZS, *hzsCBA*); ammonia monooxygenase (AMO, *amoCAB*); particulate methane monooxygenase (pMMO, *pmoCAB*); cyanase (CYN, *cynS*); and urease (URE, *ureABC*).

The first step of canonical denitrification is nitrate (NO_3^-) reduction to nitrite (NO_2^-) (Fig. 1.3). Nitrate is utilized by microorganisms for respiration, a process initiated via dissimilatory nitrate reductase (Kuypers, Marchant, and Kartal 2018). Nitrate reduction can also occur through assimilation, as nitrogen is essential for building up all forms of biomass (Kuypers, Marchant, and Kartal 2018). Nitrate reduction is often driven by organic carbon as electron donor in a heterotrophic metabolism. It can also occur autotrophically, coupled to

inorganic electron donors, such as hydrogen, reduced iron and sulfur species, and even methane (Kuypers, Marchant, and Kartal 2018). A membrane-bound nitrate reductase NAR (catalytic subunit NarG) and/or a periplasmic nitrate reductase NAP (catalytic subunit NapA) are the enzymes responsible for dissimilatory nitrate reduction to nitrite (Moreno-Vivián et al. 1999). Many bacteria carry genes encoding both enzymes (*narG*, and *napA*, respectively) (Philippot 2002). Either of these two enzymes can be involved in canonical denitrification and DNRA processes, though the NAP reductase is considered as a more common enzyme amongst DNRA microorganisms (Asamoto et al. 2021; Heylen and Keltjens 2012). In contrast to NAR, which is located in the cytoplasm and is related to the generation of proton motive force, NAP reductase does not contribute directly to the energy conservation (Moreno-Vivián et al. 1999). As for nitrate reduction prior to assimilation into biomass, assimilatory nitrate reductases (NAS) and also assimilatory nitrite reductases (cNIR, encoded by *nasB* and *nirB*) are involved. NAS is located in the cytoplasm and relies on ATP consuming transporters to provide nitrate inside the cell (Kuypers, Marchant, and Kartal 2018). Therefore, as an energy-consuming process, assimilatory nitrate reduction is found mostly when ammonia is at low availability in the environment (Kuypers, Marchant, and Kartal 2018). Given that nitrite produced from either of these two reduction processes can feed into downstream DNRA, the DNRA-catalyzing periplasmic cytochrome c nitrite reductase (ccNIR) (encoded by genes *nrfAH*) are viewed as markers for this process, despite other types of DNRA enzymes have also been reported (C. J. Smith et al. 2007; Tikhonova et al. 2006; Atkinson et al. 2007; Huang et al. 2020).

In contrast, canonical denitrification then proceeds via the reduction of nitrite (NO_2^-) to nitric oxide (NO), mediated by the classical denitrification marker genes *nirK* and *nirS*. These genes encode either a Cu-containing nitrite reductase (Cu-NIR), or a heme-containing cd_1 nitrite reductase (cd_1 -NIR), respectively, which catalyze the respiratory reduction of nitrite to nitric oxide (Braker et al. 2000). However, microorganisms that are not known for

canonical denitrification, but for other nitrogen cycling processes, can also carry *nirK* and/or *nirS* genes, including anaerobic ammonium-oxidizing bacteria, nitrite-oxidizing bacteria, and aerobic ammonia-oxidizing bacteria (Bartossek et al. 2010). The next step of the canonical denitrification, microbial nitric oxide (NO) reduction, produces the potent greenhouse gas nitrous oxide (N₂O). In addition to the respiration of nitric oxide by microbes, this step also plays a critical role as a detoxification process, as nitric oxide is known as a toxin (Kuypers, Marchant, and Kartal 2018). Two subunits of the nitric oxide reductases (NOR) cytochrome bc complex are encoded by *norB* and *norC* genes (Braker and Tiedje 2003). The final step of the canonical denitrification involves the reduction of nitrous oxide (N₂O) to dinitrogen gas (N₂), which is mediated by nitrous oxide reductase (NOS). The *nosZ* gene, which encodes nitrous oxide reductase, has been widely utilized as a marker gene to evaluate the potential of nitrous oxide consumption in the environment (Orellana et al. 2014).

Generally, denitrification and DNRA are controlled by the molar ratios of carbon to nitrogen (C/N). Carbon limited scenarios (i.e. low C/N ratio), as found in anoxic soils and marine sediment, can prioritize denitrification (Hardison et al. 2015; T. Rütting et al. 2011). In contrast, nitrate limited scenarios (i.e. high C/N ratio) can prioritize the DNRA process, as reported for rumen, anaerobic digester sludge, or chemostat bioreactors (van den Berg et al. 2016; Tiedje et al. 1983). However, niche partitioning between denitrification and DNRA processes in many habitats including lower-order streams remains unclear. Understanding respective process controls will be relevant for grasping the bottlenecks of nitrate elimination, as DNRA does not remove nitrogen from aquatic ecosystems.

1.4.2 Nitrification

On the oxidative side of the N-cycle, canonical nitrification involves two successive major steps, mediated by different microbial groups. The first major step refers to the process by which ammonia (NH₃) is oxidized to nitrite (NO₂⁻), with hydroxylamine (NH₂OH) as the

major intermediate (Fig. 1.3). The second major step is nitrite (NO_2^-) oxidation to nitrate (NO_3^-). The first step of ammonia oxidation is typically performed by aerobic autotrophs, ammonia-oxidizing bacteria (AOB) or ammonia-oxidizing archaea (AOA) (Cardarelli, Bargar, and Francis 2020). Typical AOBs are found within the *Nitrosomonadaceae* (*Betaproteobacteria*) and *Nitrosococcaceae* (*Gammaproteobacteria*) (Cardarelli, Bargar, and Francis 2020). AOA, on the other hand, mainly belong to the *Thaumarchaeota* (now classified as class *Nitrososphaeria* within the phylum *Crenarchaeota*) (Bayer et al. 2019; Parks et al. 2018), including members of the *Nitrososphaeraceae* and *Nitrosopumilaceae* (Jung et al. 2021). Both AOA and AOB can perform ammonia oxidation to hydroxylamine (NH_2OH) through a multi-subunit ammonia monooxygenase (AMO) enzyme (Kuypers, Marchant, and Kartal 2018). The *amoA* gene encoding the subunit A of AMO is widely used as marker gene to interrogate the diversity and abundance of AOA and AOB populations in complex environments (Rotthauwe, Witzel, and Liesack 1997). Quantification of the *amoA* gene has shown that AOA are frequently found to be more abundant than AOB in the soil environment (Tobias Rütting et al. 2021; Di et al. 2009; Sterngren, Hallin, and Bengtson 2015). However, while many *amoA*-carrying members of *Thaumarchaeota* are capable of oxidizing ammonia, it is likely not all of them exhibit this ability. Some members might be able conserve energy through alternative metabolisms (e.g., hydrogen oxidation), although the confirmation of these specific reductants necessitates additional culture-based studies (Abby et al. 2018; Yuchun Yang et al. 2021; Alves et al. 2019).

The recent discovery of complete ammonia oxidation (comammox) has revealed another important driver of ammonia oxidation in various environments (Van Kessel et al. 2015; F. Xia et al. 2018). Some members within the *Nitrospira* lineage, previously well-known for nitrite oxidation, have been shown to oxidize ammonia directly to, without the prior involvement of either an AOA and AOB partner (Daims et al. 2015). Apart from

autotrophic ammonia oxidation, inorganic or organic reduced nitrogen can also be oxidized heterotrophically by chemoorganotrophic bacteria and eukaryotes (e.g., fungi) (Stein 2014; T. Zhu et al. 2015).

The current understanding on the environmental distribution of these three types of ammonia oxidizers is still incomplete. Although AOA, AOB, and comammox bacteria can co-occur in various environments, AOB are typically reported as the dominant organisms under nitrogen-rich conditions, while AOA play a more significant role in relatively oligotrophic systems (L. Zhang, Guan, and Jiang 2021; Leininger et al. 2006; Verhamme, Prosser, and Nicol 2011; Yuyin Yang et al. 2016). Ammonia-oxidizing populations, such as *Nitrosospira* spp. (e.g., *N. briensis* and *N. multiformis*) and *Nitrososphaera viennensis*, are also known to decompose organic nitrogen, such as urea via ureases, to generate extra ammonia that can promote net community growth (Tourna et al. 2011; Burton and Prosser 2001). Within the AOB, it has been reported that the *Nitrosospira* genus is often dominant in terrestrial environments, especially in unfertilised soil and even under limited oxygen conditions, whereas *Nitrosomonas* phylotypes are typically more abundant in fertilised and ammonia-rich environments (Aigle, Prosser, and Gubry-Rangin 2019; Norton et al. 2002; Wagner et al. 1996; S. Xia et al. 2005).

1.5 Links between microbial nitrogen and sulfur cycling in the streambed

1.5.1 Sulfide oxidation as driver of nitrate reduction

Both reductive pathways in microbial nitrogen cycling discussed above (denitrification and DNRA) can be linked to the oxidation of reduced inorganic sulfur species. When sulfide is the electron donor, it can be oxidized to sulfate by chemolithoautotrophic sulfur-oxidizing bacteria (SOB), which are often facultative aerobes capable of respiring nitrate or oxygen. Sulfide oxidation can involve several intermediates, such as thiosulfate ($S_2O_3^{2-}$) and elemental sulfur (S), before releasing the most oxidized form of sulfur, sulfate (+6). The 15-gene sulfur-

oxidation *sox* gene cluster is one of most important systems for sulfur oxidation by diverse bacteria (Friedrich et al. 2000). Here, seven genes (*soxXYZABCD*) are encoding four periplasmic proteins, SoxXA, SoxYZ, SoxB and Sox(CD)₂ (Friedrich et al. 2005). This multi-enzyme complex is responsible for oxidizing reduced sulfur compounds stepwise to sulfate, yet it is not catalytically active when present alone (Friedrich et al. 2005; Wu et al. 2021). The importance of sulfur dehydrogenase SoxCD has been underscored according to its presence and absence in bacterial genomes. The presence of SoxCD is considered to prevent sulfur particles or polysulfide accumulation, whereas the absence of SoxCD can lead to the accumulation of elemental sulfur or polysulfides (Friedrich et al. 2005). Still, sulfur-oxidizing bacteria lacking SoxCD can utilize alternative genes and pathways to further oxidize zero-valent sulfur to sulfite, and ultimately to sulfate.

Representatives of the sulfur-oxidizing bacteria are often found within the phylum *Campylobacterota* (Waite et al. 2017; Parks et al. 2018). More specifically, members previously within the *Epsilonproteobacteria* class, such as *Sulfuricurvum* and *Sulfurimonas* (family *Sulfurimonadaceae*), and *Sulfurovum* (family *Sulfurovaceae*), are known to oxidize reduced sulfur species couple to nitrate reduction (Campbell et al. 2009; Waite et al. 2017). Members of the *Sulfurimonas* genus have been well-studied, as all species tested so far carry a periplasmic nitrate reductase catalytic alpha-subunit (NapA) (Y. Han and Perner 2015). Some of them harbor a complete *napAGHBFLD* operon (Cai, Shao, and Zhang 2015). The special structure of NapA expressed within *Sulfurimonas* enables them to utilize nitrate even in the low μM range (Vetriani et al. 2014; Y. Han and Perner 2015). They are considered ubiquitous in the environment and have been detected in aquifers, salt marsh and marine sediments, and/or even hydrothermal vents (Thomas et al. 2014; Handley et al. 2014; Y. Han and Perner 2015). Other common sulfur-oxidizing bacteria including members of the genera *Bacillus* (phylum *Firmicutes*), *Aquifex* (phylum *Aquificota*), and *Thiobacillus* (class *Betaproteobacteria*).

1.5.2 Sulfide production by sulfate reducing bacteria

Sulfide and its aqueous forms in the environment (e.g., H₂S (gas), HS⁻, and S²⁻) is typically produced by dissimilatory sulfate-reducing bacteria (SRB) in anoxic compartments. They are widely distributed in the terrestrial subsurface, and typically utilize a variety of electron acceptors besides sulfate (SO₄²⁻), including thiosulfate (S₂O₃²⁻), sulfite (SO₃²⁻), elemental sulfur (S), and partially also nitrate and nitrite (Bell et al. 2020). Common electron donors for the SRB would be organic acids and alcohols, products of prior fermentations, or also molecular hydrogen. Some SRBs are known for an incomplete oxidation of organic compounds, releasing acetate as the end product, whereas others are capable of completely mineralizing organic electron donors to CO₂ (Muyzer and Stams 2008).

In dissimilatory sulfate reduction, the direct reduction of sulfate to sulfite is considered thermodynamically unattractive. Here, SRB will first activate sulfate to adenosine 5'-phosphosulfate (APS) by ATP sulfurylase (ATPS) (encoded by the *sat* genes) (Rabus et al. 2015). APS is then reduced to sulfite by APS reductase (encoded by *apsAB*) (Wu et al. 2021). The detection of functional genes, such as *dsrAB* and *aprAB*, represents a reliable approach to identify and quantify SRB in environmental samples (Coskun et al. 2019; Muyzer and Stams 2008). The *Desulfobacterota* (formerly classified as class *Deltaproteobacteria*) are particularly important in this respect, as they constitute a large proportion of dissimilatory sulfate-reducing bacteria and carry genes (*dsrAB*) encoding for dissimilatory sulfite reductase (Müller et al. 2015). Reported bacterial populations that are capable of reducing sulfate belong to a variety of bacterial taxa, including the phyla *Proteobacteria*, *Desulfobacterota*, *Firmicutes*, *Nitrospirota*, and *Thermodesulfobiota* (Waite et al. 2020). Though some archaea (within the *Crenarchaeota*) can also reduce sulfate, these are not typically detected at terrestrial study sites (G. P. Li et al. 2014). Genomic evidence shown that some of the recently reported ultra-small members of the Candidate Phyla Radiation (CPR) bacteria, such as

members within phylum *Patescibacteria*, can also carry genes encoding sulfate adenylyltransferase (*sat*), dissimilatory sulfite reductase delta subunit (*dsrD*), therefore also suggesting a potential role in sulfur transformation processes (Bell et al. 2022; Tian et al. 2020; Alvarado et al. 2022). In addition to the canonical reduction of sulfate to sulfide, some sulfate-reducing bacteria (SRB) can also employ a reverse Dsr (dissimilatory sulfite reductase) pathway, mediated by the products of *dsrAB* and *dsrMKJOP*, to oxidize elemental sulfur to sulfite, and further to sulfate in a reverse adenylyl phosphosulfite reductase (Apr) and sulfate adenylyl transferase (Sat) reaction (Tsallagov et al. 2019). Here, reduced sulfur species can serve as effective electron donors that can be coupled to respiration with electron acceptors such as oxygen or nitrate. All of the different oxidative and reductive microbial pathways introduced in the above section clearly illustrate, that microbial nitrogen and sulfur cycling in the environment can be closely interlinked.

1.6 The Ammer catchment and the Schönbrunnen subcatchment

Extrapolating laboratory-derived data on pollutant turnover to the natural environment remains a major scientific challenge, as data recorded in the lab often fail to adequately capture the complex ecological processes occurring *in-situ*. The collaborative research project (CRC) 1253 CAMPOS – “Catchments as Reactors: Metabolism of Pollutants on the Landscape Scale” coordinated by the University of Tübingen aimed to advance the understanding towards the *in-situ* fate and turnover rates of anthropogenic contaminants in a catchment of the river Ammer (length of the Ammer River is 25 km², and the catchment area is 134 km²) in south-west Germany. The Ammer catchment is a groundwater feeding area with stable catchment discharge (mean = 1.1 m³/s) due to the presence of karstic limestones and large karst springs (Ying Liu et al. 2013). The land-use of the catchment is predominantly agricultural (71%), followed by urban (17%) and forested areas (12%) (Grathwohl et al. 2013). Pollutants derived from agricultural activities, such as nitrate (20-50 mg L⁻¹), are of

major concern in the Ammer catchment (Schwientek, Osenbrück, and Fleischer 2013). Nitrate enters the fluvial system of the Ammer catchment mainly through baseflow, which originates from several major sources: direct agricultural inputs, groundwater from the underlying karstic limestone and gypsum aquifer, effluents from wastewater treatment plants, and discharge from the drinking water softening facilities (Schwientek, Osenbrück, and Fleischer 2013). The highest nitrate concentration in surface water is typically observed during the dry summer season (Schwientek, Osenbrück, and Fleischer 2013). The low hydraulic conductivity of the loamy soils in the Ammer catchment and the underlying karstic rocks have been proposed to promote vertical water flow, resulting in the enrichment of baseflow with nitrate (Schwientek, Osenbrück, and Fleischer 2013). Moreover, sedimentary polycyclic aromatic hydrocarbons (PAHs) found in the Ammer River and streams are indicative of non-agricultural contamination due to impacts from early urban and industrial activities in the catchment (Ying Liu et al. 2013). Therefore, the Ammer catchment is a promising model system to implement state-of-the-art multidisciplinary research approaches aimed at studying *in-situ* pollutant turnover across multiple scales within the catchment.

There were more than eight multidisciplinary subprojects within the frame of the CAMPOS project, covering mechanisms of contaminant transportation, transformation and accumulation in distinct landscape compartments, including rivers, groundwater-surface water interface of lower-order streams, floodplains, fractured and karstic aquifer, and surrounding soils. Among all of these compartments, rivers are a key integrator, as all water from the catchment essentially converges towards the river. The river also connects aquatic environments and directly affects water quality beyond the catchment scale. Aquifers beneath the floodplains are considered as a vulnerable compartment to agrochemicals. This is because deeper fractured aquifers are typically less reactive towards pollutants due to the limited availability of oxygen and carbon sources. Small agricultural streams are the primary receiver

of agricultural pollutants and have the potential to serve as major reactive compartments, especially at the interface between groundwater and surface water in the streambed. This interface often features steep redox gradients and therefore forms a redox transition zone. It has the potential to act as a reactive hot spot for biogeochemical processes. Overall, all of these compartments are interconnected and essential to understand the fate of contaminants in the catchment. Apart from the agricultural pollutants (e.g., nitrate, herbicide like glyphosate), other major chemical pollutants targeted in CAMPOS involved persistent organic chemicals (POPs), general pharmaceuticals and personal care products (PPCPs). They were collectively investigated as micropollutants as they were detected in concentrations ranges of nano- to micrograms. Transdisciplinary research data collected from all subprojects was also integrated in innovative modelling frameworks for pollutant fate and transport at the landscape scale.

Within the frame of the CAMPOS project, this dissertation focused on studying lower-order agricultural streams, and the interface between groundwater and surface water in the streambed. As a sub-catchment of the Ammer catchment, the Schönbrunnen was selected as the main study site of my project. The catchment features a channelized and straightened first-order agricultural stream. This catchment was selected due to the presence of local groundwater and alluvial sediment, which suggest a presumed intense interaction between the stream and groundwater, as well as the presence of high pollutant concentrations (e.g., up to 60 mg L^{-1} nitrate). Furthermore, seasonal dynamics, geology and land use characteristics, and connectedness with circumambient first- and second-order streams (e.g., the second-order stream Käsbach) were also considered in this project. The Schönbrunnen stream joins the sulfate-rich second-order stream Käsbach in its downstream section, where the flow enters the Käsbach alluvial floodplain. A detailed description of the Schönbrunnen subcatchment is reported in the below MATERIALS AND METHODS (i.e. 2.1.1) section.

1.7 Processes of hydrologic turnover

Both nitrification and denitrification can be taken to be controlled by not only respective microbial populations, but also in stream hydrological processes (Stefan Krause et al. 2013; Nogaro et al. 2010). Recent studies have shown that re-structured agricultural lower-order streams can not only collect water from the surrounding landscape, but can steadily interact with the surrounding groundwater along successive and seasonally variable gaining (groundwater exfiltration) or losing (stream water infiltration) reaches (T. P. Covino and McGlynn 2007; Mallard, McGlynn, and Covino 2014; Z.-Y. Zhang et al. 2021). Stream and groundwater exchange processes in the Schönbrunnen have been identified via a series of hydrological monitoring approaches by the CAMPOS consortium, including measuring of stream discharge, groundwater hydraulic gradients, salt tracer tests, and ^{222}Rn (Jimenez-Fernandez et al. 2022). Substantial bidirectional exchange fluxes between the stream and surrounding groundwater were observed for successive reaches of the stream (Fig. 2.1.1 & Fig. 2.1.2). As a result, solutes, including nitrate and sulfate, and relevant biochemical processes, pass the streambed sediments via successive stream water and groundwater interactions, controlled by either upward or downward fluxes of water.

This sequential bidirectional infiltration and exfiltration of water along the flow of a river or stream has been termed as hydrologic turnover (Mallard, McGlynn, and Covino 2014; T. Covino, McGlynn, and Mallard 2011). Hydrologic turnover leads to the replacement of water from streams with groundwater, or water fractions from shallow aquifers with stream water. This typically occurs over more prolonged time scales and flow distances, compared to typical hyporheic flow driven by streambed morphology. However, the description of hydrologic turnover in previous studies did not address how the spatial heterogeneity of net water exchange might affect water chemistry, and more importantly, the streambed microbial communities and their activities.

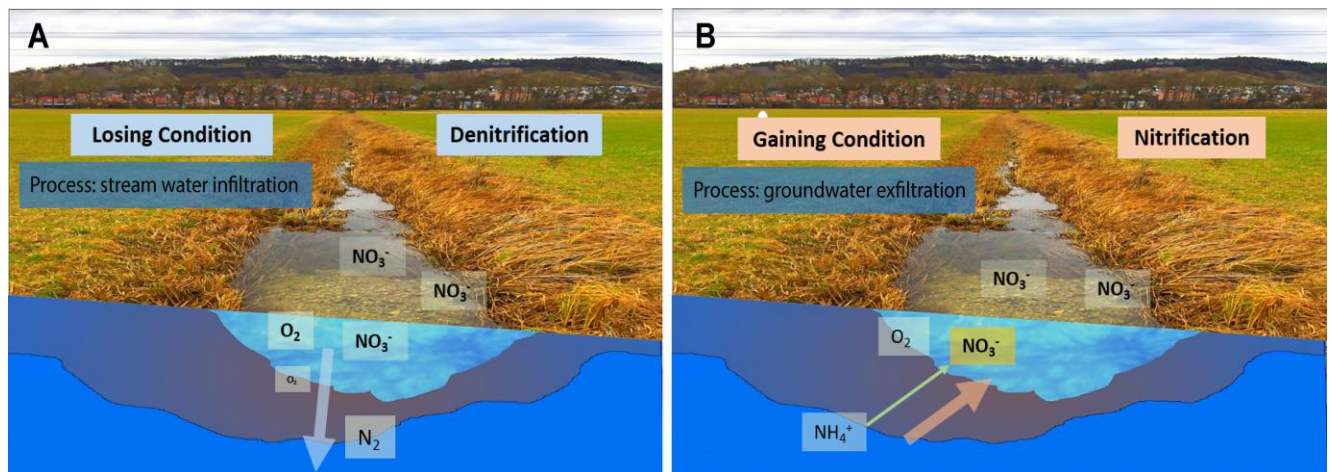


Fig. 1.4: Conceptual illustration of the impact of bidirectional water exchange on nitrogen transformations in the streambed. (A) Stream water losing condition and stream water infiltration process. (B) Stream water gaining condition and groundwater exfiltration process.

This bidirectional water exchange can substantially influence the biogeochemistry of the stream, depending on the local availability of electron donors, such as organic carbon, reduced iron and/or sulfur species in the sediment. Reactive hot-spots for denitrification may thus be generated in the streambed especially in stream water infiltration areas (Trauth et al. 2018). The stage of the stream can rise higher than the surrounding aquifer, which can lead to the infiltration of stream water into the groundwater Fig. 1.4 (A). In this scenario, the stream water, which is rich in nitrate, brings oxygen into the streambed and induces aerobic respiration. Once the water reaches deeper depths and the anoxic zone, denitrification might then be stimulated. In contrast, a decline in the stream water stage can trigger groundwater exfiltration into the stream Fig. 1.4 (B). In such a scenario, anoxic groundwater that is rich in ammonium can reach the oxic surface of the streambed and trigger nitrification, resulting in the release of secondary nitrate back into the stream. Although the importance of this secondary nitrate loading in agricultural streams remains unclear, it is another environmental concern and should not be overlooked (Peterson et al. 2001; John H. Duff and Triska 2000; Storey, Williams, and Fulthorpe 2004). Additionally, the impact of oxygen and redox

gradients, as affected by stream water infiltration and groundwater exfiltration, on the partitioning of reactivity in the streambed remains sparsely addressed.

1.8 Assembly of streambed microbial communities

As streambed microbial communities are one of the primary drivers of pollutant turnover in the stream, it is essential to further investigate the ecological mechanisms structuring their composition and distribution in the streambed. The assembly of microbial communities in the streambed of lower-order streams may also be impacted by bidirectional water exchange, but has not been addressed to date.

Typical factors affecting community assembly can be divided into two categories: deterministic and stochastic processes (Stegen et al. 2012; 2015). Deterministic processes can force the community composition to develop in two opposite major ways, homogeneous selection and variable selection (Fig. 1.5). As the term suggests, homogeneous selection forces communities to become more similar to each other. In contrast, variable selection induces the formation of more distinct community endpoints. Environmental filtering (abiotic) and interspecies interactions (biotic) (e.g., antagonistic and synergistic interactions) are considered as deterministic processes (Stegen et al. 2012). In accordance, communities affected by the same environmental conditions should be expected to become more similar over time (Fillinger, Hug, and Griebler 2019). Within stochastic processes, homogenizing dispersal and dispersal limitation lead to more similar and dissimilar communities, respectively, regardless of environmental and interspecies conditions. Homogenizing dispersal suggests that microorganisms within a community can freely move to another environment and become part of the local community there, for example, due to dynamic hydrological processes and/or connectivity (Stegen et al. 2013). On the contrary, dispersal limitations indicate that communities are unable to interact or move to a more favorable environment, for example, due to insufficient hydrological connectivity between two niche spaces (Fillinger,

Hug, and Griebler 2019). Apart from these two characterized categories, there is a third category including all undominated processes that can also affect communities. It is often the case that either deterministic selection or stochastic dispersal is not strong or consistent enough to reshape microbial communities (Stegen et al. 2015).

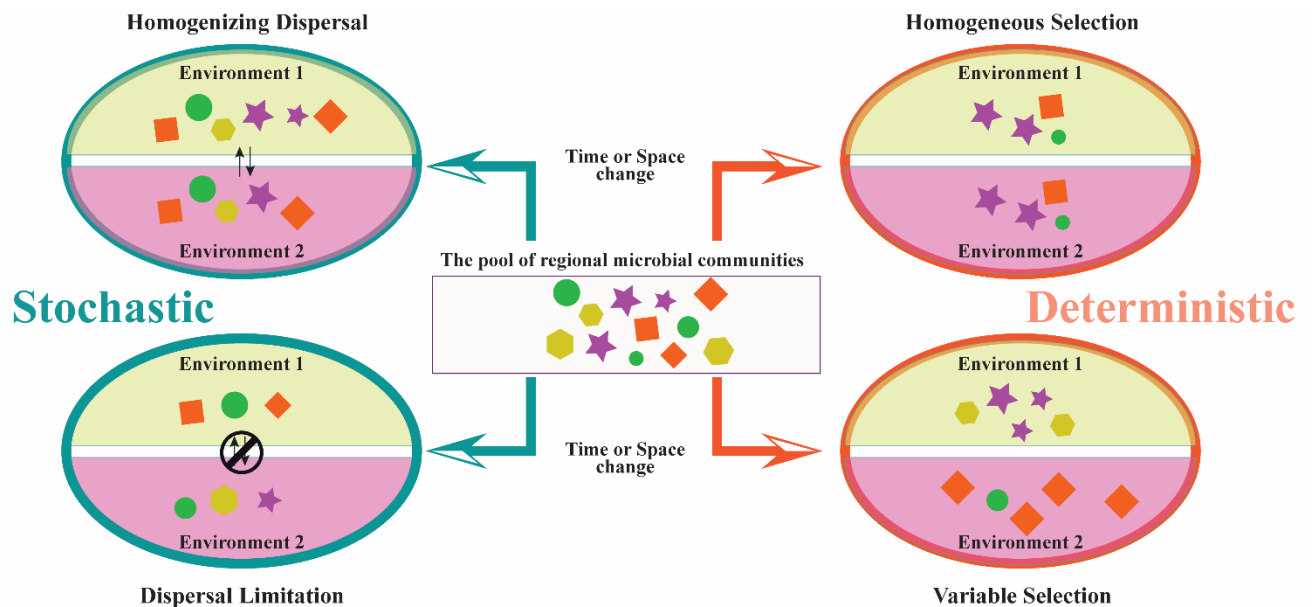


Fig. 1.5: Schematic illustration of microbial community assembly processes investigated in the dissertation. Microbial communities from two environments affected homogeneous selection process become more similar regardless of the space distance. In contrast, variable selection results in two different community compositions in two environments regardless of the space distance. Homogenizing dispersal leads to two more similar communities likely due to the connectivity between two environments, whereas dispersal limitation leads to two more different communities likely due to poor connectivity between two environments.

The analysis of community assembly processes has become a mainstream aspect in microbial ecology studies, especially after the advancement of high-throughput sequencing (Zhou and Ning 2017; Lindström and Langenheder 2012). In addition, the development of a series of null models (detailed in section 2.1.5) has allowed to quantitatively determine whether communities are structured via deterministic or stochastic processes (Stegen et al. 2013; 2012; Zhou and Ning 2017). Therefore, such analysis allow studies conducted in

different environmental systems to become comparable, and further deepen our understanding of microbial community assembly and dispersal in natural habitats.

A number of studies have been addressing microbial community assembly in rivers and streams. Results from these studies report, that sediment microbial communities are typically distinct to those found in the surrounding water bodies, suggesting a depth-dependent stratification in alluvial aquifers (Saup et al. 2019; Danczak et al. 2016; E. B. Graham et al. 2017). Particularly, variable selection was suggested for microbial communities in deeper sediment depths (e.g., deeper than 50 cm). Instead, homogenizing selection was reported in the shallow depths, as microbial communities were very similar to those found in the river water, evidencing the impact of hyporheic flow (E. B. Graham et al. 2017). For example, when organic carbon is delivered to the hyporheic zone, heterotrophic groups are often stimulated leading to the overall similarity between river water and streambed communities (Briggs et al. 2015). Longitudinally, successions in microbial community structure have been investigated from headwaters to large rivers and even estuaries, and are taken to reflect local stream characteristics, landscape type, and anthropogenic impact (Crump et al. 2004; Hullar, Kaplan, and Stahl 2006; Winter et al. 2007; Battin et al. 2008; Liao et al. 2019; Stegen et al. 2016). Moreover, stochastic assembly may likely be directly induced by hydrologic transport, including inconsistent hydrologic mixing and interstitial flow (E. B. Graham et al. 2017; E. B. Graham and Stegen 2017). In this dissertation, I have applied null models of community assembly to the streambed samples taken from the Schönbrunnen, in order to gain a better understanding of the impact of agricultural activities and bidirectional water exchange on the assembly of streambed microbial community, as these questions have yet to be fully clarified.

1.9 Molecular approaches to dissect streambed microbiomes

Interrogating the distribution, diversity, and biogeochemical importance of complex microbial communities in the environment may require a polyphasic and cultivation-independent approach. A reliable and popular technology often applied to interrogate environmental microbial communities is high-throughput sequencing (Taberlet et al. 2012). Previous studies have employed high-throughput sequencing techniques, such as 454 pyrosequencing (H. Kim et al. 2018; Lin et al. 2012) and Illumina-based sequencing (Ward et al. 2019; Stegen et al. 2018; Nelson et al. 2019; Staley et al. 2013), to investigate microbial communities in higher-order streams and/or rivers. Through examining 16s rRNA gene sequences, these studies have generated deep sequencing data on microbial communities within the hyporheic zone. In contrast, hyporheic zone microbial community structure analysis using denaturing gradient gel electrophoresis (DGGE) (Feris et al. 2003; Hamonts et al. 2014) or terminal-restriction fragment length polymorphism (T-RFLP) (Febria et al. 2012), which are relatively more labor-intensive, were unable to provide proper resolution to identify and quantify specific microbial populations. More recent studies have used Illumina-based sequencing to interrogate lower-order stream microbiomes by targeting 16S rRNA genes (Laperriere et al. 2020; Caillon et al. 2021; E. F. Jones et al. 2020; Michaels et al. 2022; Saup et al. 2019). These studies have investigated the overall response of microbial communities to environmental stressors, and identified changes in diversity and composition at the community level. However, none of these study sites were conducted in an agricultural subcatchment, and many did not perform analysis to trace specific functional capacities of microbial communities.

More powerful long-read high-throughput sequencing technologies, such as sequencing platforms developed by Pacific Biosciences (PacBio) or Oxford Nanopore, have been applied also in the microbial ecology field (Albertsen 2023; Karst et al. 2021). These

long-read sequencing techniques now allow for the generation of much longer reads than Illumina-based sequencing (Fig. 1.6B). This also enables long-read amplicon sequencing of full-length 16S rRNA gene and other functional gene amplicons (Z. Wang et al. 2022; Lam et al. 2020; B. Zhu et al. 2020; Sachs et al. 2022; Jakus, Blackwell, Osenbrück, et al. 2021). Results obtained from long-read sequencing platforms can offer superior phylogenetic resolution to Illumina-based sequencing (short-read) for detecting specific taxa in a complex community, and can also overcome primer bias (Lam et al. 2020). The sequencing strategy used by PacBio platforms, as utilized also in this dissertation, is the single-molecule real-time (SMRT) sequencing approach (Eid et al. 2009). After generating amplicons of the target gene, the preparation of PacBio SMRTbell libraries first ligates adapters to double-stranded DNA, resulting in a circular template (Fig. 1.6A) (Goodwin, McPherson, and McCombie 2016). This single molecule of DNA template is then placed inside a SMRT Cell, which contains millions of tiny wells known as zero-mode waveguides (ZMW). The polymerase is fixed to the bottom of each well and focuses on a single molecule of DNA, incorporating labelled nucleotides in a process that emits light that will be detected in real-time. Under the Circular Consensus Sequencing (CCS) mode of a PacBio platform, as used in my project, each DNA template will then be sequenced multiple times, as the polymerase repeatedly moves along the circular template inside the well. These repeatedly generated reads are then aligned and analyzed by algorithms provided by the manufacturer, to generate a highly accurate consensus read (Fig. 1.6A).

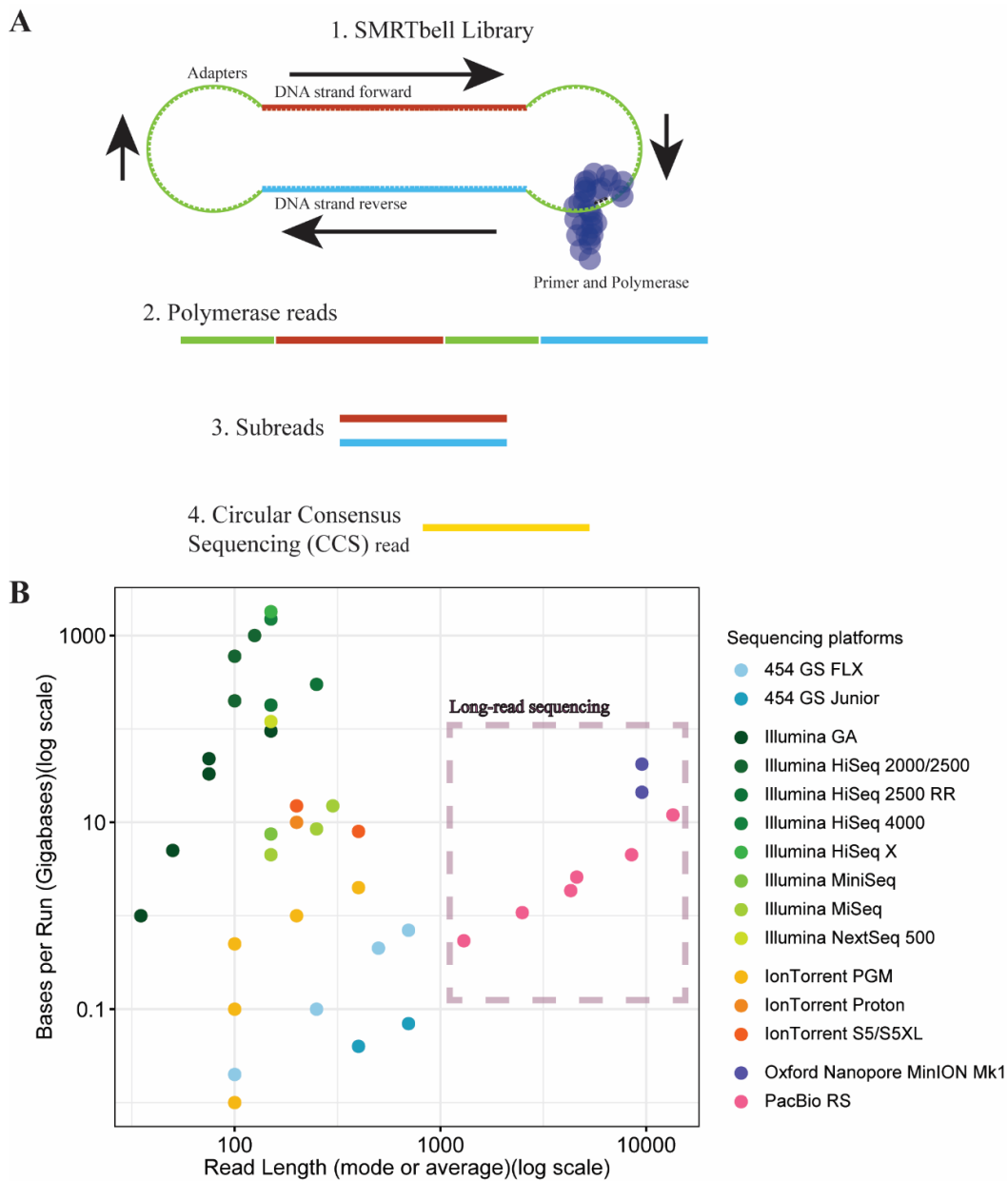


Fig. 1.6: Conceptual overview of PacBio long-read amplicon sequencing starting from the (A) library preparation; (B) presented throughput metrics for different sequencing platforms since their first instrument version came out. (B) is adapted from the online report (Nederbragt 2016). Data (until the year 2016) for (B) was acquired from the same source.

Furthermore, Oxford Nanopore sequencing detects DNA composition of a single-strand DNA template instead of monitoring incorporation process. Each nanopore senses multiple bases at one time. Disruption of ionic current when a nucleotide passes through the nanopore will be recorded (Goodwin, McPherson, and McCombie 2016). Despite the advantages mentioned above, results generated via amplicon sequencing often lack a more

detailed functional interpretation, especially for the large proportion of microbial lineages that remain uncultured and poorly characterized.

Next to amplicon sequencing, shotgun metagenomics can theoretically access the full genetic repertoire of microorganisms present in a given sample and provide valuable functional insights. The so-called metagenomic assembly employs computational processes to reconstruct genes and genomes from massed sequencing reads, allowing to predict ecological potentials and metabolic pathways of single microorganisms (Olson et al. 2018). A genome reconstructed in such way is known as a metagenome-assembled genome (MAG). Abundant overlapping sequence reads among short Illumina reads are important for reconstructing a single high-quality MAG (Du and Liang 2019). However, there are often gaps in between contigs of short sequence reads, which can negatively affect the quality and reliability of assembly (Overholt et al. 2020).

Long-read sequencing technologies from Oxford Nanopore and Pacific Biosciences can make assembly processes more reliable, especially for environmental samples with extremely complex microbial communities. Combining Oxford Nanopore sequencing with classical short-read sequencing (Illumina platforms) for terrestrial subsurface samples has been reported to produce meaningful ecological insights (Overholt et al. 2020). This so-called hybrid assembly approach, which was also applied in my project, employs longer sequence reads generated from an Oxford Nanopore platform as a backbone scaffold, to more reliably map much “deeper” short-read sequences, to improve the quality of the assembly. The more complete and higher quality the MAGs, the more likely they are to contain complete sets of ecophysiological informative genes, as well as copies of 16S rRNA genes. Thus, linking the functional potential of specific uncultivated microbes to specific lineages detected via amplicon sequencing becomes possible. To date, only few studies have employed a genome-

resolved metagenomics approach to investigate functional potentials of riverbed and/or streambed microbiota (Rodríguez-Ramos et al. 2022; S. Liu et al. 2020; Black and Just 2018).

Aims of the dissertation

The aim of this dissertation was to elucidate how local hydrological processes affect the distribution, diversity, and function of streambed microbiomes at the interface between an agricultural lower-order stream and adjacent groundwater. These main objectives are developed with a main focus on microbial N cycling, as outlined in three major objectives below:

The first study conducted at the Schönbrunnen subcatchment aimed at characterizing the diversity and distribution of streambed microbiota, especially typical nitrate-reducing lineages, under the impact of bidirectional water exchange. To date, studies on structural patterns of microbial communities in sediment of agricultural impacted lower-order streams remain scarce, especially in a dedicated hydrologic perspective. I addressed this research gap by interrogating sedimentary bacterial communities via qPCR and PacBio full-length 16S rRNA gene amplicon sequencing, combining with extensive hydrological dataset. Long-read amplicon sequencing was chosen to provide more reliable phylogenetic resolution on possible taxon distribution patterns associated with local hydrology characteristics. I posit that typical hydrological and geochemical parameters alone are not sufficient for understanding nitrate reduction mechanisms in such systems, and explicitly address the interplay of hydrological and microbial process controls (Harvey et al. 2013; Mulholland et al. 2008). In this first part of the dissertation, I hypothesized that sediment microbial communities along successive net gaining and losing sections of the first-order stream are distinct, and impacted by local hydrology. Especially, bidirectional water exchange fluxes can impact the distribution and diversity of nitrate-reducing populations. The results of this first study have already been published (Z. Wang et al. 2022).

Wang, Zhe, Oscar Jimenez-Fernandez, Karsten Osenbrück, Marc Schwientek, Michael Schlöter, Jan H. Fleckenstein, and Tillmann Lueders. "Streambed microbial communities in the transition zone between groundwater and a first-order stream as impacted by bidirectional water exchange." Water Research 217 (2022): 118334. <https://doi.org/10.1016/j.watres.2022.118334>

The second study investigated nitrifying-microorganisms in the Schönbrunnen streambed. To date, only few studies have focused on nitrification in agricultural impacted lower-order streams (Peterson et al. 2001; Arango and Tank 2008; Strauss and Lamberti 2002). More importantly, none of these studies were focused on ammonia-oxidizing communities, or have dissected the contribution of archaeal versus bacterial ammonia oxidizers to net ammonia turnover. A microcosm incubation experiment was conducted to investigate the growth and abundances of AOA and AOB, and a population-based reaction model was subsequently built by the CAMPOS consortium on the incubation results to address these knowledge gaps. Understanding the nitrification in context of the interaction between stream and groundwater is relevant to understanding the sources of nitrate, as anoxic groundwater exfiltration might induce secondary nitrate loading via nitrification. I hypothesize that the contribution of AOB and AOA may vary along the stream, due to local hydrological heterogeneities. I further hypothesize that the abundance of *amoA* genes *in-situ* alone may not be sufficient to understand population-specific contributions in such settings. This study combined activity- and modelling-based approaches to evaluate population-specific (i.e. members of AOA or AOB) contributions to nitrification in the streambed. By taking samples from disparate stream depths and segments and by setting up microcosm incubations, streambed ammonia oxidizers were exposed to a pulse of ammonia. Population-specific contributions were disentangled by applying chemical inhibitors (i.e. acetylene and 1-octyne), and confirmed by a population-based reactive process modeling, together with scientific collaborators of the CAMPOS project. The manuscript related to this study has been submitted and is currently under review.

The third study of the dissertation aimed to more comprehensively unravel the interactions between streambed nitrogen and sulfur cycling, and functional potentials of streambed communities. From the first study, chemolithoautotrophic nitrate reduction driven by the oxidation of reduced sulfur species has been suggested to play an important role in

certain sections of the Schönbrunnen streambed (Z. Wang et al. 2022). Both *Sulfuricurvum* and *Thiobacillus* spp. presented to be abundant but their capacity to either fully oxidize sulfide to sulfate or to canonically reduce nitrate to dinitrogen remains unclear. This was to be further elucidated using genome-centric metagenomics, and a long-read assisted hybrid sequencing and assembly approach. I posit that a complex network of “metabolic hand-offs” and shared energy conservation pathways may be relevant in microbial N- and S-cycling in the Schönbrunnen streambed. In addition, the metabolic capacities of diverse but abundant populations of the streambed remain unknown. Here, I aim to identify microbial populations capable of either complete canonical denitrification, partial denitrification, or DNRA. Biochemical pathways, functional gene abundance, as well as its contributing species were analyzed. Additionally, metagenome-assembled genomes (MAGs) were reconstructed to provide key functional insights for some of most abundant populations of the streambed, and to further elaborate on the ecological functions of the streambed microbiota as impacted by the bidirectional water exchange.

2 MATERIALS AND METHODS

2.1 Methods for nitrate-reducing microbial populations in the Schönbrunnen streambed as impacted by bidirectional water exchange

2.1.1 Site description

The Schönbrunnen stream (48.32°N latitude and 8.57°E longitude) is a first-order stream located in a predominantly agricultural area. It is a tributary of the second-order Käsbach stream, within the Ammer catchment in the west of the city of Tübingen, Germany (Fig. 2.1.1). Both hydrology and hydrochemistry of the site (Table 2.1.1) have been comprehensively described recently (Jimenez-Fernandez et al. 2022). The studied section of the stream has a length of approximately 550 m, a mean discharge of approximately 1 L s^{-1} , and drains an area of approximately 1 km^2 . The mean stream water depth varies between 5 and 13 cm. The stream section runs in the Käsbach valley, mainly filled with fine alluvial quaternary sediments overlying the geological unit of the Lower Keuper (Erfurt-Formation), dolomites, sand- and claystones, which act as the primary bedrock. Along the eastern hillslopes, the Lower Keuper is overlain by the Grabfeld-Formation of the Middle Keuper. This formation contains thick gypsum units interspersed with dolomite and limestone banks and forms a local aquifer draining hillslope groundwater towards the alluvial groundwater system (D’Affonseca, Finkel, and Cirpka 2020). The eastern hillslope groundwater exhibits higher sulfate concentrations than the alluvial groundwater. During this study, the majority of the surrounding area of the studied Schönbrunnen section was covered by meadows due to crop and fallow rotation, with the exception of the northwestern area, which was utilized as farming- and pasture-land.

Table 2.1.1: Water chemistry and hydrology of Schönbrunnen stream water and adjacent groundwater.

Sampling locations	Hydraulic conductivity K _f [m/s]	Q [L/s]	Water mixing		EC [μS/cm]	DOC [mg/L]	Na ⁺ [mg/L]	K ⁺ [mg/L]	Ca ²⁺ [mg/L]	Mg ²⁺ [mg/L]	NH ₄ ⁺ [mg/L]	NO ₃ ⁻ [mg/L]	Cl ⁻ [mg/L]	SO ₄ ²⁻ [mg/L]
			% Stream	% GW										
Schönbrunnen stream														
<i>Up-A</i>	-	0.11	0	100	1032	1.2	4.6	1.4	168	45.3	0	59.0	18.8	191
<i>Up-B</i>	-	0.57	-	-	1015	1.4	5.0	1.6	162	46.0	0	60.5	18.2	179
<i>Mid-A</i>	-	-	-	-	-	-	-	-	-	-	-	-	-	-
<i>Mid-B</i>	-	0.31	88.1	11.9	930	1.7	4.8	1.6	143	46.7	0	58.9	17.9	179
<i>Down</i>	-	-	-	-	1099	1.0	7.8	2.5	179	45.0	0	42.0	27.3	237
<i>Conf</i>	-	-	-	-	2280	1.6	18.7	6.9	512	78.8	0	31.0	38.2	1123
Groundwater (GW)														
GWS 2	2.9E-04	-	-	-	1035	1.4	4.6	1.3	168	45.1	0	64.4	19.8	201
GWS 7	5.9E-06	-	-	-	983	2.5	5.4	0.3	157	47.3	0	6.4	16.8	195
GWS 12	5.7E-04	-	-	-	956	1.3	4.8	1.5	153	47.0	0	16.6	16.5	183
GWS 15	8.0E-06	-	-	-	970	3.1	4.8	0.8	167	39.9	0.6	3.3	17.5	209
GWS 16	8.6E-04	-	-	-	780	1.9	4.9	0.8	120	35.2	0	3.1	21.7	65
GWS 23	7.1E-04	-	-	-	1004	2.8	5.0	0.7	160	47.5	0	2.8	15.6	122
GWS 25	1.8E-04	-	-	-	1950	7.1	10.3	7.0	383	63.9	3.7	4.9	33.8	409

* DOC and major ions are given as mean values of samples collected on several dates in summer.

* Original data were measured by Oscar Jimenez-Fernandez and Karsten Osenbrück within the CAMPOS project.

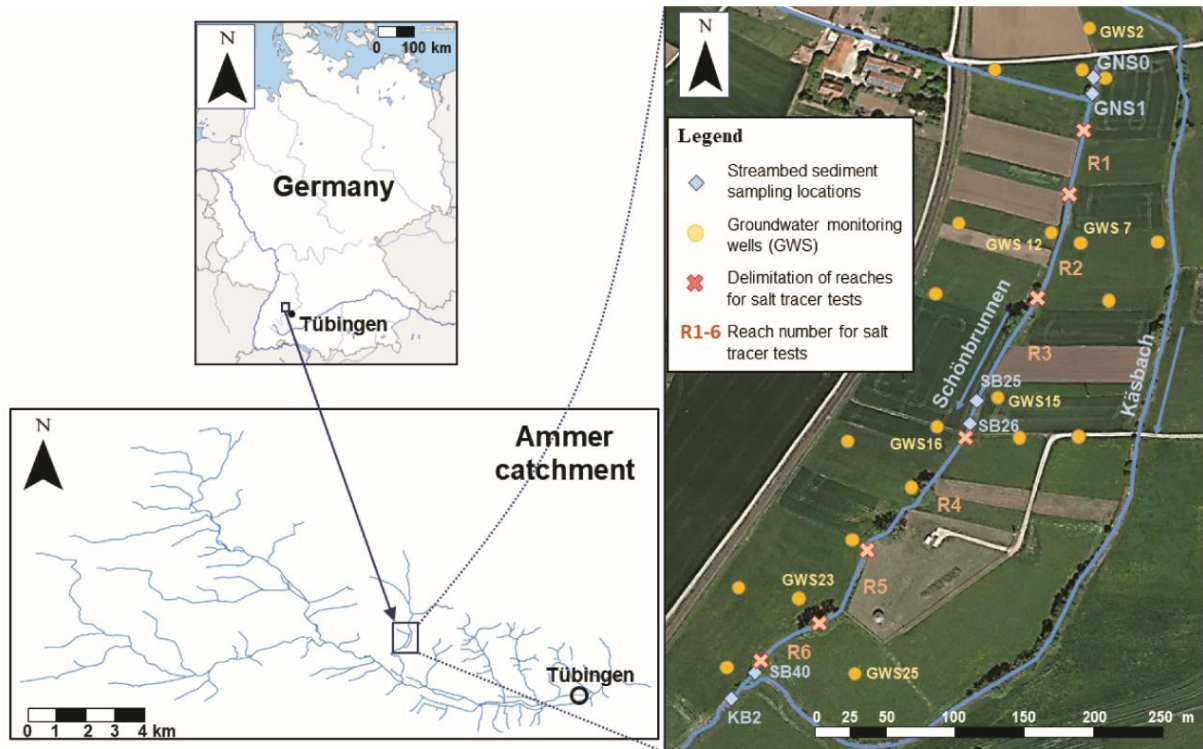


Fig. 2.1.1: Location of the first-order stream Schönbrunnen in the Ammer catchment near Tübingen, Germany. Sediment sampling locations and groundwater monitoring wells are indicated with respective symbols. These are: *Up-A* - GNS0, *Up-B* - GNS1, *Mid-A* - SB25, *Mid-B* - SB26, *Down* - SB40, *Conf* - KB2. Successive hydraulic reaches of the stream as delineated by tracer tests are indicated as R1 – R6 (Jimenez-Fernandez et al. 2022).

Table 2.1.2: Sediment sample codes according to the standardized Schönbrunnen project database.

Project site code for hydrology monitoring	Sediment sample code
GNS0	<i>Up-A</i>
GNS1	<i>Up-B</i>
SB25	<i>Mid-A</i>
SB26	<i>Mid-B</i>
SB40	<i>Down</i>
KB2	<i>Conf</i>

The streambed sediment is comprised of silty, clayey, and loamy materials. Hydraulic parameters of groundwater were calculated by performing a series of two slug tests per groundwater monitoring well (done by the project consortium). The hydraulic conductivity (k_f) of the streambed sediments was calculated by tracing a perpendicular line to groundwater

flow direction on the head contours maps. By assessing the influence of the stream on the mean groundwater levels, the hydraulic head differences (Δh) were defined at a given distance (Δl). Groundwater discharge (Q) was taken from the results of a series of tracer tests (Jimenez-Fernandez et al. 2022). Defining a fixed sediment area within each of the tracer test reaches, the hydraulic conductivity for each reach was determined. This parameter was assumed remain constant alongside the studied stream section. The permeability value (K) of the streambed was between 10^{-7} to 10^{-9} $\text{cm}^2 \cdot \text{s}^{-1}$ according to hydraulic conductivity (k_f) (Table 2.1.1) calculated using the equation below:

$$K = k_f \cdot \frac{\eta}{\rho \cdot g} \quad (1)$$

where η = dynamic viscosity was 10^{-3} Ps at 10°C , ρ = mass density of water, g = gravitational acceleration.

2.1.2 Sediment sampling

Stream sediments were collected in August 2017 at selected locations along the Schönbrunnen stream (Fig. 2.1.1 & Table 2.1.2) by taking sediment push-cores using a stainless steel piston corer (Eijkelkamp, Giesbeek, Netherlands). There had not been any major precipitation events (< 5 mm) one week preceding the sampling campaign (Agrometeorology of Baden-Württemberg 2017). After coring, sediments were dispensed onto clean plastic furrows, and sediment subsamples were collected using sterile spatula at two distinct sediment depths (5 cm and 15 cm below streambed surface). Replicate cores were taken within ~ 30 cm distances from the first core to minimize lateral disturbances.

Subsamples were stored in sterile 50 mL PE tubes (Fisher Scientific GmbH, Schwerte, Germany) and cooled during immediate transport back to the lab, then stored at -80°C until further processing. Some fresh sediment cores (~ 25 cm in length) were also stored in sterilized glass cylinders in duplicates, covered with 5 cm of stream water, before transport to

the 15 °C sample storage room in the lab, which was similar to the average stream water temperature 13.2 °C during the sampling month.

2.1.3 Hydrological description and water chemistry.

The interaction between the stream and adjacent groundwater of the site, and the hydrologic turnover were quantified by repeated field measurements and tracer tests done between summer 2017 and summer 2018 (Jimenez-Fernandez et al. 2022). In brief, the Schönbrunnen stream was divided into six reaches (R1 – R6) characterized by distinct and seasonally variable net water gains or losses to or from the stream, respectively (Fig. 2.1.1 & Fig. 2.1.2). Water exchange fluxes in the summer season were characterized by net gaining conditions in the further upstream of the reach R1 (major water source of the Schönbrunnen owing to the spring), generally net losing but locally variable conditions in midstream R2 to R4, and again mostly gaining but locally variable conditions in downstream R5 and R6 (Fig. 2.1.2A). However, gross water fluxes in both directions (infiltration and exfiltration) occurred in all reaches. These reach-scale exchange fluxes had been further investigated with salt tracer tests (Jimenez-Fernandez et al. 2022). Gaining conditions were relatively more important in downstream R5 and R6, whereas locally variable but generally net losing conditions were observed in midstream reaches (R2 and R4). For R3, salt tracers indicated a similar magnitude of stream water gaining and losing fluxes (Fig. 2.1.2A).

Water samples for major ions and DOC (dissolved organic carbon) analyses were obtained from the stream and the surrounding network of groundwater monitoring wells in August 2018. For both stream and groundwater samples, 100 mL and 25 mL samples were taken in glass bottles and filtered through 0.45 µm filters (MillexHA, Darmstadt, Germany) within 48 hours for the analysis of major ions and DOC, respectively. The samples were kept at 4°C in the dark upon analysis. Major ions were determined by the project consortium on an ion chromatography (Dionex DX 500, Thermo Fisher Scientific, Waltham, MA, USA; LOQ =

0.1 mg/L for chloride and nitrate, and 0.3 mg/L for sulfate). The DOC sample's pH was adjusted to 2 and measured on a TOC analyzer (elementar HighTOC, Langenselbold, Germany).

At selected locations, sediment porewater was sampled using mini piezometers (≤ 2.5 mL min⁻¹) with depth differentiation (0-30 cm below streambed) (Fig. S1) (J. H. Duff et al. 1998). All samples were filtered and kept at 4 °C in the dark until further analysis as mentioned above. Stream water electrical conductivity (EC) was monitored using vented pressure transducers integrated in CTD probes with data loggers (UIT GmbH, Dresden, Germany) which were installed *in situ*. Groundwater EC ($\pm 0.5\%$ of value; temperature compensation to 25°C) was measured in the field by hand-held probes (WTW GmbH, Weilheim in Oberbayern, Germany). The assessment of other parameters, including discharge Q, water mixing ratios, and groundwater heads, were described in an accompanying study of the project consortium (Jimenez-Fernandez et al. 2022). In brief, the discharge rate (Q) was determined by utilizing the documented water level data and applying the following equation (Henderson 1966):

$$Q = \frac{8}{15} C \sqrt{2g} \tan \frac{\theta}{2} h^{\frac{5}{2}} \quad (2)$$

where Q is discharge (L/s), C is a non-dimensional runoff coefficient, g is the gravitational acceleration, θ is the angle degree included between the sides of the V-notch weir, and h is the pressure head (m) which corresponds to the height of the upstream water surface in relation to the vertex of the V-notch weir. Water mixing ratios were calculated based on the endmember mixing analysis, which took in to account the stream discharge (Q), and the local variable sulfate concentrations, used in the calculation as a tracer to indicate the groundwater contribution. Moreover, contours of groundwater heads were generated using interpolation (natural neighbor) of hydraulic head data collected from monitoring wells installed at the Schönbrunnen study site (Fig. 2.1.1).

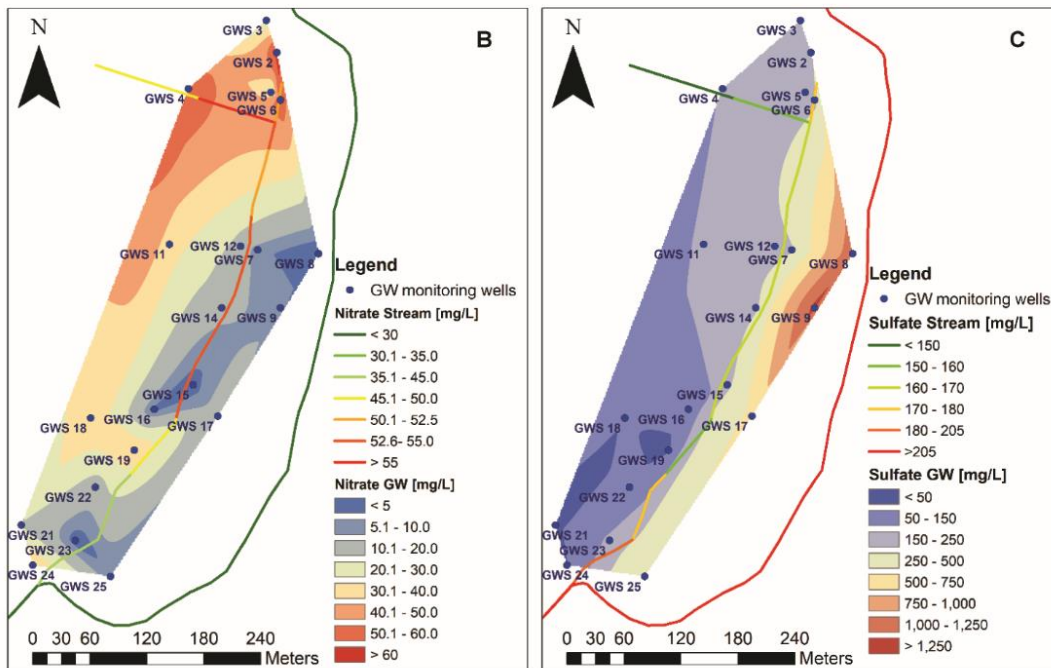
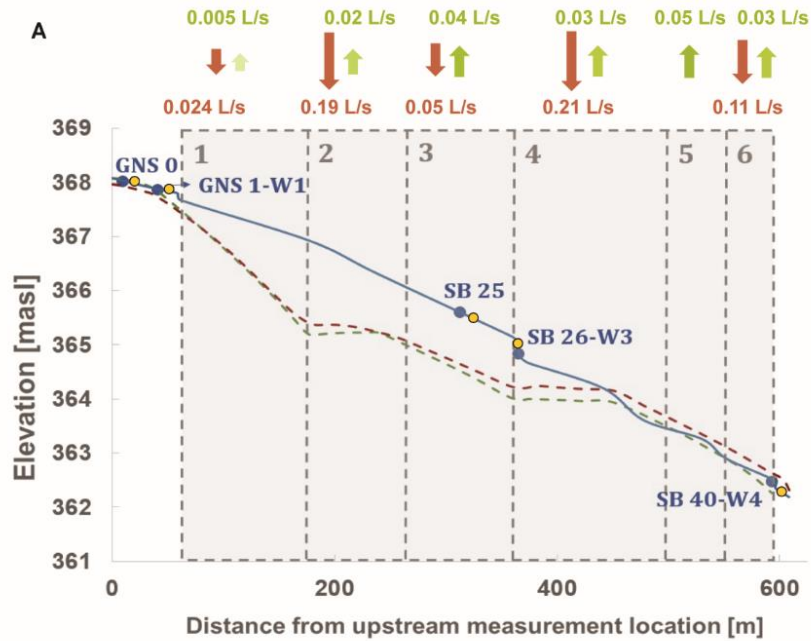


Fig. 2.1.2: Stream-groundwater exchange fluxes, and maps of nitrate and sulfate concentration. (A) Stream-groundwater exchange fluxes, stream water elevation, and groundwater heads of the Schönbrunnen site. *Data were provided by the project consortium and are necessary to describe the setting of the site investigated in the dissertation (Jimenez-Fernandez et al. 2022).* Numbers suggest gross bidirectional stream-groundwater exchange fluxes determined by tracer tests. The length of the arrows indicates the magnitude of stream water gain (green color) and loss (red color). The plot shows stream water elevation and groundwater heads. The blue color line represents the stream water stage. The two dashed lines represent groundwater head elevations 10 meters away from the Schönbrunnen, from either the western side (blue color) - or the eastern side (green color). The head elevations were extracted from the interpolated groundwater contour map (Jimenez-Fernandez et al. 2022). V-notch weirs installed in the field are shown as blue dots. Locations for sediment sampling are shown as yellow dots. (B) Contour maps of concentrations of nitrate and (C) sulfate mapped for both stream and groundwater of the Schönbrunnen and Käsbach catchment in summer 2018.

2.1.4 Nucleic acid extraction and 16S rRNA gene amplicon sequencing

Samples from replicate sediment cores of each location and depth were homogenized before further processing. Genomic DNA of sediment samples was extracted as described elsewhere (Pilloni et al. 2012) with minor modifications (all was done at 4 °C). In brief, sediment samples were first subjected to bead beating to mechanically disrupt cells, followed by lysis using lysozyme and proteinase K. The nucleic acid was then extracted using a phenol-chloroform-isoamyl alcohol method. In practice, about 0.6 g wet sediment was used for each DNA extraction, and DNA was extracted in triplicates from each sample. DNA quality and quantity in extracts was determined with agarose gel electrophoresis and by using the Quant-iT PicoGreen dsDNA Assay Kit (Thermo Fisher, Waltham, USA) on an MX3000p cyclor (Agilent, Santa Clara, USA).

For full-length 16S rRNA gene sequencing, a two-step PCR was performed. The first amplification was done with the KAPA HiFi HotStart PCR Kit (Kapa Biosystems, Boston, MA, USA) and universal primers for the bacterial 16S rRNA gene (forward and reverse) tailed with PacBio universal sequence adapters (Table 2.1.3).

Table 2.1.3: Universal primer set used for amplifying the full-length 16S rRNA gene from each sediment sample.

Primer	5' Block	PacBio universal sequence adapters	16S rRNA gene primer
*27F:	/5AmMC6/	gcagtcgaacatgtagctgactcaggtcac	AGRGTTYGATYMTGGCTCAG
**1492R:	/5AmMC6/	tggatcactgtgcaagcatcacatcgtag	RGYTACCTTGTTACGACTT

Each 25 µl PCR reaction contained 1x KAPA HiFi GC buffer, 0.3 mM dNTPs, 0.3 µM of each forward and reverse primer, 0.03 U KAPA HiFi Hot Start DNA polymerase, and ~2 ng template DNA. PCR involved 30 cycles of denaturation at 95 °C for 30 s, annealing at 57 °C for 30 s, and extension at 72 °C for 60 s. Products of the PCR amplification were purified with the MicroElute® Cycle-Pure Kit (Omega Bio-Tek, Georgia, USA), following the manufacturer's instructions. The quality and concentration of purified PCR products was

confirmed on a Fragment Analyzer 5200 System (Agilent, Santa Clara, CA, USA), using a DNF-473 NGS Fragment Analysis Kit (1-6000bp) (Advanced Analytical Technologies, Ames, IA, USA). The subsequent second PCR reaction included, also in 25 µl, 1x KAPA HiFi GC buffer, 0.3 mM dNTPs, 0.24 µM of PacBio barcoded Universal F/R primers (PacBio, Menlo Park, CA, USA), 0.02 U KAPA HiFi Hot Start DNA polymerase, and 0.05 ng template DNA. The cycling conditions were identical to the first PCR reaction, but with 20 cycles only. The PCR products from the second amplification were purified with AMPure PB beads (PacBio, Menlo Park, CA, USA) according to the manufacturer's instructions. The quality and concentration of purified PCR products was checked on an Agilent 2100 Bioanalyzer system (Agilent, Santa Clara, CA, USA). Sequencing library construction was performed utilizing the SMRTbell® Template Prep Kit 1.0, following the PacBio documentation “Procedure & Checklist – Amplification of Full-Length 16S Gene with Barcoded Primers for Multiplexed SMRTbell Library Preparation and Sequencing” (version June, 2018) (Callahan et al. 2019). The sequencing of the libraries was performed using a PacBio Sequel platform at the Research Unit for Comparative Microbiome Analyses, Helmholtz Zentrum München, Germany.

2.1.5 Sequencing data analysis

I processed raw sequencing data using the SMRTLink implemented secondary analysis platform provided by PacBio (version 6.0) to generate demultiplexed sequences and Circular Consensus Sequence (CCS) reads, which were converted to .fastq files (Table S1.1). Primers were trimmed using CUTADAPT v1.14 (Martin 2011). Reads lengths were filtered and retained by Geneious R10 (Biomatters, New Zealand) to an average range of 1400-1600 bp. Samples with a total read number <1500 were excluded (n=3) from downstream analysis. Sequence data were deposited in the European Nucleotide Archive (ENA) with the study accession number: PRJEB49634.

Sequence data were further processed in R (version 3.5.0) (R Core Team 2018) using the DADA2 (version 1.10.1) algorithms for quality filtering, generating high accuracy exact amplicon sequence variants (ASVs) with single-nucleotide resolution, and chimera removal, according to the "DADA2 + PacBio" workflow (Callahan et al. 2019). However, I did not manually discard ASVs low in abundance across all samples prior to taxonomic classification. IDTAXA Classifier (Wright 2016; Murali, Bhargava, and Wright 2018) was used with a confidence level of 50% (high) to map ASV sequences against the SILVA SSU database (release 132) for taxonomic classification (Quast et al. 2013). ASVs classified as "mitochondria", "chloroplasts", or "unclassified root" were removed. The FastTree (Price, Dehal, and Arkin 2009) algorithm was applied for generating a midpoint-rooted phylogenetic tree after ASVs sequence alignment by the DECIPHER package (version 2.12.0) (Wright 2020; 2016). Maximum likelihood phylogenetic trees were constructed for specific taxa (i.e. *Sulfuricurvum* spp. and *Thiobacillus* spp.) with MEGA-X (Kumar et al. 2018), aligned with selected reference 16S rRNA gene sequences from NCBI and IMG/M databases (I. M. A. Chen et al. 2019; Agarwala et al. 2018), using the ClustralW algorithm with default settings (1,000 bootstrap replications). Phylogenetic trees for *Sulfuricurvum* spp. and *Thiobacillus* spp. were then visualized and analyzed with iTol v6 (Letunic and Bork 2019).

I utilized raw read counts and proportions for alpha diversity and beta diversity analysis, respectively (McMurdie and Holmes 2014; Cameron et al. 2020). Alpha diversity indices, including the Shannon Index and Shannon diversity based evenness index were calculated using the Phyloseq package (version 1.28.0) (McMurdie and Holmes 2013). Differences in alpha diversity were assessed by non-parametric Kruskal-Wallis analysis in combination with Dunn's tests for multiple comparisons, and Benjamini-Hochberg correction for multiple comparisons using DescTools package (version 0.99.41) (Signorelli 2020). Bray-Curtis dissimilarities calculated to demonstrate differences in microbial community composition among samples at the family level using hierarchical clustering method (average-

linkage) and non-metric multi-dimensional scaling (NMDS) using the vegan package (version 2.5-5) (Oksanen et al. 2016). Similarity percentage analysis (SIMPER) was applied to evaluate which taxa contributed to the structural differences of two communities using the vegan package (permutations = 1000) (version 2.5-5) (Oksanen et al. 2016).

Bacterial community structure was also investigated in order to evaluate the assembly mechanisms under the impact of bidirectional water exchange in the streambed. Therefore, a two-step null model approach, taking both phylogenetic distance and abundance into consideration, was applied as first-step. This is based on the assumption that phylogenetically close taxa are more likely to have similar ecological niches (Stegen et al. 2013). We first calculated β -mean nearest taxa distance (β -MNTD) in order to quantify the phylogenetic distance of a species in one community to its closest relatives in another. β -MNTD was calculated with 999 randomizations. Then β -nearest taxon index (β -NTI), which represents the number of standard deviations between the observed β -MNTD and the mean of the null distribution, was calculated to indicate whether species in two compared communities are phylogenetically significantly more close or different than expected by chance. If $|\beta\text{-NTI}| > 2$, a significant deviation from the null distribution is assumed; indicating that species in two compared communities are phylogenetically significantly more close or distinct. Likely, this is because of deterministic environmental selection processes, such as homogeneous and variable selection. If $|\beta\text{-NTI}| < 2$, dispersal-based and other stochastic processes should be further examined. I applied the Bray-Curtis distance based Raup-Crick index (RC_{bray}) (Chase and Myers 2011) to evaluate stochastic assembly mechanisms. RC_{bray} only requires species occurrence and abundance in one community. $|\text{RC}_{\text{bray}}| > 0.95$ suggests that two communities have significantly more or less common species than expected by chance; indicating homogenizing dispersal or dispersal limitation and drift processes. $|\text{RC}_{\text{bray}}| < 0.95$ indicates drift or undominated processes. RC_{bray} was also calculated with 999 randomizations. In assembly analysis, all samples were rarefied to 1800 reads (seed = 123), the minimum number

of reads among all samples. Reads from duplicate samples were merged using the Picante package (version 1.7) (Kembel et al. 2010). Moreover, in this analysis, I omitted samples from the confluence and only applied this approach to samples with comprehensive hydrological metadata.

Correlations between gene abundances and geodesic distance were calculated using Spearman correlation and least square linear models in the R package stats (version 4.0.3), respectively (R Core Team 2018). Major packages used for data visualization include Phyloseq (version 1.34.0), ggplot2 (version 3.3.2), Tidyverse (version 1.3.0), ComplexHeatmap (version 2.7.6.1002), ggpubr (version 0.4.0), ComplexUpset (version 1.1.0) (McMurdie and Holmes 2013; Wickham 2016; Wickham et al. 2019; Gu, Eils, and Schlesner 2016; Kassambara 2021; Krassowski 2021; C. Li 2020). Phylogenetic trees for *Sulfuricurvum* spp. and *Thiobacillus* spp. were then visualized and analyzed with iTol v6 (Letunic and Bork 2019).

2.1.6 Quantitative PCR (qPCR) of bacterial 16S rRNA and nitrite reduction genes

Abundances of bacterial 16S rRNA, *nirK*, and *nirS* genes were determined via qPCR on an MX3000p qPCR System (Agilent, Santa Clara, USA). The primers used are listed in Table 2.1.4. Triplicate DNA extracts per sample were quantified in technical duplicates. For bacterial 16S rRNA genes, 40 μ L reactions consisting of 1 x Takyon SYBR MasterMix (Eurogentec, Cologne, Germany) with 0.6 μ L 50 x ROX reference dye (Thermo Fisher Scientific, Waltham, MA, USA), 0.2 μ M bovine serum albumin (BSA) (Roche Diagnostics GmbH, Basel, Switzerland), 0.3 μ M of each of the forward and reverse primer and 2 μ L of adequately diluted DNA template were used. For amplification of the nitrite reductase genes, all components were identical except that 1 x Brilliant III Ultra-Fast qPCR Master Mix (Agilent, Santa Clara, CA, USA) was used in 40 μ L qPCR reactions.

Table 2.1.4: Primer sets and annealing temperatures used for gene abundance measurements through qPCR.

Genes	Primers	Primer Sequences (5'-3')	Length of the primer	Annealing temperature
Bac. 16S rRNA (Schwieger and Tebbe 1998)	Ba519f	CAGCMGCCGCGGTAATA	17	54 °C
	Ba907r	CCGTCAATTTCCTTTGAGTTT	20	
<i>nirS</i> (Throbäck et al. 2004)	nirS-Cd3aF	G TSAACG TSAAGGARACSGG	20	58 °C
	nirS-R3cd	GASTTCGGRTGSGTCTTSAYGAA	24	
<i>nirK</i> (Henry et al. 2004)	nirK876	ATYGGCGGVCA YGGCGA	17	58 °C
	nirK1040	GCCTCGATCAGRTRRTGGTT	20	

The temperature and cycling profile for each assay were as follows: initial denaturation at 95 °C (3 min), 35 – 40 cycles of denaturation at 95 °C (30 s) , annealing at a given temperature (30 s), elongation at 72 °C (30 s), followed by a final a melting at 95 °C (30 s) and a melting curve recorded between 60 and 95 °C. Primer annealing temperature was set to 54 °C for bacterial 16S genes, and to 58 °C for *nirK* and *nirS* genes, respectively. Standardization was done via ten-fold dilution series of synthetic gene fragments (gBlocks, Integrated DNA Technologies, Leuven, Belgium) of known concentration covering all respective primer sites. For 16S rRNA genes, a 980 bp-fragment of the *E. coli* 16S rRNA gene was used. For *nirK*, a 450 bp-fragment of the respective gene of *Sinorhizobium meliloti* 1021 and for *nirS*, a 660 bp-fragment of the respective gene of *Pseudomonas stutzeri* DSM 4166 was employed. Each standard curve reached R-square value greater than 0.99 and amplification efficiency of all genes was at 100 ± 15 %. Absolute abundances of target genes were reported as copies g^{-1} of fresh sediment (g_{ww}^{-1} of sediment). Relative abundances of nitrite reductases are shown as the \log_{10} ratio of each gene to the bacterial 16S rRNA gene copies g_{ww}^{-1} of sediment.

2.2 Methods for nitrification in the Schönbrunnen streambed

2.2.1 Study site and sample collection

The study site is the same as described in section 2.1.1. Stream sediments described in this chapter were collected in June 2020 by taking sediment push-cores using a stainless-steel piston corer (Eijkelkamp, Giesbeek, Netherlands). After coring, sediments were placed onto a clean plastic furrow-shape tray for depth differentiation. Subsamples from two distinct depths (5 cm and 15 cm below surface) were collected using sterile spatula and stored in sterile 50 mL PE tubes (Fisher Scientific GmbH, Schwerte, Germany). All samples were then transported to the lab along with dry ice and processed within three days. Before the collection of sediment at the Schönbrunnen, the studied area did not experience major precipitation or flooding events within a month.

Stream water and adjacent groundwater samples were collected in 1 L glass bottles after the collection of sediment samples. Water samples were then filtered through 0.22 μm Corning™ Sterile Disposable Filter Systems (Corning Incorporated Life Sciences, Acton, MA, USA) within 48 hours. Mini piezometers (≤ 2.5 mL/min) were applied for acquiring pore-water samples from the sediment (J. H. Duff et al. 1998). All filtered samples were kept at 4 °C in the dark until further analysis by ion chromatography (Table S2.1) (done by the project consortium) (Dionex DX 500, Thermo Fisher Scientific, Waltham, MA, USA).

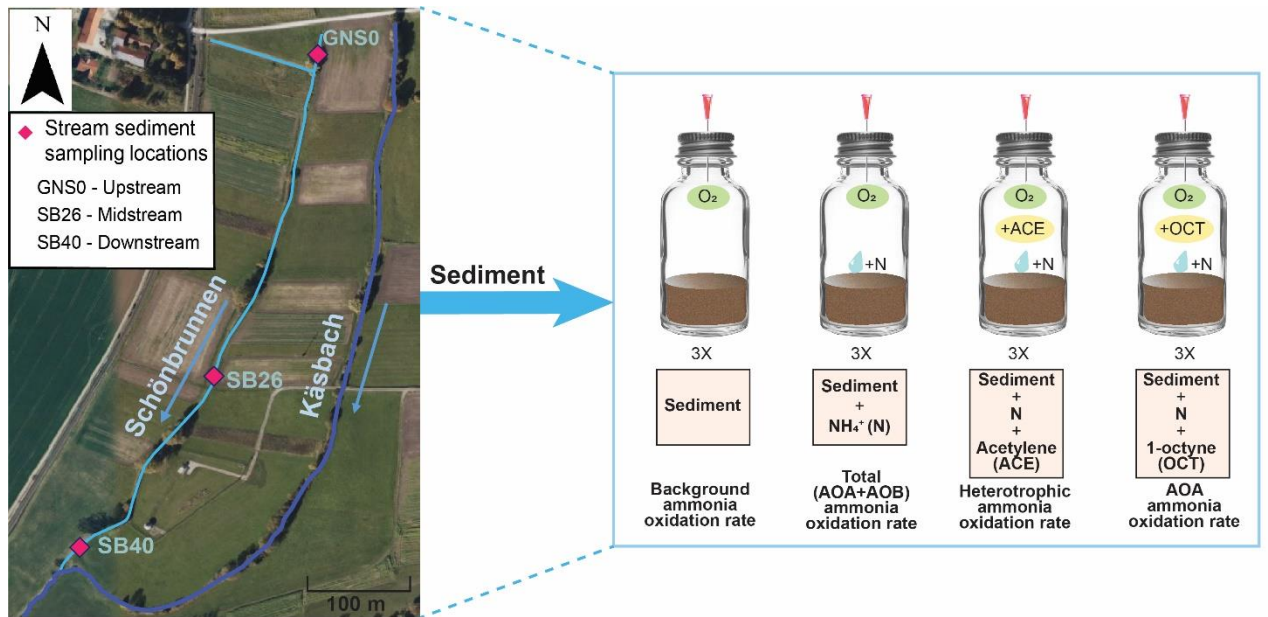


Fig. 2.2.1: Location of the Schönbrunnen stream and schematic description of the microcosm setup. Ammonia-oxidation activity in streambed sediments (sampled at 5 and 15 cm depth) obtained from upstream (Up), midstream (Mid), and downstream (Down) sections of the Schönbrunnen was investigated. Sediment microcosms were prepared with three replicates for each treatment: sediment amended with ammonium (Sedi + N), sediment amended with ammonium and acetylene (Sedi + N + ACE), sediment amended with ammonium and 1-octyne (Sedi + N + OCT), and a control treatment.

2.2.2 Sediment sample processing and microcosm setup

Fresh sediments obtained at Schönbrunnen were preprocessed for microcosm incubation (Fig. 2.2.1). Samples included streambed sediment obtained at 5 cm and 15 cm depths from three stream segments: upstream, midstream, and downstream. Larger pebbles and debris were manually removed from the samples before transfer to the lab. Within 24-h, sediments were sieved through sterilized analytical sieves with successive mesh sizes of 8.0 mm and 2.0 mm, to remove coarser particles and plant material. Sediments from replicate cores were then blended, and the remaining unnecessary materials were again removed manually to assure the preservation of the homogenized wet sediment slurry. The gravimetric water content of sieved sediment was measured prior to the microcosm experiments setup. Sediment slurries were prepared with $10\% \pm 2.6\%$ (dry weight) sediment inoculum in sterilized simulated stream water medium (Table 2.2.1). The final pH of the slurry was 7.5.

Each portion of blended slurry (46 ± 1 g) was then added to sterilized 125 ml MK-bottles (Müller+Krempel, Bülach, Switzerland), sealed with a rubber top and an aluminum cap. All incubations were adjusted to a final volume of 45 ml. In total, three sets of treatment groups and three sets of control groups were prepared per depth and per stream segment (Fig. 2.2.1).

Table 2.2.1: Simulated stream water medium modified from a previous study (De La Torre et al. 2008).

NaCl	1.0 g
MgCl ₂ ·6H ₂ O	0.4 g
CaCl ₂ ·2H ₂ O	0.1 g
KCl	0.5 g
NaHCO ₃	0.4 g
Vitamin solution	1.0 ml
Trace element solution	1.0 ml
Selenite-tungstate solution	1.0 ml
Phosphate buffer	1.0 ml
ddH ₂ O	Add to total 1000 ml (pH 7.0)

All treatment groups were supplemented with ammonium (0.5 mM final concentration). There were three treatment groups (Fig. 2.2.1): (1) an incubation group amended with ammonium without chemical inhibitors. This was set up for determining total ammonia oxidation from both heterotrophic and autotrophic microbial communities. (2) An incubation group amended with ~ 6 μ M acetylene, to infer the contribution of heterotrophic ammonia oxidation (the activity of both AOA and AOB is supposed to be inhibited by acetylene). (3) An incubation group amended with ~ 4 μ M 1-octyne, to infer the contribution of AOA-driven ammonia oxidation (the activity of AOB is supposed to be inhibited by 1-octyne). The acetylene and 1-octyne stock solutions were prepared as reported previously (Giguere et al. 2015). In a first control group, a "dead" control was set up to determine abiotic ammonia oxidation. For this group, the sediment slurry was treated with three repetitive

cycles of autoclaving (121°C, 20 min) and also amended with ammonium to a final concentration of 0.5 mM. A second control group contained live slurry without ammonium amendment. The third control group contained mixed stream-water from three stream segments, without sediments. These control incubations were further mixed with the same simulated stream water medium as used for all slurry incubations and supplemented with 0.5 mM ammonium, to assess ammonia oxidation in stream water. Actual stream water accounted for 60% of the volume; the final composition was similar as in all other treatments. All incubations were prepared in triplicates except for the water control group, which was prepared in duplicates. Incubation was performed in the dark at 15°C and the microcosms were agitated on an orbital shaker with a constant speed of ~90 rpm for 14 days, maintaining ambient oxygen conditions until the end of the incubation. Slurry samples for subsequent DNA isolation were taken on days 0, 5, 10 and 14. Samples taken from days 0 and 14 were processed for qPCR analyses of 16S rRNA and *amoA* genes.

To collect samples for ammonium measurements, 2 ml of homogenized slurry sample were centrifuged at 14000 rpm for 5 mins. The supernatant was further filtered through a 0.22 µm nylon syringe filter (Sigma-Aldrich, Darmstadt, Germany) and stored at -20°C until further measurement. The sediment pellets were stored at -80°C for subsequent molecular-biological analyses. The pH of each incubation was between 7.4 and 7.6 throughout the incubation. During the process of sample collection, incubations were opened to ensure ambient oxygen conditions. After the sampling, microcosms were again tightly sealed. Acetylene and 1-octyne were replenished subsequently to reestablish inhibitory concentrations. The determination of ammonium concentrations was performed according to a colorimetric method described previously (Gadkari 1984). Concentrations of nitrite and nitrate were quantified by ion-exchange chromatography (Metrohm, Herisau, Switzerland) in the Analytical Chemistry Keylab of the BayCEER, University of Bayreuth.

Moreover, a process-based model was conceived and calibrated by our project consortium, using the experimental data generated by this microcosm experiment, the detailed modeling of nitrification is reported in the supporting information SI.2 for a complete account. The respective manuscript is under review at the time of dissertation submission.

2.2.3 DNA isolation and amplicon sequencing

Isolation of genomic DNA from preprocessed sediment samples was conducted according to a protocol mentioned in the section 2.1.4. Extracted DNA was then quantified with a Qubit Fluorometer (Thermo Fisher Scientific, Waltham, MA). Amplicons of the V4 region of prokaryotic 16S rRNA genes were amplified using the NEBNext® High-Fidelity 2X PCR Master Mix (New England Biolabs GmbH, Frankfurt am Main, Germany), and universal Illumina-adaptor primers 515f (5'-GTGYCAGCMGCCGCGGTAA-3') and 806Rn (5'-GGACTACNVGGGTWTCTAAT-3') (Caporaso et al. 2011; Parada, Needham, and Fuhrman 2016; Apprill et al. 2015). Bacterial *amoA* genes were amplified using 1 x Brilliant III Ultra-Fast qPCR Master Mix (Agilent, Santa Clara, CA, USA), and adaptor primers *amoA*-1F (5'-GGGGTTTCTACTGGTGGT-3') and *amoA*-2R (5'-CCCCTCKGSAAAGCCTTCTTC-3') (Rotthauwe, Witzel, and Liesack 1997). Then 16S rRNA and *amoA* gene amplicons from duplicate DNA extracts (always replicate a and replicate b from each sampling spot) were pooled separately before sequencing, as all three microcosms replicates followed similar dynamics in nitrate concentrations during incubation. Further library preparation (Nextera, Illumina) and sequencing on an Illumina MiSeq platform (Illumina, San Diego, CA, United States) using 250 bp paired-end with v2 chemistry. The sequencing was performed by Microsynth AG in Switzerland.

2.2.4 qPCR measurements

The quantification of prokaryotic 16S rRNA genes and *amoA* was performed on a real-time PCR system CFX96 (Biorad, Feldkirchen, Germany) and calibrated using standard

curves from serially diluted synthetic gene fragments of known concentration (gBlocks, Integrated DNA Technologies Leuven, Belgium). For bacterial 16S rRNA genes, a 980 bp-fragment of the *Aromatoleum toluolicum* T^T (AF12946) was used. A 980 bp-fragment from *Methanosarcina barkeri* DSM 800 (NR_025303) was used for Archaeal 16S rRNA genes. For bacterial *amoA* genes, a 730 bp-fragment of the *Nitrosomonas europaea* ATCC 19178 (JN099309.1) was used. A 874 bp-fragment from Candidatus Nitrosotenuis cloacae SAT1 (CP011097) was used for archaeal *amoA* genes.

Each standard curve reached an R-square value greater than 0.99. All replicate samples for qPCR analyses were quantified in technical duplicates, and the reaction efficiency was between 80% and 92% for all target genes. Reactions were performed in a total volume of 40 µl, containing 20 µl Brilliant III Ultra-Fast SYBR Green qPCR Master Mix (Agilent, Santa Clara, CA, USA), 0.25 µl 50 µM primer, 0.4 µl 20 µg/µl BSA (Roche, Rotkreuz, Switzerland) and 2 µl DNA template. The primers used to amplify the target genes are shown in Table 2.2.2. qPCR thermal profiles were as follows: initial denaturation at 95 °C (3 min), 35–40 cycles of denaturation at 95 °C (30 s), annealing at a given temperature (30 s), elongation at 72 °C (30 s), followed by a final melting at 95 °C (30 s), and a melting curve recorded between 55 and 95 °C. The annealing temperature of the primer was set to 52 °C for bacterial 16S rRNA genes, 56 °C for archaeal 16S rRNA genes, 56 °C for bacterial *amoA* genes, and 57 °C for archaeal *amoA* genes.

Table 2.2.2: Primers for qPCR amplification of bacterial and archaeal 16S rRNA genes and *amoA* genes.

Genes	Primers	Sequence (5'-3')	Annealing temperature	Reference
Bacterial 16S rRNA genes	Ba519f Ba907r	CAGCMGCCGCGGTAATA CCGTCAATTCCTTTGAGTTT	52 °C	(Lane D.J. 1991)
Archaeal 16S rRNA genes	Ar109f Ar912rt	ACKGCTCAGTAACACGT GTGCTCCCCGCAATTCCTTTA	56 °C	(Lueders, Pommerenke, and Friedrich 2004)
Bacterial <i>amoA</i> genes	amoA-1F amoA-2R	GGGGTTTCTACTGGTGGT CCCCTCKGSAAAGCCTTCTTC	57 °C	(Rotthauwe, Witzel, and Liesack 1997)
Archaeal <i>amoA</i> genes	Arch-amoAF Arch-amoAR	STAATGGTCTGGCTTAGACG GCGGCCATCCATCTGTATGT	56 °C	(Francis et al. 2005)

2.2.5 Sequencing data analysis

Raw sequencing data of bacteria/archaeal 16S rRNA gene amplicons were first processed using Cutadapt (version 1.14) (Martin 2011) to trim primers. Trimmed adapter and primer-free sequences were then processed using the DADA2 package (version 1.16.0) (Callahan et al. 2016) in R (version 4.0.3) (R Core Team 2018) to merge forward and reverse reads, infer the exact amplicon sequence variants (ASVs), and remove PCR chimeras. In total 10399 ASV sequences were imported into the IDTAXA Classifier in package DECIPHER (version 2.18.1) (Wright 2016; Murali, Bhargava, and Wright 2018), using a confidence level of 50% (high), to map ASV sequences against the SILVA SSU database (release 138) for taxonomic classification (Quast et al. 2013). ASVs classified as "mitochondria", "chloroplasts", or "unclassified root" were removed. In addition, ASVs with an abundance <0.0001% across all samples were removed. Total reads were rarefied to 19400 reads per sample, which was the lowest number of reads observed among all samples, without sacrificing fully observed richness. The final cleaned ASV table contained 9589 ASVs and further analyzed for the alpha and beta diversity and visualized mainly with the phyloseq

(version 1.34.0), ggplot2 (version 3.3.2), and vegan (version 2.5-6) packages (Ginestet 2011; McMurdie and Holmes 2013; Oksanen et al. 2016) in R.

2.2.6 Bacteria *amoA* gene amplicon sequences analysis

Raw sequencing data of bacteria *amoA* gene amplicons were processed with nf-core/ampliseq v2.0.0 (Ewels et al. 2020; Straub et al. 2020) using Nextflow v21.03.0.edge (DI Tommaso et al. 2017) and singularity v3.4.2 (Kurtzer, Sochat, and Bauer 2017) (done by the project consortium). Processed bacterial *amoA* sequences were grouped into Operational Taxonomic Units (OTUs) with a 95% similarity threshold in R version 3.6.1 (R Core Team 2018) with DECIPHER v2.14.0 (Wright 2016). Primers were trimmed, and untrimmed sequences were discarded with Cutadapt version 3.2 (Martin 2011). Adapter and primer-free sequences were processed with DADA2 v1.18.0 (Callahan et al. 2016) to eliminate PhiX contamination, trim reads (before median quality drops below 25; forward reads were trimmed at 232 bp and reverse reads at 229 bp), correct errors, merge read pairs (adjusted to $\text{minOverlap} = 7$, $\text{maxMismatch} = 0$; $\text{minOverlap} = 5$ yielded only one additional ASV with 53 reads in only one sample, we chose to disregard this ASV and continue with $\text{minOverlap} = 7$), and remove polymerase chain reaction (PCR) chimeras. At this point, 11,972 amplicon sequencing variants (ASVs) were obtained across all samples. Next, bacterial *amoA* ASVs were then further grouped into Operational Taxonomic Units (OTUs) with a 95% similarity threshold in R version 3.6.1 (R Core Team 2018) with DECIPHER v2.14.0 (Wright 2016). 764 of 1,104 OTU sequences were exactly 452 bp long, 340 OTUs with other lengths were filtered out because they were not *amoA* sequences according to BLASTn (Altschul et al. 1990). The final OTU table was rarefied to 46,570 reads per sample, which was the lowest number of reads observed in a single sample. The rarefied OTU tables were further used to analyze the alpha and beta diversity and visualized mainly with the phyloseq (version 1.34.0), ggplot2 (version 3.3.2), and vegan (version 2.5-6) packages (Ginestet 2011; McMurdie and

Holmes 2013; Oksanen et al. 2016) in R. The FastTree (Price, Dehal, and Arkin 2009) algorithm was applied for generating a midpoint-rooted phylogenetic tree after OTU sequence alignment by the DECIPHER package (version 2.12.0) (Wright 2016). Maximum likelihood phylogenetic trees were constructed for amoA OTUs with MEGA-X (Kumar et al. 2018), aligned with selected reference bacterial amoA gene sequences from NCBI databases (Agarwala et al. 2018), using the ClustalW algorithm with default settings (1,000 bootstrap replications). Instead, differential abundance analyses were performed using unrarefied reads negative binomial model which accounts for library size differences in DESeq2 (version 1.30.1) package (Love, Huber, and Anders 2014; McMurdie and Holmes 2014).

2.3 Methods for metagenomics of the Schönbrunnen streambed microbiome

2.3.1 Sample collection and sulfide measurement

Same as the description in previous sections, this study targeted the same 550 m Schönbrunnen stream segment (section 2.1.1). Streambed sediment samples described in this chapter were collected in early September 2018, still taken to represent the summer season. Samples were collected from two different depths (roughly 5 cm and 15 cm below streambed surface), and six distinct sampling locations corresponding to the Upstream_a (*Up-A*), Upstream_b (*Up-B*), Midstream_a (*Mid-A*), Midstream_b (*Mid-B*), Downstream (*Down*), Confluence (*Conf*) in previous chapters. The observations reported in this chapter will only focus on the sample set from this specific sampling time. Sample collection details were the same as in section 2.1.2. Note that selected samples for metagenomics sequencing were from *Up-A*, *Mid-A*, *Mid-B*, *Down*, and *Conf*. Both of depths (5 cm and 15 cm) were always included, except for *Up-A* and *Conf*, where only the 15 cm and 5 cm samples were sequenced, respectively, due to budget limitations.

To provide additional chemistry evidence to demonstrate the presence of reduced sulfur species. Oxygen (outside tip diameter 90-110 μm) and H_2S microsensors (outside tip diameter 175-225 μm) (UNISENSE A/S, Aarhus, Denmark) were applied to determine the concentration of oxygen, and total sulfide at top 6 cm of fresh (within five days of the sampling time) sediment samples (Fig. S3.2). Given that H_2S microsensors directly measure the concentration of H_2S (gas) and total sulfide equilibrium is comprised of HS^- , S_2^- , and H_2S , total sulfide can be calculated from the concentration of HS^- when $\text{pH} < 9$ (Jeroschewski, Steuckart, and Kuhl 1996). Therefore, pH electrode (outside tip diameter 90-110 μm) (UNISENSE A/S, Aarhus, Denmark) was also employed to determine the pH of the top surface of the sediments.

2.3.2 DNA extraction and sequencing

Genomic DNA was extracted from sediment samples based on the protocol described in section 2.1.4. In short, duplicate sediment samples obtained from the Schönbrunnen were homogenized first prior to the DNA extraction. For amplicon sequencing, about 0.6 g wet sediment from each sample (n=36) was processed for DNA extraction. Each sample was extracted in triplicates. DNA quality and quantity in extracts was first confirmed with agarose gel electrophoresis, then through the Quant-iT PicoGreen dsDNA Assay Kit (Thermo Fisher, Waltham, USA) on an MX3000p cycler (Agilent, Santa Clara, USA). For metagenomics sequencing, in total greater than 5 µg DNA dissolved in Tris buffer were prepared for each sample (n=8). As I employed two metagenomics sequencing techniques, 1 µg DNA was used for Illumina-based shotgun metagenomic sequencing, whereas more than 4 µg DNA was sent for Nanopore-based whole genome sequencing. No replicates were included in metagenomics sequencing. DNA quality and quantity in extracts was checked and determined by NanoDrop ND-1000 (Thermo Fisher, Waltham, USA) and Qubit 4 Fluorometer (Thermo Fisher, Waltham, USA).

For full-length 16S rRNA gene amplicon sequencing, a two-step PCR was performed as described in the section 2.1.4. Sequencing library construction was performed using the SMRTbell® Template Prep Kit 1.0, following the PacBio documentation “Procedure & Checklist – Amplification of Full-Length 16S Gene with Barcoded Primers for Multiplexed SMRTbell Library Preparation and Sequencing” (version June, 2018) (Callahan et al. 2019). The libraries were sequenced on a PacBio Sequel platform by the Research Unit Comparative Microbiome Analysis at Helmholtz Zentrum München. For metagenomic sequencing, DNA samples were sent to CeGaT (Tübingen, Germany) for Illumina sequencing (PE150, ~15Gb data output per sample) on a Novoseq 6000 platform, and to GenXone (Złotniki, Poland) for Nanopore (~10-15 Gb data output per sample) on a PromethION platform. DNA sequencing

libraries for shotgun metagenomic sequencing were prepared using a TrueSeq DNA PCR Free kit (Illumina, San Diego, USA).

2.3.3 16S rRNA gene amplicon data processing and analysis

With the assistance of PacBio SMRTLink secondary analysis platform, I processed raw amplicon sequencing data as described in section 2.1.5. However, after primer trimming, the nf-core/ampliseq v2.0.0 (Ewels et al. 2020; Straub et al. 2020) pipeline in Nextflow v21.04.1 (DI Tommaso et al. 2017) and singularity v3.4.2 (Kurtzer, Sochat, and Bauer 2017) was applied to further process the data (done by the project consortium).

DADA2 (version 1.10.1) algorithms and the "DADA2 + PacBio" workflow were specifically applied for quality filtering, generating ASVs, chimera removal, and taxonomy classification (Callahan et al. 2019). Note that for this dataset, the "pseudo-pooling" (--sample_inference pseudo) option, in which samples are analyzed independently after sharing information (Callahan et al. 2019) was applied. I also manually adjusted the "max_ee" option, in which represents maximal expected number of errors in a sequencing read that result in the filter out of this read, to 12 in order to conserve more reads. After this, samples with a total read number <1500 were excluded (n=5) from downstream analysis. ASV sequences were mapped within DADA2 against the SILVA SSU database (release 138) for taxonomic classification (Quast et al. 2013).

2.3.4 Metagenome assembly and binning

Short sequence reads from the Illumina platform and long sequence reads from the Nanopore platform were processed with nf-core/mag v1.0.0 (<https://zenodo.org/record/3589528>) for quality control, hybrid assembly, assembled genome binning and taxonomic annotation (Krakau et al. 2022; Jakus, Blackwell, Straub, et al. 2021) using Nextflow v19.10.0 (DI Tommaso et al. 2017) and singularity v3.0.3 (Kurtzer, Sochat,

and Bauer 2017) (done by the project consortium). In detail, FastQC v0.11.8 (Andrews 2010) and fastp v0.20.0 (S. Chen et al. 2018) were applied for the short-reads quality control and Illumina adapter removal. Those reads mapped with Bowtie2 v2.3.5 identified as PhiX genome (Enterobacteria phage WA11, GCA_002596845.1, ASM259684v1) were excluded and removed (Langmead and Salzberg 2012). In contrast, long-read quality was checked with NanoPlot v1.26.3 (De Coster et al. 2018). Adapters were trimmed with Porechop v0.2.3_seqan2.1.1 (Bonenfant, No  , and Touzet 2023). Contamination from *Escherichia* virus Lambda (PRJNA485481, GCA_000840245.1) was filtered out by Nanolyse v1.1.0 (De Coster et al. 2018). After this, hybrid assembly was performed with metaSPAdes v3.13.1 (Nurk et al. 2017) and checked by QUAST v5.0.2 (Gurevich et al. 2013). MAGs constructed from assembled contigs were then binned with MetaBAT2 v2.13 (Kang et al. 2019). The completeness and contamination was determined with BUSCO v3.0.2 (Waterhouse et al. 2018) using 148 near-universal single-copy orthologs from OrthoDB v9 (Zdobnov et al. 2017).

Assembled metagenomes (n=8) were further processed by the Integrated Microbial Genome and Microbiome Expert Review (IMG/MER) pipeline v 5.0 (The U.S. Department of Energy Joint Genome Institute) for annotation and subsequent data analysis (I. M. A. Chen et al. 2019). The comprehensive IMG/MER annotation pipeline includes, but is not limited to functional protein families from COG (Tatusov et al. 2003), Pfam (Mistry et al. 2021), TIGRFAM (Haft, Selengut, and White 2003), Cath-Funfam (Sillitoe et al. 2013), SuperFamily (Gough et al. 2001), KEGG Orthology (KO) Terms (Kanehisa et al. 2016), and Enzyme Commission (EC) numbers (Kotera et al. 2004) derived from KO Term assignments. Sequencing depths of selected functional genes per sample as shown in Fig. 3.3.3 and Fig. S3.1, were calculated based on Bowtie2 mapping results and JGI output information (i.e. file

jgi_summarize_bam_contig_depths) and are in the following sections referred to as the gene's relative abundance.

Selected MAGs with acceptable quality (n=73) (contamination between 5%-25%, and completeness >50%) were re-analyzed for genome taxonomy using the most updated genome taxonomy database GTDB-Tk v2 (Chaumeil et al. 2022), so that taxonomic information would be in general comparable with amplicon sequencing data. Mixed-effects model with the poisson family of residuals was conducted with default setting via lme4 package (version 1.1.28) (Bates et al. 2015). In this case, selected nitrogen-reducing genes and sulfur oxidation genes were processed separately as two grouping variables. HUMAnN 3.0 was employed to run with default settings against the default database for the purpose of pathway abundance calculation, and taxonomic, strain-level profiling (Beghini et al. 2021). Differentially abundant pathways for each section of Schönbrunnen were determined using MaAsLin2 (version 1.4.0; normalization = TSS, transform= LOG, and standardize = TRUE) linear model fitting with FDR < 0.05 (Mallick et al. 2021). Moreover, in general, downstream data analyses and data visualization were primarily done in R (version 4.0.3) (R Core Team 2018) and employed similar R packages as described for section 2.1.5.

3 RESULTS

3.1 Nitrate-reducing microbial populations in the Schönbrunnen streambed as impacted by bidirectional water exchange

3.1.1 Hydrology and hydrochemistry of the Schönbrunnen stream

Nitrate concentrations in Schönbrunnen stream water and the alluvial aquifer were repeatedly measured by our project consortium over several years, and a representative set of water chemistry data corresponding to the summer sampling season is shown in Fig. 2.1.2 (B). Nitrate was generally highest in the northwestern, most upstream section of the Schönbrunnen, with concentrations $> 50 \text{ mg L}^{-1}$, consistent with the intensive agricultural activities around the stream. This was also reflected in the highest nitrate concentrations ($\geq 60 \text{ mg L}^{-1}$) found in the surrounding groundwater monitoring wells of the northwestern hillslope (e.g., GWS 2 and GWS 6). Interestingly, the high nitrate concentrations clearly decreased along the course of the Schönbrunnen, and were lowest ($< 30 \text{ mg L}^{-1}$) before the confluence with the Käsbach. Even though the farming activities varied over the years, the general trend of decreasing nitrate concentrations from upstream to downstream of the Schönbrunnen remains the same (Fig. S1.1). At selected streambed locations, fine-scale depth-resolved pore water analyses of nitrate, nitrite, and DOC were also conducted (Fig. S1.2). These data showed a strong decline of nitrate concentrations between 0 and 20 cm below the streambed, which was also the depth ($\sim 10\text{-}20 \text{ cm}$ below streambed) where pore water DOC concentrations were highest (Fig. S1.2). Similar to nitrate concentrations in the stream, nitrate concentrations in groundwater decreased with increasing distance from the north-western hillslope. In contrast to nitrate concentrations, sulfate concentrations in the stream increased over the Schönbrunnen reaches, with concentrations $> 200 \text{ mg L}^{-1}$ at the confluence (Fig. 2.1.2C). Sulfate concentrations were generally lower in groundwater from the northwestern hillslope, but higher in eastern groundwater ($> 1200 \text{ mg L}^{-1}$) in between Käsbach and Schönbrunnen, indicative of groundwater influenced by gypsum associated dissolution

processes flowing from the east. The ditch upstream of R1 was also characterized by elevated sulfate concentrations ($> 170 \text{ mg L}^{-1}$) (Fig. 2.1.2C), indicative of sulfate-rich groundwater entering the stream in this upstream net gaining section.

3.1.2 Bacterial communities in streambed sediments

Triplicate sampling of sediment microbial communities was done in three major sections of the Schönbrunnen, two upstream locations (*Up-A* and *Up-B*: further upstream of R1), two in the midstream net losing sections (*Mid-A*: R3. *Mid-B*: boundary of R3-R4), as well as one location each in the downstream net gaining section (*Down*: boundary of R6) and directly after the confluence with the Käsbach (*Conf*). For all sampling locations, I conducted full-length 16S rRNA gene amplicon sequencing for 5 and 15 cm depths, corresponding to the presumed nitrate reduction zone (Fig. S1.2). Alpha diversity indices were similar ($H' = 5.27 \pm 0.88$) across all Schönbrunnen sediment samples (Fig. 3.1.1), whereas confluence samples displayed a significantly lower diversity both at 5 and at 15 cm depth (Dunn's Kruskal-Wallis, $p < 0.01$). Samples from *Up-A* and the two midstream locations showed greater Evenness (J') (Dunn's Kruskal-Wallis, $p < 0.05$) than the confluence samples. Depth had no consistent effect on diversity indices, although some significant differences were observed for specific locations. For instance, *Up-A* 5 cm samples showed a higher Shannon diversity (Dunn's Kruskal-Wallis, $p < 0.01$) than the corresponding 15 cm samples.

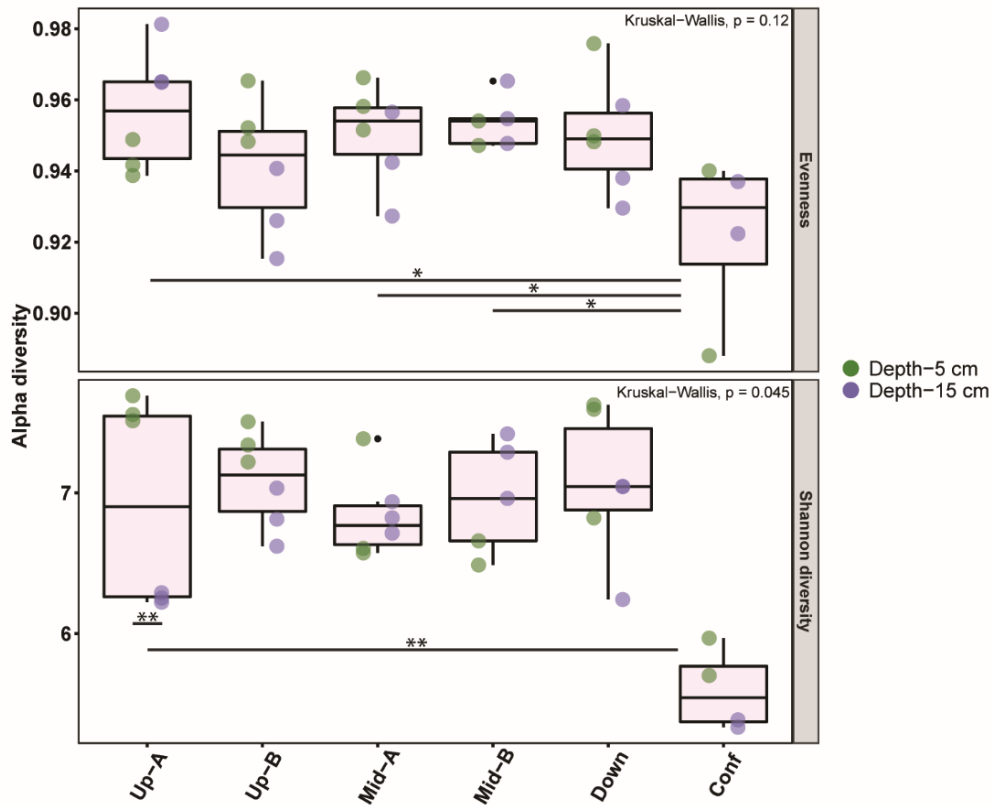


Fig. 3.1.1: Alpha diversity of sediment bacterial communities in the Schönbrunnen streambed. Shannon diversity (H') and Shannon diversity based Evenness (J') for 16S rRNA gene sequencing data are plotted for each sampling depth and sampling location. Boxplots indicate the mean Shannon diversity and evenness at each sampling location. Asterisks indicate significant differences in Kruskal-Wallis tests with Dunn's Multiple Comparison post-tests (*: $p < 0.05$; **: $p < 0.01$).

Hierarchical clustering of Bray-Curtis dissimilarities between samples revealed three major clusters (Fig. 3.1.2). Samples from the confluence formed a disparate cluster, connoting that taxonomic composition was distinct here from all other samples. A second, major cluster mainly comprised samples from 5 cm depth, as well as one set of 15 cm samples (*Mid-B*). The majority of the third cluster contained samples from 15 cm depth, plus one set of shallow depth samples from *Mid-A*. Generally, triplicate (or duplicate) libraries were grouped closely, except for one replicate of the *Down* 5 cm site, which was more similar to the *Mid-B* 15 cm samples, possibly reflecting small-scale local heterogeneities of the sampled streambed.

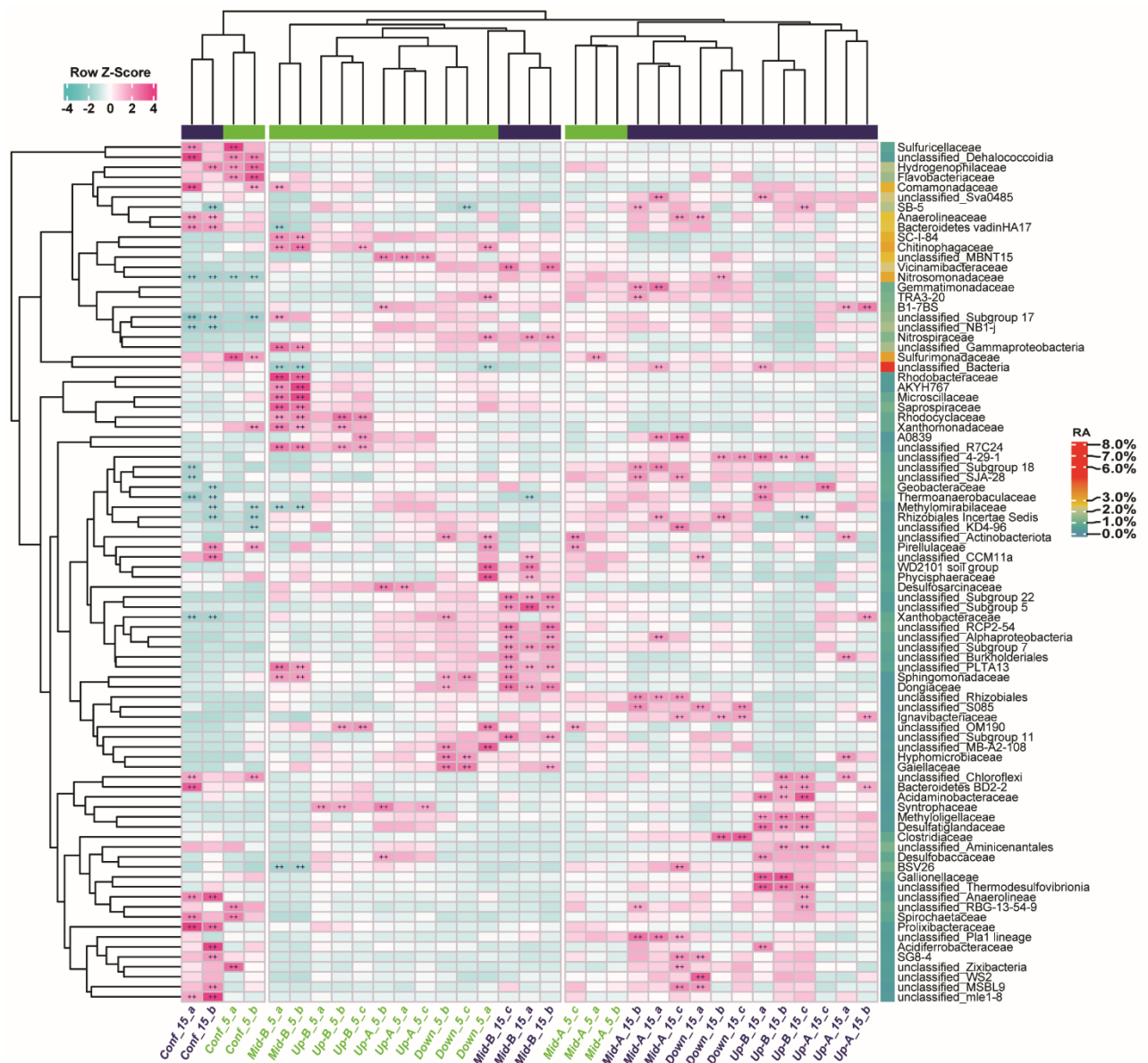


Fig. 3.1.2: Heatmap of the most abundant family-level microbial taxa in the Schönbrunnen streambed and hierarchical clustering analysis based on Bray-Curtis dissimilarity between samples (ASV level). Z-scores were calculated based on relative abundance (RA) of ASVs agglomerated at the family level. Families with cumulative relative abundances lower than 7% over all samples were excluded from the plot. The last column on the right side of the heatmap depicts the mean relative abundance of each family across all samples. Sample names on the bottom of the heatmap are color-coded to indicate sampling depths (green: 5 cm, purple: 15 cm). Cells were highlighted with ‘++’ symbols if $|Z\text{-Score}| > 2$.

The 9024 unique ASVs identified could be assigned to 55 phyla (Table S2). All samples were dominated by three phyla, *Proteobacteria* (2173 ASVs), *Bacteroidota* (1125 ASVs), and *Acidobacteriota* (1160 ASVs), which all together accounted for up to ~50% of each library. In total, 429 families were assigned. *Nitrosomonadaceae* (216 ASVs),

Chitinophagaceae (187 ASVs), and *Vicinamibacteraceae* (391 ASVs) appeared as the most abundant families within those three dominant phyla, respectively, accounting for ~10% relative abundance of the respective phylum on average. *Chitinophagaceae* were generally more abundant in 5 cm samples, while *Nitrosomonadaceae* were mostly more abundant in 15 cm samples, especially mid- and downstream. In addition to these phyla, the *Sulfurimonadaceae* (phylum *Campylobacterota*) were the most abundant family (mean relative abundance 3.5%), especially in 5 cm samples taken at the midstream and at the confluence. From up- to downstream and the confluence, 12% (1083 ASVs) of all ASVs belonging to 167 families were shared between at least five out of the six sampling locations (Fig. 3.1.3A). As for the five locations within the Schönbrunnen, 793 ASVs were presented from up- to downstream. The samples from 5 cm generally shared a greater number of common ASVs than samples from 15 cm depth (Fig. 3.1.3B & Fig. 3.1.3C).

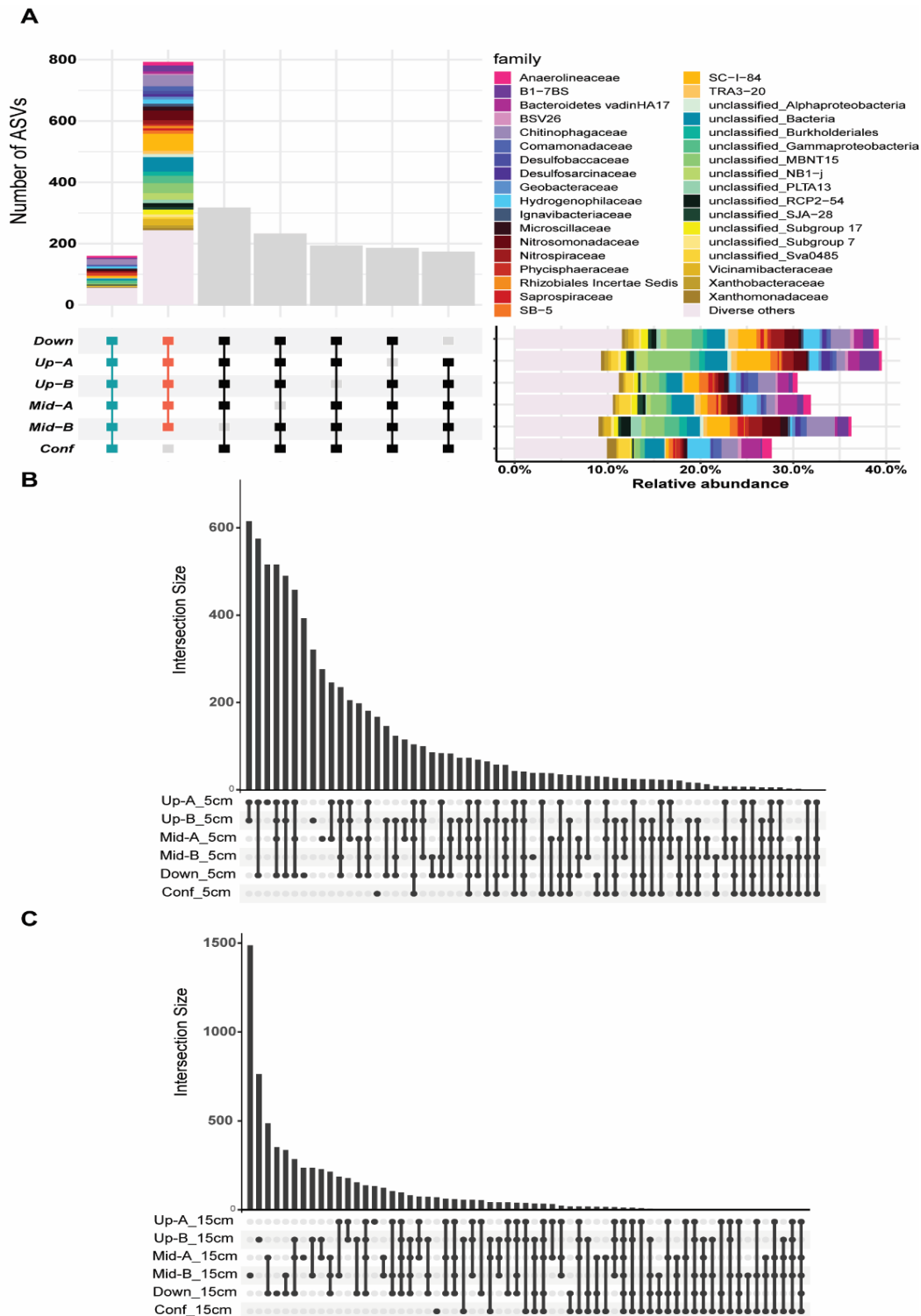


Fig. 3.1.3: Intersection of streambed ASVs. (A) UpSet plot on ASVs shared by at least five sampling locations. In total, 1083 ASVs in 167 families were plotted here. However, only the top 35 families, which have most of the shared ASVs in at least five sampling locations, were plotted with different color codes. Other ASVs presented in at least five sampling locations were merged into “Diverse others”. The bottom bar plot showed the relative abundance of these 1083 ASVs in all ASVs of a sampling location. (B) and (C) UpSet plots show the number of ASVs shared by 5 cm samples and 15 cm samples, respectively.

Differences in bacterial community structure along the Schönbrunnen were further investigated via non-metric multidimensional scaling (NMDS) and similarity percentage (SIMPER) analyses (Fig. 3.1.4). The 5 cm samples generally featured a higher abundance of typical heterotrophic, aerobic or facultative anaerobic microbial lineages. These included *Rhodanobacteraceae* (dominated by *Ahniella* spp.), *Rhodobacteraceae* (dominated by *Rhodobacter* and *Tabrizicola* spp.), *Microscillaceae* (dominated by *Chryseolinea* spp.), *Xanthomonadaceae* (dominated by *Arenimonas* spp.), *Chitinophagaceae* (dominated by *Dinghuibacter* and *Terrimonas* spp.), and the *Saprospiraceae*. Members of the *Rhodocyclaceae* were also particularly abundant in 5 cm samples taken from *Up-B* and *Mid-B* (~2-3%), mainly including reads associated with *Denitratisoma*, *Dechloromonas*, and *Rhodocyclus* spp. (Fig. 3.1.5). However, samples from 5 cm depth of *Up-A*, *Mid-A*, and *Down* also featured taxa similarly abundant at 15 cm depth of *Mid-B*. These included the *Nitrosomonadaceae* (~3%) and *Nitrospiraceae* (~1%). In contrast, the dissimilarity of bacterial communities observed in other samples from 15 cm depth was mainly driven by typical anaerobic or microaerophilic lineages. This included typical fermenters (*Anaerolineaceae*, *Anaerovoracaceae*, *Clostridiaceae*, and *Prevotellaceae*), potential sulfate reducers (*Desulfobaccaceae* and *Thermodesulfovibrionia*), but also potential iron-oxidizing bacteria within the *Gallionellaceae* (*Sideroxydans* spp.). The confluence samples were clearly distinguished from the other Schönbrunnen samples. Taxa typical for inorganic reduced sulfur oxidation (*Sulfuricellaceae*, *Sulfurimonadaceae*, and *Thiobacillus* spp. within the *Hydrogenophilaceae*) were among the major drivers of dissimilarity between those samples. Moreover, *Flavobacteriaceae* (*Flavobacterium* spp.) and *Comamonadaceae* (*Rhizobacter* spp.) were also relevant for the separation of confluence samples from others.

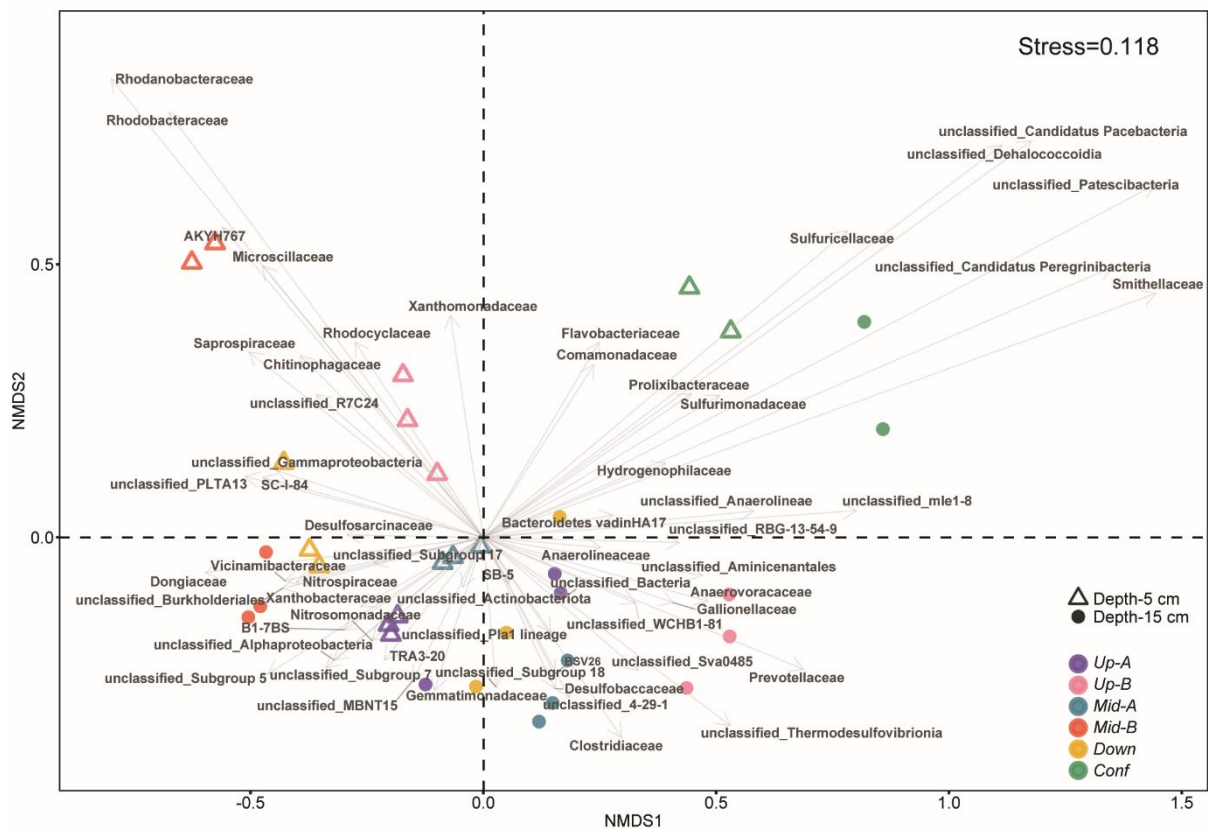


Fig. 3.1.4: Bray-Curtis distance-based non-metric multidimensional scaling (NMDS) plot of dissimilarities between streambed microbial communities grouped at the family-level. Selected taxa contributing significantly ($p < 0.05$, sum total $> 50\%$) to dissimilarities between samples (indicated via SIMPER analyses) were projected onto the NMDS plot. The arrow length and direction of each plotted taxon reflect its contribution on driving dissimilarities for a given sample.

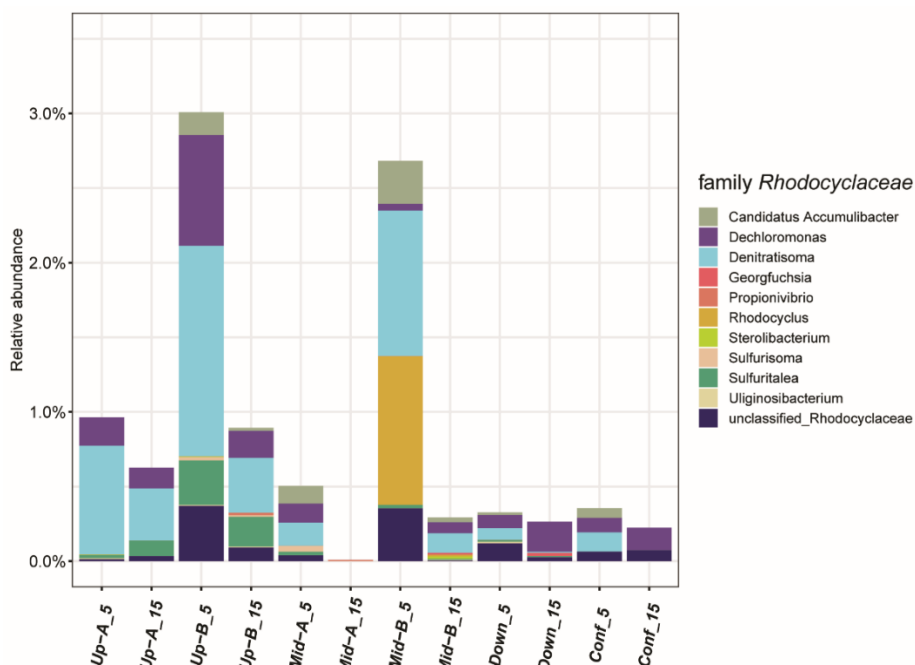


Fig. 3.1.5: Relative abundance of members within the *Rhodocyclaceae* across samples from the Schönbrunnen streambed. Different colors represent all genus-level taxa detected in this study within the family *Rhodocyclaceae*.

Typical sulfur-oxidizing bacteria (SOB) were rather abundant throughout the Schönbrunnen sediments, not only at the confluence (Fig. 3.1.2). Considering their potential role in linking sulfur and nitrogen cycling in the streambed, their distribution at ASV-level was further investigated, facilitated by the high resolution of full-length 16S rRNA amplicon reads. We specifically focused on ASVs within two dominating genera, *Sulfuricurvum* spp. (relative abundance up to 14.79%) and *Thiobacillus* spp. (relative abundance up to ~5.6%). *Sulfuricurvum* spp. was the only taxon within the *Sulfurimonadaceae* detected in this study. *Thiobacillus* spp. (73 ASVs; took up 99.88% of the family *Hydrogenophilaceae*) and unclassified *Hydrogenophilaceae* (2 ASVs; took up 0.12% of the family *Hydrogenophilaceae*) were genera detected within *Hydrogenophilaceae*. In total, 65 ASVs were identified within the genus *Sulfuricurvum*, including 34 of them were only detected within Schönbrunnen samples, such as the most dominant ASV9 (relative abundance up to ~1.99%) (Fig. 3.1.6A). However, some ASVs, especially ASV2 and ASV8 (relative abundance up to 3.71% and 3.23%, respectively), were found exclusively in the confluence samples. Another typical sulfur-oxidizing lineage detected was *Thiobacillus*. Here, out of 73 ASVs detected in total (Fig. 3.1.6B), only two ASVs appeared specifically enriched at the confluence, ASV19 (relative abundance up to ~1.26%) and ASV127 (relative abundance up to ~0.61%). In the Schönbrunnen streambed, ASV3 (relative abundance up to ~1.12%) and ASV291 (relative abundance up to ~0.33%) were relatively more abundant. For further context on the detected ASVs, ASVs within both *Sulfuricurvum* spp. and *Thiobacillus* spp. were embedded in phylogenetic dendrograms (Fig. 3.1.7A & Fig. 3.1.7B). The phylogenetic tree of *Sulfuricurvum* spp. revealed, that Schönbrunnen and confluence ASVs were separated into two distinct clusters (nominated Schönbrunnen cluster and Käsbaach cluster) (Fig. 3.1.7A). The phylogenetic tree of *Thiobacillus* spp. suggested, that Schönbrunnen and confluence ASVs of *Thiobacillus* spp. were closely related to *Thiobacillus thioparus*, whereas

ASV19 and ASV291 were more related to *Thiobacillus thiophilus* and *Thiobacillus denitrificans*, respectively (Fig. 3.1.7B).

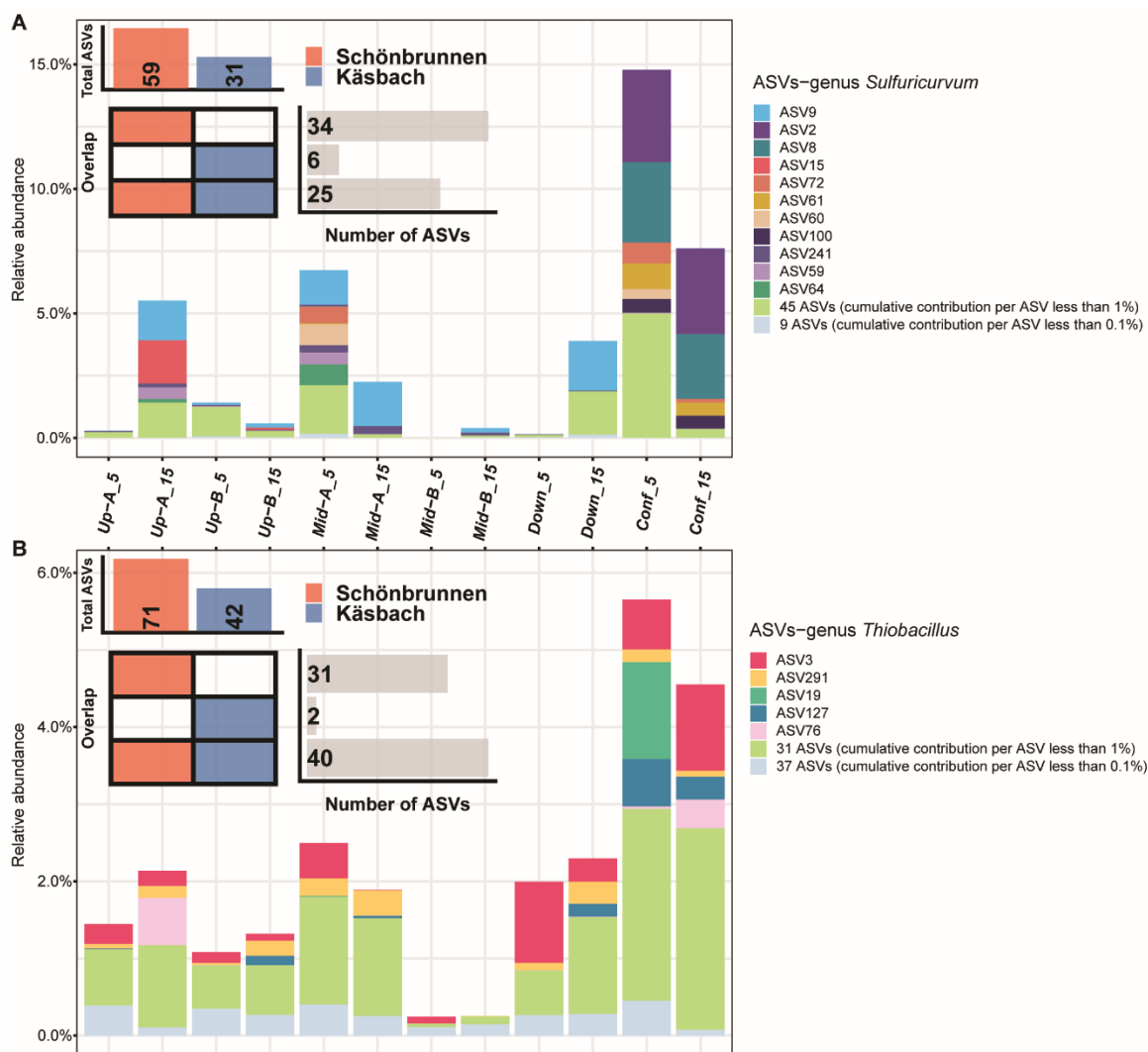


Fig. 3.1.6: Relative abundance of potential sulfur-oxidizing bacterial populations across samples of the Schönbrunnen streambed. (A) *Sulfuricurvum* spp., and (B) *Thiobacillus* spp. are resolved at the ASV level. The upset plots show the number of unique or shared ASVs within either of these two genera within Schönbrunnen or Käsbach (i.e. after confluence) samples. Most abundant ASVs are plotted with distinct colors, whereas lower abundance ASVs are merged into two categories: ASVs with a cumulative abundance < 1% across all samples (light green color), and ASVs with a cumulative abundance < 0.1% across all samples (light blue color).

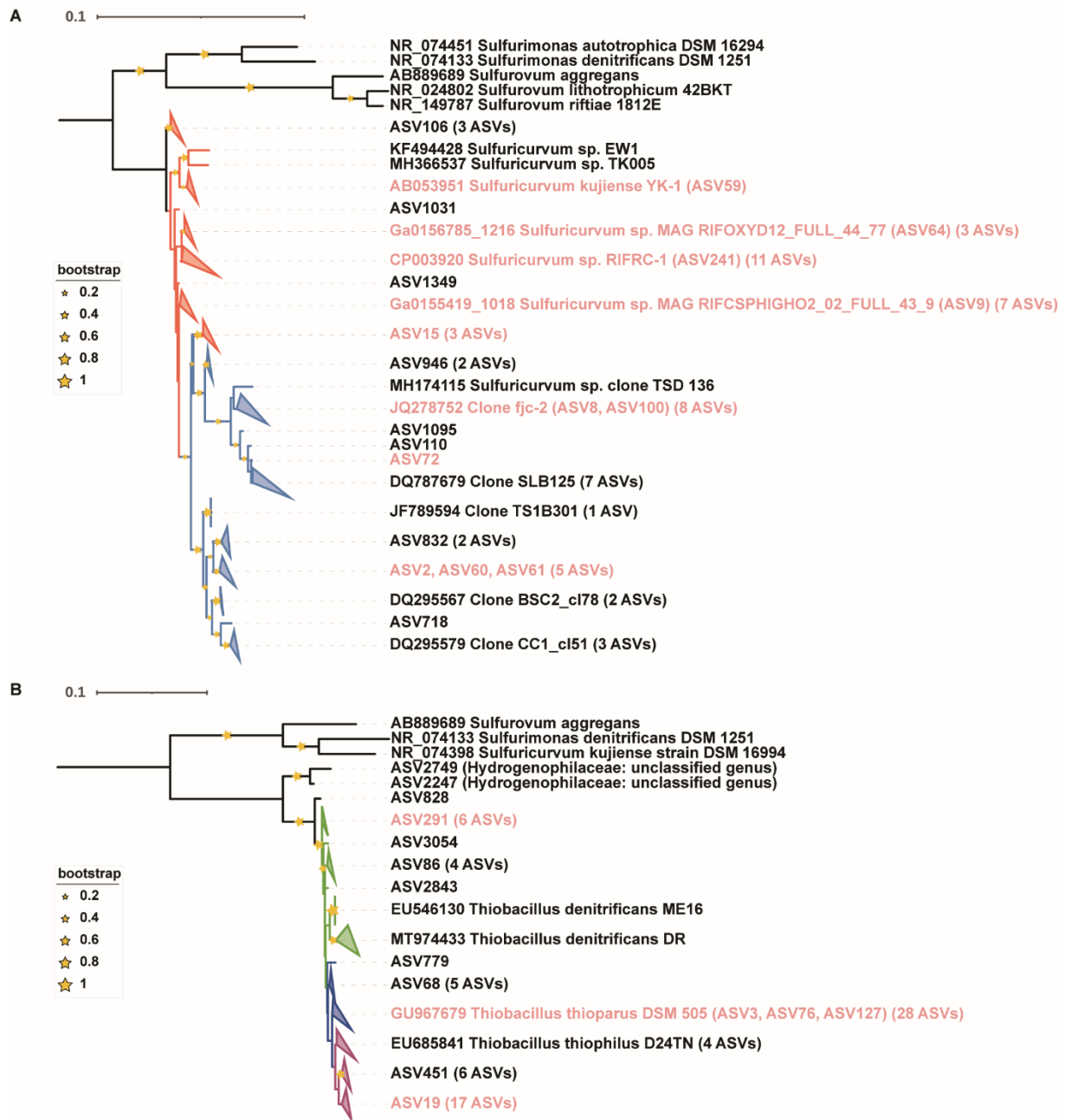


Fig. 3.1.7: Maximum likelihood tree of *Sulfuricurvum* and *Thiobacillus* ASVs. (A) all *Sulfuricurvum* ASVs detected in this study. Tree branches associated with the Schönbrunnen cluster are shown in red color, whereas branches of the Käsbach cluster are plotted in blue color. In addition, labels of the most abundant ASVs (corresponding to ASVs with distinct colors in Fig. 3.1.6) are highlighted in red color. The number of ASVs shown in parentheses (e.g., 6 ASVs) indicates the number of ASVs collapsed in a clade. Similarly, (B) shows the phylogeny of all *Thiobacillus* ASVs detected in this study. However, different colors for tree branches here represent three likely affiliation of ASVs with *T. denitrificans* in green, *T. thioparus* in blue, and *T. thiophilus* in red.

3.1.3 Streambed microbial community assembly

To investigate the potential impact of bidirectional water exchange on the assembly of bacterial communities in the streambed, the β -nearest taxon (β -NTI) and RC_{bray} indices were inferred. The importance of deterministic versus stochastic microbial community assembly can thus be estimated (Stegen et al. 2013; 2012). For samples in this study, over half of pairwise comparisons resulted in β -NTI values > 2 , significantly different from the expectation of the null model (Fig. 3.1.8). This indicated that the community assembly of Schönbrunnen sediments was largely triggered by deterministic variable selection. A $|\beta\text{-NTI}|$ index < 2 generally suggests that a pair of samples is likely to be selected by stochastic processes. The RC_{bray} index was calculated to further delineate these patterns. An RC_{bray} index < -0.95 or > 0.95 indicates that two samples share more ASVs or fewer ASVs than expected, respectively. I assumed that homogenizing dispersal could be relevant between samples from 5 cm and 15 cm of the same sampling location, depending on the local hydraulic conditions. Indeed, a homogenizing dispersal was suggested at *Up-A* and *Mid-A*. Moreover, a longitudinal homogenizing dispersal was observed between 5 cm samples of *Up-A* and *Mid-A*, and between 15 cm samples of *Mid-A* and *Down*.

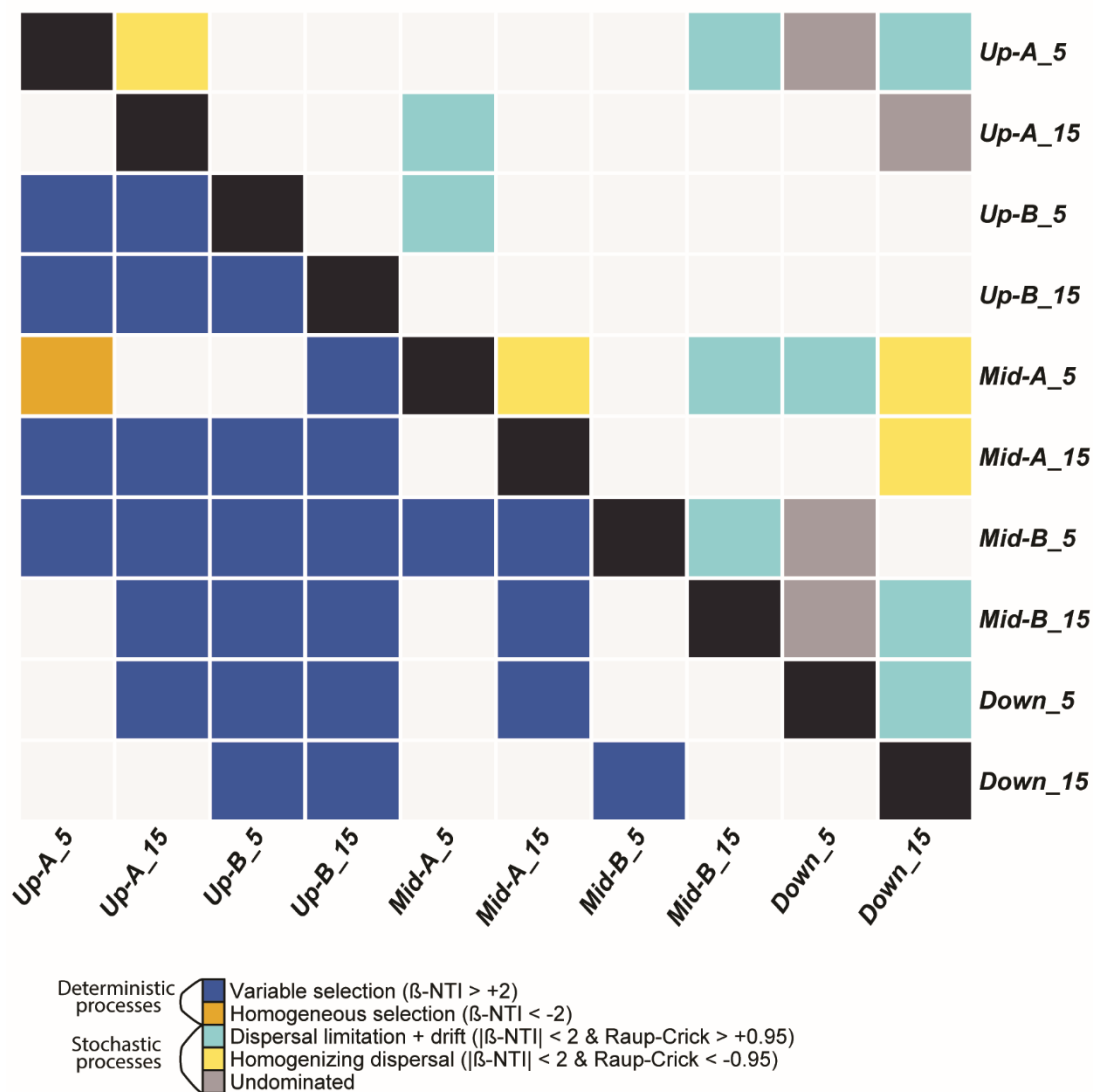


Fig. 3.1.8: Heatmap for the β -NTI values (lower left triangle) and the RC_{bray} values (upper right triangle). Deep blue and yellow colors in the lower triangle indicate deterministic processes, including variable selection and homogeneous selection, to dominate in pairwise comparison, respectively. Similarly, light blue and yellow colors in the upper triangle represent stochastic assembly mechanisms, such as dispersal limitation or homogenizing dispersal, respectively.

3.1.4 Quantification of denitrifying communities

In addition to 16S rRNA gene amplicon sequencing, I also quantified absolute abundances of bacterial 16S rRNA and nitrite reduction genes, indicative of denitrifying communities, over the Schönbrunnen streambed. Bacterial 16S rRNA genes ranged from $9.1 \pm 2.5 \times 10^6$ to $9 \pm 0.8 \times 10^7$ copies g_{ww}^{-1} of sediment (Fig. 3.1.9A). *nirK* genes were more abundant than *nirS* across all samples, ranging from $2.2 \pm 1.2 \times 10^5$ to $5.3 \pm 2.5 \times 10^6$ copies

$\text{g}_{\text{ww}}^{-1}$ of sediment. The abundance of bacterial 16S rRNA genes was positively correlated with the abundance of *nirK* ($r = 0.791, p < 0.001$; Pearson's) and *nirS* ($r = 0.909, p < 0.001$; Pearson's) genes. A notable increase in the relative abundance of *nirK* genes to up to ~10% of total bacterial 16S rRNA gene counts was observed from upstream to downstream samples, especially at 15 cm depth (Fig. 3.1.9B). A positive linear relationship ($p < 0.05$, Adjusted $R^2 = 0.235$) was noted between the relative abundance of *nirK* and the geodesic distance from upstream to confluence.

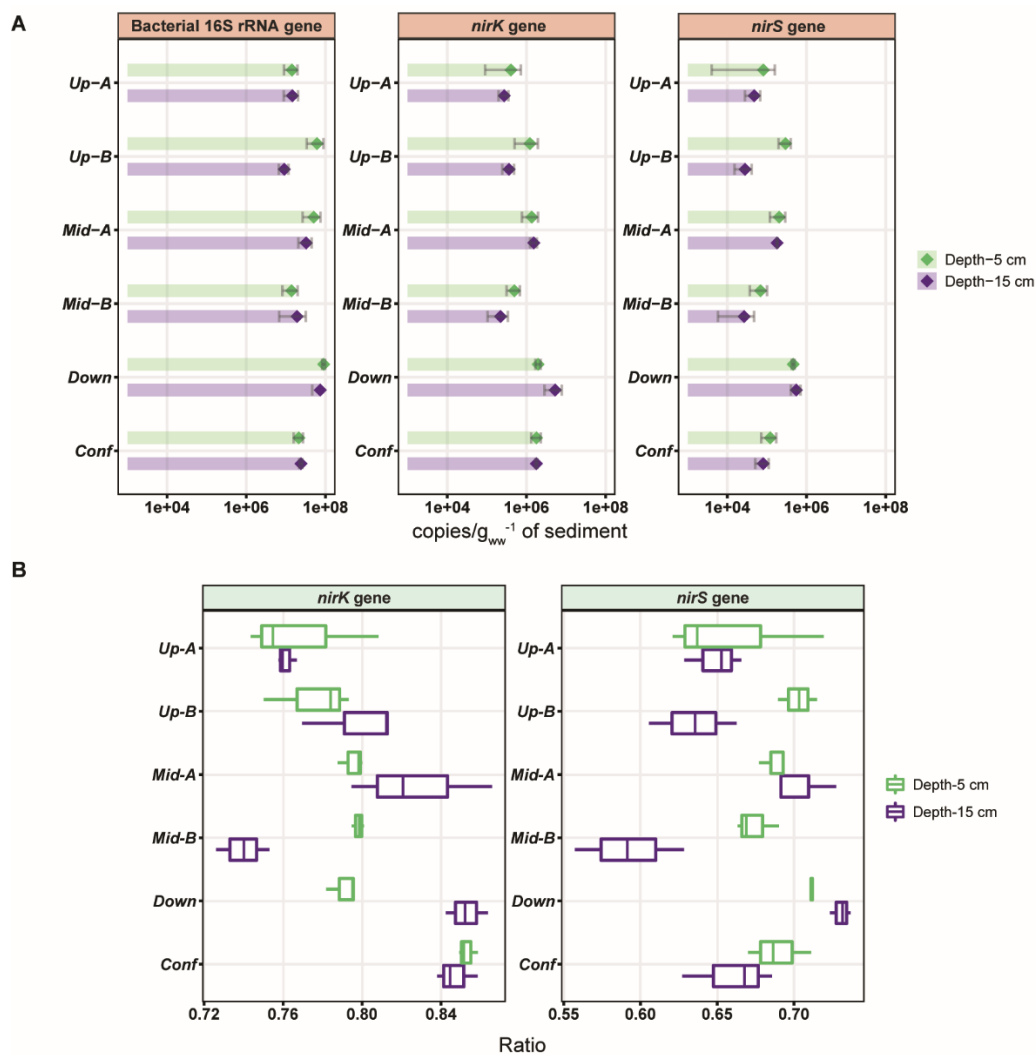


Fig. 3.1.9: Abundances of streambed denitrification communities. (A) Abundances of bacterial 16S rRNA, *nirK*, and *nirS* genes in sediments of the Schönbrunnen streambed quantified via qPCR. Gene abundances were calculated as gene copies per g of wet sediment ($\text{g}_{\text{ww}}^{-1}$ of sediment). The standard deviation of gene abundances in biological ($n = 3$) and technical ($n = 2$) replication are shown as error bars. (B) Relative abundances of *nirK* and *nirS*

versus total bacterial 16S rRNA gene counts. Ratios were calculated as ratios of log₁₀-transformed qPCR counts as shown in (A).

3.2 Nitrification in the Schönbrunnen streambed

After investigating the impact of bidirectional water exchange on nitrate reduction in section 3.1, the next aim of my thesis was to study the nitrification and nitrifying microorganisms in the Schönbrunnen streambed.

3.2.1 *In-situ* community composition of streambed microbiomes

Prior to the microcosm experiment, I again analyzed streambed microbiota of up-, mid- and downstream sections of the Schönbrunnen to infer initial *in-situ* microbial-community composition also for samples taken in summer of 2020. All fresh samples (T0) showed similar ASV-based Shannon diversity ($H' = 6.3-7.4$) with insignificant depth differences, except for samples taken from the midstream section. The Shannon diversity for midstream 5 cm samples ($H' = 7.2$) was significantly greater than midstream 15 cm samples ($H' = 5.1$) (Fig. 3.2.1). The top 20 most abundant families took up similar proportion of total microbiota (40%-60%) at all sampling spots before the incubation (Fig. 3.2.2). Potential sulfur-oxidizing populations, such as members of the *Sulfurimonadaceae* (relative abundance up to 17.7%) and *Hydrogenophilaceae* (relative abundance up to 6.4%), were among the dominant taxa in the Schönbrunnen streambed. Amongst presumed AOB lineages, the *Nitrosomonadaceae* appeared most abundant (relative abundance up to 3.2%) and were dominated by the genus-level taxa MND1 and Ellin6067 (Fig. 3.2.2 & Fig. 3.2.3 & Fig. 3.2.4). *Nitrosomonadaceae* were generally more abundant in upstream and downstream samples (Fig. 3.2.3), previously identified as net gaining sections of the stream as described in the section 2.1.3 (Jimenez-Fernandez et al. 2022). Their abundance was also generally greater in 5 cm depths than in 15 cm depths. A similar distribution pattern was also observed also for

potential nitrite-oxidizing bacteria (NOB) within the *Nitrospiraceae* (dominated by reads affiliated with the genus *Nitrospira*).

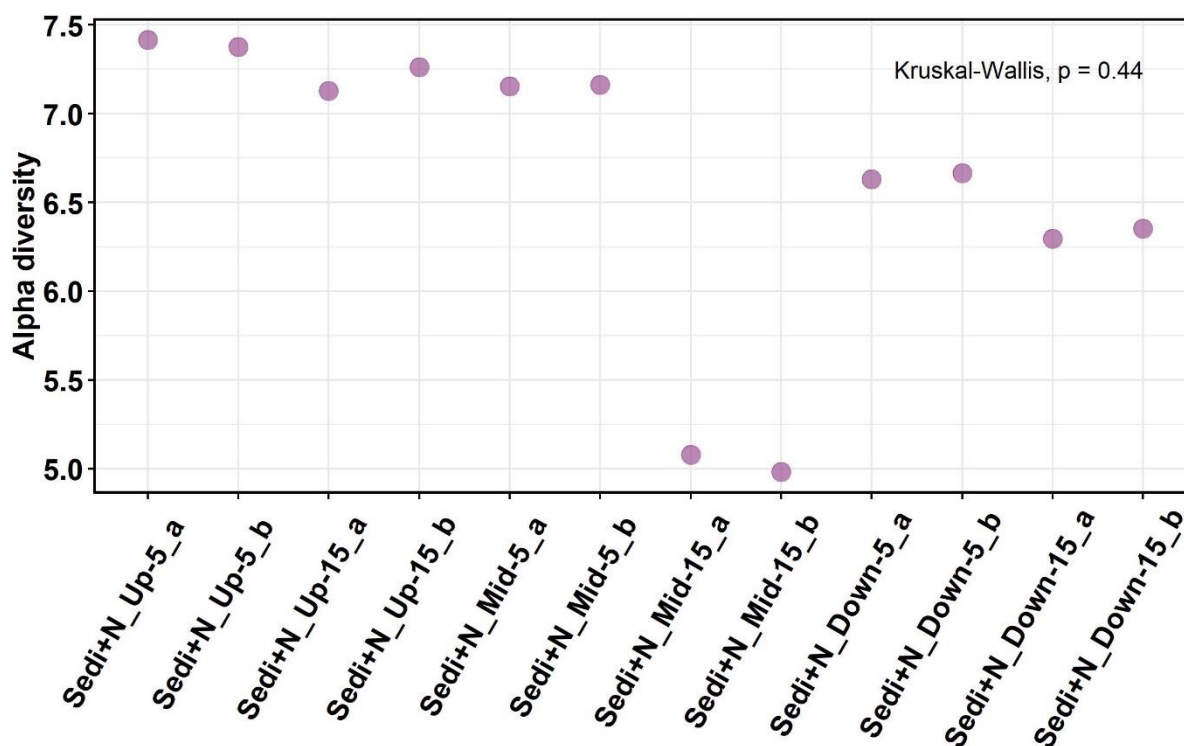


Fig. 3.2.1: *In-situ* Shannon diversity index (H') in all sediment samples. “Up”, “Mid”, and “Down” in the sample name on X-axis suggest sampling location upstream, midstream, and downstream, respectively. The sample name suffix “a” and “b” suggests biological duplicates.

In contrast, AOA were less abundant taxa in 16S amplicon libraries. For instance, members of the *Nitrososphaeraceae* had a mean relative abundance of ~0.3%, while the *Nitrosopumilaceae* had a mean relative abundance of only < 0.1% (Fig. 3.2.3). However, a characteristic distribution pattern along the Schönbrunnen was also observed for AOA (Fig. 3.2.3). Resembling the distribution of the bacterial *Nitrosomonadaceae*, members of the *Nitrososphaeraceae* also were more abundant in upstream and downstream samples and in 5 cm sediments.

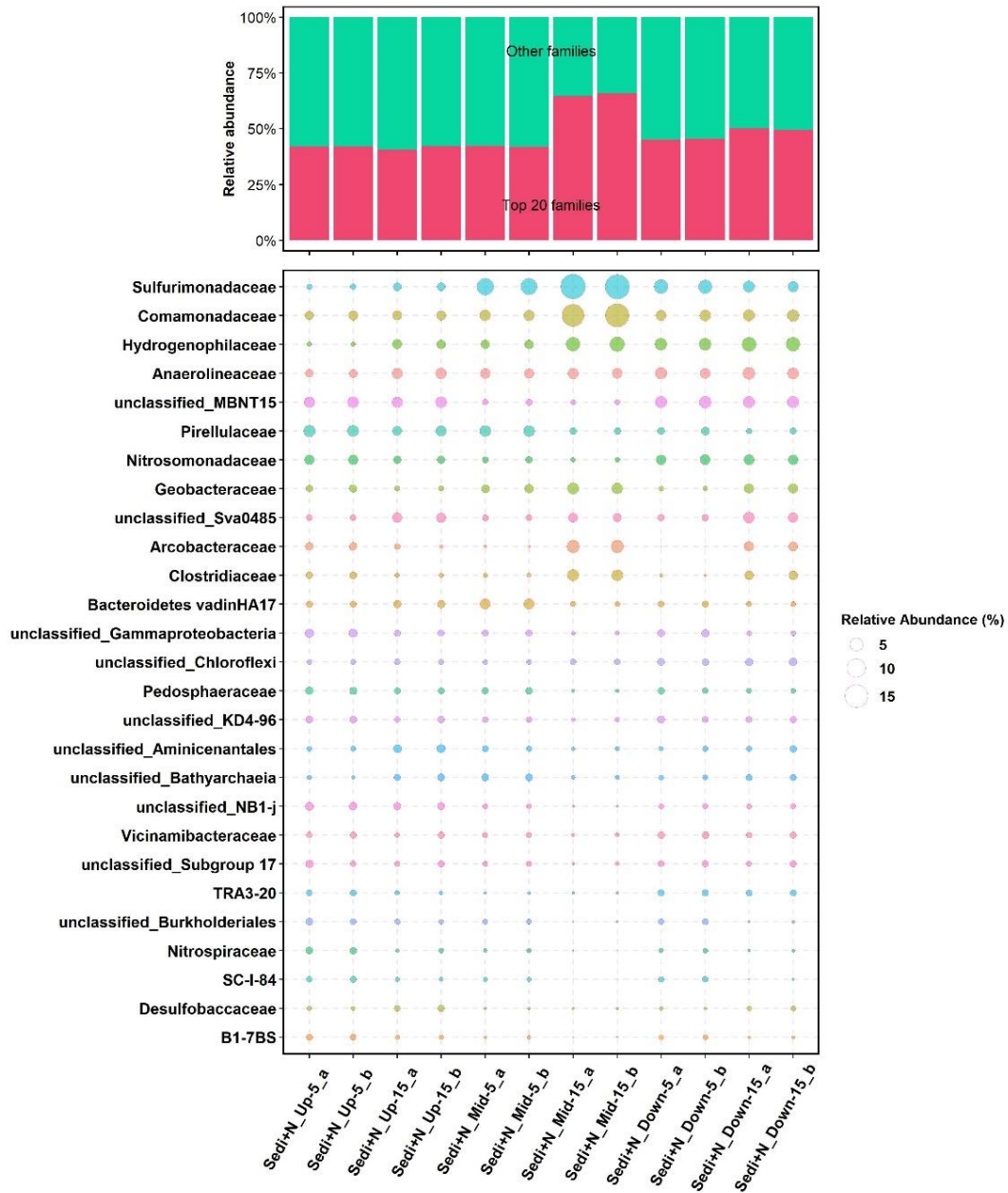


Fig. 3.2.2: Relative abundance of top 20 most abundant microbial communities at the family level detected in Schönbrunnen sediments prior to the microcosm incubation (a.k.a. T0). “Up”, “Mid”, and “Down” in the sample name on X-axis suggest sampling location upstream, midstream, and downstream, respectively. The sample name suffix “a” and “b” suggests biological duplicates. The bar plot on top showed the cumulative abundance of top 20 most abundant family in red color, whereas the green color represents the proportion of other less (OTUs with cumulative relative abundance in all samples less than 7% were classified within this category.) abundant microbial communities at the family level. The bubble plot below showed relative abundance of each taxon within top 20 most abundant microbial communities to all detected microbial communities of a sample.

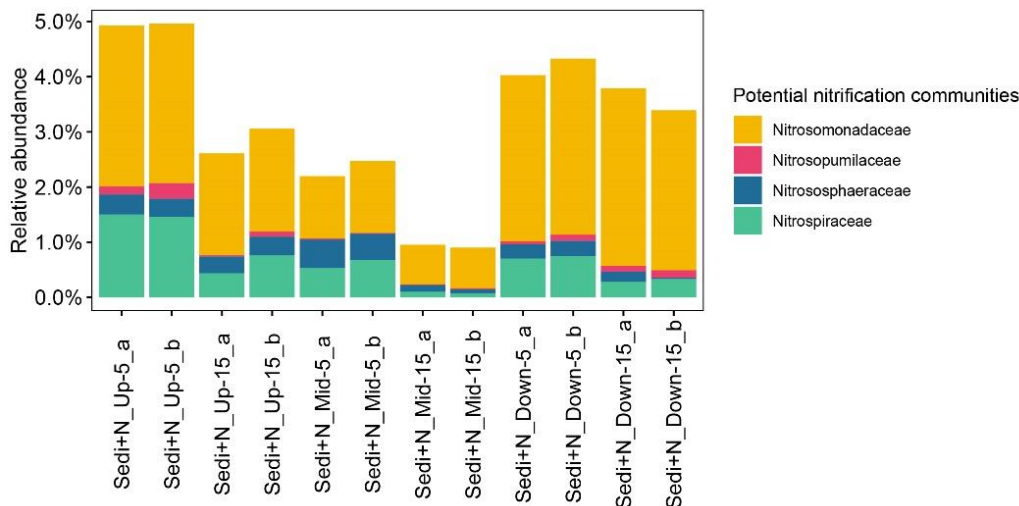


Fig. 3.2.3: Relative abundances of taxa affiliated with well-known nitrifiers in generated amplicon libraries of streambed sediments before microcosm incubation (T0). Shown are members of the AOB (*Nitrosomonadaceae*) and AOA (*Nitrosopumilaceae*, *Nitrososphaeraceae*) and the nitrite-oxidizing bacteria (*Nitrospiraceae*).

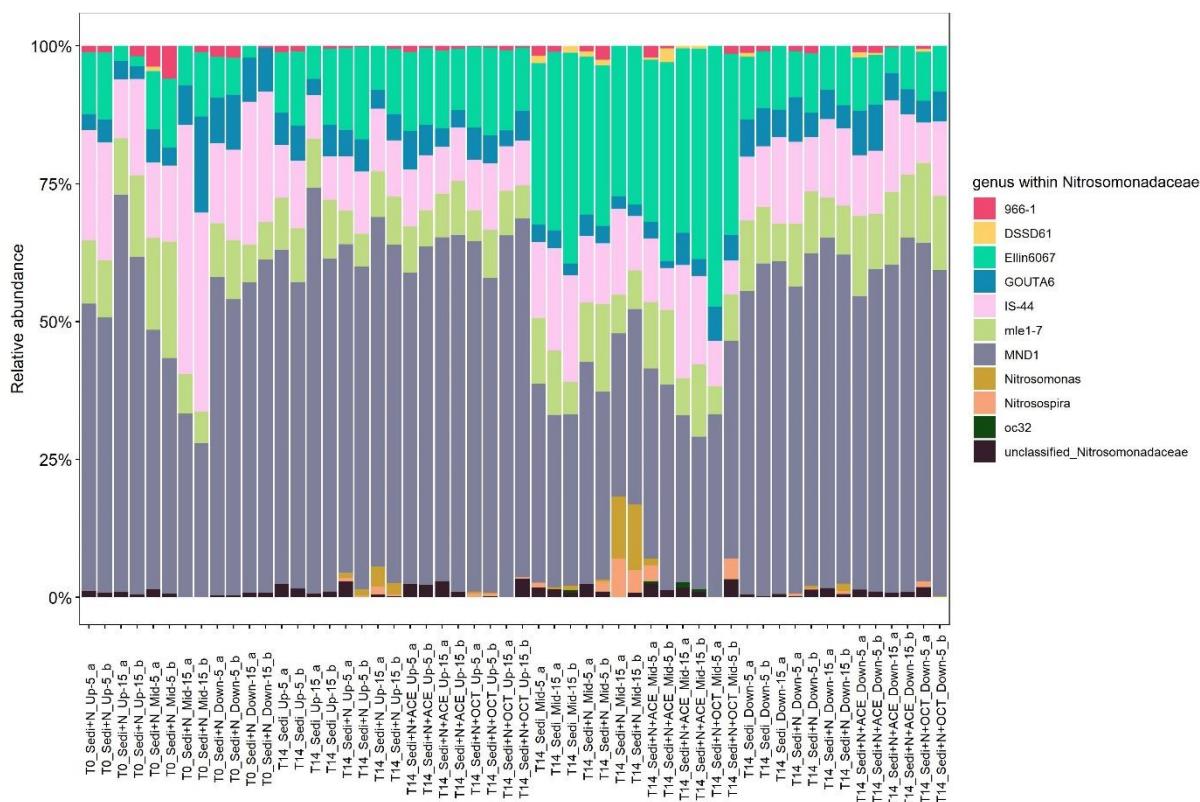


Fig. 3.2.4: Relative abundance of *Nitrosomonadaceae*-affiliated ASVs clustered at the genus level before and after the microcosm incubation. These plotted genera represent all ASVs detected within the *Nitrosomonadaceae*. T0 on X-axis represents day 0 of the microcosm incubation, whereas T14 represents the day 14 of the incubation. “Up”, “Mid”, and “Down” on X-axis suggest sampling location upstream, midstream, and downstream, respectively. “N” stands for the ammonium supplemented incubations. “OCT” suggests 1-octyne treated incubations, whereas “ACE” suggests acetylene treated incubations. The sample name suffix “a” and “b” suggests biological duplicates.

3.2.2 Microcosm incubation experiments

To further dissect not only the longitudinal distribution, but also the potential activity of streambed ammonia-oxidizing populations, a microcosm experiment was set up with distinct chemical inhibitors. Potential nitrification rates and population growth were measured during the 14-d incubation period.

3.2.2.1 Ammonia oxidation

Initial NH_4^+ concentrations were approximately 0.4 mM in all microcosms amended with ammonium (Fig. 3.2.5 & Fig. 3.2.6 & Fig. 3.2.7). This concentration was expected and corresponded to the upper ammonium concentration range measured at the Schönbrunnen field site (Table S2.1). In microcosms amended with ammonium but no inhibitors, as proxy for potential *in-situ* nitrification activity, the dynamics of ammonium and nitrate concentrations over time were similar for the different stream segments (Fig. 3.2.5 & Fig. 3.2.6 & Fig. 3.2.7). Ammonium concentrations decreased throughout the incubation and were fully depleted after 14 days for sediments from all sampling spots and depths. Nitrate was not detected at the beginning of the incubation, but final nitrate concentrations increased to up to 1.4 mM after 14 days, thus three-fold exceeding initial ammonium concentrations, surprisingly. Ammonium depletion and nitrate accumulation were delayed in 15 cm-microcosms compared to 5 cm sediments (e.g., Fig. 3.2.5). However, final nitrate concentrations were comparable in microcosms from both sediment depths.

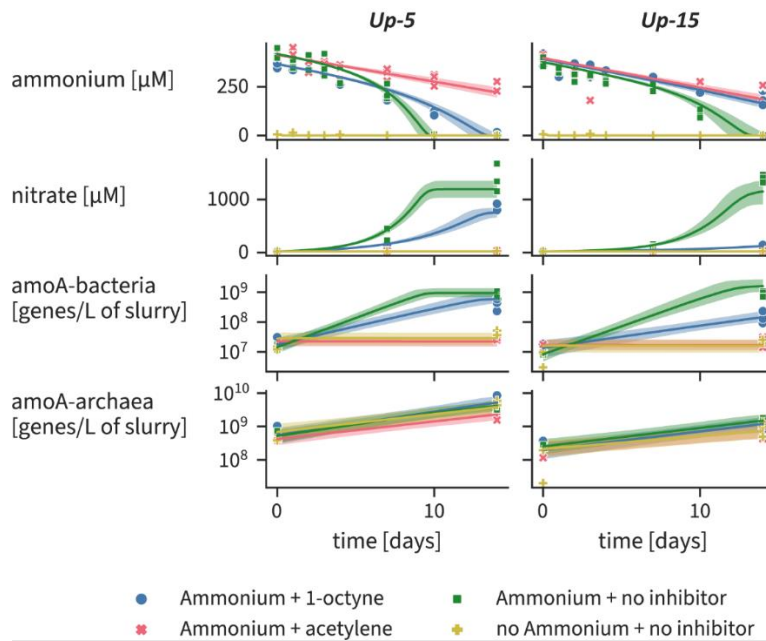


Fig. 3.2.5: Measured and simulated microcosm experiment results (upstream). Time series of ammonium, nitrate, and bacterial/archaeal *amoA* gene concentrations for microcosm from upstream 5 cm and 15 cm sediment samples. Shaded areas span between the 10th and 90th percentile, and lines represent the median of the simulated concentrations. Measurements from different biological replicates are indicated by separate points.

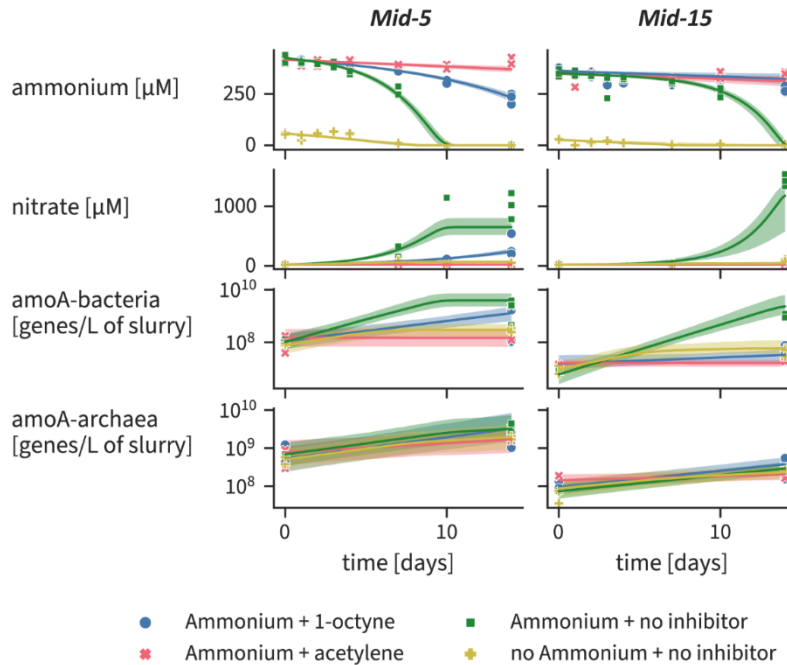


Fig. 3.2.6: Measured and simulated microcosm experiment results (Midstream). Time series of ammonium, nitrate, and bacterial/archaeal *amoA* gene concentrations for microcosm from midstream 5 cm and 15 cm sediment samples. Shaded areas span between the 10th and 90th percentile, and lines represent the median of the simulated concentrations. Measurements from different biological replicates are indicated by separate points.

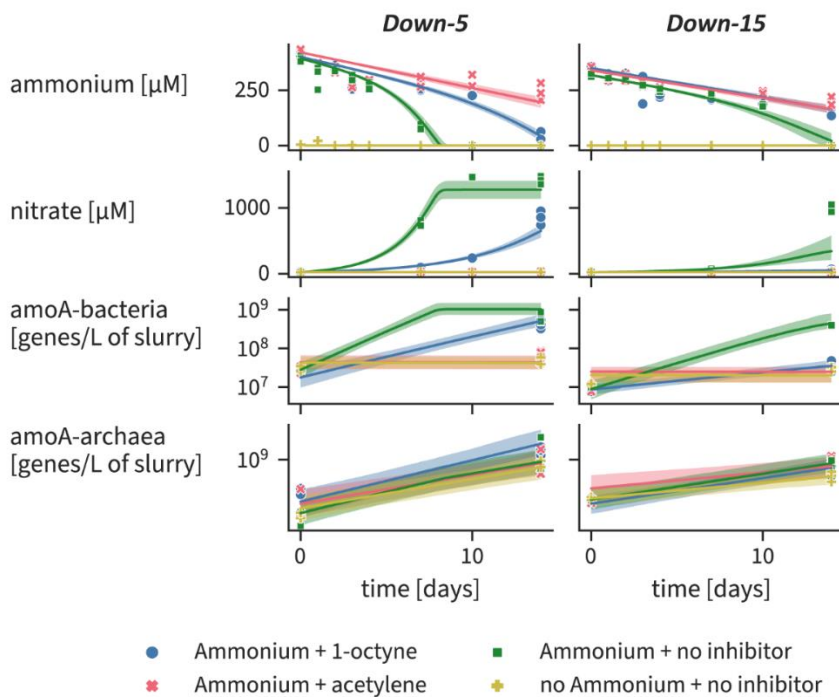


Fig. 3.2.7: Measured and simulated microcosm experiment results (downstream). Time series of ammonium, nitrate, and bacterial/archaeal *amoA* gene concentrations for microcosm from downstream 5 cm and 15 cm sediment samples. Shaded areas span between the 10th and 90th percentile, and lines represent the median of the simulated concentrations. Measurements from different biological replicates are indicated by separate points.

Microcosms amended with different chemical nitrification inhibitors exhibited distinct temporal patterns of ammonium concentrations over incubation (e.g., Fig. 3.2.5). Microcosms amended with ammonium and 6 μM acetylene (inhibitor of autotrophic nitrification by AOA and AOB) served as a proxy for measuring nitrification by heterotrophic microorganisms. Within this treatment, ammonium remained at constant concentration and no nitrate formation could be detected in all microcosms (5 cm and 15 cm). Microcosms amended with 4 μM 1-octyne (inhibitor of nitrification by AOB) served as a proxy for measuring nitrification by AOA. Here, a marked decrease of ammonium was detected, especially in the 5 cm-microcosms. In contrast to the increase of nitrate to up to 0.9 mM in upstream microcosms, 15 cm-microcosms supplemented with 1-octyne showed only a minor decrease in ammonium (of up to 0.2 mM) and nitrate remained below the detection limit after 14 days. Control microcosms (i.e. contained only sediments without amendment of ammonium and chemical

inhibitors) showed neither a decrease of ammonium, nor nitrate production over the incubation period (excluded from the plot). Apart from microcosms with sediments, two sets of control groups amended with stream water only showed no changes in ammonium concentration (excluded from the plot).

Bacterial and archaeal 16S rRNA and *amoA* genes in microcosm samples were quantified via qPCR as a proxy for total microbial populations and ammonia oxidizer abundances during incubation, respectively (Fig. 3.2.5 & Fig. 3.2.6 & Fig. 3.2.7 & Table S2.4). The abundance of bacterial 16S rRNA genes ($\sim 10^8$ copies $\text{g}_{\text{ww}}^{-1}$ sediment) was roughly one order of magnitude greater than the abundance of archaeal 16S rRNA genes prior to incubation. *In-situ* archaeal *amoA* abundances ranged from 4×10^5 to 2×10^6 gene copies $\text{g}_{\text{ww}}^{-1}$ sediment, thus exceeding the abundance of bacterial *amoA* genes, ranging from 3.5×10^4 to 3.6×10^5 gene copies $\text{g}_{\text{ww}}^{-1}$ sediment. Archaeal *amoA* gene counts showed a moderate increase (reaching up to $1.91 \times 10^7 \pm 2.72 \times 10^6$ gene copies $\text{g}_{\text{ww}}^{-1}$ after the incubation) in all microcosms over the incubation. In contrast, bacterial *amoA* genes abundances increased by up to two orders of magnitude in several microcosms (reaching up to $1 \times 10^7 \pm 5.6 \times 10^6$ gene copies $\text{g}_{\text{ww}}^{-1}$ after incubation). An increase of bacterial *amoA* abundances was only observed in microcosms with nitrate production (that is, in treatments without inhibitor and with 1-octyne, always in 5cm microcosms, and only upstream for 15cm microcosms).

3.2.2.2 Simulated dynamics of nitrogen and ammonia oxidizing communities

Note: The Model was conceived and calibrated by our project partners Anna Störiko and Holger Pagel of the Universities of Tübingen and Universities of Hohenheim, respectively, using the experimental data generated by myself. Since both, experiment and modelling are crucial to interpret nitrification activities in my microcosm experiment, these are both reported on in this section. No credit is claimed by the PhD candidate on the modelling itself. A detailed description of the modelling approach is given in section SI.2 for a complete account, and as the respective manuscript is under review at the time of dissertation submission.

Overall, the simulations of the reaction model reflected the patterns of measured concentrations of chemicals and functional genes (e.g., Fig. 3.2.5). Model-predicted ammonium concentrations decreased consistently over time in treatments with ammonium and no inhibitors, or with 1-octyne. The strongly reduced ammonium depletion in treatments with acetylene was also captured by the model. According to the model, the observed slight ammonium depletion was attributed to the incorporation of ammonium into microbial biomass. The model further correctly captured the observed increase of nitrate in the ammonium-amended microcosms without an inhibitor or with 1-octyne, and nitrate rise to levels exceeding the initial ammonium concentration. Only in microcosms *Mid-5* and *Down-15*, the model underestimated final nitrate concentrations (Fig. 3.2.6 & Fig. 3.2.7).

A comparison of the prior and posterior parameter distribution revealed how well the measurements constrained the model parameters controlling ammonia oxidation. For example, the posterior distributions of half-saturation constants for archaeal ammonia oxidation, and the 1-octyne-inhibition parameter for AOA were nearly identical to prior distributions (Fig. S2.2 & Table S2.2), and only little information was gained from the data. Other posterior distributions, however, were characterized by strong shifts of the distributions compared to prior parameter distributions, or much narrower parameter ranges. For example, maximum ammonia oxidation rates shifted to larger values for AOB, but to smaller values for AOA. Also, K_{AOB} shifted to smaller values, which were in the lower range of reported experimental values (Jung et al., 2021). Moreover, no substantial differences in parameter estimates were observed between microcosms from different stream segments (Fig. S2.2). Moreover, parameter differences based on sediment depth were small, but noticeable for some parameters, such as the 1-octyne inhibition (measured by estimated f_{inhib}) and maximum specific ammonia oxidation rate.

The model-based posterior estimates of total nitrification, that is, nitrification rates integrated over time (Fig. S2.1), revealed the contributions of AOA and AOB to nitrification in the microcosms. AOB appeared almost exclusively responsible for ammonia oxidation, whereas AOA played a very minor role, particularly when ammonium was added to the microcosms. The calculated median contribution of AOB in the treatments amended with ammonium and without inhibitors exceeded 96% for all sediment samples. When AOB were partly inhibited by 1-octyne, the model-estimated contribution of AOA to nitrification was no longer negligible, but still much lower than that of AOB (median values for AOA range from 1% to 25%). Archaeal nitrification reached the highest contribution in microcosms where no ammonium was added (median values between 2% and 78%).

3.2.3 Diversity and composition of AOB gene pools in microcosms

As the ammonia oxidation appeared to be primarily driven by AOB in the investigated sediments, I further interrogated the diversity of AOB gene pools via sequencing of *amoA* amplicons. A total of 764 OTUs were generated at 95% sequence similarity cutoff. Observed OTUs richness and Shannon indices were calculated for each of the stream segments before and after the incubation (Fig. 3.2.8). Generally, AOB *amoA* gene pools from 5 cm samples showed a higher richness and Shannon diversity than those from 15 cm samples. Upstream samples had the lowest richness (mean=93 OTUs) in comparison to midstream (mean=219) and downstream samples (mean=178). In addition, richness after incubation (T14) was generally equal or greater than before (T0). Downstream 5 cm microcosms (amended with ammonium) had the highest total number (370) of AOB *amoA* OTUs after incubation. Shannon diversity was generally consistent with observed *amoA* richness (Fig. 3.2.8). AOB *amoA* diversity was highest in midstream and downstream 5 cm samples. There was a decrease for upstream 15 cm, midstream 15 cm, and downstream 5 cm samples during

incubation. Moreover, I did not observe treatment-specific patterns for either richness or diversity indices.

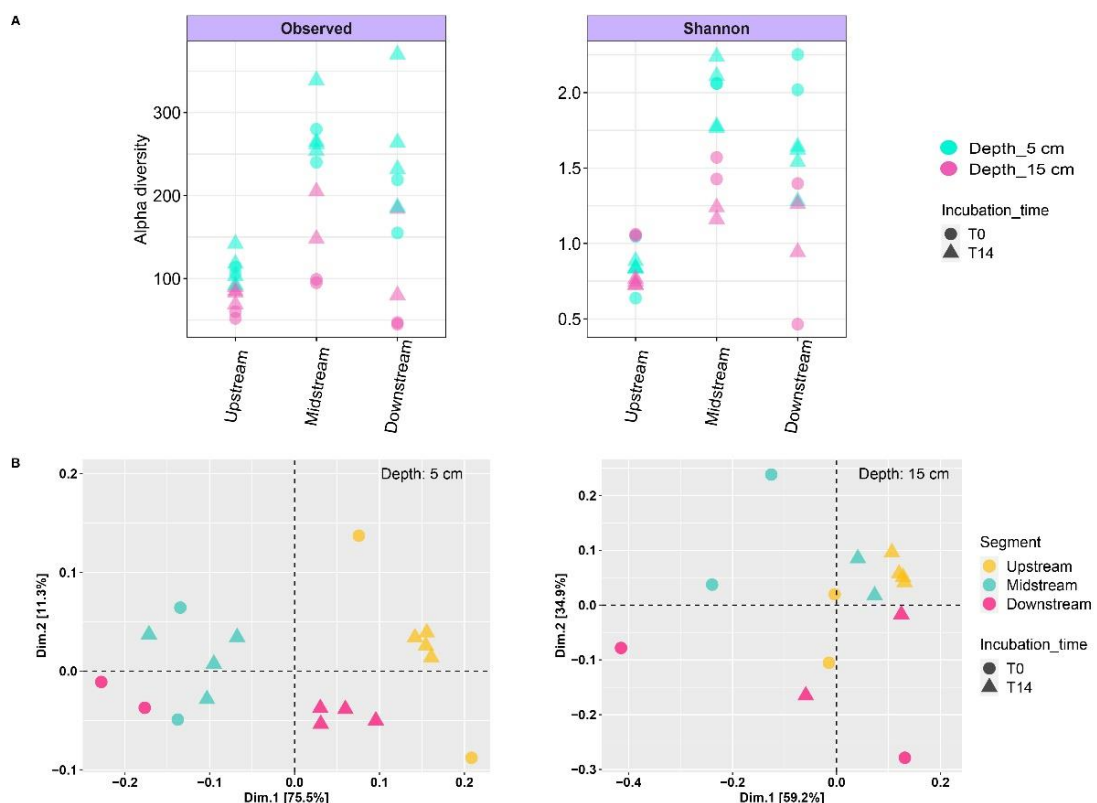


Fig. 3.2.8: Alpha diversity and PCA plots of bacterial *amoA* OTUs. (A). Observed richness (“Observed”) and Shannon diversity (“Shannon”) indices of bacterial *amoA* OTUs in 5 cm depth and 15 cm depth before (T0) and after incubation (T14). (B). PCA plots of bacterial *amoA* OTUs in 5 cm depth and 15 cm depth of different stream segments (upstream, midstream, and downstream) before (T0) and after incubation (T14).

The composition of *amoA* gene pools indeed varied between stream segments, with incubation time, and depth (Fig. 3.2.8B). For 5 cm sediments, the upstream *amoA* gene pools appeared separated from midstream and downstream samples before the incubation (T0). After incubation (T14), samples from upstream, midstream, and downstream formed three distinct clusters, while *amoA* composition in upstream and downstream samples shifted most markedly from T0 samples. Yet, the shift of *amoA* communities was not significant for midstream samples. At 15 cm depth, very similar *amoA* gene pools were observed for almost

all samples at day 14, despite heterogeneity at day 0. Overall, there was no clear community shift observed within the different treatment groups (Excluded from the plot).

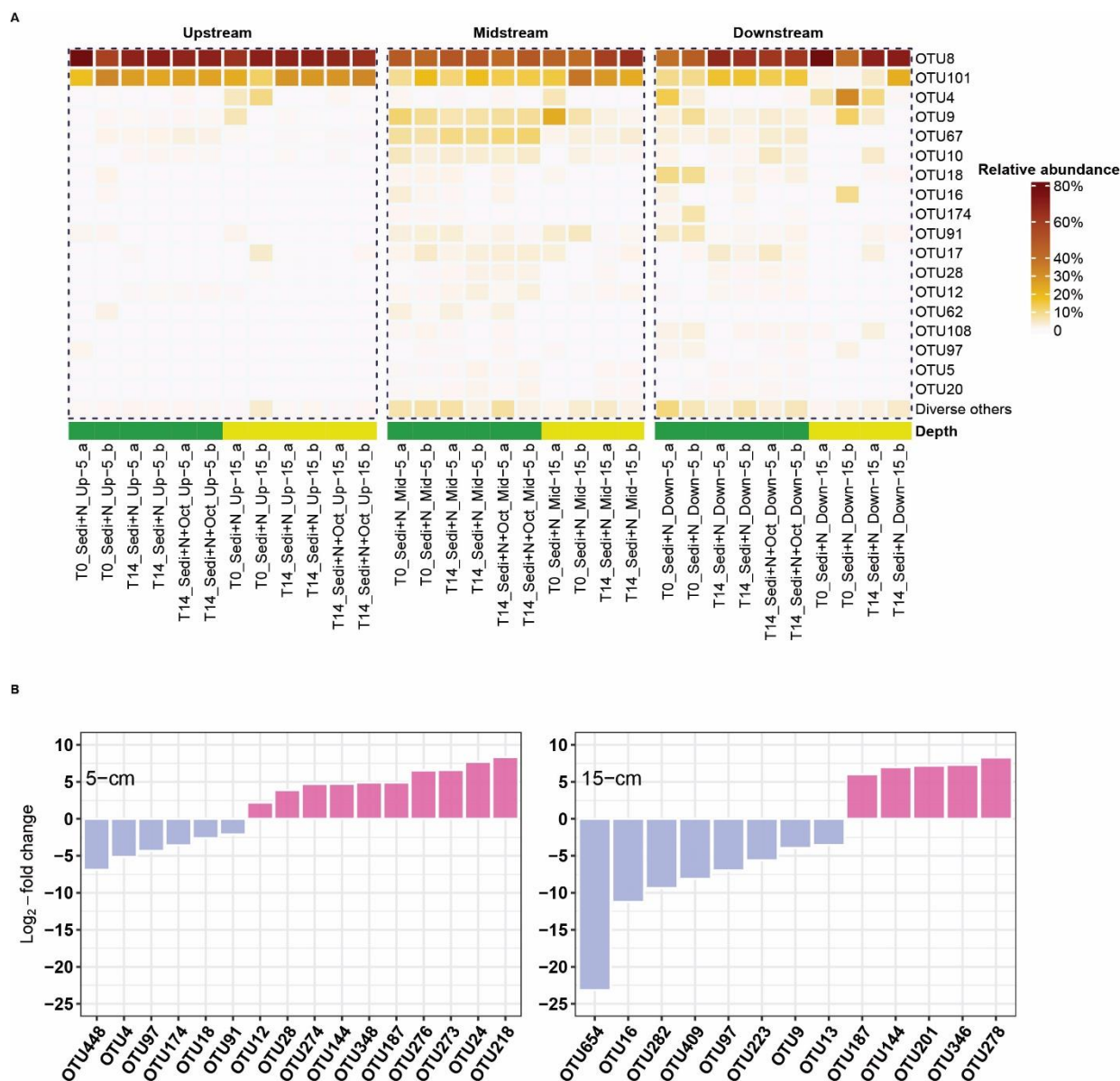


Fig. 3.2.9: Shift of bacterial *amoA* diversity before and after incubation. (A). Relative abundance of bacterial *amoA* OTUs before (T0) and after (T14) incubation in different treatments, stream segments, and depths of two replicate microcosms. Two major treatments were included: sediment amended with ammonium (Sedi+N), and sediment amended with ammonium and 1-octyne (Sedi+N+OCT). “Up”, “Mid”, and “Down” in the sample name on X-axis suggest sampling location upstream, midstream, and downstream, respectively. The sample name suffix “a” and “b” suggests biological duplicates. Low abundant OTUs were merged into “Diverse others” (when a OTU’s cumulative abundance in all samples < 2%). (B). Bacterial *amoA* OTUs whose abundance differed before (T0) and after (T14) incubation in each depth across two major treatments mentioned above.

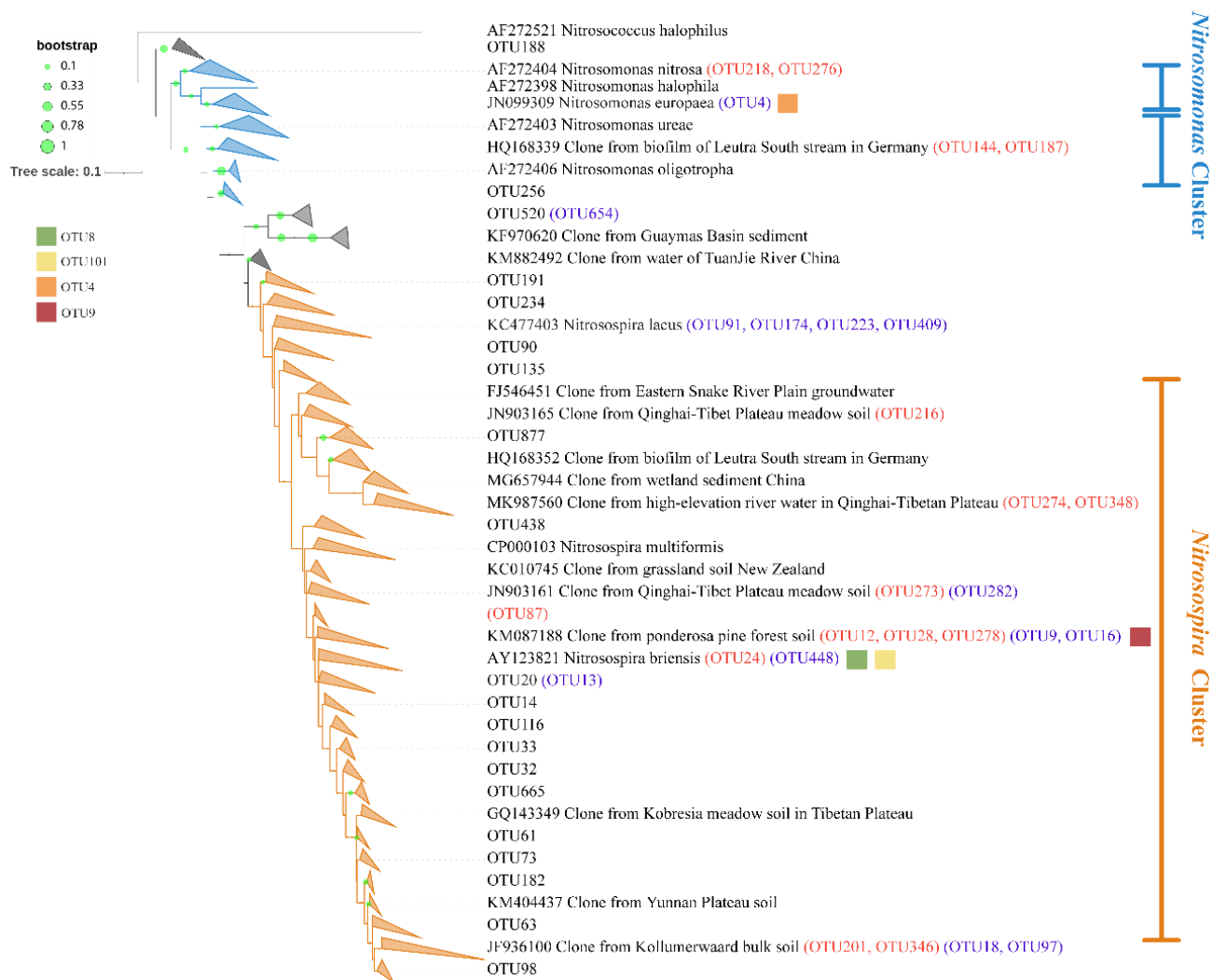


Fig. 3.2.10: Maximum likelihood phylogenetic tree generated from a nucleotide-based alignment of all bacterial *amoA* OTU sequences detected in this study from distinct depths and treatment groups. Colored squares indicated phylogenetic affiliations of four most abundant OTUs from Fig. 3.2.9A. Blue color clusters are at least 85% identical to *Nitrosomonas* isolates, whereas red color clusters are at least 85% identical to *Nitrospira* isolates. OTU names in red color parentheses represented OTUs whose abundance positively changed after incubation as shown in Fig. 3.2.9B, whereas OTU names in purple color parentheses represented OTUs whose abundance negatively changed after incubation as shown in Fig. 3.2.9B. Within each branch on the tree (triangle symbol), more OTUs were collapsed within this branch if these OTU's average branch length distance to their leaves is below 85%.

Among the 764 OTUs of bacterial *amoA* detected, the mean relative abundance of OTU8, OTU101, OTU4, and OTU9 in all samples was 87.6% (Fig. 3.2.9). OTU8 (mean relative abundance 60%) and OTU101 (mean relative abundance 19.4%) were the most predominant OTUs in almost all samples, whereas OTU4 was more abundant in T0 samples,

and OTU9 was more abundant in midstream and downstream samples. Phylogenetic analysis revealed that 57 out of 764 OTUs were clustered with *Nitrosomonas amoA* sequences, while the rest was grouped with *Nitrospira*. Thus suggests *Nitrospira* spp. as dominant and widely distributed bacterial nitrifiers in the Schönbrunnen sediments. OTU4 was identified as *Nitrosomonas* sequences (100% identical to *N. europaea*). OTU8, OTU101, and OTU9 were *Nitrospira* or *Nitrospira*-like sequences (Fig. 3.2.10). These three dominant OTUs were related to *N. briensis* (87-89% identity).

The bacterial *amoA* OTUs that were differentially abundant after the incubation were identified (Fig. 3.2.9B; $p_{\text{adj}} < 0.05$). Of all the bacterial *amoA* OTUs detected in this study, 13 of these had significant greater abundances after incubation in microcosms amended with ammonium. In general, there were more OTUs of which the abundance increased in 5 cm samples than in 15 cm samples. Two OTUs (OTU144 and OTU187), which were affiliated with *Nitrosomonas* lineages, were found more abundant after incubation in both depths. Further OTUs were more prevalent after the incubation in one specific depth only; they mostly clustered with *Nitrospira* sequences. (Fig. 3.2.9 & Fig. 3.2.10). Interestingly, two of the most abundant OTUs (OTU9 and OTU4) were less abundant after incubation.

3.3 Metagenomics of the Schönbrunnen streambed microbiome

As the third part of the dissertation, my main objective was to evaluate the functional potentials, especially functions on nitrogen and sulfur cycling, of streambed microbial communities through metagenomics sequencing. A list of the MAGs with acceptable quality with completeness and contamination information is shown in Table S3.1. Besides this, sulfide measurement conducted on streambed sediment samples provided solid evidence that total sulfide concentrations can reach $\sim 50 \mu\text{M}$ at a depth of 2 cm (Fig. S3.2). Therefore, genomics evidence shown in this section is more meaningful as both reduced sulfur species and nitrate can co-present at the same space under the top surface sediment of the Schönbrunnen streambed.

3.3.1 The streambed microbiome compared via amplicon and shotgun metagenomic sequencing

In this section, a total of eight samples from shotgun metagenomic sequencing and 31 samples from amplicon sequencing taken in summer (September) of the year 2018 were subjected to streambed microbiome analyses. I first compared streambed bacterial communities by these two sequencing approaches (Fig. 3.3.1). In sum, shotgun metagenomic sequencing detected a total of 376 bacterial families, in contrast to a total of 660 bacterial families detected in amplicon libraries (both excluding “unclassified Bacteria”, those not assigned at the phylum level or above). The majority of families observed in shotgun metagenomics were also recovered by amplicon sequencing. Amongst the 30 most abundant families detected by amplicon sequencing, 12 were also observed and ranked as most abundant taxa in shotgun metagenomics, including typical reduced sulfur oxidizing lineages, such as the *Hydrogenedensaceae* (dominated by *Thiobacillus* spp.), as well as typical nitrogen-cycling lineages. These lineages included the *Comamonadaceae* (dominated by *Acidovorax* spp.), *Nitrosomonadaceae* (dominated by MND1), *Xanthobacteraceae* (dominated by *Bradyrhizobium* spp.), and *Xanthomonadaceae* (dominated by *Arenimonas*

spp.). These taxa were also found to be abundant in the previous sampling season, as described in the section 3.1 (Z. Wang et al. 2022). Moreover, other typical sediment and aquatic lineages were also observed to be abundant, such as the *Clostridiaceae* (dominated by genus *Clostridium sensu stricto* 13), the *Oxalobacteraceae* (dominated by *Massilia* spp.), and the *Pirellulaceae* (dominated by *Pirellula* spp.). Members of the *Planococcaceae* (dominated by *Paenisporosarcina* spp.) were identified as the most abundant (mean relative abundance of 9.5%) taxon by amplicon sequencing. Most of these abundant families belonged to the *Proteobacteria*, regardless of the sequencing approach. However, overall taxon ranking was mostly inconsistent between both sequencing approaches. Shotgun metagenomic sequencing detected a larger number of unclassified families to be dominant in samples than amplicon sequencing. Specifically, the *Actinobacteriota* and the *Chloroflexi* were clearly more highly represented in shotgun metagenomic data than in amplicon libraries.

In the domain Archaea, 28 families (excluding “unclassified Archaea”) were found in the samples via shotgun metagenomic sequencing based on 16S rRNA genes (Fig. 3.3.2). Reads classified as Archaea took up only 3% of total 16S rRNA genes detected by shotgun metagenomics. Full-length amplicon sequencing was not applied for archaeal communities and thus cannot be compared here. In metagenomics, ammonia-oxidizing archaeal lineages, including the *Nitrosopumilaceae* and *Nitrososphaeraceae*, were amongst the most abundant lineages detected. Apart from that, some typical methanogens within the families *Methanosaetaceae*, *Methanosarcinaceae*, *Methanoregulaceae*, and *Methanocellaceae* were also abundant. Unclassified Bathyarchaeia and *Nitrososphaeraceae* were the most abundant archaeal lineages detected across all metagenomic samples. In general, samples taken from deeper depths (~15cm) showed more diverse Archaea. Typical methanogenic lineages were also more abundant in deeper depths, especially in the metagenomic sample of *Mid-B_15*.

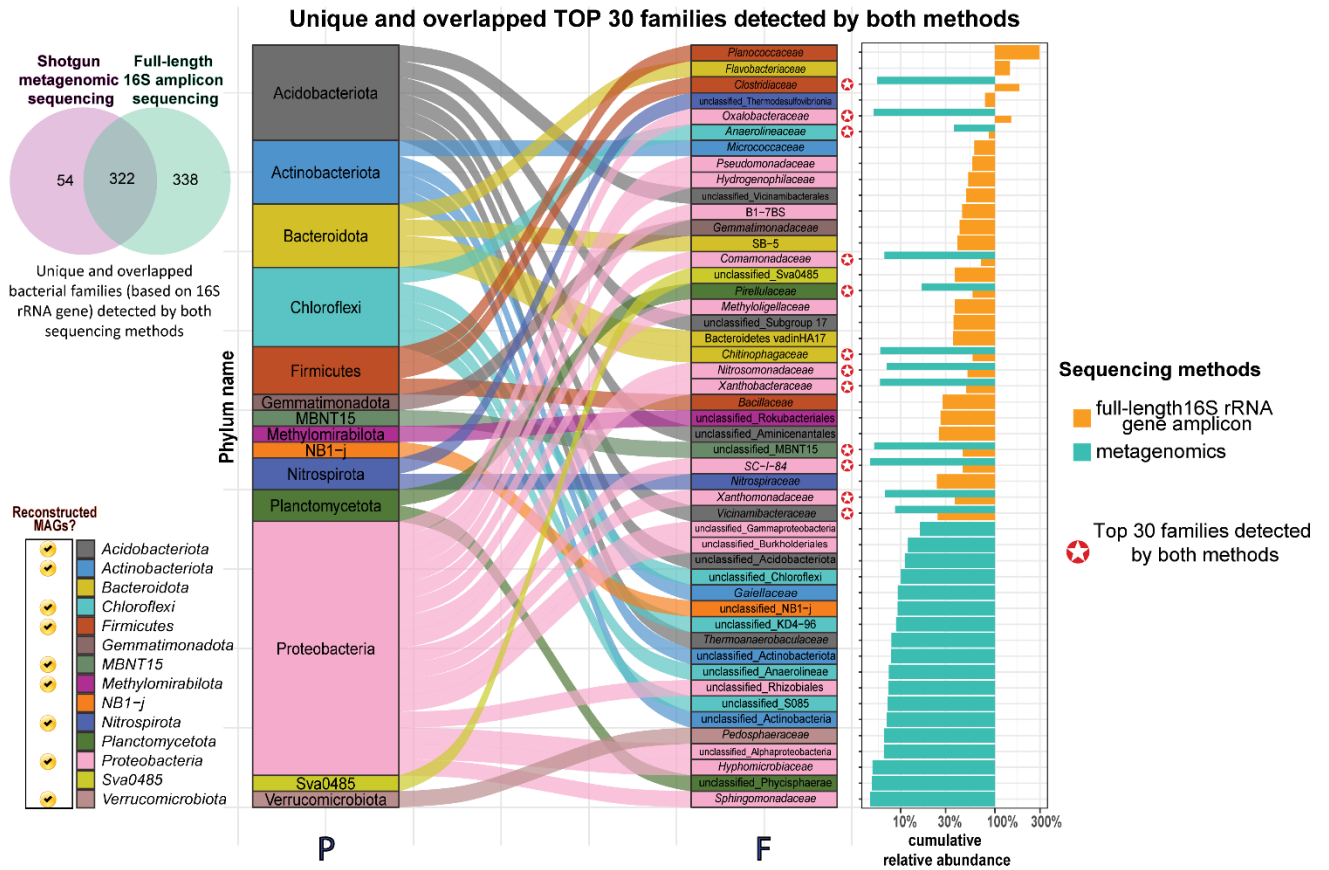


Fig. 3.3.1: Top 30 most abundant streambed microbial lineages detected at the family level. Unique and overlapping top-30 most abundant (cumulative abundance amongst all samples) families detected by either amplicon or metagenomics sequencing (based on 16S rRNA genes detected) are shown in the column F. Families detected by both sequencing approaches and ranked amongst the top-30 most abundant are marked by a star symbol. Cumulative abundances were log₁₀-transformed. Phylum level grouping of families amongst the top 30 are shown in the column P. Y-axis of the column P indicates number of families within a phylum. On the left-bottom side, phyla with at least one representative reconstructed MAG are highlighted with a yellow symbol.

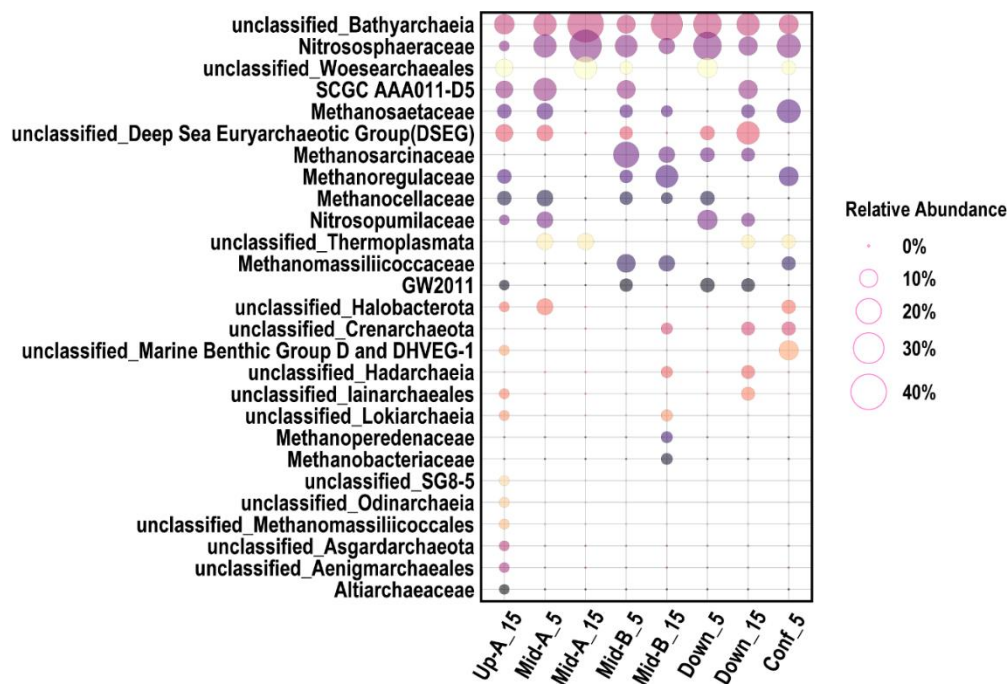


Fig. 3.3.2: Archaeal communities at the family level detected by shotgun metagenomic sequencing (based on 16S rRNA genes detected in all samples). Taxa on the Y-axis are ranked from high to low (top to bottom) according to the total relative abundance in all samples.

3.3.2 Linking microbial nitrogen and sulfur cycling

In section 3.1, a possible link between microbially-mediated nitrogen and sulfur cycling in the Schönbrunnen was first proposed via amplicon sequencing. In this section, I considered all relevant functional genes annotated from shotgun metagenomics data to further interrogate metabolic potentials for a presumed nitrate reduction driven by reduced sulfur species in the streambed. Overall, a strong correlation was observed between reduced sulfur oxidation gene families (sox genes) and nitrate reduction gene clusters, as suggested by a mixed-effect model ($p < 0.001$) (Fig. 3.3.3). Generally, nitrate reduction genes and reduced sulfur oxidation genes had similar relative abundance in *Mid-A* and *Down* samples, regardless of the depth. Conversely, gene abundances showed depth patterns at *Mid-B*. Both nitrate reduction genes and reduced sulfur oxidation genes had greater abundance in the 5 cm than the 15 cm *Mid-B* sample. Moreover, despite there was an overall positive correlation between nitrogen and sulfur cycling genes, not all genes were positively correlated with each other. For

instance, *nirS* genes were not correlated to any reduced sulfur oxidation genes (Fig. 3.3.3).

Similarly, *sorAB* genes had no significant correlation with any nitrate reduction genes.

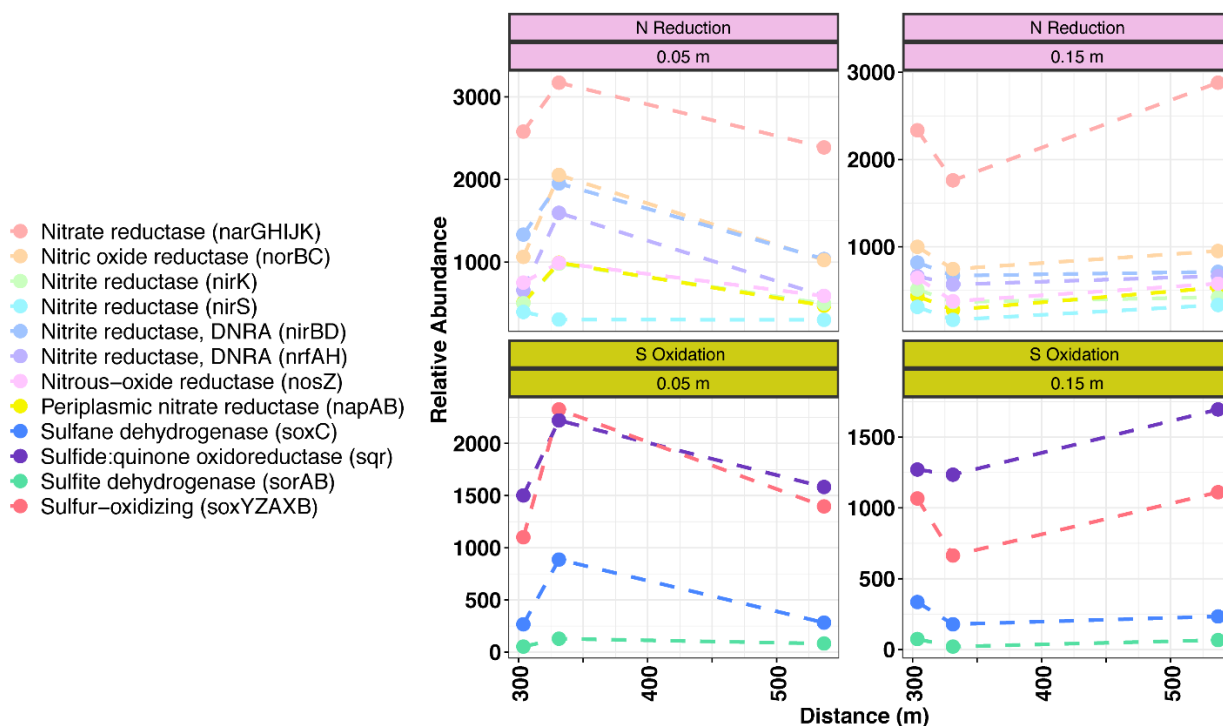


Fig. 3.3.3: Links between nitrate reduction and reduced sulfur oxidation genes observed from the mixed-effect model. Y-axis shows gene relative abundances (read-normalized sequencing depth) detected via shotgun metagenomic sequencing in samples taken from three stream segments. X-axis indicates distance to the boundary of the upstream study area (i.e. stream water source) of the Schönbrunnen. Three points plotted in the figure, from the left to right, represent metagenome sample *Mid-A*, *Mid-B*, and *Down*.

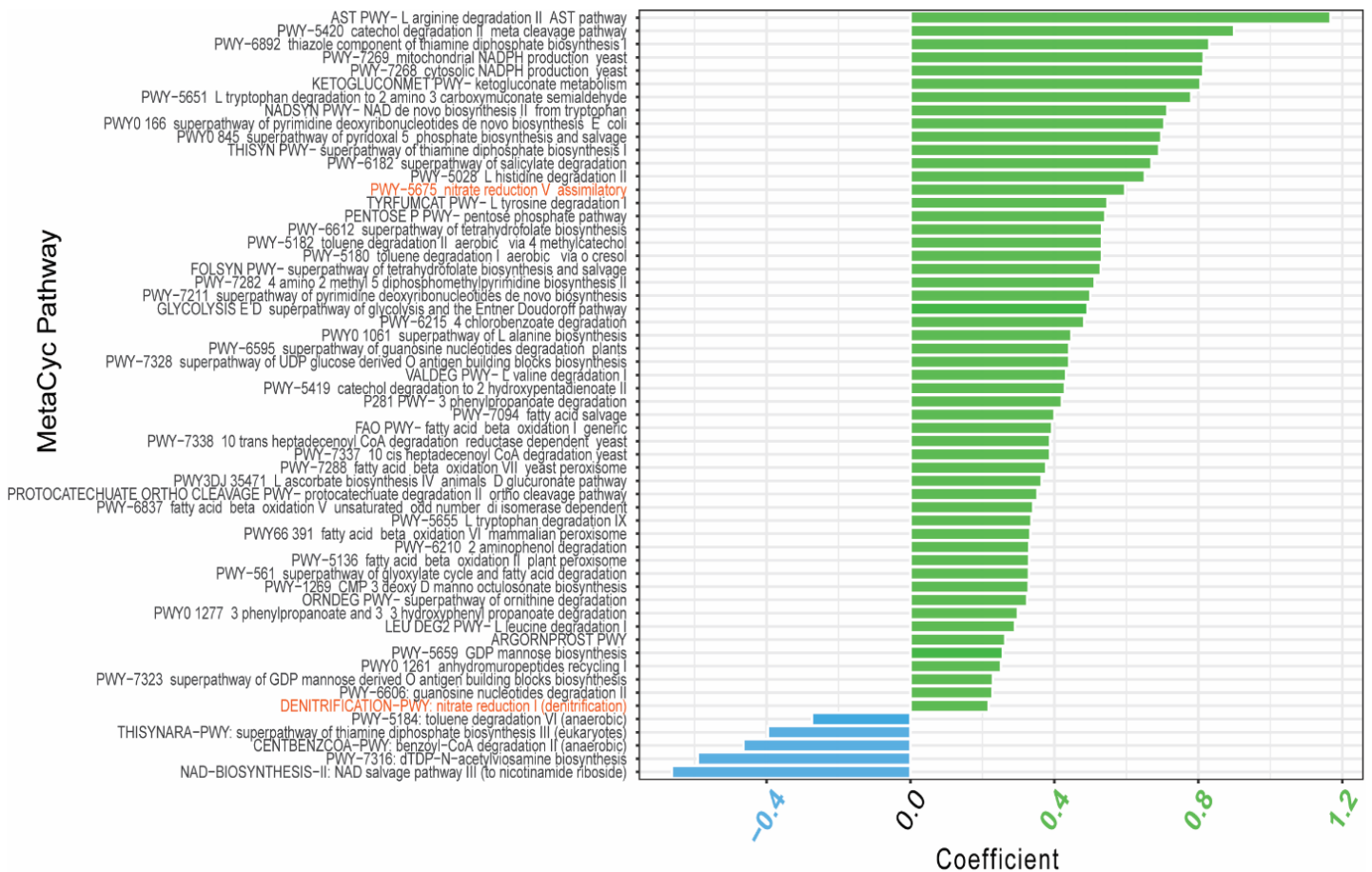


Fig. 3.3.4: Differential abundance of pathways in samples taken from 5 cm (green color) and 15 cm depth (blue color) based on MetaCyc definitions. A greater Z-score standardized coefficient from the MaAsLin2 indicates a higher effect size.

3.3.3 Metabolic capacity of the streambed microbiome

The application of the HUMAnN (HMP Unified Metabolic Analysis Network) 3.0 workflow enabled the identification of key metabolic pathways from metagenomic samples (Fig. 3.3.4). The metabolic capacity of the streambed microbiome was to be suggested from these results. In total, 483 pathways were identified based on MetaCyc pathway definitions. Multiple pathways related to sulfate reduction and nitrate reduction processes were identified. Pathway distribution in metagenomic samples was also investigated in a depth-resolved approach (5 cm vs. 15 cm) (Fig. 3.3.4). In comparison to 15 cm samples, samples from 5 cm depth showed greater differences in pathway abundances. Interestingly, plant-derived carbon decomposition, herbicide degradation (e.g., chlorobenzoate degradation), assimilatory nitrate

reduction, and canonical denitrification pathways were found to be significantly more abundant in the 5 cm depths. Other pathways that were highly abundant at 5 cm were related cellular anabolism, such as sugar and vitamin biosynthesis. In contrast, several pathways related to the anaerobic biodegradation of aromatic compounds were more abundant in 15 cm samples.

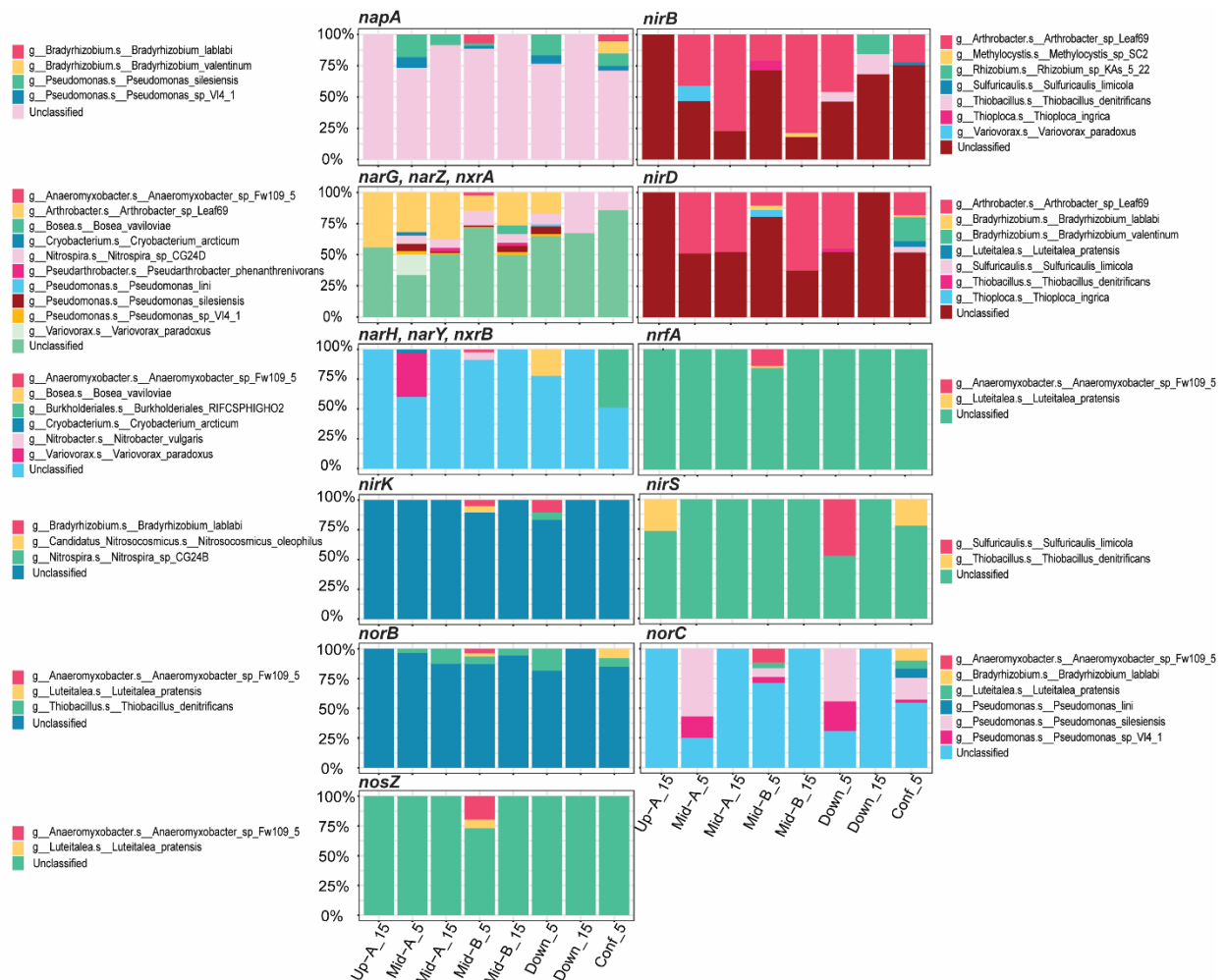


Fig. 3.3.5: Relative abundance of key nitrate reduction gene families as attributed to species-level taxa via HUMAnN 3.0. These included genes encoding for the enzymes of nitrate reduction, *i.e.* nitrate reductase (*napA* and *narG*), nitrite reductase (*nirK* and *nirS*), nitrite reductase for DNRA (*nirBD* and *nrfA*), nitric oxide reductase (*norBC*), and nitrous oxide reductase (*nosZ*).

Besides well-characterized pathways, specific gene families from the metagenome were also considered as markers of the metabolic capacity of the streambed microbiota. By

mapping gene sequences against a UniProt Reference Cluster (UniRef) database (i.e. UniRef90), gene families extracted by HUMAnN were then assigned at the species-level, to suggest the contribution of certain species to given capacities. Especially, I tried to evaluate the contribution of given taxa to representative nitrogen and sulfur cycling genes (Fig. 3.3.4 & Fig. 3.3.5, Table 3.3 & Table 3.4). Despite abundant functional genes involved in nitrogen or sulfur cycling were detected via shotgun metagenomic sequencing, only a very limited proportion of these genes could be classified to species-level taxa. Unclassified gene affiliations suggested that gene sequences did not hit any species-level records within the UniRef90 database.

For the genes encoding nitrate reductases, such as *napA* and *narG*, diverse species were found to be contributing populations, including *Bradyrhizobium* and *Pseudomonas* spp. (Fig. 3.3.5). *Arthrobacter* spp. (class *Actinobacteria*) contributed more than 40% of the *narG*, *narZ*, and *nxrA* gene pools. Yet, their contribution decreased from upstream to confluence samples. Reads of the characteristic DNRA gene *nrfA* could generally not be classified to any species, except to *Anaeromyxobacter* sp. Fw109-5 (class *Myxococcia*). In contrast, another set of typical DNRA genes, *nirBD*, had multiple contributors identified, including species within *Arthrobacter*, *Methylocystis* (class *Alphaproteobacteria*), and *Bradyrhizobium* spp. (Fig. 3.3.5). In fact, *Arthrobacter* contributed nearly 50% of *nirBD* reads in midstream samples. Moreover, typical sulfur-oxidizing populations including *Thiobacillus denitrificans* and *Sulfuricaulis limicola* (class *Gammaproteobacteria*) were also amongst the major DNRA gene contributors, especially in samples from downstream and the confluence.

Amongst canonical denitrification potentials, reads of *nirK* and *nirS* were mostly unclassified. Major taxa identified to contribute to genes of the nitric oxide reductase (*norBC*) and nitrous oxide reductase (*nosZ*) included *Anaeromyxobacter*, *Pseudomonas*, *Thiobacillus* and *Luteitalea* spp. (class *Vicinamibacteria*). *norBC* reads of *Pseudomonas* and *Thiobacillus*

spp. were clearly more frequent in 5 cm samples than 15 cm samples. On the contrary, DNRA metagenome reads (*nirBD*) of the Gram-positive *Arthrobacter* spp. were more prominently represented in 15 cm samples. Intriguingly, genes of the anammox-characteristic hydrazine oxidoreductase *hzo*, hydrazine synthase *hzsABC*, and hydrazine dehydrogenase *hdh*, were classified neither via IMG/MER gene annotations, nor via the UniRef90 database.



Fig. 3.3.6: Relative abundance of key sulfate reduction and reduced sulfur oxidation gene families as attributed to species-level taxa via HUMAnN 3.0. These included genes encoding for the sulfate adenylyl transferase (*Sat*), dissimilatory sulfite reductase (*dsrAB*), adenylyl phosphosulfite reductase (*aprAB*), thiosulfate reductase (*phsA*), reduced sulfur oxidizing multienzyme set Sox (*soxXYZABCD*), sulfide-quinone oxidoreductase (*sqr*).

Gene families that encode for key sulfur-cycling enzymes, such as sulfate adenylyltransferase (*sat*) or dissimilatory sulfite reductase (*dsrA*), were largely not attributed to any species-level taxa (Fig. 3.3.6). Here, *Thiobacillus denitrificans* and *Sulfuricaulis limicola* were two major species observed to harbor these sulfate-reducing genes. Their contribution to *sat* and *dsrA* gene pools increased from upstream to downstream. In general, identified taxa were relatively more frequent at the confluence.

3.3.4 Metabolic potentials of key populations of the streambed as revealed by metagenome assembled genomes (MAGs)

Short-read and long-read data generated by metagenomic sequencing was assembled via a hybrid approach, as well as via Illumina short-read only approaches. As hybrid assembly approaches produced better assembly results (Fig. 3.3.7), only these results are reported and discussed in the following section of this dissertation. The reconstruction of MAGs yielded more than 74 unique (based on Average Nucleotide Identity, ANI) MAGs with at least acceptable quality (contamination between 5%-25%, and completeness >50%) (Fig.3.3.7 & Table S3.1). None of these MAGs were annotated to Archaea. Three MAGs were considered as high-quality (contamination less than 5%, and completeness above 90%). Two of these high quality MAGs were classified as *Actinobacteriota* (*Kineosporiaceae*, *Micromonosporaceae*) according to the Genome Taxonomy Database (GTDB), and one of them belong to the *Proteobacteria* (*Gammaproteobacteria*). However, none of these taxa were represented in the top-30 most abundant families as first shown by amplicon sequencing results (Fig. 3.3.1). Both *Actinobacteriota* MAGs hosted an apparent capacity to fix nitrogen and to be involved in nitric oxide reduction.

Many of the lower-quality MAGs also carried genes relevant for nitrate reduction and/or sulfur oxidation. The majority of these reconstructed MAGs carried genes encoding a nitrate reductase. Besides this, genes encoding for DNRA markers (i.e. *nirBD*, *nrfAH*) were

also represented in some MAGs. These included the MAGs SA.74_Acidobacteriota (class *Vicinamibacteria*), S04.19_Nitrospirota (family *Nitrospiraceae*), S04.16_Proteobacteria (class *Gammaproteobacteria*), SD.34_Proteobacteria (class *Gammaproteobacteria*) SD.32_Desulfobacterota (class MBNT15), SA.70_Nitrospirota (unclassified class), S04.22_Nitrospirota (family *Nitrospiraceae*), and SA.54_Nitrospirota (class *Thermodesulfovibrionia*). Many of these DNRA MAGs were placed within the phylum *Nitrospirota* and the class *Gammaproteobacteria*. Still, *nosZ* genes, encoding nitrous oxide reductases, were not found in any of these specific MAGs. Moreover, the MAGs S04.16_Proteobacteria (class *Gammaproteobacteria*) and k01.33_Gammaproteobacteria (class *Gammaproteobacteria*) contained the *soxXAYZB* and *sqr* genes, and therefore were identified as potential sulfur oxidizers. Based on the other genomic capacity observed for these MAGs (Fig. 3.3.8), the majority of these MAGs seemed to represent facultatively heterotrophic microorganisms.

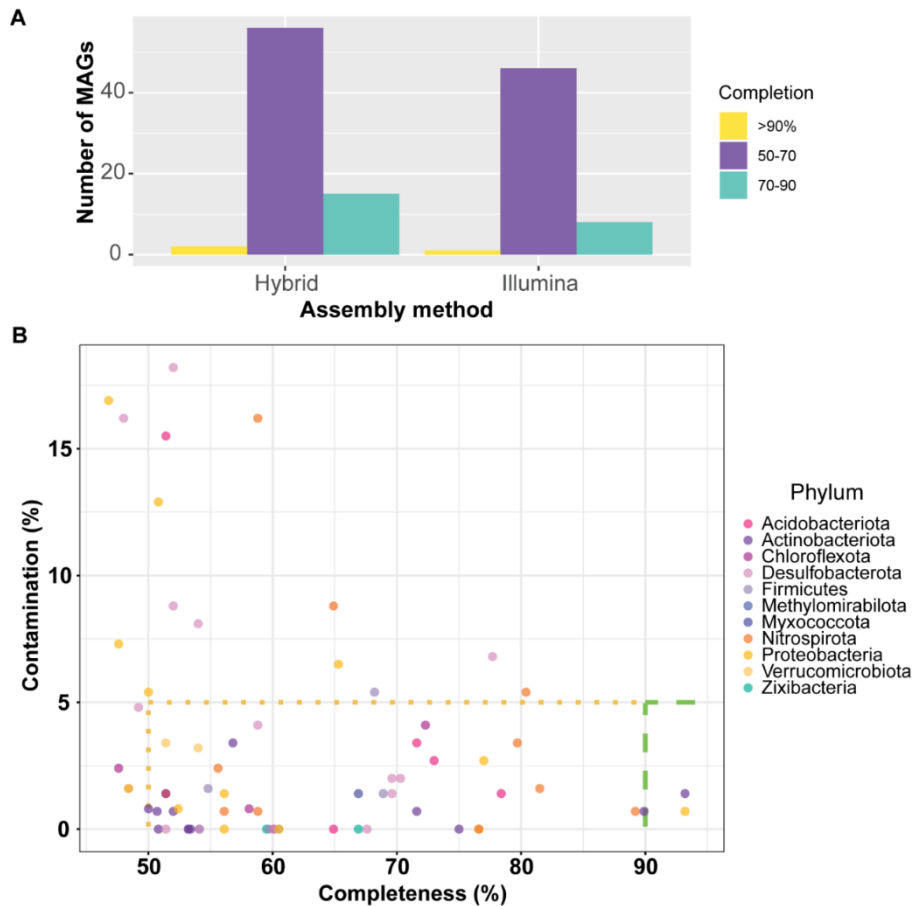


Fig. 3.3.7: Quality of metagenome-assembled genomes (MAGs) reconstructed from streambed samples. (A) MAG obtained via two distinct assembly approaches, Illumina short-reads only and a hybrid assembly (both Illumina short-reads and Nanopore long-reads contained). (B) Quality of single MAGs with completeness and contamination percentage plotted on X- and Y-axis, respectively.

Some but not all of the MAGs also contained at least one copy of partial or complete 16S rRNA genes (Fig. 3.3.8). The longer 16S rRNA genes recovered enabled a robust taxonomic placement of the respective taxa, and for a match between data from shotgun metagenomics and full-length amplicon sequencing. For example, 16S rRNA genes of the MAGs SA.54_Nitrospirota (class *Thermodesulfovibrionia*) and k01.33_Gammaproteobacteria (class *Gammaproteobacteria*) allowed to classify these to belong to the taxa *Thermodesulfovibrio* spp. and to the unclassified B1-7BS (i.e. MAG k01.33) lineage as first found in amplicon data, respectively.

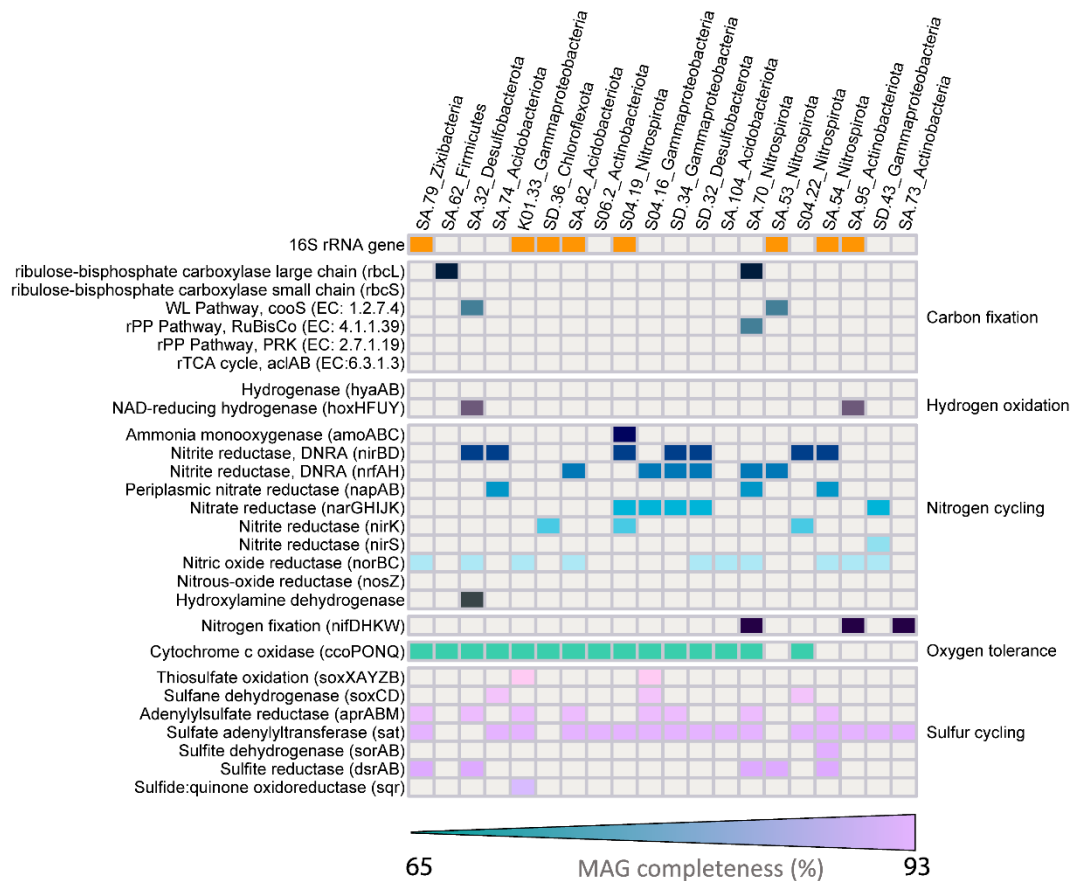


Fig. 3.3.8: Functional features within selected MAGs of the streambed microbiota. MAG quality increases from the left to the right. MAGs that contained a partial or complete 16S rRNA gene sequence are denoted with an orange square.

3.3.5 Core bacterial populations of the Schönbrunnen streambed over three years

Roughly three years of sampling were conducted to identify core microbiome components of the Schönbrunnen streambed and to evaluate their most relevant functional capacities and their distribution. Abundance-occupancy distributions were inferred to identify such core ASVs over different depths (Fig. 3.3.10). Core taxa were defined as those taxa detected in least 50% of amplicon libraries, regardless of their abundance.

Over the three years of sampling, a total of 3187 ASVs were detected across all libraries (Fig. 3.3.9). However, core ASVs were affiliated to only a limited number of families according to the abundance-occupancy distributions. Overall, more core taxa were identified in the 5 cm depths rather than at 15 cm, including typical nitrifying populations within the

Nitrospiraceae and the *Nitrosomonadaceae*. In addition, the *Xanthobacteraceae* (dominated by *Bradyrhizobium*) and the *Hydrogenophilaceae* (dominated by *Thiobacillus*) were also among core communities. Most notably, ASVs of the family-level taxon B1-7BS (*Gammaproteobacteria*) were detected in all 5 cm samples over all three years, regardless of the location. However, *Sulfurcurivum* (*Sulfurimonadaceae*) did not appear to be prevalent and abundant in all sampling seasons.

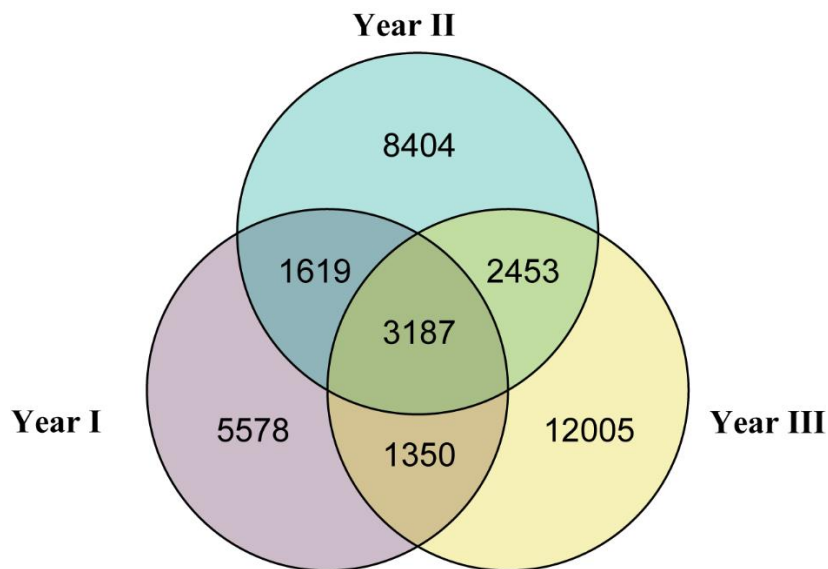


Fig. 3.3.9: Number of unique and shared ASVs based on the by sampling year.

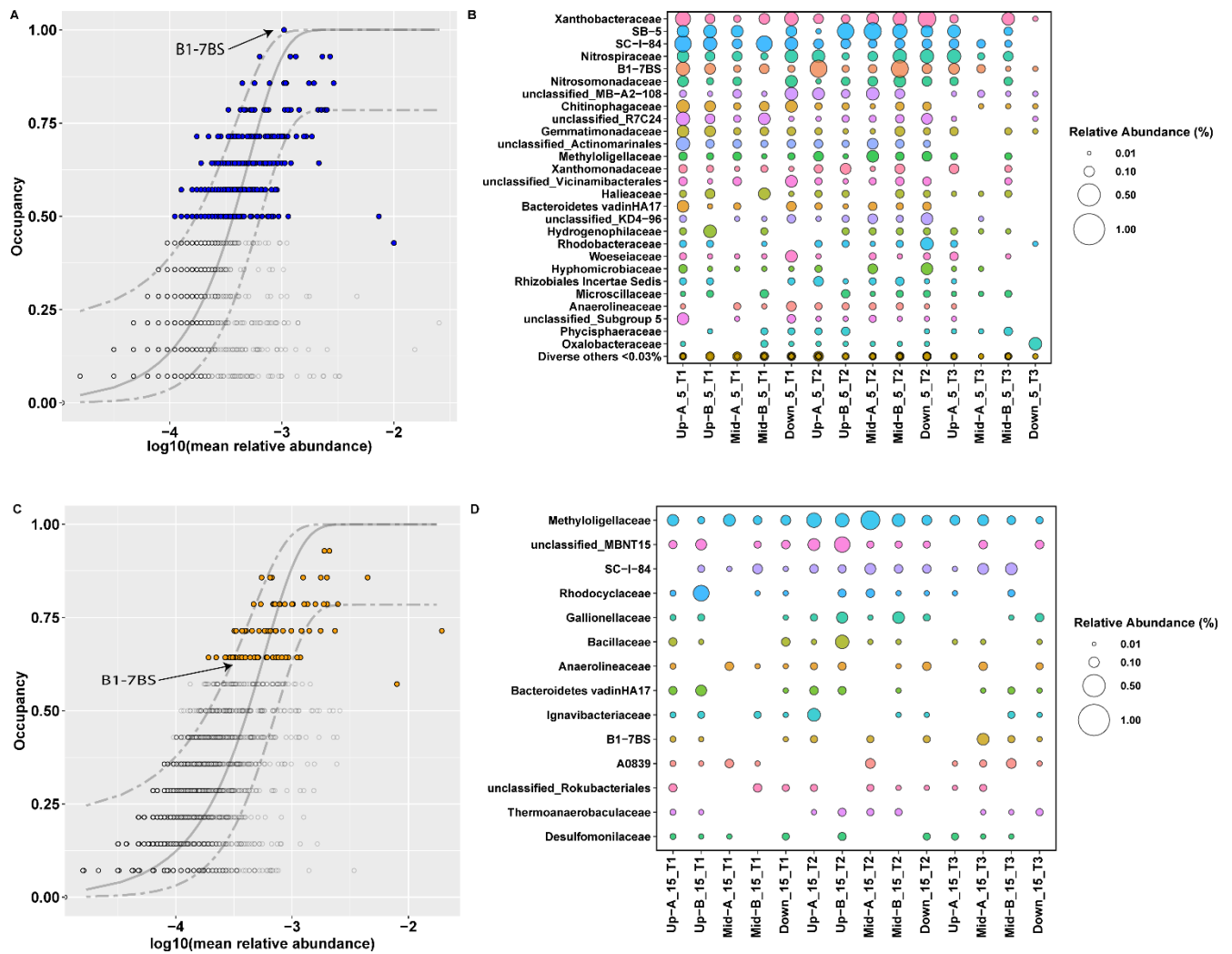


Fig. 3.3.10: Core microbiome in the Schönbrunnen streambed sediments. Each point in the figure (A) and (C) represents a taxon plotted based on its mean log₁₀ transformed relative abundance, and occupancy, in 5 cm and 15 cm samples, respectively. The solid grey line represents the neutral model built involving all taxa. Gray color dashed lines are 95% confidence intervals around the model fit. Those points fall outside of the dashed lines suggest these taxa are deterministically selected (e.g., environmental selection), rather than neutrally presented (e.g., dispersal limitation). Figure (B) and (D) plotted the relative abundance all deterministically selected taxa, in 5 cm and 15 cm samples, respectively. The X-axis represents the sampling location and sampling time (T1=year 1, T2=year 2, and T3=year 3).

4 DISCUSSION

In the investigated stream under the impact of hydrological turnover, not only downward water infiltration fluxes, but also upward groundwater exfiltration fluxes have contributed to the formation of a highly active transition zone in the streambed, which is of great relevance for water quality and the general reactivity of the stream system. The intricate interplay of such hydrological and biogeochemical processes in shaping sedimentary bacterial communities and their activities in nitrogen cycling has not been addressed prior to our study. As will be discussed in the conclusions below, strategies to enhance such bidirectional water exchange in the streambed of agricultural lower-order streams harbor a great potential for nitrate removal in agricultural catchments (Z. Wang et al. 2022). Nonetheless, only few studies have extensively characterized streambed microbiomes and their functional roles in comparable ecosystems to date. In the following Discussion section, I will first direct my attention on stream nitrate loads and nitrate removal microbes. I will elaborate on the impact of bidirectional water exchange on nitrate levels in the stream, and the varying distribution and diversity of potential nitrate-reducing microbial communities. Then I will shift the focus to nitrification – to discuss key ammonia-oxidizing microbial populations and their activities. Finally, functional potentials of diverse of streambed microbial communities will be discussed, with the aim of corroborating the functional significance of signature microbes identified in the first and second studies. Overall, studies discussed here can contribute more insights to help us understand the reactivity of the streambed of agricultural lower-order streams as controlled by hydrological and biological processes.

4.1 Nitrate-reducing microbial populations in the Schönbrunnen streambed as impacted by bidirectional water exchange

4.1.1 Bidirectional water exchange as a control of water chemistry and streambed bacterial communities

The influence of bidirectional water exchange on the biogeochemistry of lower-order streams may represent an under-regarded mechanism for the control of solute fluxes in catchments (Jimenez-Fernandez et al. 2022). Hydrological analyses reported in this study delineate the Schönbrunnen from upstream to downstream, of which upstream and downstream sections were identified as net gaining, whereas midstream sections were identified as net losing reaches, irrespective of small-scale local heterogeneities of gross bidirectional fluxes revealed by salt tracer tests (e.g., location *Mid-A*). It has been previously proposed that such net losing reaches could represent reactive hot spots for denitrification along infiltrating river water (Trauth et al. 2018). Under losing conditions, microbial denitrification will largely depend on sediment-borne electron donors and on DOC that is still available after oxygen depletion from the infiltrating stream water. Water leaving the Schönbrunnen in midstream net losing sections, however, may not immediately return to the stream, or return to the stream as groundwater exfiltration only after a prolonged travel distance and mixing with the surrounding groundwater. Mixing of stream and groundwater is not likely in the first few decimeters below the streambed. This differentiates the hydrologic setting of the Schönbrunnen from typical hyporheic flow and hyporheic exchange processes, in which stream water infiltrates into the streambed and directly returns to the stream over short flow distances, mainly induced by complex streambed morphology (Bayani Cardenas and Wilson 2006; Hester, Young, and Widdowson 2013).

However, if nitrate reduction is largely associated with infiltrating water fluxes, nitrate concentrations in the stream water of net losing reaches (e.g., midstream) should remain relatively constant. This was indeed observed in our study (Fig. 2.1.2B). Instream nitrate

concentrations only decreased in downstream net gaining reaches (R5 and R6), where adjacent groundwater depleted in nitrate (Fig. 2.1.2B) and enriched in sulfate (and likely also sulfide or other reduced sulfur species as evidenced in Fig. S3.2) entered the Schönbrunnen. Under gaining scenarios, mixing of groundwater and reduced solutes with the stream water in shallower depths of the streambed should thus result in a distinct reactivity compared to sections of stream water infiltration. Over the Schönbrunnen longitudinal profile, nitrate concentrations appeared tentatively negatively correlated with that of sulfate, indicating that sulfur and nitrogen cycling in downstream net gaining reaches were possibly linked.

Bidirectional water exchange fluxes may not only affect water chemistry, but also shape streambed bacterial communities. The high spatial variability of abiotic factors that determined the local presence and relative abundance of microbial taxa should be apparent in strong deterministic variable selection patterns (Dini-Andreote et al. 2015) over the Schönbrunnen stream. In accordance, microbial communities in top streambed sediments of the Schönbrunnen mostly showed high β NTI values (> 2), indicating strong variable selection (Stegen et al. 2013). This was consistent with previous studies on river sediment bacterial community assembly (Danczak et al. 2016; E. B. Graham et al. 2017). However, dispersal-based stochastic processes, especially homogenizing dispersal processes ($RC_{\text{Bray}} < 0.95$), were found in samples from typical net gaining reaches (e.g., *Up-A*, and *Down*). Homogenizing dispersal patterns can be an indicator of the actual physical transport of organisms (Stegen et al. 2016) and thus might infer the impact of groundwater exfiltration under the specific hydrologic setting of Schönbrunnen.

Homogenizing dispersal patterns were also observed at *Mid-A*, which was located in reach R3 predominated by net losing conditions according to groundwater heads (Fig. 2.1.2A & 3.1.8). However, several lines of circumstantial evidence indicate that *Mid-A* might also be impacted by local exfiltration fluxes of groundwater, similar to upstream and downstream

samples. On the one hand, bidirectional gross fluxes are likely in all reaches. Tracer tests showed that the magnitude of gaining and losing water fluxes in R3 could be comparable (Fig. 2.1.2A). On the other hand, the *Mid-A* 5 cm samples showed similar bacterial community composition as other 15 cm samples, whereas *Mid-B* appeared more representative of the generally net losing conditions midstream (Fig. 3.1.2). Moreover, the presence of a greater abundance of ASVs affiliated with *Sulfuricurvum* spp. was also observed at *up-A*, and *down*, two obvious groundwater exfiltration spots. Such local heterogeneities in gross hydrologic fluxes and streambed microbiomes were fortuitously recovered in our study. As the streambed permeability of the Schönbrunnen is consistently low according to our estimation, the transport of microbial populations and homogenizing processes due to bidirectional water fluxes can be further constrained (Saup et al. 2019). Yet apart from bidirectional water fluxes, substrate factors like fine-scale geochemical heterogeneities (e.g., redox potential and pH), or the sediment matrix may also be relevant in controlling local communities (E. B. Graham et al. 2017; Vos et al. 2013; Jorgensen et al. 2012; Pett-Ridge, Silver, and Firestone 2006). To further document and quantify such patterns at smaller scales, a more comprehensive spatial sampling grid per reach may clearly be necessary in the future.

Dispersal-based assembly processes can lead to rather maladapted local communities and can therefore restrict the biogeochemical potentials and functional stability of specific local communities (E. B. Graham and Stegen 2017). However, in this study, dispersal-based assembly processes were found at locations dominated by exfiltration, in concert with a high abundance of sulfur-oxidizing and autotrophic nitrate-reducing bacteria. Thus, chemolithoautotrophic mechanisms rather than canonical heterotrophic denitrification processes seemed to be prioritized at groundwater exfiltration sections. The extent of the contribution of chemolithoautotrophic nitrate reduction versus physical mixing between nitrate-depleted exfiltrating groundwater and stream water to overall nitrate removal from the

stream in downstream sections remains to be further elucidated. Nevertheless, such fine-scale heterogeneities in exchange fluxes and microbial community structure in streambed sediments have not been reported to date, but present as relevant indicators of streambed reactivity *in situ*.

4.1.2 Hydrological impact on microbial communities potentially involved in nitrate reduction

16S rRNA gene amplicon sequencing data presented in this study suggested that distinct mechanisms could be driving microbial nitrate reduction in the streambed of different sections of the Schönbrunnen. Firstly, the net losing sections appeared to be associated with an increased abundance of heterotrophic denitrifiers in the streambed. Although absolute or relative abundances of denitrification genes were not the highest in this section (Fig. 3.1.9), respective sediment communities (especially in *Mid-B*) were clearly enriched in 16S-reads of typical canonical heterotrophic denitrifier lineages. These included members of the *Rhodobacteraceae* (Tosques et al. 1997; Tarhriz et al. 2013), *Flavobacteriaceae* (Tekedar et al. 2017), *Comamonadaceae* (Khan et al. 2002; J. Wang and Chu 2016), *Rhodocyclaceae* (Fahrbach et al. 2006), all known to host typical *nirK*- or *nirS*-carrying denitrifiers. The abundance of these presumed denitrifiers, especially the *Rhodocyclaceae*, was increased in 5 cm samples of *Up-B* and *Mid-B*, whereas the relative abundance of potential reduced sulfur-driven autotrophic nitrate reducers, including *Sulfuricurvum* and *Thiobacillus* (Kodama and Watanabe 2004; Beller et al. 2006), was relatively low here (Fig. 3.1.5 & Fig. 3.1.6). Dominant genera within the *Rhodocyclaceae* were well-known denitrifiers such as *Denitratisoma*, *Dechloromonas* (Fahrbach et al. 2006; Horn et al. 2005), as well as *Rhodocycilus* spp. (Tang et al. 2020). In turn, potential reduced sulfur-driven nitrate-reducing populations were more abundant in groundwater exfiltration locations, such as *Up-A*, *Mid-A*, and *Down*.

The phylogenetic tree for *Sulfuricurvum* spp. long-read amplicons revealed two major clusters of ASVs distributed between Schönbrunnen and Käsbach (Fig. 3.1.7A). Species-level taxonomy of *Sulfuricurvum* spp. reads was not completely resolved, due to the existence of only a few pure culture isolates (Kodama and Watanabe 2004; C. Han et al. 2012; X. Li et al. 2019; Fida et al. 2021). Even though the Schönbrunnen cluster was mostly related to *Sulfuricurvum kujiense* (Kodama and Watanabe 2004), the Käsbach cluster detected at the confluence did not include any previously reported *Sulfuricurvum* isolates. The currently known *Sulfuricurvum* strains are known for respiratory reduction of nitrate, but not of nitrite (Fida et al. 2021). This suggests that they may participate in incomplete denitrification and/or rely on a complex metabolic network to exchange intermediate reduction products.

In addition, the ASVs of another typical sulfide- and sulfur-oxidizer, *Thiobacillus* spp. (*Hydrogenophilaceae*), were widespread in both Schönbrunnen and confluence sediments (Fig. 3.1.6). Currently, three species have been described within the genus, *T. thioparus*, *T. thiophilus*, and *T. denitrificans* (Boden, Hutt, and Rae 2017). *T. denitrificans* is a well-defined denitrifier and carries the *nirS* genes (Beller et al. 2006). *T. thioparus* and *T. thiophilus* may perform only partial denitrification, reducing nitrate to nitrite (Hutt et al. 2017; Kellerman and Griebler 2009). Thus, both of the detected *Sulfuricurvum* and *Thiobacillus* spp. could have contributed to a sulfide- and/or other sulfur species driven nitrate reduction, especially in streambeds impacted by gaining fluxes.

It has been previously proposed that the infiltration of stream water rich in nitrate and organic carbon may trigger heterotrophic denitrification in streambeds, whereas the exfiltration of reduced groundwater could prioritize autotrophic denitrifiers and DNRA (Fig. 1.4) (Storey, Williams, and Fulthorpe 2004; E. B. Graham et al. 2017). High sulfide levels in aquatic environments has been reported to be in favour of DNRA process (Delgado Vela et al. 2020). DNRA was reported to dominate over denitrification in salt marsh sediments amended

with 100 μM sulfide (Murphy et al. 2020). Although sulfide was not routinely measured in our regular field sampling across the Schönbrunnen catchment prior to this study, total sulfide concentrations measured in sediments in the following year reached values of ~ 50 μM at a depth of 2 cm (Fig. S3.2). Apart from such exemplary porewater measurements, groundwater from the southeastern monitoring wells (e.g., GWS 25) clearly smelled sulfidic upon sampling.

Apart from *Sulfuricurvum* spp., several other lineages detected in my amplicon libraries are also known for DNRA, such as *Geobacter* spp. (van den Berg et al. 2017), members of the *Desulfocapsaceae* (Arshad et al. 2017; Bell et al. 2020), or *Sulfurimonas* spp. (Bell et al. 2020). Generally, *nirK*-carrying denitrifiers have a greater probability of harbouring a respiratory DNRA pathway (*NrfA*) as well, yet *nirS*-carrying nitrate reducers are more likely to perform complete denitrification (Helen et al. 2016). Despite some bacteria carrying both *nirK* or *nirS* genes, most known nitrate reducers only have one copy of either of the two genes (Graf, Jones, and Hallin 2014; Etchebehere and Tiedje 2005). However, even though the distribution pattern of *nirK* genes appeared more related to nitrate concentration in the stream rather than *nirS*, linking *nirK* genes with denitrification rates *in situ* must be done with caution (D. W. Graham et al. 2010; Veraart et al. 2017). To further address this, the site-specific *in-situ* denitrification rates should be determined across reaches.

4.2 Nitrification in the Schönbrunnen streambed

To better understand the contributions of ammonia-oxidizing archaea (AOA) and ammonia-oxidizing bacteria (AOB) to nitrification in the streambed, I conducted a microcosm incubation experiment with distinct chemical inhibitors, and monitored the potential nitrification rates. Together with project partners, a population-based reaction modeling was then conducted to support the interpretation of the incubation results. Despite that both of AOA and AOB lineages were widely distributed across the streambed, their contributions to nitrification were clearly disparate. My findings and the modeling conducted for the microcosm incubation experiment, as well as the importance of AOA and AOB for streambed reactivity, will be discussed in this section.

4.2.1 Simulated ammonia oxidation dynamics

The reaction model was calibrated based on the data from the incubation experiment in order to test the conceptual understanding of processes occurring in the microcosms, and to quantify the contributions of AOA and AOB to nitrification rates. In spite of the overall consistent reflection of measured chemical concentrations and functional genes, the model did underestimate final nitrate concentrations in microcosms *Mid-5* and *Down-15* (Fig. 3.2.6 & Fig. 3.2.7). This incongruence could relate to the relatively simple description of the release of surplus nitrogen from the sediment (as further discussed in section 4.2.2). However, it remains unclear why the model was unable to fit nitrate data of microcosms *Mid-5* and *Down-15* just as well as for other microcosms despite very similar observed patterns. Except for this, simulated and measured growth dynamics of AOA and AOB indeed matched the experimental observations. In particular, the model was able to reproduce the significant growth of AOB in the treatments with high nitrate production, as well as the moderate growth of AOA in all microcosm treatments, regardless of active ammonia oxidation.

The depth impact on model parameters was mostly marginal. Yet, certain differences were observed for some parameters (Fig. S2.2 & Table S2.2) that could point to ecologically interesting distinctions over depth. For example, 1-octyne inhibition (measured by estimated f_{inhib}) was stronger in 15 cm-microcosms compared to 5 cm-microcosms. Furthermore, the maximum specific ammonia oxidation rate was slightly smaller in 15 cm-microcosms, reflecting the observed slower ammonium consumption. Another factor supporting the faster oxidation of ammonium in 5 cm microcosms was the generally higher initial abundances of AOB. Taken together, the modelling of ammonia oxidizer population dynamics in our microcosms suggested a dominating contribution of AOB to streambed nitrification, clearly outcompeting their archaeal competitors in terms of activity and population growth.

4.2.2 Release of ammonium from the sediment

The formation of nitrate, the major product of nitrification, over the incubation largely exceeded the initial concentration of ammonium amended to the microcosms (Fig. 3.2.5 & Fig. 3.2.6 & Fig. 3.2.7). Nitrification is expected to convert ammonium to equal molar concentrations of nitrate (Kuypers, Marchant, and Kartal 2018). Therefore, it seems likely that an additional source of nitrogen, possibly organic nitrogen in the sediment, may have been used as a substrate for nitrification explaining the overproduction of nitrate. Hence, overall ammonia oxidation rates can be underestimated when relying on the depletion of ammonium alone for calculations. Unlike ammonium, which can also be produced by alternative pathways such as urea hydrolysis and/or the mineralization of other organic N, the oxidative formation of nitrate is strictly attributed to nitrification under oxic conditions (Sonthiphand and Neufeld 2014; Levičnik-Höfferle et al. 2012). Therefore, nitrate production rates were selected as the key indicator of nitrification activity in our experiment and modeling approach.

In the model, the release of additional nitrogen by an ammonium production term that depends linearly on the nitrification rate (see Equation 4 in SI.2). This description is based on

the observation that additional nitrate was produced only in microcosms with active nitrification. In most microcosms, this simple empirical relationship seemed to be sufficient to describe the release process, since the disproportionate increase of nitrate observed in the data was reproduced by our model. The median model-estimated ammonium release ranged between 0.38 (*Mid-5*) and 0.85 (*Up-15*) mol of ammonium released per mol of ammonium nitrified. The fact that the model underestimated the pronounced increase of nitrate in microcosms *Mid-5* and *Down-15*, suggests that the model does not describe the ammonium release appropriately in these cases.

Members within the *Nitrosomonas*, *Nitrospira* and *Nitrososphaera* genera, among others, are known to degrade organic nitrogen compounds by hydrolysing urea with ureases, producing additional ammonia for nitrification (Burton and Prosser 2001; Tourna et al. 2011). Moreover, not only ammonia oxidizers are capable of releasing ammonia, also NOB can produce ammonia from urea and benefit by receiving additional nitrite from AOB and/or AOA. This process was described as reciprocal feeding (Koch et al. 2015). Considering that nitrate concentrations did not increase when microcosms were not amended with ammonium, this interaction between NOB and ammonia-oxidizers may be one likely explanation for the surplus ammonium released in our study. However, further analyses of total nitrogen and total organic nitrogen pools would have been necessary to comprehensively delineate these mechanisms.

4.2.3 Incomplete Inhibition of AOB by 1-Octyne

The increase of bacterial *amoA* genes in treatments with 1-octyne, concomitant with an increase in nitrate concentrations, suggests that 1-octyne in microcosms only partially inhibited ammonia oxidation by AOB. To explore this hypothesis, a parameter for the degree of inhibition by 1-octyne (f_{inhib}) was incorporated into the reaction model and estimated its value from the data. The estimated values of f_{inhib} were larger than zero, indicating

incomplete inhibition of ammonia oxidation by AOB (Fig. S2.2). The median values of inhibited rates range between 12% (*Mid-15*) to 62% (*Up-5*) of the uninhibited rate. Overall, the inhibition was stronger in the sediments from 15 cm than from 5 cm. This observation contradicts previous reports suggesting that 1-octyne is capable of robustly inhibiting AOB, both in pure culture cell suspensions and in soil microcosms (Taylor et al. 2013; Hink, Nicol, and Prosser 2017). The incomplete inhibition of AOB might be attributed to the complexity of ammonia-oxidizing communities in the investigated sediments, or sorption to limit bacterial exposure to 1-octyne. This illustrates the importance of experimental design when 1-octyne is applied to determine contributions of AOA and AOB to nitrification. Here, the growth of AOB in presence of 1-octyne helped us to infer incomplete inhibition, but this is only feasible in studies where mixotrophic AOB do not play an important role. In future work, ¹⁵N-labeled substrates could help to further determine the degree of inhibition of AOB by 1-octyne in environmental samples, and to better identify the contributions of either AOA or AOB to ammonia oxidation, under the scenario that AOA and/or AOB grow via other metabolic pathways instead of the ammonia oxidation.

In this study, the combination of partial 1-octyne-inhibition of AOB, the mixotrophic or heterotrophic growth of AOA, and the apparent presence of additional nitrogen sources very much complicated the direct inference of nitrification rates, population-specific growth rates, and the contributions of AOA and AOB to gross nitrification from experimental data alone. Here, linking the experimental data with a process-based reaction model was a clear asset to disentangle and quantify the impact of these factors, and to better estimate population-specific nitrification rates and uncertainties.

4.2.4 Contributions of AOA and AOB to ammonia oxidation

Given that archaeal *amoA* gene counts showed an increase pattern in all microcosms over the incubation, this increase was apparent regardless of inhibitory treatment. AOA

abundances in general remained within the same order of magnitude before and after incubation (Fig. 3.2.5 & Fig. 3.2.6 & Fig. 3.2.7 & Table S2.4). In contrast, there was a greater increase in bacterial *amoA* genes abundances (up to two orders of magnitude) in several microcosms suggesting a substantial growth of AOB populations. These patterns in *amoA* abundances and nitrate production suggested that the increase in bacterial *amoA* genes was strongly linked to active ammonia oxidation, whereas the moderate growth of *amoA*-carrying AOA appeared uncoupled to ammonia oxidation.

The model confirmed that AOA played a minor role in the process of the ammonia oxidation. However, the estimated contribution of archaea to nitrification in the treatments amended with ammonium was particularly high in those microcosms, where the model could not fit nitrate production very well (e.g., *M5* and *D15*). In these microcosms, nitrification rate estimates should be treated with caution, as the mismatch of nitrate data indicates that some processes influencing nitrate dynamics were not well described by the model.

Ammonium concentrations within the low μM range are considered as growth-limiting for AOB (Bollmann, Bär-Gilissen, and Laanbroek 2002). Previous studies on terrestrial samples and pure cultures indicated that AOA are better adapted to low ammonium availability, while AOB outcompete AOA at higher ammonium concentrations (Jia and Conrad 2009; Martens-Habbena et al. 2009). As our microcosms were amended with an ammonium concentration not unreasonable to be encountered *in situ* (up to 0.3 mM were measured in the field, Table S2.1), our results suggest that AOB actually dominate nitrification in the investigated agricultural stream system. In contrast, AOA were not found to be major players in ammonia-oxidation in Schönbrunnen sediments, even though they were of predominant abundance *in situ* (as per *amoA* gene qPCR). Besides concentration effects, another possible explanation of this discrepancy could be that AOA did not actually express *amoA* genes under the conditions of our experiment. The moderate population growth of AOA, independent of ammonia oxidation, could also indicate that the AOA in the streambed

might be able to survive via an alternative metabolism (Abby et al. 2018; Yuchun Yang et al. 2021; Alves et al. 2019). Alternatively, these *amoA*-possessing archaea may also lack the capacity to perform ammonia oxidation, as also observed elsewhere (Mußmann et al. 2011; Avrahami et al. 2011).

4.2.5 Diversity and composition of AOB gene pools

Despite that AOB *amoA* diversity was highest in midstream and downstream 5 cm samples, a decrease pattern was observed for upstream 15 cm, midstream 15 cm, and downstream 5 cm samples during incubation, suggesting a filtering of nitrifier populations in our experimental setup (Fig. 3.2.8). The Shannon diversity we observed in this study is overall comparable but mostly in the lower bound of values reported from other river or estuarine sediments (S. Zhang et al. 2020; Damashek et al. 2014; Y. Zhang et al. 2014; Cao et al. 2011).

In contrast to *amoA* composition shift in upstream and downstream samples after the incubation, the shift of *amoA* communities was not significant for midstream samples. This observation suggested that the supplementation of ammonium triggered AOB community shifts for upstream and downstream samples, but not for midstream samples. Upstream and downstream samples were previously shown to represent stream segments with a discharge of sulfur-rich groundwater to the stream, and sulfide concentrations in the μM range are known to significantly inhibit nitrification (Joye and Hollibaugh 1995). Water-chemistry-derived impacts on *amoA* gene diversity within the Schönbrunnen stream can thus be postulated (Z. Wang et al. 2022; Jimenez-Fernandez et al. 2022).

Overall, AOB detected in our study mostly belonged to both *Nitrosomonas* and *Nitrosospira* spp.. Similar findings have been reported from estuarine freshwater samples (Bernhard and Bollmann 2010). *Nitrosomonas europaea* (e.g., OTU4) seems a weak competitor under ammonium-limited conditions due to its relatively high K_s values and lower *in-situ* abundance compared to *Nitrosospira*-like OTUs (Bollmann, Bär-Gilissen, and

Laanbroek 2002; Koops and Pommerening-Röser 2001). High affinities towards ammonia were suggested for *Nitrosospira* by its predominant distribution in marine sediments, particularly when ammonia is lower than 10 μM (Lagostina et al. 2015). K_s values for AOB estimated with the reaction model ranged between 5 μM and 60 μM (10th and 90th percentile aggregating over all posterior samples, stream segments and depths; see also Fig. S4). This corresponds to the low end of values observed for AOB or the upper end of values for commammox bacteria. The lowest values reported for *Nitrosospira* spp. and *Nitrosomonas* strains were between 10 μM and 100 μM (Jung et al. 2021).

Our high-throughput sequencing enabled the detection of a much greater number of *amoA* OTUs (Observed richness) compared to other studies of riverine systems (Damashek et al. 2014). However, the MiSeq paired-end 250 sequencing approach was not able to cover the full length of bacterial *amoA* gene amplicons. Therefore, phylogenetic interpretations at the genus level should be done with caution as the present phylogenetic analysis does not claim to represent the total diversity of AOB (Aigle, Prosser, and Gubry-Rangin 2019).

Notwithstanding, the evidence of diverse of bacterial *amoA* genes in the lower-order agricultural stream has been observed, supporting the reactivity of the Schönbrunnen streambed. Further investigation concerning secondary nitrate loading is necessary as it can help us gain a comprehensive understanding of nitrogen turnover in agricultural small streams.

4.3 Metagenomics of the Schönbrunnen streambed microbiome

4.3.1 Diverse of microbes from the streambed revealed by amplicon and metagenomics sequencing

In this study, by using both shotgun metagenomics and amplicon sequencing, a diversity of uncultured microbial lineages were detected in streambed sediment samples. As strain isolation and cultivation often remain a challenge in the lab, fragmented information for such uncultured lineages and their ecological relevance can still be predicted via metagenome-assembled genomes (MAGs) (Albertsen et al. 2013). Especially, unclassified *Thermodesulfovibrionia* (within the *Nitrospirota*), unclassified *Vicinamibacterales* (within the *Acidobacteriota*), and unclassified *Rokubacterales* (within *Methylomirabilota*) were among most abundant taxa detected in amplicon sequencing (Fig. 3.3.1 & Fig. 3.3.2). In my metagenomic analysis, MAGs of all of these abundant taxa were recovered, including the *Nitrospirota*, *Acidobacteriota*, and *Methylomirabilota* (Fig. 3.3.8, Table S3.1). Detailed taxonomic assignment of these MAGs, e.g., MAGs SA.54 (*Thermodesulfovibrionia*), SA.53 (*Thermodesulfovibrionia*), and SA.74 (*Vicinamibacterales*) revealed that representatives of these common uncultivated lineages indeed possess a genomic capacity to reduce sulfate, or reduce nitrate in the streambed via DNRA (Fig.7 & Table S1). Members of *Thermodesulfovibrionia* have been previously enriched and reported to carry a complete DNRA pathway (Arshad et al. 2017).

Another recovered MAG (K01.33) was assigned to the *Gammaproteobacteria*. Further 16S rRNA gene-based classification indicated it to be placed within the so-far uncharacterized family-level lineage B1-7BS (Fig.3.3.8). Although B1-7BS has been detected from other terrestrial environments, including caves (Gonzalez-Pimentel et al. 2021; Jurado et al. 2020), salt marsh soils (C. Kim et al. 2023), and acidic sulfide mineral mine (D. S. Jones et al. 2017), its function and ecological importance have not been further delineated in any previous study.

The B1-7BS MAG recovered from the Schönbrunnen carried the necessary Sox protein system and therefore should potentially be able to oxidize reduced sulfur compounds.

B1-7BS was identified as a member of the core microbiome across all sediment samples taken at 5 cm depth and most samples taken at 15 cm depth for all three sampling years (2017, 2019 and 2020) (Fig. 3.3.10). Here, I propose that B1-7BS was selected (above the model fit) by the specific streambed environment and possibly due to adequate supply in reduced sulfur species in the streambed impacted by bidirectional water exchange. This demonstrates that the Schönbrunnen streambed hosts diverse and previously uncharacterized bacterial lineages of potential importance in critical sulfur and/or nitrogen turnover processes. The metabolic potential of such novel lineages can still only be partially revealed via comprehensive metagenomic sequencing approaches, due to the complexity of this ecosystem.

Moreover, methanogens, which possess the ability to generate methane, were identified in the streambed via shotgun metagenomic sequencing (Fig. 3.3.2). MAGs of some typical methanogens within the *Euryarchaeota* were detected, such as the hydrogenotrophic *Methanoregulaceae*, *Methanocellaceae*, and *Methanobacteriaceae* (*Euryarchaeota*), which utilize hydrogen gas (H₂) as the electron donor (Fones et al. 2021; Rissanen et al. 2017; Wegner and Liesack 2016). There were also MAGs of typical acetoclastic *Methanosaetaceae* (Jetten, Stams, and Zehnder 1992), and the more versatile *Methanosarcinaceae* (Boone, Whitman, and Koga 2015) detected in the streambed. Most of these methanogen MAGs were recovered from 15 cm depth of *Mid-B*, suggesting more reduced and anoxic conditions to prevail here, with limited impact by bidirectional water exchange. However, as no MAGs of any Archaea were fully reconstructed with acceptable quality, it remains unclear whether some of these methanogens could possibly be oxygen-tolerant or exhibiting a higher metabolic versatility (Berghuis et al. 2019).

Although numerous evidence in the dissertation suggested that diverse taxa can be involved in the nitrate reduction, nitrification process may not be a predominant metabolic process in the streambed as there were very limited number of *amoA* genes were detected (Fig. S3.1).

4.3.2 Linking microbial nitrogen and sulfur cycling

Results in this section support the positive correlation between nitrate reduction genes and reduced sulfur oxidation genes in the Schönbrunnen system (Fig. 3.3.3). In particular, the abundance of genes encoding the membrane-associated (NarGHI) nitrate reductase (Shao, Zhang, and Fang 2010) and sulfide-quinone oxidoreductase (SQR) were positively correlated, and tentatively decreased from 15 cm to 5 cm depths at *Mid-A*, and *Down*. These two segments were locations of groundwater exfiltration, as mentioned in the section 3.1. This again suggests that the oxidation of reduced sulfide and the reduction of nitrate were two inter-linked microbial processes in the stream. As *narG* is often used as one of the marker genes to detect denitrification, many taxa could likely be involved as suggested via the detected *narG* gene families (Fig. 3.3.5). *Arthrobacter* spp., *Nitrospira* spp., and *Pseudomonas* spp. were amongst the major contributors of *narG* gene pools, as has been reported from previous studies (Koch et al. 2015; Yixuan Liu et al. 2023; Schreiber et al. 2007; Eschbach et al. 2003). Interestingly, nitrate reduction can be an alternative survival strategy for NOB-like *Nitrospira* spp. under anoxic conditions (Koch et al. 2015; Palomo et al. 2016). In addition, *nirBD* genes, which regulates the DNRA pathway, were predominantly attributed to *Arthrobacter* spp. in the metagenome. Besides this, *nirBD* genes were also contributed by sulfur-oxidizing populations, such as *Thiobacillus* spp. and *Sulfuricaulis* spp., especially at *Down* and *Conf*. This observation was consistent with the findings of the section 4.1, in which the typical sulfur-oxidizing populations *Sulfuricurvum* spp. and *Thiobacillus* spp. were identified as signature autotrophic nitrate reducers for the streambed.

Metagenomics did also show that *nirS* genes were attributed to the sulfur-oxidizing *Thiobacillus* spp. and *Sulfuricaulis* spp., which again supports earlier findings in section 4.1, where I identified *T. denitrificans* as another key population responsible for autotrophic nitrate reduction driven by reduced sulfur species. Moreover, apart from typical sulfur-oxidizers such as *Thiobacillus* and *Sulfuricaulis* spp., also *Pseudomonas* spp. and *Bradyrhizobium* spp. (family *Xanthobacteraceae*) did contribute to sulfur oxidation genes (e.g., *soxXAYZB* and *sqr*) (Fig. 3.3.6) (Xu et al. 2016). In addition, the *Xanthobacteraceae* (dominated by *Bradyrhizobium* spp.) were one of the core taxa identified in 5 cm sediment samples collected over three years. Members of the *Bradyrhizobium* genus have been reported to oxidize thiosulfate (Masuda et al. 2010). Moreover, *Bradyrhizobium* spp. contributed to multiple nitrogen cycling gene pools, such as *napA*, *nirD*, *nirK*, and *norC*. Similar to the gammaproteobacterial B1-7BS lineage, this suggests that members of the *Xanthobacteraceae* may also have played an important role in linking nitrogen and sulfur cycling in the Schönbrunnen.

The MAGs recovered in this study also revealed that members of the *Burkholderiaceae* are likely involved in coupling nitrate reduction to the oxidation of reduced sulfur (Fig. 3.1.8). One example was MAG S04.16 (class *Gammaproteobacteria*; family *Burkholderiaceae*), which carried the sulfur-oxidizing *sox* genes, nitrate-reducing *nar* genes, as well as the *nrfAH* genes involved in DNRA. In addition, genes responsible for synthesizing the cbb3-type cytochrome c (*ccoGPONQ*) were also identified in the MAG, indicating that this member of the *Burkholderiaceae* can also thrive under oxygen-limited conditions, as typical for the Schönbrunnen and other streambeds (Hutt et al. 2017). Previously, some members within this lineage have indeed been reported to oxidize reduced sulfur species and/or to reduce nitrate, either via isolation or DNA-based stable isotope probing (Duan et al. 2020; Coenye et al. 2000; Wittke et al. 1997; B. Li et al. 2018).

Another study within the CAMPOS project which I contributed to during my dissertation project, but not reported in the results of this dissertation, was investigating deeper fractured limestone aquifers in the Ammer catchment, and targeting iron-driven autotrophic denitrification processes (Jakus, Blackwell, Straub, et al. 2021). Unclassified members of the *Burkholderiaceae* were found in that study to be able to reduce nitrate, in presence of reduced iron (II) as an electron donor, as shown in an enrichment experiment. Both *Burkholderiaceae* and *Thiobacillus* were also detected directly in the deep aquifers, and identified as important contributors to nitrate reduction regardless of heterotrophic, mixotrophic, or autotrophic processes. This observation further emphasizes the widespread distribution and the importance of these taxa in denitrification processes within the Ammer catchment, owing to their widespread distribution, diversity and metabolic versatility. Expanding the comparative genomics approach to include all relevant sequences, genomes, and MAGs generated across the different CAMPOS subprojects could yield further important insights into the metabolic potentials and diversity within these key taxa of nitrate elimination in the catchment.

Furthermore, several MAGs were also annotated to members of the *Desulfobacterota*. This phylum typically contains sulfate-reducing lineages and also syntrophic fermenters (Fig. 3.3.8 & Table S3.1) (Waite et al. 2020). Specifically, one of these MAGs was assigned to the uncultured MBNT15 lineage (MBNT15 is now classified as a phylum distantly related to the *Desulfobacterota*, according to latest SILVA SSU r138.1 release) (Parks et al. 2018; Quast et al. 2013), others to the *Desulfobacteria*, *Desulfuromonadia*, and *Desulfomonilia*, which are all well-known sulfate- or sulfur-reducing lineages (Galushko and Kuever 2019; Pfennig and Biebl 1976; DeWeerd et al. 1990). The MAGs SD.32 (MBNT15) and SA.32 (*Desulfobacterota* SM23-61) were of highest quality among all *Desulfobacterota* MAGs (Fig. 3.3.8). They were both shown to host DNRA genes, suggesting that they could also be

capable of reducing nitrate, as also reported in previous studies (Begmatov et al. 2022; Langwig et al. 2021).

As nitrate is thermodynamically more favorable than sulfate as an electron acceptor, a vertical stratification of nitrate- and sulfate-reducing populations and processes is often observed, especially for marine sediments (Bourceau et al. 2023; Canfield, Kristensen, and Thamdrup 2005). Yet, nitrate and sulfate reduction are likely to co-occur in the Schönbrunnen streambed, as the co-presence of nitrate-reducing and sulfate-reducing bacteria in many of the investigated samples. This scenario also seems in line with the concept of bidirectional water exchange, and the simultaneous or seasonally fluctuating availability of nitrate and sulfate in the streambed. A study on coastal sediments using sediment incubations and $^{35}\text{SO}_4^{2-}$ -labeling has also suggested the simultaneous occurrence of nitrate reduction and sulfate reduction (Bourceau et al. 2023). However, sulfate reduction rates were reduced in the presence of nitrate in this study. For the strain *Desulfovibrio desulfuricans*, which is capable of reducing both nitrate and sulfate, nitrate uptake affinity ($K_m = 0.05 \mu\text{mol}$) is higher than sulfate uptake affinity ($K_m = 5 \mu\text{mol}$). Still, *D. desulfuricans* switched to first reduce nitrate only when the concentration of sulfate was low ($< \sim 4 \mu\text{M}$) (Dalsgaard and Bak 1994). In addition, the above study also suggested that sulfate-reducing populations may switch their respiration to DNRA in the presence of nitrate, as over 50% of *nrfA* transcripts from fresh top surface ($< 10 \text{ cm}$) sediments were assigned to the *Desulfobacterota* (Bourceau et al. 2023). All of the information above suggests that nitrate and sulfate reduction can be linked to the same sulfate-reducing populations within the *Desulfobacterota* in the Schönbrunnen streambed, irrespective of the electron donor. It remains unclear whether possibly, also the oxidation of reduced sulfur species by these microbes could be coupled to nitrate reduction and DNRA, as recently reported for the still-enigmatic cable bacteria of the *Desulfobulbaceae* (Kjeldsen et al. 2019). In any way, a possible contribution of members of the *Desulfobacterota* to overall

nitrate reduction in the Schönbrunnen and Ammer catchment warrants further evaluation in the future. Overall, data from metagenomic sequencing suggested a complex bacterial network with a capacity for nitrate reduction, and many populations capable of only incomplete denitrification. Functional redundancy in nitrate reduction and sharing of respiratory intermediates seems likely, with key populations like the B1-7BS lineage and the *Xanthobacteraceae* present in all samples and sampling seasons, regardless of transient hydrological variations. Still, this first metagenomic study of the streambed microbiota only provides a partial coverage of the metabolic potentials of the Schönbrunnen streambed, which awaits further functional elucidation via isotopic labelling approaches and enrichment cultivation in the future.

4.3.3 Long-read sequencing to dissect sediment microbial communities at high resolution

In this dissertation, so-called third-generation long-read sequencing strategies were employed at two different levels: First, PacBio long-read sequencing of full-length 16S rRNA gene amplicons provided us with a valuable opportunity to dissect sediment bacterial communities at a robust and taxonomically very informative level of exact amplicon sequencing variants (ASVs) (Lam et al. 2020). In contrast to the much more widely used short Illumina reads, long-read ASVs can plausibly be resolved beyond the genus level (Callahan, McMurdie, and Holmes 2017). As exemplified for the species-level resolution for ASVs of sulfur-oxidizing populations in this dissertation, this may well be relevant to assess spatial patterns in investigated sub-populations and to infer their respective impact on streambed biogeochemistry. Although 16S rRNA genes assignments can only serve as a first indicator, not a diagnostic way to confirm actual process relevance within environmental microbiomes, functionally relevant context like a reliable differentiation between *T. denitrificans* and other *Thiobacillus*-related ASVs (Fig. 3.1.6) would not have been possible using shorter reads. Though PacBio long-read sequencing does not produce comparable amounts of total

sequencing output as other platforms, it can offer comparable biodiversity coverage for more frequent taxa (Lam et al. 2020). As shown in this dissertation, this can well be relevant for the functional interpretation of environmental amplicon datasets.

Next, Oxford Nanopore long-read sequencing assisted shotgun metagenomics provided an essential backbone for the hybrid assembly strategy and indeed improved the number of higher-quality MAGs obtained from the data. Valuable insights to decipher the metabolic potentials of the Schönbrunnen streambed microbiome were thus obtained. From functional gene abundances, over pathway analysis to species-level taxa contributing to certain gene pools, the information obtain from metagenome-assembled genomes (MAGs) were generally consistent with results first indicated via amplicon sequencing. However, especially the linking between streambed microbial nitrogen and sulfur cycling were much more apparent in metagenomics. Isolating strains of some of the key microbes involved from the streambed for further physiological characterization will be a time-consuming and technically challenging task, especially since several belong to uncultured and weakly characterized taxa with a lack of literature information. Still, this study and the metagenomic information conveyed may offer important first insights to move forward along this route in the future. It remains important to note that many of the MAGs reconstructed were of limited completeness and/or high contamination, despite the hybrid assembly approach. Thus, the metagenomic information on some of the intriguing and novel taxa detected is still fragmented or incomplete. In the future, to maximize the quality of reconstructed MAGs for the Schönbrunnen and comparable agricultural streams, studies should carefully reevaluate the intended sequencing depth, assembly methods (e.g., try co-assembly) (Haryono et al. 2022), and also the chosen sequencing platform (e.g., PacBio sequel II) (Lang et al. 2021). Clearly, further work should also focus on designing microcosms aimed at enriching and isolating some of the key microbes identified in this study, as well as investigating gene transcripts of

the most relevant functions to further elucidate the activity and ecophysiology of the Schönbrunn streambed microbiota.

5 CONCLUSIONS AND OUTLOOK

In this dissertation, I addressed a number of central knowledge gaps in the current understanding of microbial communities in the streambed of agricultural first-order streams as impacted by bidirectional water exchange. Firstly, this adds to a better-founded understanding of the turnover and fate of nitrogen in small streams adjacent to the agricultural area, with nitrate representing a widely enriched pollutant in groundwater around Europe. Secondly, the Schönbrunn study site provided a valuable opportunity to study the impact of bidirectional water exchange on streambed microbiota at the reach scale. Insights gained from this project can help us understand whether bidirectional water exchange can further deteriorate or possibly improve nitrate-loading scenarios in streams and groundwater. Thirdly, it was important to determine how the streambeds of small agricultural streams can act as reactors, and which function potentials and ecophysiologicals of intrinsic microbiota are most relevant in removing nitrate from the stream. Through three multidisciplinary projects, the overarching goal of the dissertation was to address these knowledge gaps and contribute to a more fundamental microbial ecology perspective of the streambeds of these clearly under investigated freshwater ecosystems.

In the first study, I show that bidirectional water exchange between an agricultural first-order stream and the surrounding alluvial aquifer is important not only for stream water chemistry, but also for sediment microbial populations and their presumed activities in attenuating agricultural solute inputs. By disentangling the stream into net gaining and losing sections, results show that sediment microbial community assembly was mostly dominated by deterministic heterogeneous assembly processes, except for zones of the streambed influenced by groundwater exfiltration. Such net gaining sections were associated with an enrichment of typical sulfur-oxidizing lineages, such as *Sulfuricurvum* and *Thiobacillus* spp., indicative of

possibly ongoing reduced sulfur-driven autotrophic nitrate attenuation processes induced by bidirectional water exchange. In contrast, canonical heterotrophic denitrifying populations were more abundant in midstream net losing reaches of the Schönbrunnen. This study thus highlights a previously overlooked importance of autotrophic physiologies in streambed nitrate reduction. Compared to more natural lower-order streams, I also reveal a reactivity of the streambed and an assembly of its microbiota strongly impacted by bidirectional water exchange fluxes rather than by bedform complexity-driven hyporheic flow. Given that the Schönbrunnen stream is located in a very typical agricultural landscape in central Europe, observations from this study are generally relevant also for other, comparable lower-order streams in agricultural lowlands, even though local explicit hydrological turnover processes and microbial communities may be distinct. Still, the observed patterns of reactivity open a door for novel management concepts for installing reactive barriers for nitrate elimination adjacent to agricultural fields. Together with other recent concepts such as the Keyline design for agricultural fields (Johansson, Brogaard, and Brodin 2022; Ryan et al. 2015), this may help to retain more water and nutrients within agricultural catchments.

My second study has interrogated ammonia-oxidizing populations in the streambed, to assess their possible involvement in secondary nitrate loading of the stream. Results clearly showed that despite a much higher *in-situ* abundance of AOA, a higher reactivity towards incoming ammonium pulses was specifically attributed to AOB in the microcosm experiment. Observations in this study indicated that using *in-situ* functional gene abundance alone is not sufficient to evaluate functional importance of ammonia oxidizers in streambeds. Both *Nitrosomonas* and *Nitrospira* populations were identified as important contributors to nitrification in streambed sediments. Even though we observed pronounced differences in AOB community diversity and abundance *in situ*, overall ammonia-oxidation rates were comparable for microcosms of distinct stream segments. This suggests that environmental

filtering by a pulse of ammonium and sufficient oxygen supply within microcosms readily selected for similar populations of AOB, irrespective of their original abundance *in situ*. Considering that lower-order streams are well connected not only with the surrounding soils and groundwater, but also downstream riverine ecosystems, our results substantiate the role of ammonia-oxidizing bacteria, not archaea, in controlling the oxidative efflux of nitrate originally stemming from agricultural ammonia inputs. That said, the observed overstoichiometric production of nitrate in all microcosms remained unexplained. In the future, this possible role of the streambed and its intrinsic microbiota in the secondary loading of stream water with nitrate clearly requires further scientific attention. Further work should be conducted, for instance, using different isotopically labelled nitrogen species, either in microcosms or *in situ*, to better understand the relevance of these fluxes.

Findings from the first and the second study were mainly based on data from 16S rRNA amplicon sequencing. However, inferring functional potentials for uncultured lineages detected in the streambed from 16S rRNA amplicon sequences is not reliable. Here, metagenomic sequencing, as applied in the third study, can overcome these limitations and provide a more comprehensive understanding of the functional potential of streambed microbial communities. Metagenomic sequencing successfully provided additional evidence to support the link between microbial nitrogen and sulfur cycles in the streambed. In addition, it suggests that a complex metabolic network rather than defined populations was likely contributed to denitrification and DNRA. Moreover, even canonical sulfate reducers seemed to host a potential for DNRA. The B1-7BS lineage, an as-yet uncharacterized taxon within the *Gammaproteobacteria*, was identified as an abundant and potentially important sulfur-oxidizing community *in situ*, and was detected in all samples collected over the three years of sampling. Enriching and isolating a member of this lineage would be very relevant to further elucidate their functions and ecophysiological roles *in situ*.

In the perspective of environmental engineering, the reduced sulfur-driven autotrophic denitrification conducted by the microbes investigated in this dissertation has previously been of interest as an alternative process in the waste water treatment field (Peng et al. 2015; Rittmann and McCarty 2001; Koenig and Liu 2002; Soares 2002; Zhao et al. 2004). Bacteria including *Thiomicrospira* sp. and *Thiobacillus* sp., have been specifically examined in their capability of sulfur-driven autotrophic nitrate reduction (Gadekar, Nemati, and Hill 2006; Yan Yang et al. 2018). Natural attenuation based on sulfur-driven autotrophic denitrification has a clear advantage in water treatment, as other physical and chemical approaches are often more costly and energy demanding. A better understanding of the intrinsic microbiota involved could facilitate promising treatment strategies for nitrate-burdened groundwater, due to the scanty of organic carbon necessary for canonical heterotrophic denitrification. Moreover, autotrophic processes lead to lower cell growth than heterotrophy, thus reducing risks of bacterial contamination during treatment (Sierra-Alvarez et al. 2007). Practically, both elemental sulfur and thiosulfate could be suitable substrates serving as electron donors for denitrification. Though this approach can also be problematic with the production of excess sulfate that requires further operations, its application potential should not be ignored in the design of novel remediation strategies for the widespread nitrate pollution issues (Yiwen Liu et al. 2017). In this dissertation, some foundations for possible future applications to this end have been elaborated. All relevant hydrological and microbial processes described in here should be considered, when improving current management concepts for controlling the fluxes of nitrogen in agricultural landscapes.

APPENDIX: SUPPORTING INFORMATION

SI.1 Streambed microbial communities in the transition zone between groundwater and a first-order stream as impacted by bidirectional water exchange

Table S1.1: PacBio sequences processed by SMRTLink (version 6.0) from subreads (raw reads) to Circular Consensus Sequences (CCS) reads.

Amplicon	Sample code	Raw sample name	Subreads	CCS reads	Number of passes
1	<i>Up-A</i>	17ss_01	791749	29732	16
2	<i>Up-A</i>	17ss_02	589002	23244	17
3	<i>Up-A</i>	17ss_03	510993	18640	16
4	<i>Up-A</i>	17ss_04	94450	5040	14
5	<i>Up-A</i>	17ss_05	89193	3644	14
6	<i>Up-A</i>	17ss_06	41969	3214	14
7	<i>Up-B</i>	17ss_07	313924	13382	16
8	<i>Up-B</i>	17ss_08	574149	24542	14
9	<i>Up-B</i>	17ss_09	367691	15846	16
10	<i>Up-B</i>	17ss_10	165619	7081	14
11	<i>Up-B</i>	17ss_11	716356	30923	17
12	<i>Up-B</i>	17ss_12	402309	17500	17
13	<i>Mid-A</i>	17ss_13	140353	5931	17
14	<i>Mid-A</i>	17ss_14	400455	15121	17
15	<i>Mid-A</i>	17ss_15	127435	4838	17
16	<i>Mid-A</i>	17ss_16	256302	9429	17
17	<i>Mid-A</i>	17ss_17	215721	8171	17
18	<i>Mid-A</i>	17ss_18	428174	16173	17
19	<i>Mid-B</i>	17ss_19	142209	5281	17
20	<i>Mid-B</i>	17ss_20	214753	7952	17
21	<i>Mid-B</i>	17ss_22	188779	6966	17
22	<i>Mid-B</i>	17ss_23	527820	19611	17
23	<i>Mid-B</i>	17ss_24	403187	15211	17
24	<i>Down</i>	17ss_25	195288	7235	17
25	<i>Down</i>	17ss_26	599195	22000	17
26	<i>Down</i>	17ss_27	523254	19411	17
27	<i>Down</i>	17ss_28	434595	4735	17
28	<i>Down</i>	17ss_29	394688	16036	17
29	<i>Down</i>	17ss_30	18685	14703	17
30	<i>Conf</i>	17ss_31	261526	9865	17
31	<i>Conf</i>	17ss_34	150575	4032	17
32	<i>Conf</i>	17ss_35	165553	5470	17
33	<i>Conf</i>	17ss_36	161400	5376	17

Table S1.2: Summary of taxonomy at the phylum level. The mean relative abundance of a phylum in all samples, and the number of ASVs detected within a given phylum were shown in the table. All samples were dominated by three phyla (highlighted in red color): *Proteobacteria*, *Bacteroidota*, and *Acidobacteriota*.

Rank	Phylum	Number of ASVs	Mean relative abundance
1	Proteobacteria	2173	27.7293%
2	Acidobacteriota	1160	9.2575%
3	Bacteroidota	1125	15.9077%
4	Planctomycetota	752	4.9452%
5	Chloroflexi	656	6.2494%
6	unclassified_Bacteria	518	7.6183%
7	Desulfobacterota	389	3.5120%
8	Actinobacteriota	262	1.9312%
9	Firmicutes	233	2.2400%
10	NB1-j	201	1.7083%
11	Sva0485	174	2.4328%
12	Patescibacteria	159	1.5301%
13	MBNT15	145	2.6433%
14	Myxococcota	139	0.5590%
15	Nitrospirota	124	2.2556%
16	Gemmatimonadota	116	1.4032%
17	Campilobacterota	83	3.2710%
18	RCP2-54	76	0.8137%
19	Verrucomicrobiota	65	0.2230%
20	Spirochaetota	64	0.8254%
21	Zixibacteria	46	0.4349%
22	Dependentiae	45	0.2280%
23	Methylomirabilota	43	0.4740%
24	WS2	38	0.4036%
25	Armatimonadota	37	0.1784%
26	Nitrospinota	34	0.1553%
27	WS1	20	0.0985%
28	Sumerlaeota	19	0.0600%
29	Bdellovibrionota	14	0.1079%
30	Hydrogenedentes	13	0.0281%
31	Entotheonellaeota	11	0.0357%
32	Fibrobacterota	11	0.0435%
33	Dadabacteria	10	0.1896%
34	Elusimicrobiota	8	0.0316%
35	TA06	7	0.0696%
36	Cyanobacteria	6	0.0226%
37	DTB120	6	0.0492%
38	LCP-89	6	0.0396%
39	Cloacimonadota	5	0.0970%
40	Calditrichota	4	0.0622%
41	WS4	4	0.0152%
42	SAR324 clade(Marine group B)	3	0.0062%
43	Abditibacteriota	2	0.0023%
44	Caldatribacteriota	2	0.0172%
45	Deferrisomatota	2	0.0097%
46	Fusobacteriota	2	0.0101%
47	GAL15	2	0.0084%
48	Schekmanbacteria	2	0.0076%
49	WPS-2	2	0.0027%
50	Deinococcota	1	0.0044%
51	Edwardsbacteria	1	0.0135%
52	FCPU426	1	0.0044%
53	Fermentibacterota	1	0.0070%
54	GN01	1	0.0216%
55	Modulibacteria	1	0.0044%

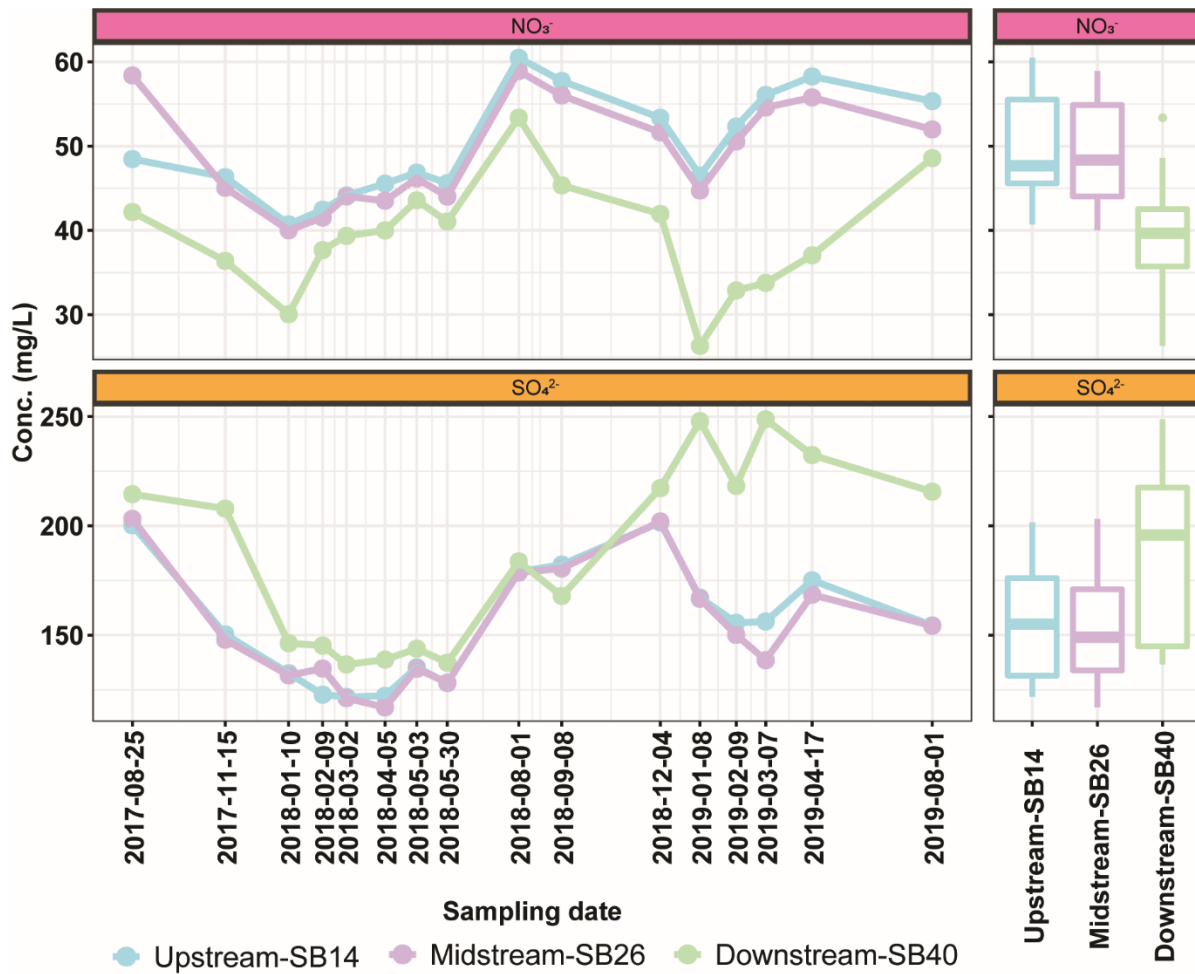


Fig. S1.1: The concentrations of nitrate and sulfate in the Schönbrunnen between the sampling years 2017 and 2019. Water samples were obtained from the upstream to the downstream. Box plots on the right side provide a summary of either nitrate or sulfate concentrations from three sampling locations between the sampling years 2017 and 2019 (original data were measured by Oscar Jimenez-Fernandez and Karsten Osenbrück within the CAMPOS project).

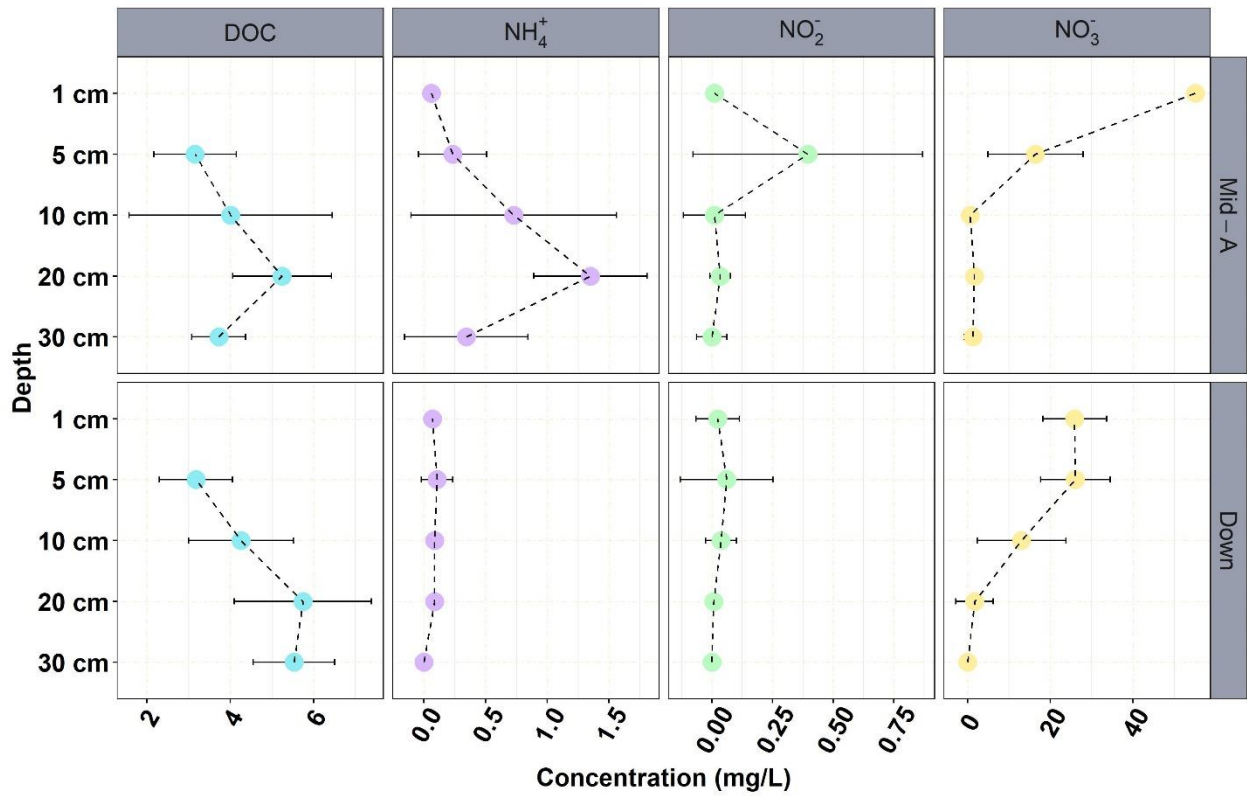


Fig. S1.2: Depth profiles of dissolved organic carbon (DOC) and nitrogen species from porewater samples collected from *Mid-A* and *Down* of the Schönbrunnen. Error bars indicated measurement variation (mean \pm standard deviation) over the summer season (duplicate samples from 4 measurement dates between July 15 and August 15) (original data were measured by Oscar Jimenez-Fernandez and Karsten Osenbrück within the CAMPOS project).

SI.2 Linking abundance and activity of ammonia-oxidizing bacteria and archaea in an agriculturally impacted first-order stream

Note: The Model was conceived and calibrated by our project partners Anna Störiko and Holger Pagel of the Universities of Tübingen and Universities of Hohenheim, respectively, using the experimental data generated by myself. Since both, experiment and modelling are crucial to interpret nitrification activities in my microcosm experiment, these are both reported on in this section. No credit is claimed by the PhD candidate on the modelling itself. A detailed description of the modelling approach is given in this section for a complete account, and as the respective manuscript is under review at the time of dissertation submission.

Process-based modeling of nitrification

A process-based model simulating nitrification in the microcosm experiments was set up to support the interpretation of the data. The model describes ammonia oxidation by AOA and AOB and their associated growth dynamics. Additionally, it reflects the growth of non-nitrifying archaea and bacteria and the growth of AOA through processes other than nitrification. Based on the initial assessment of measured dynamics of NH_4^+ , nitrate (NO_3^-), and microbial gene abundances, the modeling approach considered nitrification-controlled NH_4^+ -release from sediments and NH_4^+ uptake and incorporation by all biomass pools. Even though AOA and AOB technically oxidize ammonia (NH_3), the model was formulated with respect to ammonium (NH_4^+) concentrations, as this was the measured quantity in this study. An equilibrium-speciation calculation considering dissolved ammonia and ammonium, and gas-phase ammonia also showed that >98% is present as NH_4^+ under the conditions of the experiment. At constant pH, the ammonia concentration can be considered proportional to the ammonium concentration due to the quick equilibrium between the two species.

The oxidation of NH_4^+ and the corresponding growth of AOA and AOB through this process are described by Monod-type rate laws. The oxidation rate of NH_4^+ by group i (relating to either AOA or AOB) is given by:

$$r_{\text{NH}_4^+}^i = v_{\text{max}}^i \frac{c_{\text{NH}_4^+}}{c_{\text{NH}_4^+} + K_{\text{NH}_4^+}^i} f_{\text{inhib}B_i} \quad (1)$$

where v_{\max}^i [mol cell⁻¹ s⁻¹] is the maximum cell-specific NH₄⁺-oxidation rate, $c_{NH_4^+}$ [mol L⁻¹] and $K_{NH_4^+}^i$ [mol L⁻¹] are the NH₄⁺-concentration and half-saturation constant, and B_i [cells L⁻¹] is the cell density of group i . To account for the inhibition of nitrification rates via 1-octyne or acetylene, the rate contains the factor f_{inhib} which ranges between 0 (complete inhibition) and 1 (no inhibition). It is assumed that acetylene leads to complete inhibition of AOA and AOB. For 1-octyne, the respective values of f_{inhib} for AOA and AOB from the data were estimated. The growth rate of AOA and AOB through NH₄⁺-oxidation and, hence, nitrification, is proportional to the NH₄⁺-oxidation rate given by:

$$r_{\text{growth},NH_4^+}^i = Y_i r_{NH_4^+}^i, \quad (2)$$

where the proportionality constant is the growth yield Y_i [cells mol⁻¹].

Lacking accumulation of nitrite (NO₂⁻) during the experiment indicated that NH₄⁺-oxidation was the rate-limiting step. Therefore, production and consumption of NO₂⁻ are not considered explicitly, and the production of NO₃⁻ is directly derived from the sum of the nitrification rates:

$$\frac{dc_{NO_3^-}}{dt} = \sum_i r_{NH_4^+}^i \quad (3)$$

The NO₃⁻ amount produced in the treatments without inhibitor and with the addition of 1-octyne exceeded the NH₄⁺ amount initially added to the microcosms. However, NH₄⁺-concentrations remained constant when nitrification was inhibited entirely by acetylene. Based on this initial data evaluation, the model was formulated assuming that organic N was additionally released from the sediments and that this additional N-release depends on active nitrification. Therefore, the NH₄⁺-release from the sediment changes proportionally to the total nitrification rate:

$$r_{\text{release}}^{NH_4^+} = \alpha_{\text{release}} \sum_i r_{NH_4^+}^i, \quad (4)$$

with the proportionality factor α_{release} [1].

Many AOA are mixotrophic (Qin et al. 2014), i.e. they can not only grow from nitrification but also from the oxidation of organic carbon (C) given by:

$$r_{\text{mixotrophic}}^{\text{AOA}} = \mu_{\text{mixotrophic}}^{\text{AOA}} B_{\text{AOA}} \quad (5)$$

where $\mu_{\text{mixotrophic}}^{\text{AOA}} [s^{-1}]$ is the specific growth rate of AOA when utilizing organic C as electron donor.

Both, AOA and AOB pools decay according to a first-order rate law

$$r_{\text{dec}}^i = k_{\text{dec}}^i B_i, \quad (6)$$

with a decay coefficient $k_{\text{dec}}^i [s^{-1}]$.

The dynamics of AOA and AOB are given by summing up all growth and decay terms:

$$\frac{dB_{\text{AOA}}}{dt} = r_{\text{growth}, \text{NH}_4^+}^{\text{AOA}} + r_{\text{mixotrophic}}^{\text{AOA}} - r_{\text{dec}}^{\text{AOA}} \quad (7)$$

$$\frac{dB_{\text{AOB}}}{dt} = r_{\text{growth}, \text{NH}_4^+}^{\text{AOB}} - r_{\text{dec}}^{\text{AOB}} \quad (8)$$

The growth of microorganisms requires an N-source for biomass production. It is assumed that microorganisms use NH_4^+ as their N-source. The consumption rate of NH_4^+ for incorporation into biomass is then given by:

$$r_{\text{incorporation}} = \sum_i \beta_i r_{\text{growth}}^i \quad (9)$$

where the index i stands for archaea or bacteria, β_i is the number of moles of nitrogen per cell, and r_{growth}^i is the total growth rate of all archaea/bacteria, including nitrifiers and non-nitrifiers (Eq. 11, 12). The dynamics of NH_4^+ -concentrations are then given by:

$$\frac{d\text{NH}_4^+}{dt} = r_{\text{release}}^{\text{NH}_4^+} - \sum_i r_{\text{NH}_4^+}^i - r_{\text{incorporation}} \quad (10)$$

Our experimental data did not provide information on the metabolism of non-nitrifying organisms, but only on the total abundances of archaea and bacteria. The model therefore considers two groups (archaea and bacteria) of non-nitrifiers whose biomass is given by:

$$\frac{dX_i}{dt} = r_X^i, \quad (11)$$

with a constant growth rate r_X^i [cells L⁻¹].

The total growth rates for all archaea and bacteria are given by:

$$r_{\text{growth}}^{\text{archaea}} = r_{\text{growth},\text{NH}_4^+}^{\text{AOA}} + r_{\text{mixotrophic}}^{\text{AOA}} + r_X^{\text{archaea}} \quad (12)$$

$$r_{\text{growth}}^{\text{bacteria}} = r_{\text{growth},\text{NH}_4^+}^{\text{AOB}} + r_X^{\text{bacteria}} \quad (13)$$

Abundances of *amoA* genes were calculated from the simulated biomass of AOA and AOB assuming that a single cell contains 1 and 3 *amoA* gene copies, respectively (Lagostina et al. 2015). Abundances of 16S rRNA genes were computed for archaea and bacteria separately using the simulated summed biomass of nitrifying and non-nitrifying archaea and bacteria assuming one and two 16S rRNA gene copies per cell, respectively (Pei et al. 2010).

Parameter Estimation & Numerical Methods

The process-based model was calibrated with a Bayesian parameter-estimation approach to account for uncertainty. Prior distributions were based on literature values of the parameters (Table S2.2). It is estimated one set of parameters for each river segment (Upstream, Midstream, Downstream) and depth (5 cm, 15 cm) independently, that is, in total, six sets. Measured concentrations of ammonium and nitrate as well as *amoA* and 16S rRNA gene concentrations were used to calculate the likelihood for Bayesian inference. The data were assumed to follow a normal distribution centered about simulated concentrations (ammonium) or log-transformed concentrations (nitrate, gene counts). The log-transformation was applied to remove a concentration-dependence of measurement standard deviations in the nitrate and gene data. We then assumed a constant measurement error that was identical for all treatments and estimated it jointly with reaction parameters through Bayesian inference. Nitrate and *amoA* data contain information about nitrification rates and bacterial growth that is necessary to constrain the model. However, ammonium data were much more abundant, leading to a model fit that would be biased towards a better fit of ammonium concentrations.

Therefore, we weighted the data standard deviations by the number of measurements per data type in each microcosm, giving larger weights to scarcer measurements.

The reaction model represents a system of ordinary differential equations (ODEs) that we defined and solved with the Python package Sunode (Seyboldt, 2021). The equations are solved with the backward-differentiation-formula (BDF) solver as implemented in the SUNDIALS library (Hindmarsh et al., 2005), which is wrapped by Sunode. The posterior distribution is sampled with the No U-Turn Sampler (NUTS) using the Python package PyMC (Salvatier et al., 2016). We ran two independent Markov chains, generating 1000 samples in each chain. Convergence was assessed by comparing within-chain and between-chain variance with the \hat{R} -criterion (Vehtari et al., 2021). Details of the Bayesian parameter-estimation method for the reaction model are shown in the following section. The script for the reaction model is publicly available (<http://dx.doi.org/10.5281/zenodo.7460717>).

Bayesian Parameter Estimation for the Reaction Model

Prior Distributions

Prior parameter distributions were based on literature parameter values and physical constraints. For most parameters, a log normal distribution was chosen for the prior to ensure positivity. In general, broad priors that span several orders of magnitude were chosen. The hyper parameters of the distribution were chosen such that the distribution covers the range of reported parameter values, or that its mode is set to a reported value, when only one value was available. The inhibition factor f_{inhib} ranges between 0 and 1. Therefore, a Beta distribution was selected for the prior. Since 1-octyne is meant to inhibit ammonia-oxidizing bacteria (AOB) but not ammonia-oxidizing archaea (AOA), the parameters for the Beta distribution were chosen such that the distribution is close to one (no inhibition) for AOA. For AOB, values close to zero (complete inhibition) were favored, but some probability was also given to larger values (up to 60 %, meaning partial inhibition). Table S2.2 provides an overview of

the chosen prior distributions. Table S2.3 shows the parameters that were not estimated but fixed at literature parameter values, namely the numbers of *amoA* and 16S rRNA genes per cell.

Preprocessing of measurement data

While *amoA* and 16S rRNA gene data are given in units of genes per mass of wet sediment obtained by centrifuging the slurry in the microcosms, the model computes gene concentrations in units the genes per volume of liquid in the slurry. To compare the simulated with the measured concentrations, both quantities were converted to units of genes copies per volume of slurry.

For a few individual data points, one out of three biological replicates was excluded for the model calibration because the behavior of the corresponding microcosms deviated strongly from the other two biological replicates. In total, the following points were excluded:

1. Gene data at T14 of replicate 1 in the *Mid-5* microcosm because, unlike in the other replicates, they were below the detection limit or an order of magnitude lower than the other replicates.
2. Nitrate data in replicate 1 of the *Down-15* microcosms, because it did not show any nitrification activity.
3. The first replicate of nitrate in *Mid-5* at T7, because nitrate dynamics are inconsistent with the other two replicates. While it might be debatable if this data points should be removed, its exclusion did not considerably change the results.

Posterior Distributions

Posterior distributions of microbial kinetic parameters for AOA and AOB are shown in Fig. S2.2.

Table S2.1: Schönbrunnen stream discharge (Q) and major water chemistry parameters in both the stream water and adjacent groundwater measured in the sampling month (June 2020).

Sampling locations	Q [L/s]	EC [μS/cm]	Ca ²⁺ [mmol/l]	NH ₄ ⁺ [mmol/l]	NO ₃ ⁻ [mmol/l]	Cl ⁻ [mmol/l]	SO ₄ ²⁻ [mmol/l]
<i>Up</i>		1053	4.05	0	0.84	0.46	1.63
<i>Mid</i>	0.37	954	3.18	0	0.91	0.46	1.76
<i>Down</i>	-	989	3.78	0	0.64	0.43	1.88
Groundwater (GW)							
GWS 2	-	1049	4.03	0	0.89	0.46	1.69
GWS 8	-	2600	16.08	5.5	0.01	0.43	11.85
GWS 12	-	941	3.73	0	0.54	0.43	0.02
GWS 19	-	849	3.05	0	0.58	0.36	0.51
GWS 23	-	1057	4.38	0.01	0.02	0.37	1.68
GWS 26	-	1380	6.85	0.03	0	0.29	4.07

Table S2.2: Model parameters of the reaction model and the corresponding prior distributions for the Bayesian estimation of parameter values. (Prosser and Nicol 2012; Jung et al. 2011; 2021; Tourna et al. 2011; Song et al. 2017; Ding 2010; Cortassa et al. 2002; Loferer-Kröbächer, Klima, and Psenner 1998)

Parameter	Symbol	Unit	Hyperparameters		Ref.
			μ	σ	
<i>Parameters with Lognormal distribution¹</i>					
Maximum NH ₄ ⁺ oxidation rate for AOA	r_{\max}^{AOA}	mol cell ⁻¹ s ⁻¹	-43.4	1.0	2
Maximum NH ₄ ⁺ oxidation rate for AOB	r_{\max}^{AOB}	mol cell ⁻¹ s ⁻¹	-40.4	1.0	2
Half-saturation constant for AOA	$K_{\text{NH}_4^+}^{\text{AOA}}$	M	-14.5	1.0	3
Half-saturation constant for AOB	$K_{\text{NH}_4^+}^{\text{AOB}}$	M	-9.2	1.0	3
Growth yield for AOA	Y_{AOA}	cells mol ⁻¹	32.2	0.5	4
Growth yield for AOB	Y_{AOB}	cells mol ⁻¹	28.7	0.5	2
Mixotrophic growth rate constant of AOA	$\mu_{\text{mixotrophic}}^{\text{AOA}}$	s ⁻¹	-13.9	1.0	5
Decay constant of AOA and AOB	k_{dec}	s ⁻¹	-18.3	0.5	6
NH ₄ ⁺ release relative to its oxidation rate	α_{release}	mol mol ⁻¹	-2.0	1.0	7
Growth rate of non-nitrifying archaea	r_X^{archaea}	cells L ⁻¹ s ⁻¹		1.0	8
Growth rate of non-nitrifying bacteria	r_X^{bacteria}	cells L ⁻¹ s ⁻¹		1.0	8
Nitrogen content of archaeal biomass	β_{archaea}	mol cell ⁻¹	-34.5	1.0	9
Nitrogen content of bacterial biomass	β_{bacteria}	mol cell ⁻¹	-34.5	1.0	9
Initial concentration of AOA in treatment <i>j</i>	$B_{\text{AOA},j}^0$	cells L ⁻¹		0.5	10
Initial concentration of AOB in treatment <i>j</i>	$B_{\text{AOB},j}^0$	cells L ⁻¹		0.5	10
Initial concentration of archaea in treatment <i>j</i>	$X_{\text{arch},j}^0$	cells L ⁻¹		0.5	10
Initial concentration of bacteria in treatment <i>j</i>	$X_{\text{bac},j}^0$	cells L ⁻¹		0.5	10
<i>Parameters with Beta distribution¹¹</i>					
Inhibition factor of 1-octyne for AOA	$f_{\text{inhib}}^{\text{AOA}}$	-	100	1.0	12
Inhibition factor of 1-octyne for AOB	$f_{\text{inhib}}^{\text{AOB}}$	-	1	5.0	12

¹ The parameters μ and σ are the mean and standard deviation of the (normally distributed) logarithmic variable, using the natural logarithm. ² Prosser and Nicol (2012) ³ Jung et al. (2021) ⁴ Jung et al. (2011)
⁵ Tourna et al. (2011) ⁶ Ding (2010) and Song et al. (2017) ⁷ The prior was chosen such that the release rate is considerably smaller than ammonium oxidation (centering at about 13%), since ammonium did not accumulate.
⁸ The prior was based on a back-of-the-envelope calculation using the data. ⁹ Based on a biomass composition of CH_{1.8}O_{0.5}N_{0.2} (Cortassa, 2002), and a cell weight of about 10⁻¹³ g/cell to 10⁻¹² g/cell (Loferer-Kröbächer et al., 1998).
¹⁰ The mean for initial biomass concentrations is based on the measured initial gene abundances averaged over all treatments and replicates. ¹¹ α and β are the shape parameters of the Beta distribution.
¹² See section "Prior distributions"

Table S2.3 Parameters for the reaction model of the microcosm experiments that were set to fixed values. (Lagostina et al. 2015; Pei et al. 2010)

Parameter	Value	Unit	Reference
Number of <i>amoA</i> copies in AOA	1	genes/cell	Lagostina et al. (2015)
Number of <i>amoA</i> copies in AOB	3	genes/cell	Lagostina et al. (2015)
16S rRNA gene copies in AOA	1	genes/cell	Pei et al. (2010)
16S rRNA gene copies in AOB	1	genes/cell	Pei et al. (2010)
16S rRNA gene copies in other archaea	1	genes/cell	Pei et al. (2010)
16S rRNA gene copies in other bacteria	2	genes/cell	Pei et al. (2010)

Table S2.4. Bacterial and archaeal 16S rRNA genes and *amoA* genes copy numbers in per gram wet sediment of Schönbrunnen streambed sediments before (0-day) and after (14-day) the microcosm incubation as determined by quantitative PCR. qPCR results are shown as the mean value from replicate microcosms (n=2 for before incubation data; n=3 for after incubation data) and technical replicates (n=2) of each microcosm.

Before incubation (0-day):

UNIT: gene copies / g wet sediment	bacterial 16S rRNA genes		bacterial <i>amoA</i>		archaeal 16S rRNA genes		archaeal <i>amoA</i>	
SD: standard deviation	Mean	STD	Mean	STD	Mean	STD	Mean	STD
Up-5cm-no Ammonium + no inhibitor	1.75E+08	1.30E+07	5.42E+04	5.85E+03	2.72E+07	6.99E+05	1.48E+06	4.94E+04
Up-15cm-Ammonium + no inhibitor	2.55E+08	5.89E+07	5.22E+04	1.00E+04	2.56E+07	6.68E+06	2.48E+06	7.60E+03
Up-5cm-Ammonium + acetylene	2.40E+08	1.04E+07	6.18E+04	6.78E+03	3.63E+07	5.33E+06	1.85E+06	1.70E+05
Up-5cm-Ammonium + 1-octyne	3.26E+08	8.22E+07	7.64E+04	3.29E+04	3.91E+07	1.28E+07	2.70E+06	1.01E+06
Up-15cm-no Ammonium + no inhibitor	7.53E+07	5.59E+07	2.15E+04	1.00E+04	2.20E+07	1.58E+07	3.50E+05	2.82E+05
Up-15cm-Ammonium + no inhibitor	1.67E+08	4.46E+07	3.03E+04	1.92E+03	5.61E+07	n<3	8.66E+05	n<3
Up-15cm-Ammonium + acetylene	1.32E+08	6.99E+07	4.71E+04	1.62E+04	3.54E+07	1.61E+07	6.37E+05	2.85E+05
Up-15cm-Ammonium + 1-octyne	1.97E+08	1.48E+07	5.78E+04	n<3	5.51E+07	n<3	1.15E+06	n<3
Mid-5cm-no Ammonium + no inhibitor	3.25E+08	6.19E+07	2.99E+05	2.85E+04	9.10E+07	1.51E+07	1.64E+06	3.58E+05
Mid-5cm-Ammonium + no inhibitor	4.18E+08	2.28E+07	3.68E+05	7.62E+04	1.14E+08	3.96E+06	2.10E+06	3.30E+04
Mid-5cm-Ammonium + acetylene	2.83E+08	1.32E+08	3.63E+05	2.11E+05	7.85E+07	3.73E+07	2.06E+06	9.04E+05
Mid-5cm-Ammonium + 1-octyne	2.84E+08	4.10E+06	3.98E+05	4.05E+04	8.36E+07	6.79E+06	2.63E+06	1.09E+06
Mid-15cm-no Ammonium + no inhibitor	1.38E+08	4.16E+07	3.05E+04	9.21E+03	1.07E+07	3.49E+06	1.75E+05	5.64E+04
Mid-15cm-Ammonium + no inhibitor	1.80E+08	2.65E+07	3.16E+04	1.74E+03	1.52E+07	1.74E+06	2.49E+05	1.92E+03
Mid-15cm-Ammonium + acetylene	2.42E+08	6.05E+06	4.92E+04	2.42E+03	2.55E+07	1.21E+05	6.76E+05	4.42E+03
Mid-15cm-Ammonium + 1-octyne	1.94E+08	1.36E+07	4.62E+04	4.83E+03	1.84E+07	1.68E+06	4.00E+05	9.80E+04
Down-5cm-no Ammonium + no inhibitor	2.25E+08	1.86E+07	1.18E+05	2.02E+04	2.17E+07	1.45E+06	6.93E+05	7.14E+04
Down-5cm-Ammonium + no inhibitor	1.99E+08	3.18E+07	9.43E+04	2.62E+03	1.81E+07	2.61E+06	5.59E+05	1.61E+05
Down-5cm-Ammonium + acetylene	2.08E+08	5.95E+07	9.88E+04	1.30E+04	2.25E+07	6.10E+06	1.03E+06	2.98E+05
Down-5cm-Ammonium + 1-octyne	1.68E+08	2.21E+07	8.84E+04	7.07E+03	1.37E+07	2.38E+06	1.25E+06	1.73E+05
Down-15cm-no ammonium + no inhibitor	2.12E+08	5.24E+06	3.66E+04	2.80E+03	1.73E+07	2.66E+05	9.99E+05	3.58E+04
Down-15cm-Ammonium + no inhibitor	1.73E+08	3.76E+07	3.58E+04	1.25E+03	1.40E+07	2.03E+06	8.48E+05	2.38E+05
Down-15cm-Ammonium + acetylene	2.12E+08	6.40E+07	3.21E+04	2.82E+03	1.36E+07	5.65E+06	8.48E+05	6.96E+03
Down-15cm-Ammonium + 1-octyne	2.06E+08	7.77E+06	3.10E+04	4.40E+03	1.85E+07	2.98E+05	1.09E+06	4.74E+04

After incubation (14-day):

UNIT: gene copies / g wet sediment SD: standard deviation	bacterial 16S rRNA genes		bacterial <i>amoA</i> genes		archaeal 16S rRNA genes		archaeal <i>amoA</i> genes	
	Mean	STD	Mean	STD	Mean	STD	Mean	STD
Up-5cm-no Ammonium + no inhibitor	4.72E+08	4.12E+07	1.68E+05	2.56E+04	6.21E+07	6.70E+06	1.91E+07	2.72E+06
Up-15cm-Ammonium + no inhibitor	3.25E+08	1.21E+07	3.21E+06	7.31E+05	5.09E+07	8.70E+06	1.81E+07	2.77E+06
Up-5cm-Ammonium + acetylene	3.65E+08	4.33E+07	1.09E+05	1.83E+04	4.19E+07	7.19E+06	8.04E+06	1.75E+06
Up-5cm-Ammonium + 1-octyne	4.18E+08	8.82E+07	1.66E+06	5.30E+05	4.83E+07	1.77E+07	1.88E+07	8.95E+06
Up-15cm-no Ammonium + no inhibitor	2.97E+08	1.11E+08	9.80E+04	1.60E+04	5.93E+07	2.32E+07	3.99E+06	1.57E+06
Up-15cm-Ammonium + no inhibitor	3.71E+08	5.97E+07	3.55E+06	6.30E+05	7.20E+07	1.02E+07	5.52E+06	1.10E+06
Up-15cm-Ammonium + acetylene	3.58E+08	8.61E+07	1.07E+05	2.67E+04	5.92E+07	1.72E+07	3.70E+06	1.19E+06
Up-15cm-Ammonium + 1-octyne	3.51E+08	8.77E+07	4.74E+05	2.29E+05	5.23E+07	1.48E+07	3.09E+06	9.92E+05
Mid-5cm-no Ammonium + no inhibitor	6.91E+08	5.48E+07	8.47E+05	5.23E+05	1.52E+08	8.07E+07	5.93E+06	3.28E+06
Mid-5cm-Ammonium + no inhibitor	8.99E+08	4.31E+07	1.04E+07	5.55E+06	2.35E+08	2.00E+07	1.18E+07	3.18E+06
Mid-5cm-Ammonium + acetylene	8.66E+08	9.84E+07	1.14E+06	3.74E+06	1.76E+08	3.26E+07	9.19E+06	2.82E+06
Mid-5cm-Ammonium + 1-octyne	1.03E+09	1.17E+08	6.37E+06	3.21E+06	1.98E+08	3.15E+07	1.04E+07	3.72E+06
Mid-15cm-no Ammonium + no inhibitor	4.15E+08	5.07E+07	1.79E+05	3.24E+04	2.65E+07	2.41E+06	1.11E+06	1.12E+05
Mid-15cm-Ammonium + no inhibitor	4.14E+08	4.89E+07	3.72E+06	5.13E+05	2.61E+07	3.68E+06	1.19E+06	1.84E+05
Mid-15cm-Ammonium + acetylene	3.37E+08	5.57E+07	7.05E+04	1.07E+04	1.99E+07	1.85E+06	7.24E+05	7.37E+04
Mid-15cm-Ammonium + 1-octyne	4.64E+08	1.41E+08	2.03E+05	4.09E+04	3.32E+07	7.94E+06	1.43E+06	5.11E+05
Down-5cm-no Ammonium + no inhibitor	4.96E+08	2.65E+07	1.95E+05	3.18E+04	3.55E+07	1.83E+06	3.41E+06	2.19E+05
Down-5cm-Ammonium + no inhibitor	5.11E+08	1.35E+08	2.02E+06	7.50E+05	3.79E+07	1.21E+07	3.75E+06	2.25E+06
Down-5cm-Ammonium + acetylene	5.86E+08	1.46E+08	2.75E+05	6.62E+04	3.21E+07	6.32E+06	3.00E+06	9.95E+05
Down-5cm-Ammonium + 1-octyne	6.03E+08	5.87E+07	1.70E+06	2.84E+05	4.57E+07	1.98E+06	5.38E+06	4.65E+05
Down-15cm-no ammonium + no inhibitor	5.67E+08	9.61E+07	1.11E+05	1.10E+04	2.91E+07	3.50E+06	2.51E+06	3.56E+05
Down-15cm-Ammonium + no inhibitor	6.14E+08	6.63E+07	1.37E+06	6.07E+05	3.21E+07	1.83E+06	2.99E+06	2.08E+05
Down-15cm-Ammonium + acetylene	6.79E+08	2.94E+07	1.09E+05	9.67E+03	3.22E+07	4.90E+06	3.33E+06	6.03E+05
Down-15cm-Ammonium + 1-octyne	5.71E+08	4.88E+07	1.31E+05	3.55E+04	2.25E+07	3.78E+06	2.74E+06	2.80E+05

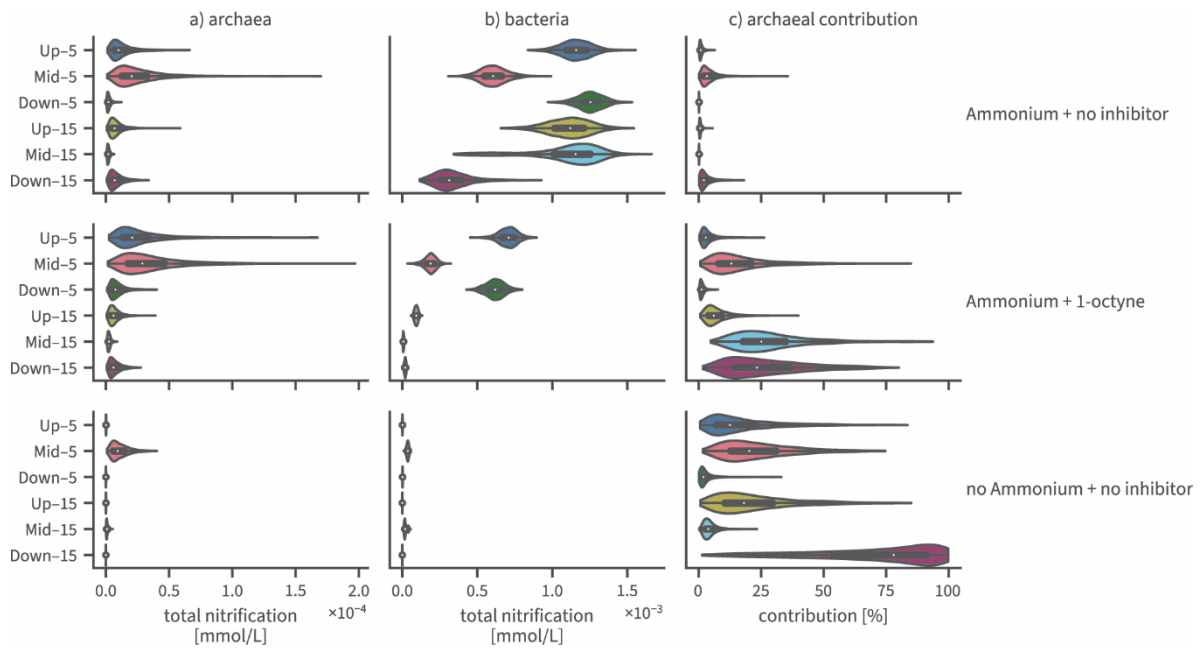


Fig. S2.1: Posterior estimates of nitrification rates in the different microcosms for archaea (a) and bacteria (b), integrated over the duration of the experiment. (c) Contribution of archaea to total nitrification.

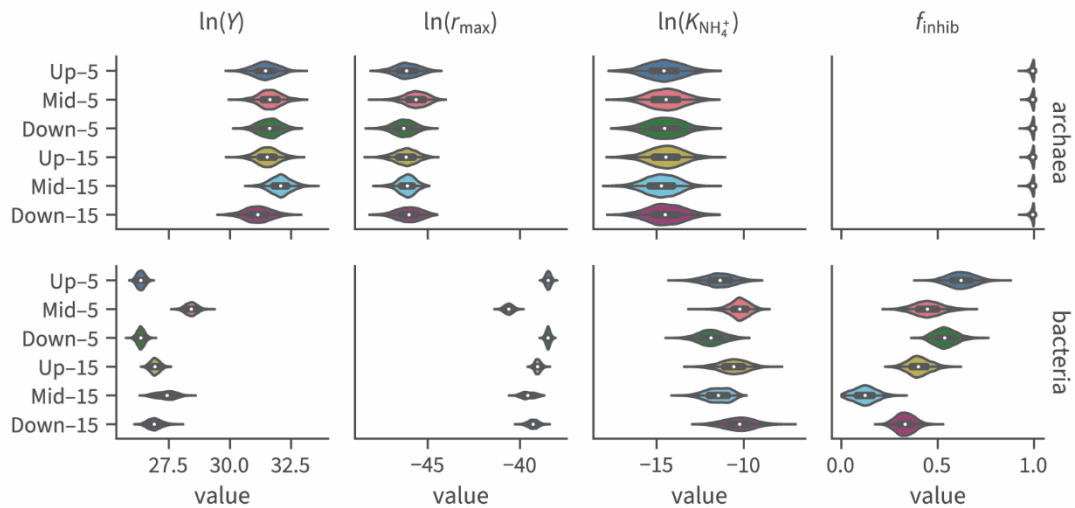


Fig. S2.2: Posterior distributions of model parameters describing the oxidation of ammonium and growth of AOA and AOB for microcosms from different stream segments and depths. Y is the growth yield of ammonium oxidation, r_{\max} is the maximum cell-specific reaction rate, $K_{\text{NH}_4^+}$ is the half-saturation constant, and f_{inhib} is the inhibition constant of 1-octyne.

SI.3 Deciphering microbial nitrogen and sulfur cycling in lower-order agricultural stream sediments using genome-resolved long-read metagenomics

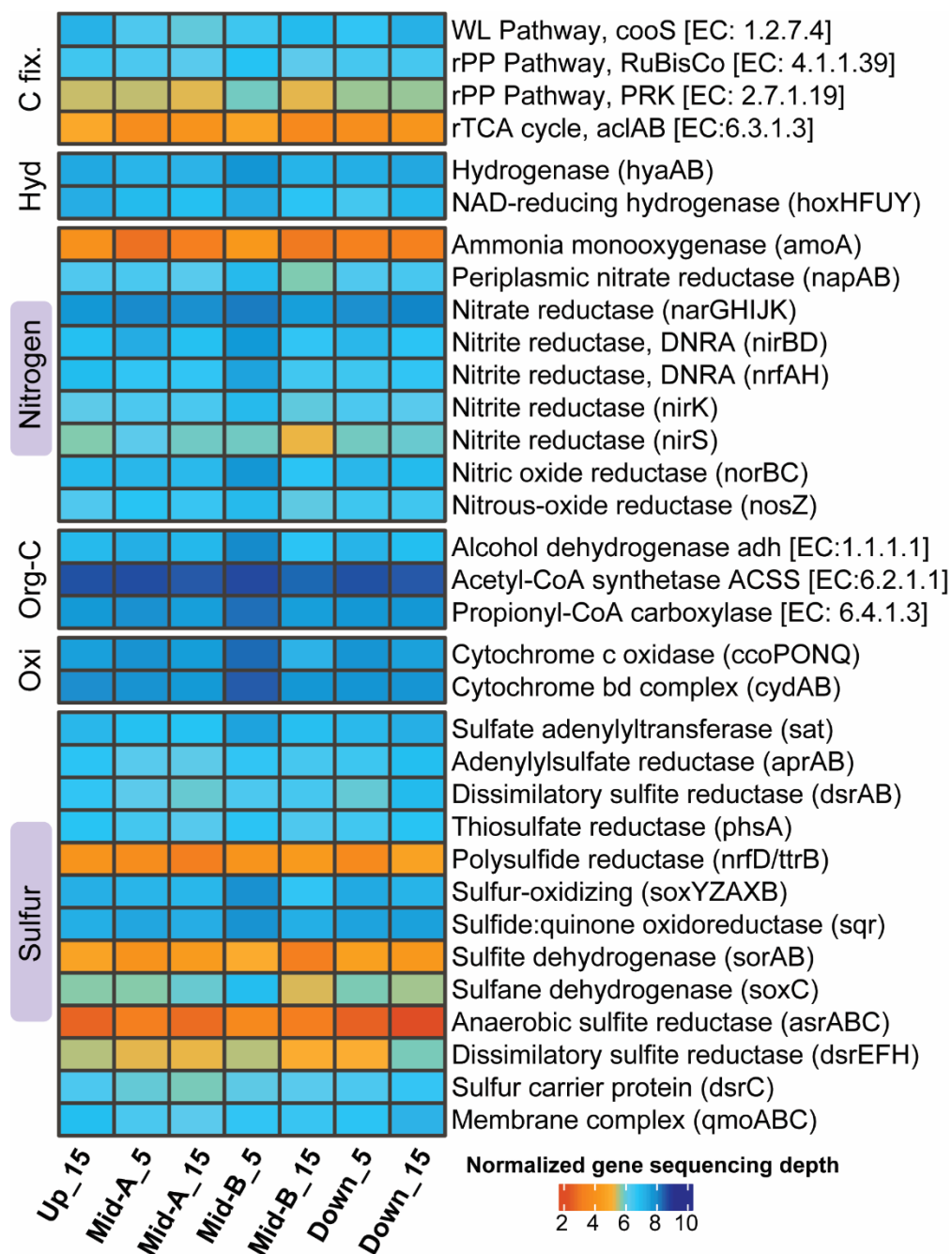


Fig S3.1: Abundance of selected functional genes responsible for nitrogen or sulfur metabolism distributed throughout the Schönbrunnen sediment. Abundance of functional genes are shown as log-transformed gene count after normalization by shotgun metagenomic sequencing depth. Abbreviations: carbon fixation (C fix), hydrogen oxidation (Hyd), organic carbon (Org-C), oxidative phosphorylation (Oxi), dissimilatory nitrate reduction to ammonia (DNRA). Data and figure were prepared together with Daniel Straub within the CAMPOS project.

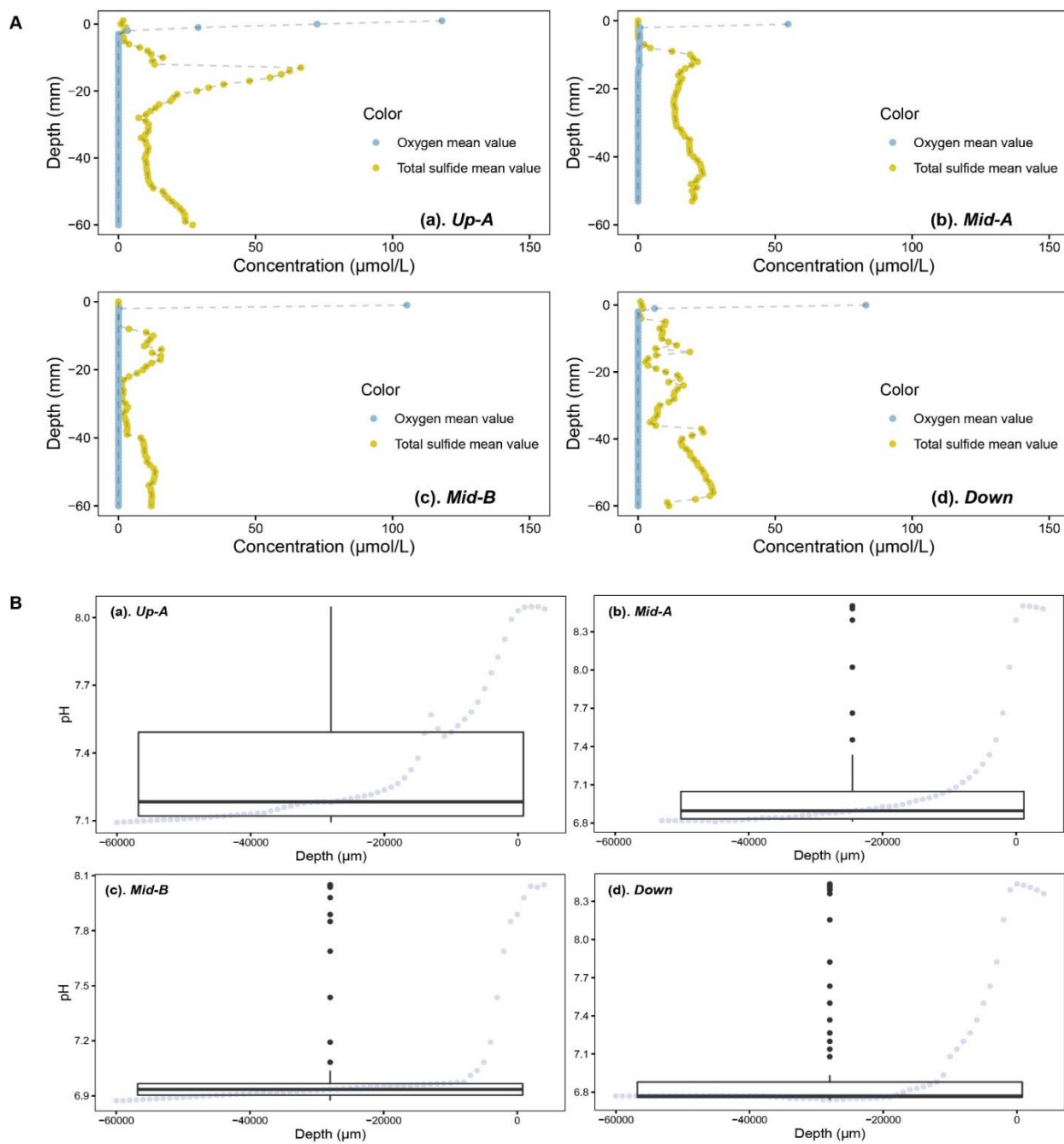


Fig. S3.2 (A). Microprofiles of total sulfide and oxygen, and (B). pH determined by microsensors in Schönbrunnen sediment samples collected from distinct stream sections. The initial measurement point was demonstrated as depth 0, then the MicroProfiling System move vertically until depth 6 cm. Technical replicates and error bars were not shown on the plot for aesthetic reason. In Fig. S3B., each blue dot represented each measurement depth, whereas the box plot was used to indicate mean pH value in top 6 cm of a sampling location.

Table S3.2: List of top 200 abundant pathways based on MetaCyc definitions. The abundance of metabolic pathways was based on the calculation output from the HUMAN3.

MetaCyc Pathways	Up-A_15	Mid-A_5	Mid-A_15	Mid-B_5	Mid-B_15	Down_5	Down_15	Conf_5
ILEUSYN-PWY: L-isoleucine biosynthesis I (from threonine)	11176.78	9256.13	7149.55	16735.77	13398.79	9614.49	13838.75	10723.35
VALSYN-PWY: L-valine biosynthesis	11176.78	9256.13	7149.55	16735.77	13398.79	9614.49	13838.75	10723.35
PWY-7111: pyruvate fermentation to isobutanol (engineered)	11176.78	9256.13	7149.55	16735.77	13244.99	9614.49	13838.75	10723.35
BRANCHED-CHAIN-AA-SYN-PWY: superpathway of branched chain amino acid biosynthesis	10453.31	8533.63	6769.76	15463.82	13104.65	9107.26	13060.55	9970.54
PWY-5103: L-isoleucine biosynthesis III	10453.31	8533.63	6769.76	15463.82	13074.95	9107.26	13060.55	9970.54
PWY-7219: adenosine ribonucleotides de novo biosynthesis	9534.17	8279.31	6082.09	14455.21	13187.79	8688.09	12448.11	9871.98
PWY-7220: adenosine deoxyribonucleotides de novo biosynthesis II	8994.89	9150.68	6832.47	15607.16	11811.10	8832.87	11433.89	9585.30
PWY-7222: guanosine deoxyribonucleotides de novo biosynthesis II	8994.89	9150.68	6832.47	15607.16	11811.10	8832.87	11433.89	9585.30
PWY-7228: superpathway of guanosine nucleotides de novo biosynthesis I	9066.60	8777.40	6526.62	15084.55	11912.12	8581.33	11437.10	9351.21
PWY-7221: guanosine ribonucleotides de novo biosynthesis	8700.79	8246.83	6128.69	14283.98	11362.05	8097.10	10994.09	8862.56
PWY-7208: superpathway of pyrimidine nucleobases salvage	7947.71	7442.27	6025.98	13576.77	11082.30	7886.35	10202.71	8560.97
PWY-7229: superpathway of adenosine nucleotides de novo biosynthesis I	8472.53	7178.78	5509.20	11444.28	12030.10	7548.95	10440.55	7491.23
PWY-6126: superpathway of adenosine nucleotides de novo biosynthesis II	8336.78	7253.12	5548.84	11690.54	11645.17	7532.83	10350.68	7578.83
PWY-6125: superpathway of guanosine nucleotides de novo biosynthesis II	6338.99	6553.21	4864.28	10341.84	10037.01	6620.69	8530.84	7053.09
PWY-6122: 5-aminoimidazole ribonucleotide biosynthesis II	6869.35	5380.49	4414.08	10431.87	10269.14	6567.10	9304.72	6824.17
PWY-6277: superpathway of 5-aminoimidazole ribonucleotide biosynthesis	6869.35	5380.49	4414.08	10431.87	10269.14	6567.10	9304.72	6824.17
PWY-7197: pyrimidine deoxyribonucleotide phosphorylation	6768.38	5168.54	4768.60	10773.71	9302.41	6453.29	9083.03	6450.61
PWY-841: superpathway of purine nucleotides de novo biosynthesis I	6212.71	6079.52	4451.38	9727.43	9561.92	6390.22	8545.15	6396.42
FASYN-INITIAL-PWY: superpathway of fatty acid biosynthesis initiation (E. coli)	6611.10	5959.93	4015.16	9629.89	9092.71	6471.42	8597.70	6949.01
ARGSYN-PWY: L-arginine biosynthesis I (via L-ornithine)	6749.72	5548.94	4103.08	9944.24	9038.08	6223.02	8862.13	6753.66
PWY-7400: L-arginine biosynthesis IV (archaeobacteria)	6722.37	5521.06	4088.37	9900.57	9002.16	6192.25	8830.88	6723.21
PWY-6123: inosine-5'-phosphate biosynthesis I	5922.29	5878.03	4111.25	9962.09	8940.96	6278.63	8382.32	6889.15
PWY-5686: UMP biosynthesis I	6751.94	6162.35	4074.14	9459.88	9023.51	6238.02	7998.69	6356.94
ARGSYNBSUB-PWY: L-arginine biosynthesis II (acetyl cycle)	6560.27	5407.96	3955.36	9564.81	8820.83	6272.65	8750.96	6632.56
PWY-6124: inosine-5'-phosphate biosynthesis II	5669.78	5737.46	3997.55	9610.72	8793.29	6129.72	8267.23	6758.67
PWY-3841: folate transformations II (plants)	6342.55	6284.47	3997.21	9640.17	8631.86	5968.03	7867.47	6033.43
TRNA-CHARGING-PWY: tRNA charging	6065.55	5331.18	3859.50	8915.16	8875.38	5536.74	7757.24	5569.88
TCA: TCA cycle I (prokaryotic)	5792.66	5186.27	4329.00	8213.55	8426.23	5899.44	8255.05	5557.01
PWY-1042: glycolysis IV	6165.48	5053.44	3850.47	8769.82	8334.91	5293.03	7543.73	5290.84
PWY-6121: 5-aminoimidazole ribonucleotide biosynthesis I	5707.62	5002.36	3750.32	8083.11	8593.32	5782.66	7659.29	5447.83
PWY-5695: inosine 5'-phosphate degradation	5490.03	5114.48	3749.09	7968.92	8427.46	5570.15	7337.36	5063.32
PWY-3001: superpathway of L-isoleucine biosynthesis I	4523.15	4747.24	3609.55	7519.34	7186.02	4902.10	7011.83	5023.32
PWY-2942: L-lysine biosynthesis III	4915.52	4495.77	3306.56	7267.59	7711.91	4902.81	6657.35	4591.87
GLYCOLYSIS: glycolysis I (from glucose 6-phosphate)	5078.01	4494.09	3346.51	7444.94	7039.35	4826.86	6039.41	4668.93
PWY-6609: adenine and adenosine salvage III	4367.54	4567.13	3401.44	6603.58	8397.73	4772.14	6033.90	4238.48
COA-PWY-1: superpathway of coenzyme A biosynthesis III (mammals)	4966.42	4356.20	2844.17	6470.54	7598.55	4562.91	6826.58	4565.04
NONOXIPENT-PWY: pentose phosphate pathway (non-oxidative branch) I	4541.55	4181.26	2992.48	6982.68	7390.49	5004.49	6454.64	4510.23
PWY-6969: TCA cycle V (2-oxoglutarate synthase)	4875.77	4055.60	3477.00	6583.19	7015.66	4726.94	6912.45	4233.57
CALVIN-PWY: Calvin-Benson-Bassham cycle	4874.57	4340.32	3105.52	6508.81	7002.93	4773.67	6326.35	4533.44

HISTSYN-PWY: L-histidine biosynthesis	4440.48	4577.24	3429.21	6935.01	6661.22	4861.74	5530.78	4831.86
PWY-5097: L-lysine biosynthesis VI	4720.28	4243.51	3088.33	6867.33	6798.18	4595.83	6427.78	4367.88
PWY-5973: cis-vaccenate biosynthesis	3872.89	5228.15	3139.48	8120.28	4833.77	4905.53	4516.97	5911.78
SER-GLYSYN-PWY: superpathway of L-serine and glycine biosynthesis I	4308.88	4531.04	3305.18	7541.62	5298.33	4627.27	5391.85	4839.71
COA-PWY: coenzyme A biosynthesis I (prokaryotic)	4664.22	3982.95	2524.35	5927.09	6916.36	4218.73	6369.28	4176.49
GLUTORN-PWY: L-ornithine biosynthesis I	4656.22	3656.34	2762.33	6477.70	6220.89	4252.37	6007.29	4613.31
PANTO-PWY: phosphopantothenate biosynthesis I	4583.97	3938.90	2853.62	5212.47	7247.05	4395.21	6312.53	3571.02
PWY-6700: queuosine biosynthesis I (de novo)	4088.14	4215.14	2829.73	6200.82	6234.16	4101.20	5729.51	4274.77
PWY-5484: glycolysis II (from fructose 6-phosphate)	4296.11	4019.68	2946.56	6357.54	6180.76	4345.70	5389.47	3908.92
1CMET2-PWY: folate transformations III (E. coli)	3646.90	4682.15	3051.75	6005.34	6156.09	4526.02	5185.33	4145.34
UDPNAGSYN-PWY: UDP-N-acetyl-D-glucosamine biosynthesis I	3996.18	3783.38	2782.07	5267.60	7164.39	4353.57	5601.12	3836.30
PWY-5188: tetrapyrrole biosynthesis I (from glutamate)	3795.73	3891.87	2795.38	5424.41	6846.76	4377.48	5833.71	3708.39
PWY-7663: gondoate biosynthesis (anaerobic)	3360.71	4786.69	2780.94	7265.28	4159.49	4395.50	3888.61	5397.04
ANAGLYCOLYSIS-PWY: glycolysis III (from glucose)	4077.71	3441.66	2395.00	5495.43	5813.83	4231.84	5571.36	4598.66
PEPTIDOLYCANSYN-PWY: peptidoglycan biosynthesis I (meso-diaminopimelate containing)	3596.37	3797.47	2669.04	5353.37	6710.38	4176.13	5538.91	3644.89
PWY-5690: TCA cycle II (plants and fungi)	3945.10	3430.97	2989.32	5263.64	6113.79	4075.48	5866.73	3592.40
PWY-6386: UDP-N-acetylmuramoyl-pentapeptide biosynthesis II (lysine-containing)	3594.83	3756.13	2698.17	4975.24	6816.62	4222.43	5560.08	3485.91
COMPLETE-ARO-PWY: superpathway of aromatic amino acid biosynthesis	3624.57	3876.79	2776.82	5729.51	5903.12	4235.49	5077.89	3878.86
PWY-6385: peptidoglycan biosynthesis III (mycobacteria)	3551.59	3764.42	2598.51	5212.14	6523.82	4130.97	5494.28	3546.26
PWY-6387: UDP-N-acetylmuramoyl-pentapeptide biosynthesis I (meso-diaminopimelate containing)	3447.79	3682.14	2599.41	5081.77	6567.70	4046.94	5368.30	3502.01
PWY-724: superpathway of L-lysine, L-threonine and L-methionine biosynthesis II	3652.81	3733.65	2778.77	5827.60	5363.19	3841.68	4873.34	3837.39
THRESYN-PWY: superpathway of L-threonine biosynthesis	3258.20	3622.54	2728.81	5543.29	5497.91	3714.84	5309.34	3736.52
ARO-PWY: chorismate biosynthesis I	3395.65	3653.02	2610.03	5336.32	5602.96	4001.63	4740.40	3601.73
PWY-6163: chorismate biosynthesis from 3-dehydroquinate	3414.78	3637.07	2588.49	5099.59	5826.89	4047.04	4787.15	3453.28
NONMEVIPP-PWY: methylerythritol phosphate pathway I	3640.53	3242.17	2361.09	4854.55	6330.11	3768.14	5251.44	3360.75
PANTOSYN-PWY: superpathway of coenzyme A biosynthesis I (bacteria)	4009.92	3387.65	2350.25	4833.34	6109.38	3502.49	5409.73	2915.79
PWY-7198: pyrimidine deoxyribonucleotides de novo biosynthesis IV	2720.02	3310.86	2718.17	6077.04	5019.23	3743.61	3778.83	4080.58
PWY0-162: superpathway of pyrimidine ribonucleotides de novo biosynthesis	2270.18	4502.89	2425.90	5196.12	4285.00	4333.49	4036.85	4084.12
PWY-6703: preQ0 biosynthesis	2823.13	3248.22	2255.40	4709.31	5559.88	3698.40	4142.48	3314.65
PYRIDNUCSYN-PWY: NAD de novo biosynthesis I (from aspartate)	3495.72	3159.63	2229.61	4430.44	5353.68	3456.59	4628.31	2862.55
HSERMETANA-PWY: L-methionine biosynthesis III	3565.52	2951.75	2364.95	5148.92	4716.73	3061.02	4492.15	3052.08
RIBOSYN2-PWY: flavin biosynthesis I (bacteria and plants)	3034.83	3095.95	2059.21	4182.20	5434.18	3382.42	4361.12	2990.01
CITRULBIO-PWY: L-citrulline biosynthesis	2580.15	3196.45	2417.38	5537.53	4561.09	3060.68	3237.08	3750.44
TRPSYN-PWY: L-tryptophan biosynthesis	3081.47	3326.59	2216.11	3915.92	4899.49	3456.90	4202.43	2739.35
PWY-4242	3026.10	3074.77	2048.71	3466.48	5902.86	3282.26	4378.45	2636.57
PWY-4984: urea cycle	2341.37	3129.60	2367.47	5571.55	4316.74	2887.06	2935.03	3783.03
PWY-7383: anaerobic energy metabolism (invertebrates, cytosol)	2810.06	2818.92	2250.46	3981.20	4615.43	3416.26	4659.16	2708.10
PWY-5104: L-isoleucine biosynthesis IV	4125.47	1561.31	1476.63	3968.72	6326.70	2562.90	4865.75	2263.20
ANAEROFrucAT-PWY: homolactic fermentation	2853.97	2804.40	2021.07	4437.26	4815.27	3183.47	3722.33	3251.70
OANTIGEN-PWY: O-antigen building blocks biosynthesis (E. coli)	3208.55	3059.40	2051.83	3852.50	4717.99	3481.83	4074.09	2625.42
DTDRHAMSYN-PWY: dTDP-β-L-rhamnose biosynthesis	3161.78	3063.34	1946.13	4725.89	4050.76	3203.74	3677.87	2756.24
HISDEG-PWY: L-histidine degradation I	2273.42	3206.68	2085.95	4545.11	4374.05	2919.11	2944.93	3747.35
DAPLYSINESYN-PWY: L-lysine biosynthesis I	2502.86	3002.77	1951.51	4635.47	3722.79	3290.98	3490.35	3436.82
PWY-7234: inosine-5'-phosphate biosynthesis III	1607.99	3997.75	2396.25	5024.45	4433.53	3686.89	1148.36	3393.35

GLYCOGENSYNTH-PWY: glycogen biosynthesis I (from ADP-D-Glucose)	3116.17	2526.71	2030.12	4438.02	4072.20	2963.43	3911.60	2325.04
PWY-7199: pyrimidine deoxyribonucleosides salvage	2213.30	3241.19	2208.06	4100.56	4683.13	2764.83	2737.97	3079.13
PWY-5723: Rubisco shunt	2554.93	2444.48	1753.97	3591.85	3896.85	3461.69	3719.29	3114.46
P105-PWY: TCA cycle IV (2-oxoglutarate decarboxylase)	1888.20	3194.10	2451.73	4372.20	3681.67	2943.57	2243.42	3166.45
PWY-5464: superpathway of cytosolic glycolysis (plants), pyruvate dehydrogenase and TCA cycle	2711.88	2624.55	2064.37	5259.09	2431.47	2704.24	2639.76	3227.90
P42-PWY: incomplete reductive TCA cycle	3346.13	1970.11	1795.74	4442.62	4287.04	2088.47	3228.78	2285.73
PWY-6270: isoprene biosynthesis I	2773.82	2494.58	1732.41	3113.53	5073.97	2654.54	3356.66	2161.01
PWY-5918: superpathway of heme b biosynthesis from glutamate	2388.30	2555.26	1944.82	3445.93	3798.42	3073.08	3844.38	2272.41
HEME-BIOSYNTHESIS-II: heme b biosynthesis I (aerobic)	1800.10	2827.90	1596.90	3301.67	4649.90	2754.93	3556.12	2626.87
PWY-5345: superpathway of L-methionine biosynthesis (by sulfhydrylation)	2105.80	2569.81	2031.09	4346.76	3688.15	2541.84	2905.20	2736.74
PWY66-409: superpathway of purine nucleotide salvage	1966.29	2141.32	1907.16	4505.57	3388.65	2874.66	2758.57	2744.18
PWY0-1586: peptidoglycan maturation (meso-diaminopimelate containing)	2793.11	2616.30	1276.34	3369.09	2139.43	3207.18	3910.94	2691.73
PWY-7560: methylerythritol phosphate pathway II	2542.84	2287.50	1576.49	3174.59	4736.72	2432.34	3056.31	2128.97
GLYCOLYSIS-TCA-GLYOX-BYPASS: superpathway of glycolysis, pyruvate dehydrogenase, TCA, and glyoxylate bypass	1594.42	3312.00	2309.21	3325.15	3516.31	2571.97	1803.38	2746.72
GLYOXYLATE-BYPASS: glyoxylate cycle	2142.03	2205.54	1898.51	3200.25	3610.67	2507.66	3274.53	2206.08
PWY-5173	1921.22	2231.85	1455.56	4700.59	1816.08	2284.38	3016.51	3002.00
PWY-4981: L-proline biosynthesis II (from arginine)	2325.25	2433.18	1705.68	3600.21	2719.86	2421.28	2321.15	2490.65
TCA-GLYOX-BYPASS: superpathway of glyoxylate bypass and TCA	1203.27	2964.78	2073.37	3649.68	3666.90	2264.91	1318.02	2781.91
METSYN-PWY: superpathway of L-homoserine and L-methionine biosynthesis	1831.82	2417.52	1484.60	3569.18	1986.85	2309.02	2446.83	2779.32
PWY66-399: gluconeogenesis III	1970.47	2131.04	1357.47	3453.83	2564.62	2183.92	2391.43	2748.56
GLUCONEO-PWY: gluconeogenesis I	1874.60	2212.65	1351.85	3800.60	2293.64	2210.33	2405.29	2475.51
MET-SAM-PWY: superpathway of S-adenosyl-L-methionine biosynthesis	1686.59	2347.98	1524.14	3589.80	2065.70	2199.89	2273.97	2725.51
PWY-5667: CDP-diacylglycerol biosynthesis I	1882.88	1742.05	1403.69	2582.62	3848.44	2142.62	3171.31	1623.02
PWY0-1319: CDP-diacylglycerol biosynthesis II	1882.88	1742.05	1403.69	2582.62	3848.44	2142.62	3171.31	1623.02
SO4ASSIM-PWY: assimilatory sulfate reduction I	1679.97	2213.28	1511.61	4008.78	2682.12	1918.69	2012.55	2347.56
PWY0-862: (5Z)-dodecenoate biosynthesis I	1382.34	2234.72	1511.38	3509.09	2588.00	2048.10	2121.64	2921.12
PWY-5347: superpathway of L-methionine biosynthesis (transsulfuration)	1764.36	2237.02	1464.12	3192.70	2092.21	2286.04	2520.53	2411.30
P23-PWY: reductive TCA cycle I	1654.16	1473.67	1527.69	4437.98	1811.12	1509.44	2791.22	2603.06
PHOSLIPSYN-PWY: superpathway of phospholipid biosynthesis I (bacteria)	2001.09	1843.46	1323.58	2732.42	2995.03	2025.63	3105.78	1711.21
FASYN-ELONG-PWY: fatty acid elongation -- saturated	1239.30	2608.77	1267.60	3510.27	2084.70	2079.54	2102.40	2804.10
PWY66-398: TCA cycle III (animals)	1758.47	2071.96	1658.61	3954.37	1852.02	2046.70	1648.36	2487.60
P4-PWY: superpathway of L-lysine, L-threonine and L-methionine biosynthesis I	1693.38	2207.05	1497.59	2983.60	2314.19	2300.90	2325.80	2012.56
PWY-7664: oleate biosynthesis IV (anaerobic)	1209.82	2434.16	1258.90	3371.20	2095.66	1992.14	2037.08	2722.75
PWY-7388: octanoyl-[acyl-carrier protein] biosynthesis (mitochondria, yeast)	1166.02	2462.92	1182.16	3280.67	2027.80	1967.58	2064.63	2650.89
PWY0-1296: purine ribonucleosides degradation	972.96	1610.66	1341.23	3387.28	3283.50	1823.30	1754.10	2352.92
PWY0-781: aspartate superpathway	1462.52	2123.33	1414.55	2643.36	2184.46	2214.42	2109.77	1991.10
PWY-5100: pyruvate fermentation to acetate and lactate II	2404.04	1444.88	1283.91	3256.46	2615.23	1435.21	1789.03	1621.60
PWY-7371: 1,4-dihydroxy-6-naphthoate biosynthesis II	1487.80	1025.33	1249.39	2962.69	2408.80	1743.45	3178.17	1546.53
PWY-5920: superpathway of heme b biosynthesis from glycine	1333.88	1804.22	1290.11	2705.45	2679.44	1909.42	2002.54	1846.11
PWY0-1479: tRNA processing	1598.66	1721.38	995.66	2634.32	2197.95	2066.04	2300.56	2054.48
PWY-241: C4 photosynthetic carbon assimilation cycle, NADP-ME type	813.19	2338.58	1399.55	2890.98	1904.76	2203.59	1661.64	1959.75
PWY-5913: partial TCA cycle (obligate autotrophs)	732.14	2140.81	1464.85	2967.13	1876.24	2077.37	1610.38	2188.93
PWY-7237: myo-, chiro- and scylo-inositol degradation	2115.91	1518.71	1326.38	3647.28	1687.81	1478.86	1436.55	1697.87
PWY-6282: palmitoleate biosynthesis I (from (5Z)-dodec-5-enoate)	1007.39	2233.63	1053.32	2949.56	1742.89	1742.57	1772.99	2387.74

PWY-7117: C4 photosynthetic carbon assimilation cycle, PEPC type	852.52	2037.54	1376.89	2563.18	2220.13	2172.94	1795.48	1759.12
PWY-5189: tetrapyrrole biosynthesis II (from glycine)	1075.25	1552.92	1103.53	2845.27	2346.39	1536.73	1487.17	2205.01
PWY-6549: L-glutamine biosynthesis III	1026.47	1679.69	1334.81	3004.74	1676.97	1718.45	1679.86	1914.36
ASPASN-PWY: superpathway of L-aspartate and L-asparagine biosynthesis	1612.06	1361.83	1146.30	2436.96	1935.29	1585.60	2160.14	1567.00
PWY-6936: seleno-amino acid biosynthesis (plants)	968.67	1648.11	1376.18	2807.89	2145.31	1417.81	1375.27	1826.28
PWY0-1415: superpathway of heme b biosynthesis from uroporphyrinogen-III	1343.29	1726.93	1039.30	1909.92	1714.00	2072.88	2126.99	1500.94
HEMESYN2-PWY: heme b biosynthesis II (oxygen-independent)	1274.86	1886.39	985.32	1820.79	1534.98	2145.59	1991.64	1715.23
PWY-5989: stearate biosynthesis II (bacteria and plants)	948.39	1991.45	963.40	2611.42	1602.20	1570.75	1535.08	2052.08
PWY4FS-7: phosphatidylglycerol biosynthesis I (plastidic)	1626.70	1217.96	863.29	1437.76	2254.37	1579.03	2630.78	1033.19
PWY4FS-8: phosphatidylglycerol biosynthesis II (non-plastidic)	1626.70	1217.96	863.29	1437.76	2254.37	1579.03	2630.78	1033.19
PWY-5154: L-arginine biosynthesis III (via N-acetyl-L-citrulline)	1328.28	1525.15	810.04	2389.83	1222.48	1386.01	1743.28	1912.88
PWY-6737: starch degradation V	1417.85	1747.13	1049.08	2208.16	1623.51	1428.55	1064.89	1290.54
FERMENTATION-PWY: mixed acid fermentation	887.43	1372.17	1162.19	2779.19	1461.95	1395.30	1054.77	1694.95
BIOTIN-BIOSYNTHESIS-PWY: biotin biosynthesis I	1061.64	1553.77	789.90	1727.05	1498.55	1690.43	1831.93	1601.73
PWY-6168: flavin biosynthesis III (fungi)	1674.36	1900.19	945.44	1988.93	1382.78	1239.12	1164.53	1195.18
HOMOSER-METSYN-PWY: L-methionine biosynthesis I	1074.54	1531.91	897.47	2186.35	1114.30	1428.71	1439.17	1772.50
PWY-6519: 8-amino-7-oxononanoate biosynthesis I	1002.06	1491.82	732.88	1691.01	1356.12	1583.61	1691.24	1652.11
PWY-6305: superpathway of putrescine biosynthesis	849.95	1371.49	1202.36	2217.46	1782.71	1145.55	893.95	1452.25
PWY-7254: TCA cycle VII (acetate-producers)	199.08	2350.85	1593.33	1168.36	2985.03	1628.88	78.72	788.08
PWY-6353: purine nucleotides degradation II (aerobic)	950.24	1044.73	838.86	2034.05	1535.76	1430.18	1368.67	1384.17
SULFATE-CYS-PWY: superpathway of sulfate assimilation and cysteine biosynthesis	973.58	1183.30	846.34	2655.48	1255.50	1198.03	633.17	1791.35
PWY-5855: ubiquinol-7 biosynthesis (early decarboxylation)	1219.03	1113.82	674.15	1819.15	788.10	1423.00	1647.71	1360.31
PWY-5856: ubiquinol-9 biosynthesis (early decarboxylation)	1219.03	1113.82	674.15	1819.15	788.10	1423.00	1647.71	1360.31
PWY-5857: ubiquinol-10 biosynthesis (early decarboxylation)	1219.03	1113.82	674.15	1819.15	788.10	1423.00	1647.71	1360.31
PWY-6708: ubiquinol-8 biosynthesis (early decarboxylation)	1219.03	1113.82	674.15	1819.15	788.10	1423.00	1647.71	1360.31
PWY-6608: guanosine nucleotides degradation III	959.98	1052.17	686.78	1603.98	1398.59	1279.28	1421.93	1320.25
PWY-2941: L-lysine biosynthesis II	191.71	1977.81	1302.32	938.61	2831.44	1426.63	209.35	407.59
PWY66-389: phytol degradation	622.41	1359.02	959.80	1848.08	1105.03	1179.03	769.71	1294.78
PWY0-1297: superpathway of purine deoxyribonucleosides degradation	647.93	1152.17	736.87	1872.28	1299.67	1140.48	977.17	1140.31
ARG+POLYAMINE-SYN: superpathway of arginine and polyamine biosynthesis	1027.81	875.41	571.15	1886.89	1213.30	1263.01	1051.71	1027.46
REDCITCYC: TCA cycle VI (Helicobacter)	344.24	1379.48	1089.01	1677.28	1456.03	1084.72	499.70	1310.61
P108-PWY: pyruvate fermentation to propanoate I	1114.06	842.45	611.06	1889.62	920.39	800.62	1227.51	1262.88
SALVADEHYPOX-PWY: adenosine nucleotides degradation II	826.25	912.41	592.83	1388.01	1202.30	1113.02	1228.46	1155.79
PWY0-1298: superpathway of pyrimidine deoxyribonucleosides degradation	709.04	1060.62	649.96	1235.80	1691.53	1052.83	1130.43	808.83
PWY-5676: acetyl-CoA fermentation to butanoate II	858.83	778.77	746.93	2107.10	621.92	878.72	707.37	1199.54
PWY-7384: anaerobic energy metabolism (invertebrates, mitochondrial)	704.31	807.46	559.56	1732.13	768.47	538.85	1023.19	1080.27
PWY0-1241: ADP-L-glycero-β-D-manno-heptose biosynthesis	922.02	640.17	423.97	1422.09	973.67	641.94	1294.85	878.06
PWY-6588: pyruvate fermentation to acetone	502.28	536.21	518.09	1546.93	1255.42	642.50	567.73	978.18
PWY-6876: isopropanol biosynthesis (engineered)	502.28	536.21	518.09	1546.93	1255.42	642.50	567.73	978.18
P124-PWY: Bifidobacterium shunt	763.73	572.78	484.96	1531.75	648.51	705.84	663.84	1017.53
PWY-821: superpathway of sulfur amino acid biosynthesis (Saccharomyces cerevisiae)	195.87	832.09	657.22	1357.71	980.02	864.96	463.33	984.37
PWY-5121: superpathway of geranylgeranyl diphosphate biosynthesis II (via MEP)	550.46	1357.98	715.33	778.38	430.17	1101.25	498.33	844.46
PWY-7332: superpathway of UDP-N-acetylglucosamine-derived O-antigen building blocks biosynthesis	959.80	668.09	415.27	1457.15	839.20	452.54	848.10	548.26
PWY-1269: CMP-3-deoxy-D-manno-octulosonate biosynthesis	402.13	1370.62	546.30	1184.18	325.32	973.44	580.44	775.36

METH-ACETATE-PWY: methanogenesis from acetate	1456.04	355.78	214.20	350.47	1679.29	524.12	1237.07	319.02
PWY-5101: L-isoleucine biosynthesis II	862.80	323.29	416.54	1386.36	1471.74	396.13	678.89	596.36
PWY-6151: S-adenosyl-L-methionine salvage I	213.86	871.32	646.41	992.92	1609.89	522.91	181.49	506.10
NAGLIPASYN-PWY: lipid IVA biosynthesis (E. coli)	398.98	821.18	310.96	677.05	596.70	1051.51	778.96	863.72
URSIN-PWY: ureide biosynthesis	177.26	961.45	642.64	798.20	978.67	922.10	342.43	653.12
PWY-7210: pyrimidine deoxyribonucleotides biosynthesis from CTP	949.43	1652.66	217.71	417.83	85.59	1122.61	40.32	988.53
PWY66-367: ketogenesis	452.36	604.21	438.03	1117.20	535.24	673.78	495.17	938.42
FAO-PWY: fatty acid & beta;-oxidation I (generic)	148.81	1360.95	333.92	639.74	481.62	784.04	508.73	961.71
PWY-7392: taxadiene biosynthesis (engineered)	399.31	1197.89	615.57	623.24	320.56	959.50	389.67	709.92
POLYAMSYN-PWY: superpathway of polyamine biosynthesis I	575.45	485.72	316.45	1077.05	681.92	730.68	573.43	567.44
PWY-7184: pyrimidine deoxyribonucleotides de novo biosynthesis I	858.64	1537.41	196.28	376.82	77.03	1017.77	36.28	896.73
PWY-6545: pyrimidine deoxyribonucleotides de novo biosynthesis III	856.60	1489.86	196.11	376.72	77.04	1012.83	36.30	896.26
PWY-7389: superpathway of anaerobic energy metabolism (invertebrates)	686.24	515.35	360.36	1074.57	464.17	475.61	785.19	456.21
PWY-7242: D-fructuronate degradation	629.46	493.21	308.72	845.24	773.72	446.31	624.97	579.98
PWY0-42: 2-methylcitrate cycle I	472.47	633.67	315.79	817.62	473.15	402.12	579.27	559.58
GLYCOCAT-PWY: glycogen degradation I	104.63	504.76	247.38	834.03	454.59	838.80	659.43	589.41
COLANSYN-PWY: colanic acid building blocks biosynthesis	269.77	637.30	278.93	727.68	471.67	664.10	528.59	648.99
GLYCOLYSIS-E-D: superpathway of glycolysis and the Entner-Doudoroff pathway	300.47	754.68	312.30	1006.33	178.02	644.62	182.09	827.35
PWY-6590: superpathway of Clostridium acetobutylicum acidogenic fermentation	459.90	536.86	330.22	795.83	804.80	355.12	579.64	264.24
PYRIDNUCSAL-PWY: NAD salvage pathway I (PNC VI cycle)	419.62	221.86	186.63	707.27	908.54	371.56	744.28	489.98
PWY-7094: fatty acid salvage	241.99	563.31	279.98	862.45	280.96	565.33	246.40	978.12
PWY-5747: 2-methylcitrate cycle II	436.07	631.61	284.84	759.35	433.18	373.85	569.74	527.87
PYRIDOSYN-PWY: pyridoxal 5'-phosphate biosynthesis I	489.53	1310.18	156.35	594.42	248.70	513.75	150.42	528.65
PWY-7527: L-methionine salvage cycle III	62.34	687.28	511.14	291.06	1731.14	378.60	120.71	187.88
PWY-7115: C4 photosynthetic carbon assimilation cycle, NAD-ME type	531.68	438.08	298.19	854.38	393.22	406.67	650.85	355.69
P161-PWY: acetylene degradation (anaerobic)	322.29	793.74	343.27	664.23	542.72	410.13	402.87	432.67
PWY-6527: stachyose degradation	723.45	525.54	224.02	473.62	986.32	282.28	491.27	131.81
PWY-6317: D-galactose degradation I (Leloir pathway)	550.04	578.94	250.59	525.67	823.95	316.50	428.53	334.90
NADSYN-PWY: NAD de novo biosynthesis II (from tryptophan)	165.60	856.66	458.25	878.53	107.71	675.78	36.56	605.09
PWY-622: starch biosynthesis	142.41	375.62	280.42	822.38	512.95	562.08	573.12	479.33
PWY-6897: thiamine diphosphate salvage II	542.81	346.90	313.68	669.16	561.49	336.96	574.77	350.88
PWY66-422	550.04	578.94	250.59	525.67	823.95	316.50	428.53	160.67
PWY-5505: L-glutamate and L-glutamine biosynthesis	304.39	536.42	352.99	815.85	357.40	452.75	341.71	471.98
PWY-6507: 4-deoxy-L-threo-hex-4-enopyranuronate degradation	511.41	438.27	237.52	663.67	545.77	318.94	261.67	455.10
COBALSYN-PWY: superpathway of adenosylcobalamin salvage from cobinamide I	441.23	543.30	181.07	458.28	607.96	323.01	524.97	299.70
CENTFERM-PWY: pyruvate fermentation to butanoate	373.72	437.09	266.99	642.34	665.51	285.40	480.52	210.07
PWY-6901: superpathway of glucose and xylose degradation	361.51	549.16	325.84	943.78	162.04	396.62	223.03	395.29
PWY-1861: formaldehyde assimilation II (assimilatory RuMP Cycle)	838.51	213.97	73.93	418.04	978.91	149.68	220.75	449.82
PWY-5659: GDP-mannose biosynthesis	200.33	543.75	227.81	589.59	365.66	405.55	323.99	637.87
PWY-1361: benzoyl-CoA degradation I (aerobic)	321.38	252.66	315.83	756.27	392.18	371.20	358.19	520.53
PWY-6263: superpathway of menaquinol-8 biosynthesis II	420.26	501.49	261.19	798.95	144.53	252.83	358.36	480.32
HEXITOLDEGSUPER-PWY: superpathway of hexitol degradation (bacteria)	43.51	484.39	352.61	624.28	918.44	456.42	171.30	147.49
PENTOSE-P-PWY: pentose phosphate pathway	206.40	582.15	235.06	803.94	114.79	484.65	118.68	610.49
P461-PWY: hexitol fermentation to lactate, formate, ethanol and acetate	201.65	482.43	450.75	312.23	805.83	368.26	321.18	210.01

PWY-7357: thiamine phosphate formation from pyriothiamine and oxythiamine (yeast)	460.44	284.06	260.87	536.23	497.66	264.73	466.05	262.87
PWY-6147: 6-hydroxymethyl-dihydropterin diphosphate biosynthesis I	536.52	244.50	187.20	601.40	526.78	280.72	337.09	289.84
PWY-7539: 6-hydroxymethyl-dihydropterin diphosphate biosynthesis III (Chlamydia)	534.27	243.36	186.47	598.71	525.22	278.98	336.41	288.53
PWY-5651: L-tryptophan degradation to 2-amino-3-carboxymuconate semialdehyde	112.85	701.03	360.60	737.34	69.41	509.41	23.12	470.62
PWY-5022: 4-aminobutanoate degradation V	372.17	278.43	191.90	346.88	544.99	259.17	286.34	460.95
PWY-6859: all-trans-farnesol biosynthesis	221.48	673.26	322.25	308.12	151.22	491.95	192.85	365.52
PWY-4361: S-methyl-5-thio-α-D-ribose 1-phosphate degradation I	37.77	465.20	346.81	180.34	1187.40	241.90	73.40	115.88
LEU-DEG2-PWY: L-leucine degradation I	146.47	441.57	235.70	545.96	213.74	359.98	243.22	430.29
POLYISOPRENSYN-PWY: polyisoprenoid biosynthesis (E. coli)	205.79	636.83	245.93	366.38	164.85	388.19	154.63	374.22
ARGORNPROST-PWY	122.28	373.96	159.57	541.37	287.58	413.10	302.54	329.25
PWY-7209: superpathway of pyrimidine ribonucleosides degradation	195.24	367.12	272.81	401.89	273.64	344.29	305.54	363.98
PWY-7323: superpathway of GDP-mannose-derived O-antigen building blocks biosynthesis	166.67	421.29	175.67	435.66	294.42	321.87	243.63	422.01
GALACTUROCAT-PWY: D-galacturonate degradation I	217.52	454.57	220.76	638.42	99.76	264.88	170.48	403.56
PWY-6471: peptidoglycan biosynthesis IV (Enterococcus faecium)	304.73	166.02	0.00	714.47	236.12	343.18	421.18	268.55
PWY-7328: superpathway of UDP-glucose-derived O-antigen building blocks biosynthesis	66.92	341.56	160.07	529.05	298.76	521.34	128.55	364.28
PWY3DJ-35471: L-ascorbate biosynthesis IV (animals, D-glucuronate pathway)	74.35	314.60	160.33	569.82	144.21	400.48	368.41	364.30
ORNDEG-PWY: superpathway of ornithine degradation	0.00	343.51	0.00	802.61	445.72	372.19	0.00	402.76
PWY-7200: superpathway of pyrimidine deoxyribonucleoside salvage	342.97	540.23	318.78	491.66	204.11	217.25	91.32	113.66
PWY-6728: methylaspartate cycle	248.19	208.89	157.46	318.57	495.16	271.22	360.44	231.47
DENITRIFICATION-PWY: nitrate reduction I (denitrification)	129.31	314.54	226.34	546.44	187.70	257.23	261.24	337.56
GLUCOSE1PMETAB-PWY: glucose and glucose-1-phosphate degradation	52.82	271.92	127.78	433.55	237.53	463.38	351.98	312.02
PWY-6953: dTDP-3-acetamido-α-D-fucose biosynthesis	358.18	169.32	172.90	539.94	295.99	224.68	240.28	234.41
PWY-5675: nitrate reduction V (assimilatory)	24.34	696.85	158.78	403.66	204.45	261.64	101.20	378.20
PWY-6583: pyruvate fermentation to butanol I	296.70	217.52	95.50	427.22	420.56	137.40	337.96	223.97
POLYAMINSYN3-PWY: superpathway of polyamine biosynthesis II	120.38	293.17	154.96	495.30	373.02	186.60	285.57	180.97
PROTocatechuate-ortho-cleavage-PWY: protocatechuate degradation II (ortho-cleavage pathway)	100.88	383.87	176.30	396.73	191.73	316.89	134.48	351.95

Table S3.3: Abundance of selected nitrate reduction gene families with KO (KEGG ORTHOLOGY) number and contributing microbial species.

KO	gene family	Up-A_15	Mid-A_5	Mid-A_15	Mid-B_5	Mid-B_15	Down_5	Down_15	Conf_5	Species_contribution
K00370	<i>narG</i> , <i>narZ</i> , <i>nxrA</i>	0.0	0.0	0.0	20.5	0.0	0.0	0.0	0.0	<i>g_Anaeromyxobacter.s_Anaeromyxobacter_sp_Fw109_5</i>
K00370	<i>narG</i> , <i>narZ</i> , <i>nxrA</i>	0.0	277.1	250.7	110.1	401.6	163.7	0.0	81.2	<i>g_Arthrobacter.s_Arthrobacter_sp_Leaf69</i>
K00370	<i>narG</i> , <i>narZ</i> , <i>nxrA</i>	0.0	0.0	0.0	0.0	0.0	42.2	0.0	0.0	<i>g_Bosea.s_Bosea_vaviloviae</i>
K00370	<i>narG</i> , <i>narZ</i> , <i>nxrA</i>	0.0	23.0	0.0	0.0	0.0	0.0	0.0	0.0	<i>g_Cryobacterium.s_Cryobacterium_arcticum</i>
K00370	<i>narG</i> , <i>narZ</i> , <i>nxrA</i>	159.4	59.3	48.7	104.9	0.0	43.8	62.6	41.4	<i>g_Nitrospira.s_Nitrospira_sp_CG24D</i>
K00370	<i>narG</i> , <i>narZ</i> , <i>nxrA</i>	0.0	0.0	19.4	0.0	0.0	15.7	0.0	0.0	<i>g_Pseudarthrobacter.s_Pseudarthrobacter_phenanthrenivorans</i>
K00370	<i>narG</i> , <i>narZ</i> , <i>nxrA</i>	0.0	0.0	0.0	0.0	0.0	0.0	0.0	8.3	<i>g_Pseudomonas.s_Pseudomonas_lini</i>
K00370	<i>narG</i> , <i>narZ</i> , <i>nxrA</i>	0.0	49.4	8.8	10.8	0.0	29.8	0.0	30.1	<i>g_Pseudomonas.s_Pseudomonas_silesiensis</i>
K00370	<i>narG</i> , <i>narZ</i> , <i>nxrA</i>	0.0	22.9	5.5	7.4	0.0	15.5	0.0	7.7	<i>g_Pseudomonas.s_Pseudomonas_sp_VI4_1</i>
K00370	<i>narG</i> , <i>narZ</i> , <i>nxrA</i>	0.0	143.9	0.0	0.0	0.0	0.0	0.0	0.0	<i>g_Variovorax.s_Variovorax_paradoxus</i>
K00370	<i>narG</i> , <i>narZ</i> , <i>nxrA</i>	327.0	293.1	337.4	634.0	506.4	305.9	371.9	309.9	Unclassified
K00368	<i>nirK</i>	0.0	0.0	0.0	14.3	0.0	0.0	0.0	14.3	<i>g_Bradyrhizobium.s_Bradyrhizobium_lablabi</i>
K00368	<i>nirK</i>	0.0	0.0	0.0	14.9	0.0	0.0	0.0	0.0	<i>g_Candidatus_Nitrosocosmicus.s_Candidatus_Nitrosocosmicus_oleophilus</i>
K00368	<i>nirK</i>	0.0	0.0	0.0	0.0	0.0	0.0	0.0	8.7	<i>g_Nitrospira.s_Nitrospira_sp_CG24B</i>
K00368	<i>nirK</i>	15.8	44.8	63.7	247.6	9.9	18.4	10.6	115.0	Unclassified
K15864	<i>nirS</i>	0.0	0.0	0.0	0.0	0.0	0.0	0.0	30.9	<i>g_Sulfuricaulis.s_Sulfuricaulis_limicola</i>
K15864	<i>nirS</i>	0.0	0.0	0.0	0.0	16.5	0.0	14.6	0.0	<i>g_Thiobacillus.s_Thiobacillus_denitrificans</i>
K15864	<i>nirS</i>	9.2	30.5	28.5	62.5	45.4	29.4	51.1	34.0	Unclassified
K10944	<i>pmoA-amoA</i>	0.0	0.0	0.0	16.0	0.0	0.0	0.0	0.0	<i>g_Candidatus_Nitrosocosmicus.s_Candidatus_Nitrosocosmicus_oleophilus</i>
K10944	<i>pmoA-amoA</i>	5.7	0.0	4.0	0.0	0.0	10.4	36.8	0.0	Unclassified

K00 371	<i>narH</i> , <i>narY</i> , <i>nxrB</i>	0.0	0.0	0.0	16.1	0.0	0.0	0.0	0.0	g_Anaeromyxobacter.s_Anaeromyxobacter_sp_Fw109_5
K00 371	<i>narH</i> , <i>narY</i> , <i>nxrB</i>	0.0	0.0	0.0	0.0	0.0	98.8	0.0	0.0	g_Bosea.s_Bosea_vaviloviae
K00 371	<i>narH</i> , <i>narY</i> , <i>nxrB</i>	0.0	0.0	0.0	0.0	0.0	0.0	0.0	266.3	g_Burkholderiales_unclassified.s_Burkholderiales_bacterium_RIFCSPHIGHO2_12_FULL_69_20
K00 371	<i>narH</i> , <i>narY</i> , <i>nxrB</i>	0.0	17.8	0.0	0.0	0.0	0.0	0.0	0.0	g_Cryobacterium.s_Cryobacterium_arcticum
K00 371	<i>narH</i> , <i>narY</i> , <i>nxrB</i>	0.0	0.0	0.0	42.4	0.0	0.0	0.0	0.0	g_Nitrobacter.s_Nitrobacter_vulgaris
K00 371	<i>narH</i> , <i>narY</i> , <i>nxrB</i>	0.0	212.5	0.0	0.0	0.0	0.0	0.0	0.0	g_Variovorax.s_Variovorax_paradoxus
K00 371	<i>narH</i> , <i>narY</i> , <i>nxrB</i>	335.5	345.6	380.7	612.2	525.1	343.8	347.0	279.0	Unclassified
K00 373	<i>narJ</i> , <i>narW</i>	0.0	0.0	0.0	5.7	0.0	0.0	0.0	0.0	g_Nitrobacter.s_Nitrobacter_vulgaris
K00 373	<i>narJ</i> , <i>narW</i>	0.0	0.0	0.0	0.0	0.0	0.0	0.0	18.2	g_Pseudomonas.s_Pseudomonas lini
K00 373	<i>narJ</i> , <i>narW</i>	0.0	32.7	9.9	3.3	0.0	33.0	0.0	38.0	g_Pseudomonas.s_Pseudomonas_silesiensis
K00 373	<i>narJ</i> , <i>narW</i>	0.0	11.3	0.0	1.7	0.0	8.1	0.0	3.3	g_Pseudomonas.s_Pseudomonas_sp_VI4_1
K00 373	<i>narJ</i> , <i>narW</i>	30.3	88.3	54.5	85.8	88.7	61.7	51.7	60.2	Unclassified
K00 374	<i>narI</i> , <i>narV</i>	0.0	52.3	0.0	0.0	0.0	31.9	0.0	56.5	g_Pseudomonas.s_Pseudomonas_silesiensis
K00 374	<i>narI</i> , <i>narV</i>	0.0	0.0	0.0	0.0	0.0	5.5	0.0	0.0	g_Thiobacillus.s_Thiobacillus_denitrificans
K00 374	<i>narI</i> , <i>narV</i>	0.0	7.8	0.0	0.0	0.0	0.0	0.0	0.0	g_Variovorax.s_Variovorax_paradoxus
K00 374	<i>narI</i> , <i>narV</i>	80.6	82.4	117.8	259.4	114.6	97.8	86.9	112.5	Unclassified
K00 376	<i>nosZ</i>	0.0	0.0	0.0	57.4	0.0	0.0	0.0	0.0	g_Anaeromyxobacter.s_Anaeromyxobacter_sp_Fw109_5
K00 376	<i>nosZ</i>	0.0	0.0	0.0	20.9	0.0	0.0	0.0	0.0	g_Luteitalea.s_Luteitalea_pratensis
K00 376	<i>nosZ</i>	34.6	76.3	75.4	212.7	64.8	74.2	70.1	94.6	Unclassified
K00 362	<i>nirB</i>	0.0	196.8	130.9	85.6	340.8	122.3	0.0	60.4	g_Arthrobacter.s_Arthrobacter_sp_Leaf69
K00 362	<i>nirB</i>	0.0	0.0	0.0	0.0	13.6	0.0	0.0	0.0	g_Methylocystis.s_Methylocystis_sp_SC2
K00 362	<i>nirB</i>	0.0	0.0	0.0	0.0	0.0	0.0	14.7	0.0	g_Rhizobium.s_Rhizobium_sp_KAs_5_22
K00 362	<i>nirB</i>	0.0	0.0	0.0	0.0	0.0	0.0	0.0	6.5	g_Sulfuricaulis.s_Sulfuricaulis_limicola
K00 362	<i>nirB</i>	0.0	0.0	0.0	0.0	0.0	20.4	15.2	0.0	g_Thiobacillus.s_Thiobacillus_denitrificans
K00 362	<i>nirB</i>	0.0	0.0	0.0	30.3	0.0	0.0	0.0	0.0	g_Thioploca.s_Thioploca_ingrica

K00 362	<i>nirB</i>	0.0	57.3	0.0	0.0	0.0	0.0	0.0	0.0	g_Variovorax.s_Variovorax_paradoxus
K00 362	<i>nirB</i>	35.9	223.8	38.4	291.6	77.6	123.1	64.2	205.6	Unclassified
K00 363	<i>nirD</i>	0.0	223.7	197.4	48.2	285.1	171.1	0.0	61.4	g_Arthrobacter.s_Arthrobacter_sp_Leaf69
K00 363	<i>nirD</i>	0.0	0.0	0.0	16.1	0.0	0.0	0.0	5.4	g_Bradyrhizobium.s_Bradyrhizobium_lablabi
K00 363	<i>nirD</i>	0.0	0.0	0.0	0.0	0.0	0.0	0.0	64.5	g_Bradyrhizobium.s_Bradyrhizobium_valentinum
K00 363	<i>nirD</i>	0.0	0.0	0.0	0.0	0.0	0.0	0.0	15.2	g_Luteitalea.s_Luteitalea_pratensis
K00 363	<i>nirD</i>	0.0	0.0	0.0	0.0	0.0	0.0	0.0	14.9	g_Sulfuricaulis.s_Sulfuricaulis_limicola
K00 363	<i>nirD</i>	0.0	0.0	0.0	0.0	0.0	10.9	0.0	0.0	g_Thiobacillus.s_Thiobacillus_denitrificans
K00 363	<i>nirD</i>	0.0	0.0	0.0	25.6	0.0	0.0	0.0	0.0	g_Thioploca.s_Thioploca_ingrica
K00 363	<i>nirD</i>	39.1	233.2	215.2	368.6	170.0	198.7	48.1	174.1	Unclassified
K03 385	<i>nrfA</i>	0.0	0.0	0.0	72.7	0.0	0.0	0.0	0.0	g_Anaeromyxobacter.s_Anaeromyxobacter_sp_Fw109_5
K03 385	<i>nrfA</i>	0.0	0.0	0.0	9.1	0.0	0.0	0.0	0.0	g_Luteitalea.s_Luteitalea_pratensis
K03 385	<i>nrfA</i>	235.4	154.4	133.9	441.8	228.0	144.4	221.2	237.9	Unclassified
K04 561	<i>norB</i>	0.0	0.0	0.0	39.3	0.0	0.0	0.0	0.0	g_Anaeromyxobacter.s_Anaeromyxobacter_sp_Fw109_5
K04 561	<i>norB</i>	0.0	0.0	0.0	28.0	0.0	0.0	0.0	36.2	g_Luteitalea.s_Luteitalea_pratensis
K04 561	<i>norB</i>	0.0	11.4	40.6	65.1	23.6	70.9	0.0	33.4	g_Thiobacillus.s_Thiobacillus_denitrificans
K04 561	<i>norB</i>	321.2	302.7	281.4	885.2	389.0	313.4	336.8	386.8	Unclassified
K02 305	<i>norC</i>	0.0	0.0	0.0	16.3	0.0	0.0	0.0	0.0	g_Anaeromyxobacter.s_Anaeromyxobacter_sp_Fw109_5
K02 305	<i>norC</i>	0.0	0.0	0.0	0.0	0.0	0.0	0.0	13.2	g_Bradyrhizobium.s_Bradyrhizobium_lablabi
K02 305	<i>norC</i>	0.0	0.0	0.0	6.1	0.0	0.0	0.0	9.1	g_Luteitalea.s_Luteitalea_pratensis
K02 305	<i>norC</i>	0.0	0.0	0.0	0.0	0.0	0.0	0.0	10.3	g_Pseudomonas.s_Pseudomonas lini
K02 305	<i>norC</i>	0.0	65.1	0.0	10.3	0.0	17.2	0.0	24.1	g_Pseudomonas.s_Pseudomonas_silesiensis
K02 305	<i>norC</i>	0.0	20.6	0.0	6.9	0.0	9.7	0.0	3.4	g_Pseudomonas.s_Pseudomonas_sp_VI4_1
K02 305	<i>norC</i>	5.2	28.5	11.9	97.9	9.9	11.9	22.4	72.3	Unclassified
K02 586	<i>nifD</i>	0.0	0.0	0.0	42.9	0.0	0.0	0.0	0.0	g_Anaeromyxobacter.s_Anaeromyxobacter_sp_Fw109_5
K02 586	<i>nifD</i>	0.0	0.0	0.0	0.0	79.1	0.0	0.0	0.0	g_Methylocystis.s_Methylocystis_sp_SC2
K02 586	<i>nifD</i>	203.4	56.2	44.7	126.9	399.3	107.6	314.2	57.6	Unclassified

K02 588	<i>nifH</i>	0.0	0.0	0.0	17.7	0.0	0.0	0.0	19.0	<i>g_Bradyrhizobium.s_Bradyrhizobium_lablabi</i>
K02 588	<i>nifH</i>	0.0	0.0	0.0	0.0	0.0	0.0	0.0	4.1	<i>g_Bradyrhizobium.s_Bradyrhizobium_valentinum</i>
K02 588	<i>nifH</i>	6.0	0.0	0.0	0.0	3.8	0.0	0.0	0.0	<i>g_Methanosarcina.s_Methanosarcina_mazei</i>
K02 588	<i>nifH</i>	0.0	0.0	0.0	0.0	27.0	0.0	0.0	0.0	<i>g_Methanosarcina.s_Methanosarcina_sp_Ant1</i>
K02 588	<i>nifH</i>	0.0	0.0	0.0	0.0	242.3	0.0	0.0	0.0	<i>g_Methylocystis.s_Methylocystis_sp_SC2</i>
K02 588	<i>nifH</i>	329.0	107.5	65.7	226.1	461.6	147.1	353.1	59.2	Unclassified
K02 567	<i>napA</i>	0.0	0.0	0.0	31.1	0.0	0.0	0.0	14.9	<i>g_Bradyrhizobium.s_Bradyrhizobium_lablabi</i>
K02 567	<i>napA</i>	0.0	0.0	0.0	0.0	0.0	0.0	0.0	25.1	<i>g_Bradyrhizobium.s_Bradyrhizobium_valentinum</i>
K02 567	<i>napA</i>	0.0	39.8	8.9	8.5	0.0	22.1	0.0	25.9	<i>g_Pseudomonas.s_Pseudomonas_silesiensis</i>
K02 567	<i>napA</i>	0.0	18.6	0.0	9.3	0.0	8.9	0.0	10.2	<i>g_Pseudomonas.s_Pseudomonas_sp_VI4_1</i>
K02 567	<i>napA</i>	139.3	160.6	95.0	380.3	124.0	100.7	253.6	186.3	Unclassified
K01 430	<i>ureA</i>	0.0	220.6	320.3	85.0	389.5	175.6	0.0	98.0	<i>g_Arthrobacter.s_Arthrobacter_sp_Leaf69</i>
K01 430	<i>ureA</i>	0.0	0.0	0.0	91.3	0.0	0.0	0.0	78.4	<i>g_Bradyrhizobium.s_Bradyrhizobium_lablabi</i>
K01 430	<i>ureA</i>	0.0	0.0	0.0	0.0	0.0	0.0	0.0	52.3	<i>g_Burkholderiales_unclassified.s_Burkholderiales_bacterium_RIFCSPHIGHO2_12_FULL_69_20</i>
K01 430	<i>ureA</i>	0.0	0.0	0.0	26.7	0.0	0.0	0.0	0.0	<i>g_Candidatus_Nitrosocosmicus.s_Candidatus_Nitrosocosmicus_oleophilus</i>
K01 430	<i>ureA</i>	111.1	13.1	0.0	13.1	0.0	0.0	0.0	0.0	<i>g_Nitrospira.s_Nitrospira_sp_CG24C</i>
K01 430	<i>ureA</i>	0.0	13.1	0.0	6.5	0.0	6.5	0.0	6.5	<i>g_Pseudomonas.s_Pseudomonas_jessenii</i>
K01 430	<i>ureA</i>	0.0	6.5	0.0	0.0	0.0	0.0	0.0	0.0	<i>g_Pseudomonas.s_Pseudomonas_moraviensis</i>
K01 430	<i>ureA</i>	0.0	70.7	13.1	6.5	0.0	45.8	0.0	19.6	<i>g_Pseudomonas.s_Pseudomonas_silesiensis</i>
K01 430	<i>ureA</i>	0.0	32.7	13.1	32.7	0.0	0.0	0.0	0.0	<i>g_Pseudomonas.s_Pseudomonas_sp_VI4_1</i>
K01 430	<i>ureA</i>	0.0	39.2	0.0	0.0	0.0	0.0	0.0	0.0	<i>g_Variovorax.s_Variovorax_paradoxus</i>
K01 430	<i>ureA</i>	525.5	409.2	311.7	1150.7	226.9	405.0	371.9	552.0	Unclassified

Table S3.4: Abundance of selected sulfur cycling gene families with KO (KEGG ORTHOLOGY) number and contributing microbial species.

KO	gene family	Up-A_1_5	Mid-A_5	Mid-A_15	Mid-B_5	Mid-B_15	Dow_n_5	Dow_n_15	Con_f_5	Species_contribution
K00958	<i>sat</i>	0.0	0.0	0.0	20.3	0.0	0.0	0.0	0.0	<i>g_Candidatus_Nitrosocosmicus.s_Candidatus_Nitrosocosmicus_ol_eophilus</i>
K00958	<i>sat</i>	0.0	0.0	0.0	0.0	0.0	0.0	0.0	112.3	<i>g_Sulfuricaulis.s_Sulfuricaulis_limicola</i>
K00958	<i>sat</i>	0.2	48.5	68.3	115.9	254.7	294.7	161.0	81.4	<i>g_Thiobacillus.s_Thiobacillus_denitrificans</i>
K00958	<i>sat</i>	0.8	184.5	135.5	386.7	348.0	298.7	477.0	186.6	Unclassified
K00394	<i>aprA</i>	0.0	0.0	0.0	0.0	0.0	0.0	0.0	27.0	<i>g_Sulfuricaulis.s_Sulfuricaulis_limicola</i>
K00394	<i>aprA</i>	0.1	44.8	34.3	37.8	8.7	37.2	31.4	40.7	<i>g_Thiobacillus.s_Thiobacillus_denitrificans</i>
K00394	<i>aprA</i>	0.9	197.2	175.9	391.1	386.9	226.2	447.6	155.5	Unclassified
K00395	<i>aprB</i>	0.0	0.0	0.0	0.0	0.0	0.0	0.0	38.1	<i>g_Sulfuricaulis.s_Sulfuricaulis_limicola</i>
K00395	<i>aprB</i>	1.0	75.0	28.5	135.3	215.5	88.6	248.6	55.6	Unclassified
K11180	<i>dsrA</i>	0.0	0.0	0.0	0.0	0.0	0.0	0.0	20.4	<i>g_Sulfuricaulis.s_Sulfuricaulis_limicola</i>
K11180	<i>dsrA</i>	0.0	28.6	25.0	76.8	79.6	109.9	45.0	37.2	<i>g_Thiobacillus.s_Thiobacillus_denitrificans</i>
K11180	<i>dsrA</i>	1.0	27.2	15.1	42.6	138.7	73.4	244.5	21.3	Unclassified
K11181	<i>dsrB</i>	0.0	0.0	0.0	0.0	0.0	0.0	0.0	9.6	<i>g_Sulfuricaulis.s_Sulfuricaulis_limicola</i>
K11181	<i>dsrB</i>	1.0	60.4	45.6	60.9	106.1	58.8	186.8	26.4	Unclassified
K08352	<i>phsA</i>	0.0	0.0	0.0	24.4	0.0	0.0	0.0	0.0	<i>g_Anaeromyxobacter.s_Anaeromyxobacter_sp_Fw109_5</i>
K08352	<i>phsA</i>	1.0	55.6	62.2	75.1	134.2	81.1	216.5	55.1	Unclassified
K17222	<i>soxA</i>	0.0	0.0	0.0	57.9	0.0	0.0	0.0	22.9	<i>g_Bradyrhizobium.s_Bradyrhizobium_lablabi</i>
K17222	<i>soxA</i>	0.0	0.0	0.0	0.0	0.0	0.0	0.0	19.2	<i>g_Bradyrhizobium.s_Bradyrhizobium_valentinum</i>
K17222	<i>soxA</i>	1.0	161.6	88.3	347.0	250.8	215.9	169.3	173.5	Unclassified
K17223	<i>soxX</i>	0.0	0.0	0.0	0.0	0.0	0.0	0.0	7.6	<i>g_Sulfuricaulis.s_Sulfuricaulis_limicola</i>
K17223	<i>soxX</i>	1.0	48.4	47.3	179.1	123.8	129.7	73.2	56.2	Unclassified
K17224	<i>soxB</i>	0.0	0.0	0.0	26.3	0.0	0.0	0.0	21.3	<i>g_Bradyrhizobium.s_Bradyrhizobium_lablabi</i>
K17224	<i>soxB</i>	0.0	0.0	0.0	0.0	0.0	0.0	0.0	25.0	<i>g_Bradyrhizobium.s_Bradyrhizobium_valentinum</i>
K17224	<i>soxB</i>	0.0	0.0	0.0	0.0	0.0	0.0	0.0	9.8	<i>g_Sulfuricaulis.s_Sulfuricaulis_limicola</i>
K17224	<i>soxB</i>	0.0	0.0	0.0	7.4	0.0	0.0	0.0	0.0	<i>g_Thioplaca.s_Thioplaca_ingrica</i>
K17224	<i>soxB</i>	1.0	95.0	74.5	269.6	78.1	160.1	96.7	183.3	Unclassified
K17225	<i>soxC</i>	0.0	12.5	0.0	0.0	0.0	0.0	0.0	0.0	<i>g_Variovorax.s_Variovorax_paradoxus</i>
K17225	<i>soxC</i>	1.0	57.3	69.1	259.0	99.6	71.5	72.1	142.8	Unclassified
K17226	<i>soxy</i>	0.0	0.0	0.0	0.0	9.3	0.0	0.0	0.0	<i>g_Methylocystis.s_Methylocystis_sp_SC2</i>
K17226	<i>soxy</i>	0.0	1.5	0.0	4.9	0.0	0.0	0.0	6.5	<i>g_Pseudomonas.s_Pseudomonas_jessenii</i>
K17226	<i>soxy</i>	0.0	65.3	0.0	6.5	0.0	47.1	0.0	26.1	<i>g_Pseudomonas.s_Pseudomonas_silesiensis</i>
K17226	<i>soxy</i>	0.0	24.5	0.0	1.6	0.0	13.1	0.0	6.5	<i>g_Pseudomonas.s_Pseudomonas_sp_VI4_1</i>
K17226	<i>soxy</i>	0.0	0.0	0.0	0.0	0.0	0.0	0.0	34.0	<i>g_Sulfuricaulis.s_Sulfuricaulis_limicola</i>
K17226	<i>soxy</i>	1.0	200.1	142.1	253.2	166.5	159.5	150.8	167.1	Unclassified
K17227	<i>soxZ</i>	0.0	0.0	0.0	54.6	0.0	0.0	0.0	6.2	<i>g_Bradyrhizobium.s_Bradyrhizobium_lablabi</i>
K17227	<i>soxZ</i>	0.0	0.0	0.0	0.0	0.0	0.0	0.0	12.3	<i>g_Bradyrhizobium.s_Bradyrhizobium_valentinum</i>
K17227	<i>soxZ</i>	0.0	0.0	0.0	0.0	0.0	0.0	0.0	17.5	<i>g_Sulfuricaulis.s_Sulfuricaulis_limicola</i>
K17227	<i>soxZ</i>	0.0	0.0	0.0	0.0	0.0	10.7	0.0	0.0	<i>g_Thiobacillus.s_Thiobacillus_denitrificans</i>
K17227	<i>soxZ</i>	0.0	0.0	0.0	21.9	0.0	0.0	0.0	0.0	<i>g_Thioplaca.s_Thioplaca_ingrica</i>
K17227	<i>soxZ</i>	1.0	188.8	107.2	333.8	204.7	126.6	104.5	233.8	Unclassified
K17218	<i>sqr</i>	0.0	0.0	0.0	0.0	15.9	0.0	0.0	0.0	<i>g_Methylocystis.s_Methylocystis_sp_SC2</i>

K1721 8	<i>sqr</i>	0.0	15.5	0.0	0.0	0.0	0.0	0.0	0.0	g_Pseudomonas.s_Pseudomonas_moraviensis
K1721 8	<i>sqr</i>	1.0	169. 1	162.7	325. 9	193.1	212. 8	140.3	144. 2	Unclassified

REFERENCES

- Abby, Sophie S., Michael Melcher, Melina Kerou, Mart Krupovic, Michaela Stieglmeier, Claudia Rossel, Kevin Pfeifer, and Christa Schleper. 2018. "Candidatus Nitrosocaldus Cavascurensis, an Ammonia Oxidizing, Extremely Thermophilic Archaeon with a Highly Mobile Genome." *Frontiers in Microbiology* 9 (JAN). <https://doi.org/10.3389/fmicb.2018.00028>.
- Agarwala, Richa, Tanya Barrett, Jeff Beck, Dennis A. Benson, Colleen Bollin, Evan Bolton, Devon Bourexis, et al. 2018. "Database Resources of the National Center for Biotechnology Information." *Nucleic Acids Research* 46 (D1): D8–13. <https://doi.org/10.1093/nar/gkx1095>.
- Agrometeorology of Baden-Württemberg. 2017. "Agrarmeteorologie Baden-Württemberg." 2017. <https://www.wetter-bw.de/Agrarmeteorologie-BW/Wetterdaten/Stationskarte>.
- Aigle, Axel, James I. Prosser, and Cécile Gubry-Rangin. 2019. "The Application of High-Throughput Sequencing Technology to Analysis of AmoA Phylogeny and Environmental Niche Specialisation of Terrestrial Bacterial Ammonia-Oxidisers." *Environmental Microbiomes* 14 (1): 1–10. <https://doi.org/10.1186/s40793-019-0342-6>.
- Albertsen, Mads. 2023. "Long-Read Metagenomics Paves the Way toward a Complete Microbial Tree of Life." *Nature Methods* 20 (1): 30–31. <https://doi.org/10.1038/s41592-022-01726-6>.
- Albertsen, Mads, Philip Hugenholtz, Adam Skarszewski, Kåre L. Nielsen, Gene W. Tyson, and Per H. Nielsen. 2013. "Genome Sequences of Rare, Uncultured Bacteria Obtained by Differential Coverage Binning of Multiple Metagenomes." *Nature Biotechnology* 31 (6). <https://doi.org/10.1038/nbt.2579>.
- Altschul, Stephen F., Warren Gish, Webb Miller, Eugene W. Myers, and David J. Lipman. 1990. "Basic Local Alignment Search Tool." *Journal of Molecular Biology* 215 (3): 403–10. [https://doi.org/10.1016/S0022-2836\(05\)80360-2](https://doi.org/10.1016/S0022-2836(05)80360-2).
- Alvarado, Luis E Valentin, Sirine C Fakra, Alexander J Probst, Jonathan R Giska, Alexander L Jaffe, Luke M Oltrogge, Jacob West-Roberts, et al. 2022. "Autotrophic Biofilms Sustained by Deeply-Sourced Groundwater Host Diverse CPR Bacteria Implicated in Sulfur and Hydrogen Metabolism." *BioRxiv*, January, 2022.11.17.516901. <https://doi.org/10.1101/2022.11.17.516901>.
- Alves, Ricardo J.Eloy, Melina Kerou, Anna Zappe, Romana Bittner, Sophie S. Abby, Heiko A. Schmidt, Kevin Pfeifer, and Christa Schleper. 2019. "Ammonia Oxidation by the Arctic Terrestrial Thaumarchaeote Candidatus Nitrosocosmicus Arcticus Is Stimulated by Increasing Temperatures." *Frontiers in Microbiology* 10 (JULY). <https://doi.org/10.3389/fmicb.2019.01571>.
- Andrews, Simon. 2010. "FastQC - A Quality Control Tool for High Throughput Sequence Data. <http://www.Bioinformatics.Babraham.Ac.Uk/Projects/Fastqc/>." *Babraham Bioinformatics*.
- Apprill, Amy, Sean McNally, Rachel Parsons, and Laura Weber. 2015. "Minor Revision to V4 Region SSU rRNA 806R Gene Primer Greatly Increases Detection of SAR11 Bacterioplankton." *Aquatic Microbial Ecology* 75 (2): 129–37.

<https://doi.org/10.3354/ame01753>.

- Arango, C. P., and J. L. Tank. 2008. "Land Use Influences the Spatiotemporal Controls on Nitrification and Denitrification in Headwater Streams." *Journal of the North American Benthological Society* 27 (1): 90–107. <https://doi.org/10.1899/07-024.1>.
- Arshad, Arslan, Paula Dalcin Martins, Jeroen Frank, Mike S.M. Jetten, Huub J.M. Op den Camp, and Cornelia U. Welte. 2017. "Mimicking Microbial Interactions under Nitrate-Reducing Conditions in an Anoxic Bioreactor: Enrichment of Novel Nitrospirae Bacteria Distantly Related to *Thermodesulfobivrio*." *Environmental Microbiology* 19 (12): 4965–77. <https://doi.org/10.1111/1462-2920.13977>.
- Asamoto, Ciara K., Kaitlin R. Rempfert, Victoria H. Luu, Adam D. Younkin, and Sebastian H. Kopf. 2021. "Enzyme-Specific Coupling of Oxygen and Nitrogen Isotope Fractionation of the Nap and Nar Nitrate Reductases." *Environmental Science and Technology* 55 (8): 5537–46. <https://doi.org/10.1021/acs.est.0c07816>.
- Atkinson, Sally J., Christopher G. Mowat, Graeme A. Reid, and Stephen K. Chapman. 2007. "An Octaheme C-Type Cytochrome from *Shewanella Oneidensis* Can Reduce Nitrite and Hydroxylamine." *FEBS Letters* 581 (20): 3805–8. <https://doi.org/10.1016/j.febslet.2007.07.005>.
- Avrahami, Sharon, Zhongjun Jia, Josh D. Neufeld, J. Colin Murrell, Ralf Conrad, and Kirsten Küsel. 2011. "Active Autotrophic Ammonia-Oxidizing Bacteria in Biofilm Enrichments from Simulated Creek Ecosystems at Two Ammonium Concentrations Respond to Temperature Manipulation." *Applied and Environmental Microbiology* 77 (20): 7329–38. <https://doi.org/10.1128/AEM.05864-11>.
- Badrzadeh, Nasrin, Jamal Mohammad Vali Samani, Mehdi Mazaheri, and Alban Kuriqi. 2022. "Evaluation of Management Practices on Agricultural Nonpoint Source Pollution Discharges into the Rivers under Climate Change Effects." *Science of the Total Environment* 838 (September): 156643. <https://doi.org/10.1016/j.scitotenv.2022.156643>.
- Bartossek, Rita, Graeme W. Nicol, Anders Lanzen, Hans Peter Klenk, and Christa Schleper. 2010. "Homologues of Nitrite Reductases in Ammonia-Oxidizing Archaea: Diversity and Genomic Context." *Environmental Microbiology* 12 (4): 1075–88. <https://doi.org/10.1111/j.1462-2920.2010.02153.x>.
- Basu, Nandita B., Georgia Destouni, James W. Jawitz, Sally E. Thompson, Natalia V. Loukinova, Amélie Darracq, Stefano Zanardo, et al. 2010. "Nutrient Loads Exported from Managed Catchments Reveal Emergent Biogeochemical Stationarity." *Geophysical Research Letters* 37 (23). <https://doi.org/10.1029/2010GL045168>.
- Basu, Nandita B., Kimberly J. Van Meter, Danyka K. Byrnes, Philippe Van Cappellen, Roy Brouwer, Brian H. Jacobsen, Jerker Jarsjö, et al. 2022. "Managing Nitrogen Legacies to Accelerate Water Quality Improvement." *Nature Geoscience* 15 (2): 97–105. <https://doi.org/10.1038/s41561-021-00889-9>.
- Bates, Douglas, Martin Mächler, Benjamin M. Bolker, and Steven C. Walker. 2015. "Fitting Linear Mixed-Effects Models Using Lme4." *Journal of Statistical Software* 67 (1). <https://doi.org/10.18637/jss.v067.i01>.
- Battin, Tom J, Louis A Kaplan, Stuart Findlay, Charles S Hopkinson, Eugenia Marti, Aaron I Packman, J Denis Newbold, and Francesc Sabater. 2008. "Biophysical Controls on

- Organic Carbon Fluxes in Fluvial Networks.” *Nature Geoscience* 1 (2): 95–100. <https://doi.org/10.1038/ngeo101>.
- Bayani Cardenas, M., and J. L. Wilson. 2006. “The Influence of Ambient Groundwater Discharge on Exchange Zones Induced by Current-Bedform Interactions.” *Journal of Hydrology* 331 (1–2): 103–9. <https://doi.org/10.1016/j.jhydrol.2006.05.012>.
- Bayer, Barbara, Jana Vojvoda, Thomas Reinthaler, Carolina Reyes, Maria Pinto, and Gerhard J. Herndl. 2019. “Nitrosopumilus Adriaticus Sp. Nov. and Nitrosopumilus Piranensis Sp. Nov., Two Ammonia-Oxidizing Archaea from the Adriatic Sea and Members of the Class Nitrososphaeria.” *International Journal of Systematic and Evolutionary Microbiology* 69 (7). <https://doi.org/10.1099/ijsem.0.003360>.
- Beaulieu, Jake J., Jennifer L. Tank, Stephen K. Hamilton, Wilfred M. Wollheim, Robert O. Hall, Patrick J. Mulholland, Bruce J. Peterson, et al. 2011. “Nitrous Oxide Emission from Denitrification in Stream and River Networks.” *Proceedings of the National Academy of Sciences of the United States of America* 108 (1): 214–19. <https://doi.org/10.1073/pnas.1011464108>.
- Beghini, Francesco, Lauren J. McIver, Aitor Blanco-Míguez, Leonard Dubois, Francesco Asnicar, Sagun Maharjan, Ana Mailyan, et al. 2021. “Integrating Taxonomic, Functional, and Strain-Level Profiling of Diverse Microbial Communities with Biobakery 3.” *ELife* 10: 1–42. <https://doi.org/10.7554/eLife.65088>.
- Begmatov, Shahjahan, Alexey V Beletsky, Svetlana N Dedysh, Andrey V Mardanov, and Nikolai V Ravin. 2022. “Genome Analysis of the Candidate Phylum MBNT15 Bacterium from a Boreal Peatland Predicted Its Respiratory Versatility and Dissimilatory Iron Metabolism .” *Frontiers in Microbiology* . <https://www.frontiersin.org/articles/10.3389/fmicb.2022.951761>.
- Bell, Emma, Tiina Lamminmäki, Johannes Alneberg, Anders F. Andersson, Chen Qian, Weili Xiong, Robert L. Hettich, Manon Frutschi, and Rizlan Bernier-Latmani. 2020. “Active Sulfur Cycling in the Terrestrial Deep Subsurface.” *ISME Journal* 14 (5): 1260–72. <https://doi.org/10.1038/s41396-020-0602-x>.
- Bell, Emma, Tiina Lamminmäki, Johannes Alneberg, Chen Qian, Weili Xiong, Robert L. Hettich, Manon Frutschi, and Rizlan Bernier-Latmani. 2022. “Active Anaerobic Methane Oxidation and Sulfur Disproportionation in the Deep Terrestrial Subsurface.” *ISME Journal* 16 (6): 1583–93. <https://doi.org/10.1038/s41396-022-01207-w>.
- Beller, Harry R., Patrick S.G. Chain, Tracy E. Letain, Anu Chakicherla, Frank W. Larimer, Paul M. Richardson, Matthew A. Coleman, Ann P. Wood, and Donovan P. Kelly. 2006. “The Genome Sequence of the Obligately Chemolithoautotrophic, Facultatively Anaerobic Bacterium *Thiobacillus Denitrificans*.” *Journal of Bacteriology* 188 (4): 1473–88. <https://doi.org/10.1128/JB.188.4.1473-1488.2006>.
- Berg, Eveline M. van den, Marissa Boleij, J. Gijs Kuenen, Robbert Kleerebezem, and Mark C.M. van Loosdrecht. 2016. “DNRA and Denitrification Coexist over a Broad Range of Acetate/N-NO₃- Ratios, in a Chemostat Enrichment Culture.” *Frontiers in Microbiology* 7 (NOV): 1–12. <https://doi.org/10.3389/fmicb.2016.01842>.
- Berg, Eveline M. van den, Marina P. Elisário, J. Gijs Kuenen, Robbert Kleerebezem, and Mark C.M. van Loosdrecht. 2017. “Fermentative Bacteria Influence the Competition

- between Denitrifiers and DNRA Bacteria.” *Frontiers in Microbiology* 8 (SEP): 1–13.
<https://doi.org/10.3389/fmicb.2017.01684>.
- Berghuis, Bojk A., Feiqiao Brian Yu, Frederik Schulz, Paul C. Blainey, Tanja Woyke, and Stephen R. Quake. 2019. “Hydrogenotrophic Methanogenesis in Archaeal Phylum Verstraetearchaeota Reveals the Shared Ancestry of All Methanogens.” *Proceedings of the National Academy of Sciences of the United States of America* 116 (11).
<https://doi.org/10.1073/pnas.1815631116>.
- Bernhard, Anne E., and Annette Bollmann. 2010. “Estuarine Nitrifiers: New Players, Patterns and Processes.” *Estuarine, Coastal and Shelf Science* 88 (1): 1–11.
<https://doi.org/10.1016/j.ecss.2010.01.023>.
- Biernat, Lars, Friedhelm Taube, Iris Vogeler, Thorsten Reinsch, Christof Kluß, and Ralf Loges. 2020. “Is Organic Agriculture in Line with the EU-Nitrate Directive? On-Farm Nitrate Leaching from Organic and Conventional Arable Crop Rotations.” *Agriculture, Ecosystems and Environment* 298. <https://doi.org/10.1016/j.agee.2020.106964>.
- Black, Ellen M., and Craig L. Just. 2018. “The Genomic Potentials of NOB and Comammox Nitrospira in River Sediment Are Impacted by Native Freshwater Mussels.” *Frontiers in Microbiology* 9 (SEP). <https://doi.org/10.3389/fmicb.2018.02061>.
- Blann, Kristen L., James L. Anderson, Gary R. Sands, and Bruce Vondracek. 2009. “Effects of Agricultural Drainage on Aquatic Ecosystems: A Review.” *Critical Reviews in Environmental Science and Technology* 39 (11): 909–1001.
<https://doi.org/10.1080/10643380801977966>.
- Boano, F., J. W. Harvey, A. Marion, A. I. Packman, R. Revelli, L. Ridolfi, and A. Wörman. 2014. “Hyporheic Flow and Transport Processes: Mechanisms, Models, and Biogeochemical Implications.” *Reviews of Geophysics*.
<https://doi.org/10.1002/2012RG000417>.
- Boden, Rich, Lee P. Hutt, and Alex W. Rae. 2017. “Reclassification of Thiobacillus Aquaesulis (Wood & Kelly, 1995) as Annwoodia Aquaesulis Gen. Nov., Comb. Nov., Transfer of Thiobacillus (Beijerinck, 1904) from the Hydrogenophilales to the Nitrosomonadales, Proposal of Hydrogenophilalia Class. Nov. Withi.” *International Journal of Systematic and Evolutionary Microbiology* 67 (5): 1191–1205.
<https://doi.org/10.1099/ijsem.0.001927>.
- Bollmann, Annette, Marie José Bär-Gilissen, and Hendrikus J. Laanbroek. 2002. “Growth at Low Ammonium Concentrations and Starvation Response as Potential Factors Involved in Niche Differentiation among Ammonia-Oxidizing Bacteria.” *Applied and Environmental Microbiology* 68 (10): 4751–57.
<https://doi.org/10.1128/AEM.68.10.4751-4757.2002>.
- Bonenfant, Quentin, Laurent Noé, and Hélène Touzet. 2023. “Porechop_ABI: Discovering Unknown Adapters in Oxford Nanopore Technology Sequencing Reads for Downstream Trimming.” *Bioinformatics Advances* 3 (1): vbac085.
<https://doi.org/10.1093/bioadv/vbac085>.
- Boone, David R, William B Whitman, and Yosuke Koga. 2015. “Methanosarcinaceae.” In *Bergey’s Manual of Systematics of Archaea and Bacteria*, 1–2.
<https://doi.org/https://doi.org/10.1002/9781118960608.fbm00105>.

- Bourceau, O M, T Ferdelman, G Lavik, M Mussmann, M M M Kuypers, and H K Marchant. 2023. "Simultaneous Sulfate and Nitrate Reduction in Coastal Sediments." *ISME Communications* 3 (1): 17. <https://doi.org/10.1038/s43705-023-00222-y>.
- Braker, Gesche, and James M. Tiedje. 2003. "Nitric Oxide Reductase (NorB) Genes from Pure Cultures and Environmental Samples." *Applied and Environmental Microbiology* 69 (6). <https://doi.org/10.1128/AEM.69.6.3476-3483.2003>.
- Braker, Gesche, Jizhong Zhou, Liyou Wu, Allan H. Devol, and James M. Tiedje. 2000. "Nitrite Reductase Genes (NirK and NirS) as Functional Markers to Investigate Diversity of Denitrifying Bacteria in Pacific Northwest Marine Sediment Communities." *Applied and Environmental Microbiology* 66 (5): 2096–2104. <https://doi.org/10.1128/AEM.66.5.2096-2104.2000>.
- Briggs, Martin A., Frederick D. Day-Lewis, Jay P. Zarnetske, and Judson W. Harvey. 2015. "A Physical Explanation for the Development of Redox Microzones in Hyporheic Flow." *Geophysical Research Letters* 42 (11): 4402–10. <https://doi.org/10.1002/2015GL064200>.
- Burton, Simon A.Q., and Jim I. Prosser. 2001. "Autotrophic Ammonia Oxidation at Low PH through Urea Hydrolysis." *Applied and Environmental Microbiology* 67 (7): 2952–57. <https://doi.org/10.1128/AEM.67.7.2952-2957.2001>.
- Butturini, Andrea, Tom J. Battin, and Francesc Sabater. 2000. "Nitrification in Stream Sediment Biofilms: The Role of Ammonium Concentration and DOC Quality." *Water Research* 34 (2): 629–39. [https://doi.org/10.1016/S0043-1354\(99\)00171-2](https://doi.org/10.1016/S0043-1354(99)00171-2).
- Cai, Lin, Ming Fei Shao, and Tong Zhang. 2015. "Non-Contiguous Finished Genome Sequence and Description of *Sulfurimonas Hongkongensis* Sp. Nov., a Strictly Anaerobic Denitrifying, Hydrogen- and Sulfuroxidizing Chemolithoautotroph Isolated from Marine Sediment." *Standards in Genomic Sciences* 9 (3): 1302–10. <https://doi.org/10.4056/sigs.4948668>.
- Caillon, Florian, Katharina Besemer, Peter Peduzzi, and Jakob Schelker. 2021. "Soil Microbial Inoculation during Flood Events Shapes Headwater Stream Microbial Communities and Diversity." *Microbial Ecology* 82 (3): 591–601. <https://doi.org/10.1007/s00248-021-01700-3>.
- Callahan, Benjamin J., Paul J. McMurdie, and Susan P. Holmes. 2017. "Exact Sequence Variants Should Replace Operational Taxonomic Units in Marker-Gene Data Analysis." *ISME Journal* 11 (12): 2639–43. <https://doi.org/10.1038/ismej.2017.119>.
- Callahan, Benjamin J., Paul J. McMurdie, Michael J. Rosen, Andrew W. Han, Amy Jo A. Johnson, and Susan P. Holmes. 2016. "DADA2: High-Resolution Sample Inference from Illumina Amplicon Data." *Nature Methods* 13 (7): 581–83. <https://doi.org/10.1038/nmeth.3869>.
- Callahan, Benjamin J., Joan Wong, Cheryl Heiner, Steve Oh, Casey M. Theriot, Ajay S. Gulati, Sarah K. McGill, and Michael K. Dougherty. 2019. "High-Throughput Amplicon Sequencing of the Full-Length 16S rRNA Gene with Single-Nucleotide Resolution." *Nucleic Acids Research* 47 (18): E103. <https://doi.org/10.1093/NAR/GKZ569>.
- Camargo, Julio A., Alvaro Alonso, and Annabella Salamanca. 2005. "Nitrate Toxicity to Aquatic Animals: A Review with New Data for Freshwater Invertebrates." *Chemosphere* 58 (9): 1255–67. <https://doi.org/10.1016/j.chemosphere.2004.10.044>.

- Cameron, Ellen S., Philip J. Schmidt, Benjamin J.M. Tremblay, Monica B. Emelko, and Kirsten M. Müller. 2020. “To Rarefy or Not to Rarefy: Enhancing Microbial Community Analysis through next-Generation Sequencing.” *BioRxiv*. <https://doi.org/10.1101/2020.09.09.290049>.
- Campbell, Barbara J., Julie L. Smith, Thomas E. Hanson, Martin G. Klotz, Lisa Y. Stein, Charles K. Lee, Dongying Wu, et al. 2009. “Adaptations to Submarine Hydrothermal Environments Exemplified by the Genome of *Nautilia Profundicola*.” *PLoS Genetics* 5 (2). <https://doi.org/10.1371/journal.pgen.1000362>.
- Canfield, Donald E., Erik Kristensen, and B. Thamdrup. 2005. “Aquatic Geomicrobiology.” *Advances in Marine Biology*.
- Cao, Huiluo, Yiguo Hong, Meng Li, and Ji Dong Gu. 2011. “Diversity and Abundance of Ammonia-Oxidizing Prokaryotes in Sediments from the Coastal Pearl River Estuary to the South China Sea.” *Antonie van Leeuwenhoek, International Journal of General and Molecular Microbiology* 100 (4): 545–56. <https://doi.org/10.1007/s10482-011-9610-1>.
- Caporaso, J. Gregory, Christian L. Lauber, William A. Walters, Donna Berg-Lyons, Catherine A. Lozupone, Peter J. Turnbaugh, Noah Fierer, and Rob Knight. 2011. “Global Patterns of 16S rRNA Diversity at a Depth of Millions of Sequences per Sample.” *Proceedings of the National Academy of Sciences of the United States of America* 108 (SUPPL. 1): 4516–22. <https://doi.org/10.1073/pnas.1000080107>.
- Cardarelli, Emily L., John R. Bargar, and Christopher A. Francis. 2020. “Diverse Thaumarchaeota Dominate Subsurface Ammonia-Oxidizing Communities in Semi-Arid Floodplains in the Western United States.” *Microbial Ecology* 80 (4): 778–92. <https://doi.org/10.1007/s00248-020-01534-5>.
- Chase, Jonathan M., and Jonathan A. Myers. 2011. “Disentangling the Importance of Ecological Niches from Stochastic Processes across Scales.” *Philosophical Transactions of the Royal Society B: Biological Sciences* 366 (1576): 2351–63. <https://doi.org/10.1098/rstb.2011.0063>.
- Chaumeil, Pierre-Alain, Aaron J Mussig, Philip Hugenholtz, and Donovan H Parks. 2022. “GTDB-Tk v2: Memory Friendly Classification with the Genome Taxonomy Database.” *Bioinformatics* 38 (23): 5315–16. <https://doi.org/10.1093/bioinformatics/btac672>.
- Chen, I. Min A., Ken Chu, Krishna Palaniappan, Manoj Pillay, Anna Ratner, Jinghua Huang, Marcel Huntemann, et al. 2019. “IMG/M v.5.0: An Integrated Data Management and Comparative Analysis System for Microbial Genomes and Microbiomes.” *Nucleic Acids Research* 47 (D1): D666–77. <https://doi.org/10.1093/nar/gky901>.
- Chen, Shifu, Yanqing Zhou, Yaru Chen, and Jia Gu. 2018. “Fastp: An Ultra-Fast All-in-One FASTQ Preprocessor.” In *Bioinformatics*. Vol. 34. <https://doi.org/10.1093/bioinformatics/bty560>.
- Coenye, Tom, Enevold Falsen, Bart Hoste, Maria Ohlén, Johan Goris, John R.W. Govan, Monique Gillis, and Peter Vandamme. 2000. “Description of *Pandoraea* Gen. Nov. with *Pandoraea Apista* Sp. Nov., *Pandoraea Pulmonicola* Sp. Nov., *Pandoraea Pnomenusa* Sp. Nov., *Pandoraea Sputorum* Sp. Nov. and *Pandoraea Norimbergensis* Comb. Nov.” *International Journal of Systematic and Evolutionary Microbiology* 50 (2). <https://doi.org/10.1099/00207713-50-2-887>.

- Colglazier, William. 2015. "Sustainable Development Agenda: 2030." *Science*. American Association for the Advancement of Science. <https://doi.org/10.1126/science.aad2333>.
- Cortassa, S, M A Aon, A A Iglesias, and D Lloyd. 2002. *An Introduction to Metabolic and Cellular Engineering*. WORLD SCIENTIFIC. <https://doi.org/doi:10.1142/4874>.
- Coskun, Ömer K., Volkan Özen, Scott D. Wankel, and William D. Orsi. 2019. "Quantifying Population-Specific Growth in Benthic Bacterial Communities under Low Oxygen Using H218O." *ISME Journal* 13 (6): 1546–59. <https://doi.org/10.1038/s41396-019-0373-4>.
- Coster, Wouter De, Sven D'Hert, Darrin T. Schultz, Marc Cruys, and Christine Van Broeckhoven. 2018. "NanoPack: Visualizing and Processing Long-Read Sequencing Data." *Bioinformatics* 34 (15). <https://doi.org/10.1093/bioinformatics/bty149>.
- Covino, Tim, Brian McGlynn, and John Mallard. 2011. "Stream-Groundwater Exchange and Hydrologic Turnover at the Network Scale." *Water Resources Research* 47 (12). <https://doi.org/10.1029/2011WR010942>.
- Covino, Timothy P., and Brian L. McGlynn. 2007. "Stream Gains and Losses across a Mountain-to-Valley Transition: Impacts on Watershed Hydrology and Stream Water Chemistry." *Water Resources Research* 43 (10). <https://doi.org/10.1029/2006WR005544>.
- Crump, Byron C., Charles S. Hopkinson, Mitchell L. Sogin, and John E. Hobbie. 2004. "Microbial Biogeography along an Estuarine Salinity Gradient: Combined Influences of Bacterial Growth and Residence Time." *Applied and Environmental Microbiology* 70 (3): 1494–1505. <https://doi.org/10.1128/AEM.70.3.1494-1505.2004>.
- D'Affonseca, Fernando M., Michael Finkel, and Olaf A. Cirpka. 2020. "Combining Implicit Geological Modeling, Field Surveys, and Hydrogeological Modeling to Describe Groundwater Flow in a Karst Aquifer." *Hydrogeology Journal* 28 (8): 2779–2802. <https://doi.org/10.1007/s10040-020-02220-z>.
- Daims, Holger, Elena V. Lebedeva, Petra Pjevac, Ping Han, Craig Herbold, Mads Albertsen, Nico Jehmlich, et al. 2015. "Complete Nitrification by Nitrospira Bacteria." *Nature* 528 (7583): 504–9. <https://doi.org/10.1038/nature16461>.
- Dalsgaard, T., and F. Bak. 1994. "Nitrate Reduction in a Sulfate-Reducing Bacterium, Desulfovibrio Desulfuricans, Isolated from Rice Paddy Soil: Sulfide Inhibition, Kinetics, and Regulation." *Applied and Environmental Microbiology* 60 (1): 291–97. <https://doi.org/10.1128/aem.60.1.291-297.1994>.
- Damania, Richard. 2020. "The Economics of Water Scarcity and Variability." *Oxford Review of Economic Policy* 36 (1): 24–44. <https://doi.org/10.1093/oxrep/grz027>.
- Damashek, Julian, Jason M. Smith, Annika C. Mosier, and Christopher A. Francis. 2014. "Benthic Ammonia Oxidizers Differ in Community Structure and Biogeochemical Potential across a Riverine Delta." *Frontiers in Microbiology* 5 (DEC): 1–18. <https://doi.org/10.3389/fmicb.2014.00743>.
- Danczak, Robert E., Audrey H. Sawyer, Kenneth H. Williams, James C. Stegen, Chad Hobson, and Michael J. Wilkins. 2016. "Seasonal Hyporheic Dynamics Control Coupled Microbiology and Geochemistry in Colorado River Sediments." *Journal of Geophysical Research: Biogeosciences* 121 (12): 2976–87. <https://doi.org/10.1002/2016JG003527>.

- David, Mark B., and Lowell E. Gentry. 2000. "Anthropogenic Inputs of Nitrogen and Phosphorus and Riverine Export for Illinois, USA." *Journal of Environmental Quality* 29 (2): 494–508. <https://doi.org/10.2134/jeq2000.00472425002900020018x>.
- Delgado Vela, Jeseth, Laura A. Bristow, Hannah K. Marchant, Nancy G. Love, and Gregory J. Dick. 2020. "Sulfide Alters Microbial Functional Potential in a Methane and Nitrogen Cycling Biofilm Reactor." *Environmental Microbiology*, 0–2. <https://doi.org/10.1111/1462-2920.15352>.
- DeWeerd, Kim A., Linda Mandelco, Ralph S. Tanner, Carl R. Woese, and Joseph M. Suflita. 1990. "Desulfomonile Tiedjei Gen. Nov. and Sp. Nov., a Novel Anaerobic, Dehalogenating, Sulfate-Reducing Bacterium." *Archives of Microbiology* 154 (1). <https://doi.org/10.1007/BF00249173>.
- Di, H. J., K. C. Cameron, J. P. Shen, C. S. Winefield, M. Ocallaghan, S. Bowatte, and J. Z. He. 2009. "Nitrification Driven by Bacteria and Not Archaea in Nitrogen-Rich Grassland Soils." *Nature Geoscience* 2 (9). <https://doi.org/10.1038/ngeo613>.
- Ding, Dong. 2010. "Transport of Bacteria in Aquifer Sediment: Experiments and Modeling." *Hydrogeology Journal* 18 (3). <https://doi.org/10.1007/s10040-009-0559-3>.
- Dini-Andreote, Francisco, James C. Stegen, Jan Dirk Van Elsas, and Joana Falcão Salles. 2015. "Disentangling Mechanisms That Mediate the Balance between Stochastic and Deterministic Processes in Microbial Succession." *Proceedings of the National Academy of Sciences of the United States of America* 112 (11): E1326–32. <https://doi.org/10.1073/pnas.1414261112>.
- Doane, Timothy A. 2017. "The Abiotic Nitrogen Cycle." *ACS Earth and Space Chemistry* 1 (7): 411–21. <https://doi.org/10.1021/acsearthspacechem.7b00059>.
- Du, Huilong, and Chengzhi Liang. 2019. "Assembly of Chromosome-Scale Contigs by Efficiently Resolving Repetitive Sequences with Long Reads." *Nature Communications* 10 (1). <https://doi.org/10.1038/s41467-019-13355-3>.
- Duan, Yuhan, Zhiwei Jiang, Zheng Wu, Zhi Sheng, Xi Yang, Jingya Sun, Xiaoling Zhang, Qiao Yang, Xinwei Yu, and Jianbo Yan. 2020. "Limnobacter Alexandrii Sp. Nov., a Thiosulfate-Oxidizing, Heterotrophic and EPS-Bearing Burkholderiaceae Isolated from Cultivable Phycosphere Microbiota of Toxic Alexandrium Catenella LZT09." *Antonie van Leeuwenhoek, International Journal of General and Molecular Microbiology* 113 (11). <https://doi.org/10.1007/s10482-020-01473-8>.
- Duff, J. H., F. Murphy, C. C. Fuller, and F. J. Triska. 1998. "A Mini Drivepoint Sampler for Measuring Pore Water Solute Concentrations in the Hyporheic Zone of Sand-Bottom Streams." *Limnology and Oceanography* 43 (6): 1378–83. <https://doi.org/10.4319/lo.1998.43.6.1378>.
- Duff, John H., and Frank J. Triska. 2000. "Nitrogen Biogeochemistry and Surface–Subsurface Exchange in Streams." In *Streams and Ground Waters*, 197–220. <https://doi.org/10.1016/b978-012389845-6/50009-0>.
- Eid, John, Adrian Fehr, Jeremy Gray, Khai Luong, John Lyle, Geoff Otto, Paul Peluso, et al. 2009. "Real-Time DNA Sequencing from Single Polymerase Molecules." *Science* 323 (5910): 133–38. <https://doi.org/10.1126/science.1162986>.

- Eschbach, Martin, Henrik Möbitz, Alexandra Rompf, and Dieter Jahn. 2003. "Members of the Genus *Arthrobacter* Grow Anaerobically Using Nitrate Ammonification and Fermentative Processes: Anaerobic Adaptation of Aerobic Bacteria Abundant in Soil." *FEMS Microbiology Letters* 223 (2). [https://doi.org/10.1016/S0378-1097\(03\)00383-5](https://doi.org/10.1016/S0378-1097(03)00383-5).
- Etchebehere, Claudia, and James Tiedje. 2005. "Presence of Two Different Active NirS Nitrite Reductase Genes in a Denitrifying *Thauera* Sp. from a High-Nitrate-Removal-Rate Reactor." *Applied and Environmental Microbiology* 71 (9): 5642–45. <https://doi.org/10.1128/AEM.71.9.5642-5645.2005>.
- Ewels, Philip A., Alexander Peltzer, Sven Fillinger, Harshil Patel, Johannes Alneberg, Andreas Wilm, Maxime Ulysse Garcia, Paolo Di Tommaso, and Sven Nahnsen. 2020. "The Nf-Core Framework for Community-Curated Bioinformatics Pipelines." *Nature Biotechnology*. <https://doi.org/10.1038/s41587-020-0439-x>.
- Fahrbach, Michael, Jan Kuever, Ruth Meinke, Peter Kämpfer, and Juliane Hollender. 2006. "Denitratisoma Oestradiolicum Gen. Nov., Sp. Nov., a 17 β -Oestradiol-Degrading, Denitrifying Betaproteobacterium." *International Journal of Systematic and Evolutionary Microbiology* 56 (7): 1547–52. <https://doi.org/10.1099/ijs.0.63672-0>.
- Febria, Catherine M., Paul Beddoes, Roberta R. Fulthorpe, and D. Dudley Williams. 2012. "Bacterial Community Dynamics in the Hyporheic Zone of an Intermittent Stream." *ISME Journal* 6 (5): 1078–88. <https://doi.org/10.1038/ismej.2011.173>.
- Feris, K. P., P. W. Ramsey, C. Frazar, M. C. Rillig, J. E. Gannon, and W. E. Holben. 2003. "Structure and Seasonal Dynamics of Hyporheic Zone Microbial Communities in Free-Stone Rivers of the Western United States." *Microbial Ecology* 46 (2): 200–215. <https://doi.org/10.1007/s00248-002-0003-x>.
- Fida, Tekle Tafese, Mohita Sharma, Yin Shen, and Gerrit Voordouw. 2021. "Microbial Sulfite Oxidation Coupled to Nitrate Reduction in Makeup Water for Oil Production." *Chemosphere* 284. <https://doi.org/10.1016/j.chemosphere.2021.131298>.
- Fillinger, Lucas, Katrin Hug, and Christian Griebler. 2019. "Selection Imposed by Local Environmental Conditions Drives Differences in Microbial Community Composition across Geographically Distinct Groundwater Aquifers." *FEMS Microbiology Ecology* 95 (11). <https://doi.org/10.1093/femsec/fiz160>.
- Foley, Jonathan A., Navin Ramankutty, Kate A. Brauman, Emily S. Cassidy, James S. Gerber, Matt Johnston, Nathaniel D. Mueller, et al. 2011. "Solutions for a Cultivated Planet." *Nature* 478 (7369). <https://doi.org/10.1038/nature10452>.
- Fones, Elizabeth M., Daniel R. Colman, Emily A. Kraus, Ramunas Stepanauskas, Alexis S. Templeton, John R. Spear, and Eric S. Boyd. 2021. "Diversification of Methanogens into Hyperalkaline Serpentinizing Environments through Adaptations to Minimize Oxidant Limitation." *ISME Journal* 15 (4): 1121–35. <https://doi.org/10.1038/s41396-020-00838-1>.
- Fossen Johnson, Sarah. 2019. "Methemoglobinemia: Infants at Risk." *Current Problems in Pediatric and Adolescent Health Care* 49 (3): 57–67. <https://doi.org/10.1016/j.cppeds.2019.03.002>.
- Francis, Christopher A., Kathryn J. Roberts, J. Michael Beman, Alyson E. Santoro, and Brian B. Oakley. 2005. "Ubiquity and Diversity of Ammonia-Oxidizing Archaea in Water

- Columns and Sediments of the Ocean.” *Proceedings of the National Academy of Sciences of the United States of America* 102 (41): 14683–88.
<https://doi.org/10.1073/pnas.0506625102>.
- Friedrich, Frank Bardischewsky, Dagmar Rother, Armin Quentmeier, and Jörg Fischer. 2005. “Prokaryotic Sulfur Oxidation.” *Current Opinion in Microbiology*.
<https://doi.org/10.1016/j.mib.2005.04.005>.
- Friedrich, C. G., A. Quentmeier, F. Bardischewsky, D. Rother, R. Kraft, S. Kostka, and H. Prinz. 2000. “Novel Genes Coding for Lithotrophic Sulfur Oxidation of *Paracoccus Pantotrophus* GB17.” *Journal of Bacteriology* 182 (17).
<https://doi.org/10.1128/JB.182.17.4677-4687.2000>.
- Gadekar, S., M. Nemati, and G. A. Hill. 2006. “Batch and Continuous Biooxidation of Sulphide by *Thiomicrospira* Sp. CVO: Reaction Kinetics and Stoichiometry.” *Water Research* 40 (12). <https://doi.org/10.1016/j.watres.2006.04.007>.
- Gadkari, Dilip. 1984. “Influence of the Herbicides Goltix and Sencor on Nitrification.” *Zentralblatt Für Mikrobiologie* 139 (8): 623–31. [https://doi.org/10.1016/s0232-4393\(84\)80056-6](https://doi.org/10.1016/s0232-4393(84)80056-6).
- Galushko, Alexander, and Jan Kuever. 2019. “Desulfobacterium.” In *Bergey’s Manual of Systematics of Archaea and Bacteria*, 1–4.
<https://doi.org/https://doi.org/10.1002/9781118960608.gbm01012.pub2>.
- Giguere, Andrew T., Anne E. Taylor, David D. Myrold, and Peter J. Bottomley. 2015. “Nitrification Responses of Soil Ammonia-Oxidizing Archaea and Bacteria to Ammonium Concentrations.” *Soil Science Society of America Journal* 79 (5): 1366–74.
<https://doi.org/10.2136/sssaj2015.03.0107>.
- Ginestet, Cedric. 2011. “Ggplot2: Elegant Graphics for Data Analysis.” *Journal of the Royal Statistical Society: Series A (Statistics in Society)* 174 (1): 245–46.
https://doi.org/10.1111/j.1467-985x.2010.00676_9.x.
- Gomez-Velez, Jesus D., Judson W. Harvey, M. Bayani Cardenas, and Brian Kiel. 2015. “Denitrification in the Mississippi River Network Controlled by Flow through River Bedforms.” *Nature Geoscience* 8 (12): 941–45. <https://doi.org/10.1038/ngeo2567>.
- Gonzalez-Pimentel, Jose Luis, Tamara Martin-Pozas, Valme Jurado, Ana Zelia Miller, Ana Teresa Caldeira, Octavio Fernandez-Lorenzo, Sergio Sanchez-Moral, and Cesareo Saiz-Jimenez. 2021. “Prokaryotic Communities from a Lava Tube Cave in La Palma Island (Spain) Are Involved in the Biogeochemical Cycle of Major Elements.” *PeerJ* 9.
<https://doi.org/10.7717/peerj.11386>.
- Goodwin, Sara, John D McPherson, and W Richard McCombie. 2016. “Coming of Age: Ten Years of next-Generation Sequencing Technologies.” *Nature Reviews Genetics* 17 (6): 333–51. <https://doi.org/10.1038/nrg.2016.49>.
- Gooseff, Michael N., Diane M. McKnight, Robert L. Runkel, and John H. Duff. 2004. “Denitrification and Hydrologic Transient Storage in a Glacial Meltwater Stream, McMurdo Dry Valleys, Antarctica.” *Limnology and Oceanography* 49 (5): 1884–95.
<https://doi.org/10.4319/lo.2004.49.5.1884>.
- Gough, Julian, Kevin Karplus, Richard Hughey, and Cyrus Chothia. 2001. “Assignment of

- Homology to Genome Sequences Using a Library of Hidden Markov Models That Represent All Proteins of Known Structure.” *Journal of Molecular Biology* 313 (4). <https://doi.org/10.1006/jmbi.2001.5080>.
- Graf, Daniel R.H., Christopher M. Jones, and Sara Hallin. 2014. “Intergenomic Comparisons Highlight Modularity of the Denitrification Pathway and Underpin the Importance of Community Structure for N₂O Emissions.” *PLoS ONE* 9 (12). <https://doi.org/10.1371/journal.pone.0114118>.
- Graham, David W., Clare Trippett, Walter K. Dodds, Jonathan M. O’Brien, Eric B.K. Banner, Ian M. Head, Marilyn S. Smith, Richard K. Yang, and Charles W. Knapp. 2010. “Correlations between in Situ Denitrification Activity and Nir-Gene Abundances in Pristine and Impacted Prairie Streams.” *Environmental Pollution* 158 (10): 3225–29. <https://doi.org/10.1016/j.envpol.2010.07.010>.
- Graham, Emily B., Alex R. Crump, Charles T. Resch, Sarah Fansler, Evan Arntzen, David W. Kennedy, Jim K. Fredrickson, and James C. Stegen. 2017. “Deterministic Influences Exceed Dispersal Effects on Hydrologically-Connected Microbiomes.” *Environmental Microbiology* 19 (4): 1552–67. <https://doi.org/10.1111/1462-2920.13720>.
- Graham, Emily B., and James C. Stegen. 2017. “Dispersal-Based Microbial Community Assembly Decreases Biogeochemical Function.” *Processes* 5 (4). <https://doi.org/10.3390/pr5040065>.
- Grathwohl, Peter, Hermann Rügner, Thomas Wöhling, Karsten Osenbrück, Marc Schwientek, Sebastian Gayler, Ute Wollschläger, et al. 2013. “Catchments as Reactors: A Comprehensive Approach for Water Fluxes and Solute Turnover.” *Environmental Earth Sciences* 69 (2): 317–33. <https://doi.org/10.1007/s12665-013-2281-7>.
- Grinsven, Hans J.M. Van, Mary H. Ward, Nigel Benjamin, and Theo M. De Kok. 2006. “Does the Evidence about Health Risks Associated with Nitrate Ingestion Warrant an Increase of the Nitrate Standard for Drinking Water?” *Environmental Health: A Global Access Science Source* 5. <https://doi.org/10.1186/1476-069X-5-26>.
- Grose, Amelia L., Shannon L. Speir, Audrey N. Thellman, Martha M. Dee, and Jennifer L. Tank. 2022. “Water Transport Pathways Influence the Propagation of Field-scale NO₃--N Reductions to the Watershed Scale.” *Hydrological Processes* 36 (2): 1–13. <https://doi.org/10.1002/hyp.14476>.
- Gu, Zuguang, Roland Eils, and Matthias Schlesner. 2016. “Complex Heatmaps Reveal Patterns and Correlations in Multidimensional Genomic Data.” *Bioinformatics* 32 (18): 2847–49. <https://doi.org/10.1093/bioinformatics/btw313>.
- Guppy, Lisa, Paula Uyttendaele, Karen G Villholth, Vladimir Smakhtin, Yanyan Gao, Hui Qian, Wenhao Ren, et al. 2018. “Groundwater and Sustainable Development Goals: Analysis of Interlinkages.” *Encyclopedia of Inland Waters* 1 (1): 1–5. <http://dx.doi.org/10.1038/s41545-018-0015-9><https://doi.org/10.1016/j.jclepro.2020.121006>.
- Gurevich, Alexey, Vladislav Saveliev, Nikolay Vyahhi, and Glenn Tesler. 2013. “QUAST: Quality Assessment Tool for Genome Assemblies.” *Bioinformatics* 29 (8). <https://doi.org/10.1093/bioinformatics/btt086>.
- Haft, Daniel H., Jeremy D. Selengut, and Owen White. 2003. “The TIGRFAMs Database of

- Protein Families.” *Nucleic Acids Research*. <https://doi.org/10.1093/nar/gkg128>.
- Hamonts, Kelly, Annemie Ryngaert, Hauke Smidt, Dirk Springael, and Winnie Dejonghe. 2014. “Determinants of the Microbial Community Structure of Eutrophic, Hyporheic River Sediments Polluted with Chlorinated Aliphatic Hydrocarbons.” *FEMS Microbiology Ecology* 87 (3): 715–32. <https://doi.org/10.1111/1574-6941.12260>.
- Han, Cliff, Oleg Kotsyurbenko, Olga Chertkov, Brittany Held, Alla Lapidus, Matt Nolan, Susan Lucas, et al. 2012. “Complete Genome Sequence of the Sulfur Compounds Oxidizing Chemolithoautotroph *Sulfuricurvum kujiense* Type Strain (YK-1 T).” *Standards in Genomic Sciences* 6 (1): 94–103. <https://doi.org/10.4056/sigs.2456004>.
- Han, Yuchen, and Mirjam Perner. 2015. “The Globally Widespread Genus *Sulfurimonas*: Versatile Energy Metabolisms and Adaptations to Redox Clines.” *Frontiers in Microbiology*. <https://doi.org/10.3389/fmicb.2015.00989>.
- Handley, Kim M., Daniela Bartels, Edward J. O’Loughlin, Kenneth H. Williams, William L. Trimble, Kelly Skinner, Jack A. Gilbert, et al. 2014. “The Complete Genome Sequence for Putative H₂- and S-Oxidizer Candidatus *Sulfuricurvum* Sp., Assembled de Novo from an Aquifer-Derived Metagenome.” *Environmental Microbiology* 16 (11): 3443–62. <https://doi.org/10.1111/1462-2920.12453>.
- Hannah, David M., Benjamin W. Abbott, Kieran Khamis, Christa Kelleher, Iseult Lynch, Stefan Krause, and Adam S. Ward. 2022. “Illuminating the ‘Invisible Water Crisis’ to Address Global Water Pollution Challenges.” *Hydrological Processes* 36 (3): 1–5. <https://doi.org/10.1002/hyp.14525>.
- Hanrahan, Brittany R., Jennifer L. Tank, Martha M. Dee, Matt T. Trentman, Elizabeth M. Berg, and Sara K. McMillan. 2018. “Restored Floodplains Enhance Denitrification Compared to Naturalized Floodplains in Agricultural Streams.” *Biogeochemistry* 141 (3): 419–37. <https://doi.org/10.1007/s10533-018-0431-4>.
- Hardison, Amber K., Christopher K. Algar, Anne E. Giblin, and Jeremy J. Rich. 2015. “Influence of Organic Carbon and Nitrate Loading on Partitioning between Dissimilatory Nitrate Reduction to Ammonium (DNRA) and N₂ Production.” *Geochimica et Cosmochimica Acta* 164. <https://doi.org/10.1016/j.gca.2015.04.049>.
- Harvey, Judson W., J. K. Böhlke, Mary A. Voytek, Durelle Scott, and Craig R. Tobias. 2013. “Hyporheic Zone Denitrification: Controls on Effective Reaction Depth and Contribution to Whole-Stream Mass Balance.” *Water Resources Research* 49 (10): 6298–6316. <https://doi.org/10.1002/wrcr.20492>.
- Haryono, Mindia A.S., Ying Yu Law, Krithika Arumugam, Larry C.W. Liew, Thi Quynh Ngoc Nguyen, Daniela I. Drautz-Moses, Stephan C. Schuster, Stefan Wuertz, and Rohan B.H. Williams. 2022. “Recovery of High Quality Metagenome-Assembled Genomes From Full-Scale Activated Sludge Microbial Communities in a Tropical Climate Using Longitudinal Metagenome Sampling.” *Frontiers in Microbiology* 13. <https://doi.org/10.3389/fmicb.2022.869135>.
- Helen, Decleyre, Heylen Kim, Bjorn Tytgat, and Willems Anne. 2016. “Highly Diverse NirK Genes Comprise Two Major Clades That Harbour Ammonium-Producing Denitrifiers.” *BMC Genomics* 17 (1). <https://doi.org/10.1186/s12864-016-2465-0>.
- Henderson, F M. 1966. “Open Channel Flow Mac Millan Publishing Co.” *Inc., New York*

1966, 288–324.

- Henry, Sonia, Ezékiel Baudoïn, Juan C. López-Gutiérrez, Fabrice Martin-Laurent, Alain Brauman, and Laurent Philippot. 2004. “Quantification of Denitrifying Bacteria in Soils by NirK Gene Targeted Real-Time PCR.” *Journal of Microbiological Methods* 59 (3): 327–35. <https://doi.org/10.1016/j.mimet.2004.07.002>.
- Herzog, Skuyler, Anna Herzog Howell, and Adam Ward. 2020. “English Translation of Chappuis (1946) ‘A New Biotope of Aquatic Underground Fauna.’” *HydroShare*. <https://doi.org/10.4211/hs.d28c7b2d81a644bfba15762074230988>.
- Hester, E. T., K. I. Young, and M. A. Widdowson. 2013. “Mixing of Surface and Groundwater Induced by Riverbed Dunes: Implications for Hyporheic Zone Definitions and Pollutant Reactions.” *Water Resources Research* 49 (9): 5221–37. <https://doi.org/10.1002/wrcr.20399>.
- Heylen, Kim, and Jan Keltjens. 2012. “Redundancy and Modularity in Membrane-Associated Dissimilatory Nitrate Reduction in *Bacillus*.” *Frontiers in Microbiology* 3 (OCT). <https://doi.org/10.3389/fmicb.2012.00371>.
- Hink, Linda, Graeme W. Nicol, and James I. Prosser. 2017. “Archaea Produce Lower Yields of N₂O than Bacteria during Aerobic Ammonia Oxidation in Soil.” *Environmental Microbiology* 19 (12): 4829–37. <https://doi.org/10.1111/1462-2920.13282>.
- Holman, I. P., C. Brown, V. Janes, and D. Sandars. 2017. “Can We Be Certain about Future Land Use Change in Europe? A Multi-Scenario, Integrated-Assessment Analysis.” *Agricultural Systems* 151. <https://doi.org/10.1016/j.agsy.2016.12.001>.
- Horn, Marcus A., Julian Ihssen, Carola Matthies, Andreas Schramm, Georg Acker, and Harold L. Drake. 2005. “*Dechloromonas Denitrificans* Sp. Nov., *Flavobacterium Denitrificans* Sp. Nov., *Paenibacillus Anaericanus* Sp. Nov. and *Paenibacillus Terrae* Strain MH72, N₂O-Producing Bacteria Isolated from the Gut of the Earthworm *Aporrectodea Caliginosa*.” *International Journal of Systematic and Evolutionary Microbiology* 55 (3): 1255–65. <https://doi.org/10.1099/ijs.0.63484-0>.
- Horton, Robert E. 1945. “Erosional Development of Streams and Their Drainage Basins; Hydrophysical Approach to Quantitative Morphology.” *Geological Society of America Bulletin* 56 (3): 275–370.
- Huang, Xuejiao, Christopher G. Weisener, Jiupai Ni, Binghui He, Deti Xie, and Zhenlun Li. 2020. “Nitrate Assimilation, Dissimilatory Nitrate Reduction to Ammonium, and Denitrification Coexist in *Pseudomonas Putida* Y-9 under Aerobic Conditions.” *Bioresource Technology* 312. <https://doi.org/10.1016/j.biortech.2020.123597>.
- Hullar, Meredith A.J., Louis A. Kaplan, and David A. Stahl. 2006. “Recurring Seasonal Dynamics of Microbial Communities in Stream Habitats.” *Applied and Environmental Microbiology* 72 (1): 713–22. <https://doi.org/10.1128/AEM.72.1.713-722.2006>.
- Hutt, Lee P., Marcel Huntemann, Alicia Clum, Manoj Pillay, Krishnaveni Palaniappan, Neha Varghese, Natalia Mikhailova, et al. 2017. “Permanent Draft Genome of *Thiobacillus Thioparus* DSM 505T, an Obligately Chemolithoautotrophic Member of the Betaproteobacteria.” *Standards in Genomic Sciences* 12 (1). <https://doi.org/10.1186/s40793-017-0229-3>.

- Jakus, Natalia, Nia Blackwell, Karsten Osenbrück, Daniel Straub, James M. Byrne, Zhe Wang, David Glöckler, et al. 2021. “Nitrate Removal by a Novel Lithoautotrophic Nitrate-Reducing, Iron(II)-Oxidizing Culture Enriched from a Pyrite-Rich Limestone Aquifer.” *Applied and Environmental Microbiology* 87 (16): 1–15. <https://doi.org/10.1128/AEM.00460-21>.
- Jakus, Natalia, Nia Blackwell, Daniel Straub, Andreas Kappler, and Sara Kleindienst. 2021. “Presence of Fe(II) and Nitrate Shapes Aquifer-Originating Communities Leading to an Autotrophic Enrichment Dominated by an Fe(II)-Oxidizing Gallionellaceae Sp.” *FEMS Microbiology Ecology* 97 (11). <https://doi.org/10.1093/femsec/fiab145>.
- Jeroschewski, P., C. Steuckart, and M. Kuhl. 1996. “An Amperometric Microsensor for the Determination of H₂S in Aquatic Environments.” *Analytical Chemistry* 68 (24): 4351–57. <https://doi.org/10.1021/ac960091b>.
- Jetten, Mike S.M., Alfons J.M. Stams, and Alexander J.B. Zehnder. 1992. “Methanogenesis from Acetate: A Comparison of the Acetate Metabolism in Methanotrix Soehngeni and Methanosarcina Spp.” *FEMS Microbiology Letters* 88 (3–4). [https://doi.org/10.1016/0378-1097\(92\)90802-U](https://doi.org/10.1016/0378-1097(92)90802-U).
- Jia, Zhongjun, and Ralf Conrad. 2009. “Bacteria Rather than Archaea Dominate Microbial Ammonia Oxidation in an Agricultural Soil.” *Environmental Microbiology* 11 (7): 1658–71. <https://doi.org/10.1111/j.1462-2920.2009.01891.x>.
- Jimenez-Fernandez, Oscar, Marc Schwientek, Karsten Osenbrück, Clarissa Glaser, Christian Schmidt, and Jan H Fleckenstein. 2022. “Groundwater-Surface Water Exchange as Key Control for Instream and Groundwater Nitrate Concentrations along a First-Order Agricultural Stream.” *Hydrological Processes* 36 (2): e14507. <https://doi.org/10.1002/hyp.14507>.
- Johansson, Emma Li, Sara Brogaard, and Lova Brodin. 2022. “Envisioning Sustainable Carbon Sequestration in Swedish Farmland.” *Environmental Science & Policy* 135: 16–25. <https://doi.org/10.1016/j.envsci.2022.04.005>.
- Jones, Daniel S., Kim A. Lapakko, Zachary J. Wenz, Michael C. Olson, Elizabeth W. Roepke, Michael J. Sadowsky, Paige J. Novak, and Jake V. Bailey. 2017. “Novel Microbial Assemblages Dominate Weathered Sulfidebearing Rock from Copper-Nickel Deposits in the Duluth Complex, Minnesota, USA.” *Applied and Environmental Microbiology* 83 (16). <https://doi.org/10.1128/AEM.00909-17>.
- Jones, Erin Fleming, Natasha Griffin, Julia E. Kelso, Gregory T. Carling, Michelle A. Baker, and Zachary T. Aanderud. 2020. “Stream Microbial Community Structured by Trace Elements, Headwater Dispersal, and Large Reservoirs in Sub-Alpine and Urban Ecosystems.” *Frontiers in Microbiology* 11. <https://doi.org/10.3389/fmicb.2020.491425>.
- Jorgensen, Steffen Leth, Bjarte Hannisdal, Anders Lanzén, Tamara Baumberger, Kristin Flesland, Rita Fonseca, Lise Øvreås, et al. 2012. “Correlating Microbial Community Profiles with Geochemical Data in Highly Stratified Sediments from the Arctic Mid-Ocean Ridge.” *Proceedings of the National Academy of Sciences of the United States of America* 109 (42). <https://doi.org/10.1073/pnas.1207574109>.
- Joye, Samantha B., and James T. Hollibaugh. 1995. “Influence of Sulfide Inhibition of Nitrification on Nitrogen Regeneration in Sediments.” *Science* 270 (5236): 623–25.

<https://doi.org/10.1126/science.270.5236.623>.

- Jung, Man Young, Soo Je Park, Deullae Min, Jin Seog Kim, W. Irene C. Rijpstra, Jaap S. Sinninghe Damsté, Geun Joong Kim, Eugene L. Madsen, and Sung Keun Rhee. 2011. “Enrichment and Characterization of an Autotrophic Ammonia-Oxidizing Archaeon of Mesophilic Crenarchaeal Group I.1a from an Agricultural Soil.” *Applied and Environmental Microbiology* 77 (24). <https://doi.org/10.1128/AEM.05787-11>.
- Jung, Man Young, Christopher J. Sedlacek, K. Dimitri Kits, Anna J. Mueller, Sung Keun Rhee, Linda Hink, Graeme W. Nicol, et al. 2021. “Ammonia-Oxidizing Archaea Possess a Wide Range of Cellular Ammonia Affinities.” *ISME Journal*, no. July: 1–12. <https://doi.org/10.1038/s41396-021-01064-z>.
- Jurado, Valme, Jose Luis Gonzalez-Pimentel, Ana Zelia Miller, Bernardo Hermosin, Ilenia M. D’Angeli, Paola Tognini, Jo De Waele, and Cesareo Saiz-Jimenez. 2020. “Microbial Communities in Vermiculation Deposits from an Alpine Cave.” *Frontiers in Earth Science* 8. <https://doi.org/10.3389/feart.2020.586248>.
- Kaandorp, V. P., P. G.B. de Louw, Y. van der Velde, and H. P. Broers. 2018. “Transient Groundwater Travel Time Distributions and Age-Ranked Storage-Discharge Relationships of Three Lowland Catchments.” *Water Resources Research* 54 (7): 4519–36. <https://doi.org/10.1029/2017WR022461>.
- Kanehisa, Minoru, Yoko Sato, Masayuki Kawashima, Miho Furumichi, and Mao Tanabe. 2016. “KEGG as a Reference Resource for Gene and Protein Annotation.” *Nucleic Acids Research* 44 (D1). <https://doi.org/10.1093/nar/gkv1070>.
- Kang, Dongwan D., Feng Li, Edward Kirton, Ashleigh Thomas, Rob Egan, Hong An, and Zhong Wang. 2019. “MetaBAT 2: An Adaptive Binning Algorithm for Robust and Efficient Genome Reconstruction from Metagenome Assemblies.” *PeerJ* 2019 (7). <https://doi.org/10.7717/peerj.7359>.
- Karst, Søren M., Ryan M. Ziels, Rasmus H. Kirkegaard, Emil A. Sørensen, Daniel McDonald, Qiyun Zhu, Rob Knight, and Mads Albertsen. 2021. “High-Accuracy Long-Read Amplicon Sequences Using Unique Molecular Identifiers with Nanopore or PacBio Sequencing.” *Nature Methods* 18 (2): 165–69. <https://doi.org/10.1038/s41592-020-01041-y>.
- Kassambara, Alboukadel. 2021. “Ggpubr: ‘Ggplot2’ Based Publication Ready Plots.” *R Package Version 0.4.0*. <https://cran.r-project.org/package=ggpubr>.
- Katsanou, Konstantina, and Hrisi K. Karapanagioti. 2019. “Surface Water and Groundwater Sources for Drinking Water.” In *Handbook of Environmental Chemistry*, 67:1–19. https://doi.org/10.1007/978-94-007-140-1_140.
- Kellerman, Claudia, and Christian Griebler. 2009. “Thiobacillus Thiophilus Sp. Nov., a Chemolithoautotrophic, Thiosulfate-Oxidizing Bacterium Isolated from Contaminated Aquifer Sediments.” *International Journal of Systematic and Evolutionary Microbiology* 59 (3): 583–88. <https://doi.org/10.1099/ijs.0.002808-0>.
- Kembel, Steven W., Peter D. Cowan, Matthew R. Helmus, William K. Cornwell, Helene Morlon, David D. Ackerly, Simon P. Blomberg, and Campbell O. Webb. 2010. “Picante: R Tools for Integrating Phylogenies and Ecology.” *Bioinformatics* 26 (11): 1463–64. <https://doi.org/10.1093/bioinformatics/btq166>.

- Kessel, Maartje A.H.J. Van, Daan R. Speth, Mads Albertsen, Per H. Nielsen, Huub J.M. Op Den Camp, Boran Kartal, Mike S.M. Jetten, and Sebastian Lücker. 2015. "Complete Nitrification by a Single Microorganism." *Nature* 528 (7583): 555–59. <https://doi.org/10.1038/nature16459>.
- Khan, Shams Tabrez, Yoko Horiba, Masamitsu Yamamoto, and Akira Hiraishi. 2002. "Members of the Family Comamonadaceae as Primary Poly(3-Hydroxybutyrate-Co-3-Hydroxyvalerate)-Degrading Denitrifiers in Activated Sludge as Revealed by a Polyphasic Approach." *Applied and Environmental Microbiology* 68 (7): 3206–14. <https://doi.org/10.1128/AEM.68.7.3206-3214.2002>.
- Kim, Carol, Lorie W Staver, Xuan Chen, Ashley Bulseco, Jeffrey C Cornwell, and Sairah Y Malkin. 2023. "Microbial Community Succession Along a Chronosequence in Constructed Salt Marsh Soils." *Microbial Ecology*. <https://doi.org/10.1007/s00248-023-02189-8>.
- Kim, Heejung, Dugin Kaown, Bernhard Mayer, Jin Yong Lee, and Kang Kun Lee. 2018. "Combining Pyrosequencing and Isotopic Approaches to Assess Denitrification in a Hyporheic Zone." *Science of the Total Environment* 631–632. <https://doi.org/10.1016/j.scitotenv.2018.03.073>.
- Kjeldsen, Kasper U., Lars Schreiber, Casper A. Thorup, Thomas Boesen, Jesper T. Bjerg, Tingting Yang, Morten S. Dueholm, et al. 2019. "On the Evolution and Physiology of Cable Bacteria." *Proceedings of the National Academy of Sciences of the United States of America* 116 (38). <https://doi.org/10.1073/pnas.1903514116>.
- Koch, Hanna, Sebastian Lücker, Mads Albertsen, Katharina Kitzinger, Craig Herbold, Eva Spieck, Per Halkjaer Nielsen, Michael Wagner, and Holger Daims. 2015. "Expanded Metabolic Versatility of Ubiquitous Nitrite-Oxidizing Bacteria from the Genus *Nitrospira*." *Proceedings of the National Academy of Sciences of the United States of America* 112 (36): 11371–76. <https://doi.org/10.1073/pnas.1506533112>.
- Kodama, Yumiko, and Kazuya Watanabe. 2004. "Sulfuricurvum Kujiense Gen. Nov., Sp. Nov., a Facultatively Anaerobic, Chemolithoautotrophic, Sulfur-Oxidizing Bacterium Isolated from an Underground Crude-Oil Storage Cavity." *International Journal of Systematic and Evolutionary Microbiology* 54 (6): 2297–2300. <https://doi.org/10.1099/ijs.0.63243-0>.
- Koenig, A., and L. H. Liu. 2002. "Use of Limestone for PH Control in Autotrophic Denitrification: Continuous Flow Experiments in Pilot-Scale Packed Bed Reactors." *Journal of Biotechnology* 99 (2). [https://doi.org/10.1016/S0168-1656\(02\)00183-9](https://doi.org/10.1016/S0168-1656(02)00183-9).
- Koops, Hans Peter, and Andreas Pommerening-Röser. 2001. "Distribution and Ecophysiology of the Nitrifying Bacteria Emphasizing Cultured Species." *FEMS Microbiology Ecology* 37 (1): 1–9. [https://doi.org/10.1016/S0168-6496\(01\)00137-4](https://doi.org/10.1016/S0168-6496(01)00137-4).
- Kotera, Masaaki, Yasushi Okuno, Masahiro Hattori, Susumu Goto, and Minoru Kanehisa. 2004. "Computational Assignment of the EC Numbers for Genomic-Scale Analysis of Enzymatic Reactions." *Journal of the American Chemical Society* 126 (50). <https://doi.org/10.1021/ja0466457>.
- Krakau, Sabrina, Daniel Straub, Hadrien Gourelé, Gisela Gabernet, and Sven Nahnsen. 2022. "Nf-Core/Mag: A Best-Practice Pipeline for Metagenome Hybrid Assembly and

- Binning.” *NAR Genomics and Bioinformatics* 4 (1).
<https://doi.org/10.1093/nargab/lqac007>.
- Krassowski, Michał. 2021. “Krassowski/Complex-Upset: V1.0.2,” January.
<https://doi.org/10.5281/ZENODO.4416064>.
- Krause, S., D. M. Hannah, J. H. Fleckenstein, C. M. Heppell, D. Kaeser, R. Pickup, G. Pinay, A. L. Robertson, and P. J. Wood. 2011. “Inter-Disciplinary Perspectives on Processes in the Hyporheic Zone.” *Ecohydrology*. <https://doi.org/10.1002/eco.176>.
- Krause, Stefan, Christina Tecklenburg, Matthias Munz, and Emma Naden. 2013. “Streambed Nitrogen Cycling beyond the Hyporheic Zone: Flow Controls on Horizontal Patterns and Depth Distribution of Nitrate and Dissolved Oxygen in the Upwelling Groundwater of a Lowland River.” *Journal of Geophysical Research: Biogeosciences* 118 (1): 54–67.
<https://doi.org/10.1029/2012JG002122>.
- Kumar, Sudhir, Glen Stecher, Michael Li, Christina Knyaz, and Koichiro Tamura. 2018. “MEGA X: Molecular Evolutionary Genetics Analysis across Computing Platforms.” *Molecular Biology and Evolution* 35 (6): 1547–49.
<https://doi.org/10.1093/molbev/msy096>.
- Kurtzer, Gregory M., Vanessa Sochat, and Michael W. Bauer. 2017. “Singularity: Scientific Containers for Mobility of Compute.” *PLoS ONE* 12 (5).
<https://doi.org/10.1371/journal.pone.0177459>.
- Kuypers, Marcel M.M., Hannah K. Marchant, and Boran Kartal. 2018. “The Microbial Nitrogen-Cycling Network.” *Nature Reviews Microbiology* 16 (5): 263–76.
<https://doi.org/10.1038/nrmicro.2018.9>.
- La Torre, José R. De, Christopher B. Walker, Anitra E. Ingalls, Martin Könneke, and David A. Stahl. 2008. “Cultivation of a Thermophilic Ammonia Oxidizing Archaeon Synthesizing Crenarchaeol.” *Environmental Microbiology* 10 (3): 810–18.
<https://doi.org/10.1111/j.1462-2920.2007.01506.x>.
- Lagostina, Lorenzo, Tobias Goldhammer, Hans Røy, Thomas W. Evans, Mark A. Lever, Bo B. Jørgensen, Dorthe G. Petersen, Andreas Schramm, and Lars Schreiber. 2015. “Ammonia-Oxidizing Bacteria of the Nitrosospira Cluster 1 Dominate over Ammonia-Oxidizing Archaea in Oligotrophic Surface Sediments near the South Atlantic Gyre.” *Environmental Microbiology Reports* 7 (3): 404–13. <https://doi.org/10.1111/1758-2229.12264>.
- Lam, Theo Y.C., Ran Mei, Zhuoying Wu, Patrick K.H. Lee, Wen Tso Liu, and Po Heng Lee. 2020. “Superior Resolution Characterisation of Microbial Diversity in Anaerobic Digesters Using Full-Length 16S rRNA Gene Amplicon Sequencing.” *Water Research* 178: 115815. <https://doi.org/10.1016/j.watres.2020.115815>.
- Lane D.J. 1991. “16S/23S rRNA Sequencing.” *Nucleic Acid Techniques in Bacterial Systematics* 31 (6): 125–75. <http://doi.wiley.com/10.1002/jobm.3620310616>.
- Lang, Dandan, Shilai Zhang, Pingping Ren, Fan Liang, Zongyi Sun, Guanliang Meng, Yuntao Tan, et al. 2021. “Comparison of the Two Up-to-Date Sequencing Technologies for Genome Assembly: HiFi Reads of Pacific Biosciences Sequel II System and Ultralong Reads of Oxford Nanopore.” *GigaScience* 9 (12).
<https://doi.org/10.1093/gigascience/giaa123>.

- Langmead, Ben, and Steven L. Salzberg. 2012. "Fast Gapped-Read Alignment with Bowtie 2." *Nature Methods* 9 (4). <https://doi.org/10.1038/nmeth.1923>.
- Langwig, Marguerite V., Valerie De Anda, Nina Dombrowski, Kiley W. Seitz, Ian M. Rambo, Chris Greening, Andreas P. Teske, and Brett J. Baker. 2021. "Large-Scale Protein Level Comparison of Deltaproteobacteria Reveals Cohesive Metabolic Groups." *ISME Journal*, no. July: 1–14. <https://doi.org/10.1038/s41396-021-01057-y>.
- Laperriere, Sarah M., Robert H. Hilderbrand, Stephen R. Keller, Regina Trott, and Alyson E. Santoro. 2020. "Headwater Stream Microbial Diversity and Function across Agricultural and Urban Land Use Gradients." *Applied and Environmental Microbiology* 86 (11). <https://doi.org/10.1128/AEM.00018-20>.
- Lee, Bandy X., Finn Kjaerulf, Shannon Turner, Larry Cohen, Peter D. Donnelly, Robert Muggah, Rachel Davis, et al. 2016. "Transforming Our World: Implementing the 2030 Agenda Through Sustainable Development Goal Indicators." *Journal of Public Health Policy*. <https://doi.org/10.1057/s41271-016-0002-7>.
- Leininger, S., T. Urich, M. Schloter, L. Schwark, J. Qi, G. W. Nicol, J. I. Prosser, S. C. Schuster, and C. Schleper. 2006. "Archaea Predominate among Ammonia-Oxidizing Prokaryotes in Soils." *Nature* 442 (7104): 806–9. <https://doi.org/10.1038/nature04983>.
- Letunic, Ivica, and Peer Bork. 2019. "Interactive Tree of Life (ITOL) v4: Recent Updates and New Developments." *Nucleic Acids Research* 47 (W1). <https://doi.org/10.1093/nar/gkz239>.
- Levičnik-Höfferle, Špela, Graeme W. Nicol, Luka Ausec, Ines Mandić-Mulec, and James I. Prosser. 2012. "Stimulation of Thaumarchaeal Ammonia Oxidation by Ammonia Derived from Organic Nitrogen but Not Added Inorganic Nitrogen." *FEMS Microbiology Ecology* 80 (1): 114–23. <https://doi.org/10.1111/j.1574-6941.2011.01275.x>.
- Lewandowski, Jörg, Shai Arnon, Eddie Banks, Okke Batelaan, Andrea Betterle, Tabea Broecker, Claudia Coll, et al. 2019. "Is the Hyporheic Zone Relevant beyond the Scientific Community?" *Water (Switzerland)* 11 (11). <https://doi.org/10.3390/w11112230>.
- Li, Baoqin, Zhe Li, Xiaoxu Sun, Qi Wang, Enzong Xiao, and Weimin Sun. 2018. "DNA-SIP Reveals the Diversity of Chemolithoautotrophic Bacteria Inhabiting Three Different Soil Types in Typical Karst Rocky Desertification Ecosystems in Southwest China." *Microbial Ecology* 76 (4). <https://doi.org/10.1007/s00248-018-1196-y>.
- Li, Chenxin. 2020. "GitHub - Cxli233/Customized_upset_plots." 2020. https://doi.org/https://github.com/cxli233/customized_upset_plots.
- Li, Gao Peng, Liang Jiang, Jia Zuan Ni, Qiong Liu, and Yan Zhang. 2014. "Computational Identification of a New SelD-like Family That May Participate in Sulfur Metabolism in Hyperthermophilic Sulfur-Reducing Archaea." *BMC Genomics* 15 (1). <https://doi.org/10.1186/1471-2164-15-908>.
- Li, Xiuying, Yi Yang, Xiangfeng Zeng, Jingjing Wang, Huijuan Jin, Zhi Sheng, and Jun Yan. 2019. "Metagenome-Assembled Genome Sequence of *Sulfuricurvum* Sp. Strain IAE1, Isolated from a 4-Chlorophenol-Degrading Consortium." *Microbiology Resource Announcements* 8 (31). <https://doi.org/10.1128/mra.00296-19>.

- Liao, Hehuan, Kai Yu, Yanhua Duan, Zigong Ning, Binrui Li, Leiyu He, and Chongxuan Liu. 2019. “Profiling Microbial Communities in a Watershed Undergoing Intensive Anthropogenic Activities.” *Science of the Total Environment* 647 (October): 1137–47. <https://doi.org/10.1016/j.scitotenv.2018.08.103>.
- Lin, Xueju, James McKinley, Charles T. Resch, Rachael Kaluzny, Christian L. Lauber, James Fredrickson, Rob Knight, and Allan Konopka. 2012. “Spatial and Temporal Dynamics of the Microbial Community in the Hanford Unconfined Aquifer.” *ISME Journal* 6 (9): 1665–76. <https://doi.org/10.1038/ismej.2012.26>.
- Lindström, Eva S., and Silke Langenheder. 2012. “Local and Regional Factors Influencing Bacterial Community Assembly.” *Environmental Microbiology Reports*. <https://doi.org/10.1111/j.1758-2229.2011.00257.x>.
- Liu, Shufeng, Haiying Wang, Liming Chen, Jiawen Wang, Maosheng Zheng, Sitong Liu, Qian Chen, and Jinren Ni. 2020. “Comammox Nitrospira within the Yangtze River Continuum: Community, Biogeography, and Ecological Drivers.” *ISME Journal* 14 (10). <https://doi.org/10.1038/s41396-020-0701-8>.
- Liu, Ying, Barbara Beckingham, Hermann Ruegner, Zhe Li, Limin Ma, Marc Schwientek, Huan Xie, Jianfu Zhao, and Peter Grathwohl. 2013. “Comparison of Sedimentary PAHs in the Rivers of Ammer (Germany) and Liangtan (China): Differences between Early- and Newly-Industrialized Countries.” *Environmental Science and Technology* 47 (2): 701–9. <https://doi.org/10.1021/es3031566>.
- Liu, Yiwen, Huu Hao Ngo, Wenshan Guo, Junliang Zhou, Lai Peng, Dongbo Wang, Xueming Chen, Jing Sun, and Bing Jie Ni. 2017. “Optimizing Sulfur-Driven Mixotrophic Denitrification Process: System Performance and Nitrous Oxide Emission.” *Chemical Engineering Science* 172 (2017): 414–22. <https://doi.org/10.1016/j.ces.2017.07.005>.
- Liu, Yixuan, Yumin Zhang, Yudi Huang, Jingjing Niu, Jun Huang, Xiaoya Peng, and Fang Peng. 2023. “Spatial and Temporal Conversion of Nitrogen Using *Arthrobacter* Sp. 24S4–2, a Strain Obtained from Antarctica .” *Frontiers in Microbiology* . <https://www.frontiersin.org/articles/10.3389/fmicb.2023.1040201>.
- Loferer-Krößbacher, M., J. Klima, and R. Psenner. 1998. “Determination of Bacterial Cell Dry Mass by Transmission Electron Microscopy and Densitometric Image Analysis.” *Applied and Environmental Microbiology* 64 (2). <https://doi.org/10.1128/aem.64.2.688-694.1998>.
- Love, Michael I., Wolfgang Huber, and Simon Anders. 2014. “Moderated Estimation of Fold Change and Dispersion for RNA-Seq Data with DESeq2.” *Genome Biology* 15 (12). <https://doi.org/10.1186/s13059-014-0550-8>.
- Lueders, Tillmann, Bianca Pommerenke, and Michael W. Friedrich. 2004. “Stable-Isotope Probing of Microorganisms Thriving at Thermodynamic Limits: Syntrophic Propionate Oxidation in Flooded Soil.” *Applied and Environmental Microbiology* 70 (10): 5778–86. <https://doi.org/10.1128/AEM.70.10.5778-5786.2004>.
- Mallard, John, Brian McGlynn, and Tim Covino. 2014. “Lateral Inflows, Stream-Groundwater Exchange, and Network Geometry Influence Stream Water Composition.” *Water Resources Research* 50 (6): 4603–23. <https://doi.org/10.1002/2013WR014944>.
- Mallick, Himel, Ali Rahnavard, Lauren J. McIver, Siyuan Ma, Yancong Zhang, Long H.

- Nguyen, Timothy L. Tickle, et al. 2021. “Multivariable Association Discovery in Population-Scale Meta-Omics Studies.” *PLoS Computational Biology* 17 (11): 1–27. <https://doi.org/10.1371/journal.pcbi.1009442>.
- Martens-Habbena, Willm, Paul M. Berube, Hidetoshi Urakawa, José R. De La Torre, and David A. Stahl. 2009. “Ammonia Oxidation Kinetics Determine Niche Separation of Nitrifying Archaea and Bacteria.” *Nature* 461 (7266): 976–79. <https://doi.org/10.1038/nature08465>.
- Martin, Marcel. 2011. “Cutadapt Removes Adapter Sequences from High-Throughput Sequencing Reads.” *EMBnet.Journal* 17 (1): 10. <https://doi.org/10.14806/ej.17.1.200>.
- Masuda, Sachiko, Shima Eda, Seishi Ikeda, Hisayuki Mitsui, and Kiwamu Minamisawa. 2010. “Thiosulfate-Dependent Chemolithoautotrophic Growth of *Bradyrhizobium Japonicum*.” *Applied and Environmental Microbiology* 76 (8). <https://doi.org/10.1128/AEM.02783-09>.
- McClain, Michael E, Elizabeth W Boyer, C Lisa Dent, Sarah E Gergel, Nancy B Grimm, Peter M Groffman, Stephen C Hart, Judson W Harvey, Carol A Johnston, and Emilio Mayorga. 2003. “Biogeochemical Hot Spots and Hot Moments at the Interface of Terrestrial and Aquatic Ecosystems.” *Ecosystems*, 301–12.
- McMurdie, Paul J., and Susan Holmes. 2013. “Phyloseq: An R Package for Reproducible Interactive Analysis and Graphics of Microbiome Census Data.” *PLoS ONE* 8 (4). <https://doi.org/10.1371/journal.pone.0061217>.
- . 2014. “Waste Not, Want Not: Why Rarefying Microbiome Data Is Inadmissible.” *PLoS Computational Biology* 10 (4). <https://doi.org/10.1371/journal.pcbi.1003531>.
- Michaels, Rachel, Kevin Eliason, Teagan Kuzniar, J. Todd Petty, Michael P. Strager, Paul F. Ziemkiewicz, and Ember Morrissey. 2022. “Microbial Communities Reveal Impacts of Unconventional Oil and Gas Development on Headwater Streams.” *Water Research* 212. <https://doi.org/10.1016/j.watres.2022.118073>.
- Mistry, Jaina, Sara Chuguransky, Lowri Williams, Matloob Qureshi, Gustavo A. Salazar, Erik L.L. Sonnhammer, Silvio C.E. Tosatto, et al. 2021. “Pfam: The Protein Families Database in 2021.” *Nucleic Acids Research* 49 (D1). <https://doi.org/10.1093/nar/gkaa913>.
- Moreno-Vivián, Conrado, Purificación Cabello, Manuel Martínez-Luque, Rafael Blasco, and Francisco Castillo. 1999. “Prokaryotic Nitrate Reduction: Molecular Properties and Functional Distinction among Bacterial Nitrate Reductases.” *Journal of Bacteriology*. <https://doi.org/10.1128/jb.181.21.6573-6584.1999>.
- Mulholland, Patrick J., Ashley M. Helton, Geoffrey C. Poole, Robert O. Hall, Stephen K. Hamilton, Bruce J. Peterson, Jennifer L. Tank, et al. 2008. “Stream Denitrification across Biomes and Its Response to Anthropogenic Nitrate Loading.” *Nature* 452 (7184): 202–5. <https://doi.org/10.1038/nature06686>.
- Müller, Albert Leopold, Kasper Urup Kjeldsen, Thomas Rattei, Michael Pester, and Alexander Loy. 2015. “Phylogenetic and Environmental Diversity of DsrAB-Type Dissimilatory (Bi)Sulfite Reductases.” *ISME Journal* 9 (5): 1152–65. <https://doi.org/10.1038/ismej.2014.208>.

- Murali, Adithya, Aniruddha Bhargava, and Erik S. Wright. 2018. “IDTAXA: A Novel Approach for Accurate Taxonomic Classification of Microbiome Sequences.” *Microbiome* 6 (1). <https://doi.org/10.1186/s40168-018-0521-5>.
- Murphy, Anna E., Ashley N. Bulseco, Ross Ackerman, Joseph H. Vineis, and Jennifer L. Bowen. 2020. “Sulphide Addition Favours Respiratory Ammonification (DNRA) over Complete Denitrification and Alters the Active Microbial Community in Salt Marsh Sediments.” *Environmental Microbiology* 22 (6): 2124–39. <https://doi.org/10.1111/1462-2920.14969>.
- Mußmann, Marc, Ivana Brito, Angela Pitcher, Jaap S. Sinninghe Damsté, Roland Hatzenpichler, Andreas Richter, Jeppe L. Nielsen, et al. 2011. “Thaumarchaeotes Abundant in Refinery Nitrifying Sludges Express AmoA but Are Not Obligate Autotrophic Ammonia Oxidizers.” *Proceedings of the National Academy of Sciences of the United States of America* 108 (40): 16771–76. <https://doi.org/10.1073/pnas.1106427108>.
- Muyzer, Gerard, and Alfons J.M. Stams. 2008. “The Ecology and Biotechnology of Sulphate-Reducing Bacteria.” *Nature Reviews Microbiology* 6 (6): 441–54. <https://doi.org/10.1038/nrmicro1892>.
- Nederbragt, Lex. 2016. “Developments in NGS (Version 9).” 2016. https://figshare.com/articles/developments_in_NGS/100940.
- Needelman, Brian A., Peter J.A. Kleinman, Jeffrey S. Strock, and Arthur L. Allen. 2007. “Improved Management of Agricultural Drainage Ditches for Water Quality Protection: An Overview.” *Journal of Soil and Water Conservation* 62 (4): 171 LP – 178. <http://www.jswconline.org/content/62/4/171.abstract>.
- Nelson, Amelia R., Audrey H. Sawyer, Rachel S. Gabor, Casey M. Saup, Savannah R. Bryant, Kira D. Harris, Martin A. Briggs, Kenneth H. Williams, and Michael J. Wilkins. 2019. “Heterogeneity in Hyporheic Flow, Pore Water Chemistry, and Microbial Community Composition in an Alpine Streambed.” *Journal of Geophysical Research: Biogeosciences* 124 (11): 3465–78. <https://doi.org/10.1029/2019JG005226>.
- Newbold, J. D. 1992. “Cycles and Spirals of Nutrients.” *The Rivers Handbook. Vol. 1*, 379–408.
- Nitratbericht Deutschland. 2020. “Gemeinsamer Bericht Der Bundesministerien Für Umwelt, Naturschutz Und Reaktorsicherheit (BMUB) Sowie Für Ernährung.” Landwirtschaft Und Verbraucherschutz (BMEL). 2020. <https://www.bmu.de/download/nitratberichte>.
- Nogaro, Geraldine, Thibault Datry, Florian Mermillod-Blondin, Stephane Descloux, and Bernard Montuelle. 2010. “Influence of Streambed Sediment Clogging on Microbial Processes in the Hyporheic Zone.” *Freshwater Biology* 55 (6): 1288–1302. <https://doi.org/10.1111/j.1365-2427.2009.02352.x>.
- Norton, Jeanette M., Javier J. Alzerreca, Yuichi Suwa, and Martin G. Klotz. 2002. “Diversity of Ammonia Monooxygenase Operon in Autotrophic Ammonia-Oxidizing Bacteria.” *Archives of Microbiology* 177 (2): 139–49. <https://doi.org/10.1007/s00203-001-0369-z>.
- Nurk, Sergey, Dmitry Meleshko, Anton Korobeynikov, and Pavel A. Pevzner. 2017. “MetaSPAdes: A New Versatile Metagenomic Assembler.” *Genome Research* 27 (5). <https://doi.org/10.1101/gr.213959.116>.

- Oksanen, Jari, F. Guillaume Blanchet, Roeland Kindt, Pierre Legendre, Peter R. Minchin, R. B. O'Hara, Gavin L. Simpson, Peter Solymos, M. Henry H. Stevens, and Helene Wagner. 2016. "Vegan: Community Ecology R Package, Version 2.3-5." *Vegan: Community Ecology Package. R Package Version 2.4-1*. <https://CRAN.R-Project.Org/Package=vegan> 2 (9). <https://cran.r-project.org/package=vegan>.
- Olson, Nathan D., Todd J. Treangen, Christopher M. Hill, Victoria Cepeda-Espinoza, Jay Ghurye, Sergey Koren, and Mihai Pop. 2018. "Metagenomic Assembly through the Lens of Validation: Recent Advances in Assessing and Improving the Quality of Genomes Assembled from Metagenomes." *Briefings in Bioinformatics* 20 (4). <https://doi.org/10.1093/bib/bbx098>.
- Orellana, L. H., L. M. Rodriguez-R, S. Higgins, J. C. Chee-Sanford, R. A. Sanford, K. M. Ritalahti, F. E. Löffler, and K. T. Konstantinidis. 2014. "Detecting Nitrous Oxide Reductase (NosZ) Genes in Soil Metagenomes: Method Development and Implications for the Nitrogen Cycle." *MBio* 5 (3). <https://doi.org/10.1128/mBio.01193-14>.
- Orghidan, Tr. 1955. "Un Nou Domeniu de Viata Acvatica Subterana: 'Biotopul Hiporeic.'" *Buletin Stiintific Sectia de Biologie Si Stiinte Agricole Si Sectia de Geologie Si Geografie* 7 (3): 657–76.
- Orghidan, Traian. 2010. "A New Habitat of Subsurface Waters: The Hyporheic Biotope." *Fundamental and Applied Limnology* 176 (4): 291–302. <https://doi.org/10.1127/1863-9135/2010/0176-0291>.
- Overholt, Will A., Martin Hölzer, Patricia Geesink, Celia Diezel, Manja Marz, and Kirsten Küsel. 2020. "Inclusion of Oxford Nanopore Long Reads Improves All Microbial and Viral Metagenome-Assembled Genomes from a Complex Aquifer System." *Environmental Microbiology* 22 (9): 4000–4013. <https://doi.org/10.1111/1462-2920.15186>.
- Palomo, Alejandro, S. Jane Fowler, Arda Gülay, Simon Rasmussen, Thomas Sicheritz-Ponten, and Barth F. Smets. 2016. "Metagenomic Analysis of Rapid Gravity Sand Filter Microbial Communities Suggests Novel Physiology of *Nitrospira* Spp." *ISME Journal* 10 (11). <https://doi.org/10.1038/ismej.2016.63>.
- Parada, Alma E., David M. Needham, and Jed A. Fuhrman. 2016. "Every Base Matters: Assessing Small Subunit rRNA Primers for Marine Microbiomes with Mock Communities, Time Series and Global Field Samples." *Environmental Microbiology* 18 (5): 1403–14. <https://doi.org/10.1111/1462-2920.13023>.
- Parks, Donovan H., Maria Chuvochina, David W. Waite, Christian Rinke, Adam Skarshewski, Pierre Alain Chaumeil, and Philip Hugenholtz. 2018. "A Standardized Bacterial Taxonomy Based on Genome Phylogeny Substantially Revises the Tree of Life." *Nature Biotechnology* 36 (10). <https://doi.org/10.1038/nbt.4229>.
- Pei, Anna Y., William E. Oberdorf, Carlos W. Nossa, Ankush Agarwal, Pooja Chokshi, Erika A. Gerz, Zhida Jin, et al. 2010. "Diversity of 16S rRNA Genes within Individual Prokaryotic Genomes." *Applied and Environmental Microbiology* 76 (12): 3886–97. <https://doi.org/10.1128/AEM.02953-09>.
- Peng, Lai, Yiwen Liu, Shu Hong Gao, Xueming Chen, Pei Xin, Xiaohu Dai, and Bing Jie Ni. 2015. "Evaluation on the Nanoscale Zero Valent Iron Based Microbial Denitrification for

- Nitrate Removal from Groundwater.” *Scientific Reports* 5.
<https://doi.org/10.1038/srep12331>.
- Peterson, B. J., W. M. Wollheim, P. J. Mulholland, J. R. Webster, J. L. Meyer, J. L. Tank, E. Marti, et al. 2001. “Control of Nitrogen Export from Watersheds by Headwater Streams.” *Science* 292 (5514): 86–90. <https://doi.org/10.1126/science.1056874>.
- Pett-Ridge, Jennifer, Whendee L. Silver, and Mary K. Firestone. 2006. “Redox Fluctuations Frame Microbial Community Impacts on N-Cycling Rates in a Humid Tropical Forest Soil.” *Biogeochemistry* 81 (1): 95–110. <https://doi.org/10.1007/s10533-006-9032-8>.
- Pfennig, Norbert, and Hanno Biebl. 1976. “Desulfuromonas Acetoxidans Gen. Nov. and Sp. Nov., a New Anaerobic, Sulfur-Reducing, Acetate-Oxidizing Bacterium.” *Archives of Microbiology* 110 (1). <https://doi.org/10.1007/BF00416962>.
- Philippot, Laurent. 2002. “Denitrifying Genes in Bacterial and Archaeal Genomes.” *Biochimica et Biophysica Acta - Gene Structure and Expression*.
[https://doi.org/10.1016/S0167-4781\(02\)00420-7](https://doi.org/10.1016/S0167-4781(02)00420-7).
- Pilloni, Giovanni, Michael S. Granitsiotis, Marion Engel, and Tillmann Lueders. 2012. “Testing the Limits of 454 Pyrotag Sequencing: Reproducibility, Quantitative Assessment and Comparison to T-RFLP Fingerprinting of Aquifer Microbes.” *PLoS ONE* 7 (7). <https://doi.org/10.1371/journal.pone.0040467>.
- Price, Morgan N., Paramvir S. Dehal, and Adam P. Arkin. 2009. “Fasttree: Computing Large Minimum Evolution Trees with Profiles Instead of a Distance Matrix.” *Molecular Biology and Evolution* 26 (7): 1641–50. <https://doi.org/10.1093/molbev/msp077>.
- Prosser, James I., and Graeme W. Nicol. 2012. “Archaeal and Bacterial Ammonia-Oxidisers in Soil: The Quest for Niche Specialisation and Differentiation.” *Trends in Microbiology*.
<https://doi.org/10.1016/j.tim.2012.08.001>.
- Qin, Wei, Shady A. Amin, Willm Martens-Habbena, Christopher B. Walker, Hidetoshi Urakawa, Allan H. Devol, Anitra E. Ingalls, James W. Moffett, E. Virginia Armbrust, and David A. Stahl. 2014. “Marine Ammonia-Oxidizing Archaeal Isolates Display Obligate Mixotrophy and Wide Ecotypic Variation.” *Proceedings of the National Academy of Sciences of the United States of America* 111 (34): 12504–9.
<https://doi.org/10.1073/pnas.1324115111>.
- Quast, Christian, Elmar Pruesse, Pelin Yilmaz, Jan Gerken, Timmy Schweer, Pablo Yarza, Jörg Peplies, and Frank Oliver Glöckner. 2013. “The SILVA Ribosomal RNA Gene Database Project: Improved Data Processing and Web-Based Tools.” *Nucleic Acids Research* 41 (D1). <https://doi.org/10.1093/nar/gks1219>.
- R Core Team. 2018. “R: A Language and Environment for Statistical Computing [Computer Software]. Vienna, Austria: R Foundation for Statistical Computing.” <http://www.r-project.org/>.
- Rabus, Ralf, Sofia S. Venceslau, Lars Wöhlbrand, Gerrit Voordouw, Judy D. Wall, and Inês A.C. Pereira. 2015. “A Post-Genomic View of the Ecophysiology, Catabolism and Biotechnological Relevance of Sulphate-Reducing Prokaryotes.” In *Advances in Microbial Physiology*, 66:55–321. <https://doi.org/10.1016/bs.ampbs.2015.05.002>.
- Rissanen, Antti J., Anu Karvinen, Hannu Nykänen, Sari Peura, Marja Tirola, Anita Mäki, and

- Paula Kankaala. 2017. “Effects of Alternative Electron Acceptors on the Activity and Community Structure of Methane-Producing and Consuming Microbes in the Sediments of Two Shallow Boreal Lakes.” *FEMS Microbiology Ecology* 93 (7): 1–16. <https://doi.org/10.1093/FEMSEC/FIX078>.
- Rittmann, Bruce E, and Perry L. McCarty. 2001. “Environmental Biotechnology : Principles and Applications.” *Current Opinion in Biotechnology* 7 (3): 357–65. <http://www.sciencedirect.com/science/article/pii/S0958166996800474>.
- Rodríguez-Ramos, Josue, Mikayla A Borton, Bridget B McGivern, Garrett J Smith, Lindsey M Solden, Michael Shaffer, Rebecca A Daly, et al. 2022. “Genome-Resolved Metaproteomics Decodes the Microbial and River Sediments.” *MSystems* 7 (4): e0051622. <https://doi.org/10.1128/msystems.00516-22>.
- Röös, Elin, Bojana Bajželj, Pete Smith, Mikaela Patel, David Little, and Tara Garnett. 2017. “Greedy or Needy? Land Use and Climate Impacts of Food in 2050 under Different Livestock Futures.” *Global Environmental Change* 47. <https://doi.org/10.1016/j.gloenvcha.2017.09.001>.
- Rotthauwe, Jan Henrich, Karl Paul Witzel, and Werner Liesack. 1997. “The Ammonia Monooxygenase Structural Gene AmoA as a Functional Marker: Molecular Fine-Scale Analysis of Natural Ammonia-Oxidizing Populations.” *Applied and Environmental Microbiology* 63 (12): 4704–12. <https://doi.org/10.1128/aem.63.12.4704-4712.1997>.
- Rütting, T., P. Boeckx, C. Müller, and L. Klemetsson. 2011. “Assessment of the Importance of Dissimilatory Nitrate Reduction to Ammonium for the Terrestrial Nitrogen Cycle.” *Biogeosciences* 8 (7). <https://doi.org/10.5194/bg-8-1779-2011>.
- Rütting, Tobias, Philipp Schleusner, Linda Hink, and James I. Prosser. 2021. “The Contribution of Ammonia-Oxidizing Archaea and Bacteria to Gross Nitrification under Different Substrate Availability.” *Soil Biology and Biochemistry* 160. <https://doi.org/10.1016/j.soilbio.2021.108353>.
- Ryan, Justin G., Clive A. McAlpine, John A. Ludwig, and John N. Callow. 2015. “Modelling the Potential of Integrated Vegetation Bands (IVB) to Retain Stormwater Runoff on Steep Hillslopes of Southeast Queensland, Australia.” *Land* 4 (3). <https://doi.org/10.3390/land4030711>.
- Sachs, Corinna, Dheeraj Kanaparthi, Susanne Kublik, Anna Roza Szalay, Michael Schloter, Lars Riis Damgaard, Andreas Schramm, and Tillmann Lueders. 2022. “Tracing Long-Distance Electron Transfer and Cable Bacteria in Freshwater Sediments by Agar Pillar Gradient Columns.” *FEMS Microbiology Ecology* 98 (5): 1–12. <https://doi.org/10.1093/femsec/fiac042>.
- Saup, C. M., S. R. Bryant, A. R. Nelson, K. D. Harris, A. H. Sawyer, J. N. Christensen, M. M. Tfaily, K. H. Williams, and M. J. Wilkins. 2019. “Hyporheic Zone Microbiome Assembly Is Linked to Dynamic Water Mixing Patterns in Snowmelt-Dominated Headwater Catchments.” *Journal of Geophysical Research: Biogeosciences* 124 (11): 3269–80. <https://doi.org/10.1029/2019JG005189>.
- Scheidegger, ADRIAN E. 1965. “The Algebra of Stream-Order Numbers.” *United States Geological Survey Professional Paper* 525: 187–89.
- Schreiber, Kerstin, Robert Krieger, Beatrice Benkert, Martin Eschbach, Hiroyuki Arai, Max

- Schobert, and Dieter Jahn. 2007. "The Anaerobic Regulatory Network Required for *Pseudomonas Aeruginosa* Nitrate Respiration." *Journal of Bacteriology* 189 (11). <https://doi.org/10.1128/JB.00240-07>.
- Schullehner, Jörg, Birgitte Hansen, Malene Thygesen, Carsten B. Pedersen, and Torben Sigsgaard. 2018. "Nitrate in Drinking Water and Colorectal Cancer Risk: A Nationwide Population-Based Cohort Study." *International Journal of Cancer* 143 (1): 73–79. <https://doi.org/10.1002/ijc.31306>.
- Schwieger, Frank, and Christoph C. Tebbe. 1998. "A New Approach to Utilize PCR-Single-Strand-Conformation Polymorphism for 16S rRNA Gene-Based Microbial Community Analysis." *Applied and Environmental Microbiology* 64 (12): 4870–76. <https://doi.org/10.1128/aem.64.12.4870-4876.1998>.
- Schwientek, Marc, Karsten Osenbrück, and Matthias Fleischer. 2013. "Investigating Hydrological Drivers of Nitrate Export Dynamics in Two Agricultural Catchments in Germany Using High-Frequency Data Series." *Environmental Earth Sciences* 69 (2): 381–93. <https://doi.org/10.1007/s12665-013-2322-2>.
- Seitzinger, Sybil P., Renée V. Styles, Elizabeth W. Boyer, Richard B. Alexander, Gilles Billen, Robert W. Howarth, Bernhard Mayer, and Nico Van Breemen. 2002. "Nitrogen Retention in Rivers: Model Development and Application to Watersheds in the Northeastern U.S.A." In *Biogeochemistry*, 57–58:199–237. <https://doi.org/10.1023/A:1015745629794>.
- Shao, Ming Fei, Tong Zhang, and Herbert Han Ping Fang. 2010. "Sulfur-Driven Autotrophic Denitrification: Diversity, Biochemistry, and Engineering Applications." *Applied Microbiology and Biotechnology* 88 (5): 1027–42. <https://doi.org/10.1007/s00253-010-2847-1>.
- Shortle, J. S., and J. B. Braden. 2013. "Economics of Nonpoint Pollution." *Encyclopedia of Energy, Natural Resource, and Environmental Economics* 3–3 (January): 143–49. <https://doi.org/10.1016/B978-0-12-375067-9.00028-0>.
- Sierra-Alvarez, Reyes, Ricardo Beristain-Cardoso, Margarita Salazar, Jorge Gómez, Elias Razo-Flores, and Jim A. Field. 2007. "Chemolithotrophic Denitrification with Elemental Sulfur for Groundwater Treatment." *Water Research* 41 (6). <https://doi.org/10.1016/j.watres.2006.12.039>.
- Signorelli, Andri. 2020. "DescTools: Tools for Descriptive Statistics. R Package Version 0.99.37." *Cran*.
- Sillitoe, Ian, Alison L. Cuff, Benoit H. Dessailly, Natalie L. Dawson, Nicholas Furnham, David Lee, Jonathan G. Lees, et al. 2013. "New Functional Families (FunFams) in CATH to Improve the Mapping of Conserved Functional Sites to 3D Structures." *Nucleic Acids Research* 41 (D1). <https://doi.org/10.1093/nar/gks1211>.
- Singh, Simranjeet, Amith G. Anil, Vijay Kumar, Dhriti Kapoor, S. Subramanian, Joginder Singh, and Praveen C. Ramamurthy. 2022. "Nitrates in the Environment: A Critical Review of Their Distribution, Sensing Techniques, Ecological Effects and Remediation." *Chemosphere*. <https://doi.org/10.1016/j.chemosphere.2021.131996>.
- Smith, Cindy J., David B. Nedwell, Liang F. Dong, and A. Mark Osborn. 2007. "Diversity and Abundance of Nitrate Reductase Genes (NarG and NapA), Nitrite Reductase Genes

- (NirS and NrfA), and Their Transcripts in Estuarine Sediments.” *Applied and Environmental Microbiology* 73 (11): 3612–22. <https://doi.org/10.1128/AEM.02894-06>.
- Smith, Lesley K., Mary A. Voytek, John Karl Böhlke, and Judson W. Harvey. 2006. “Denitrification in Nitrate-Rich Streams: Application of N₂:Ar and ¹⁵N-Tracer Methods in Intact Cores.” *Ecological Applications* 16 (6): 2191–2207. [https://doi.org/10.1890/1051-0761\(2006\)016\[2191:DINSAO\]2.0.CO;2](https://doi.org/10.1890/1051-0761(2006)016[2191:DINSAO]2.0.CO;2).
- Soares, M. I.M. 2002. “Denitrification of Groundwater with Elemental Sulfur.” *Water Research* 36 (5). [https://doi.org/10.1016/S0043-1354\(01\)00326-8](https://doi.org/10.1016/S0043-1354(01)00326-8).
- Song, Hyun Seob, Dennis G. Thomas, James C. Stegen, Minjing Li, Chongxuan Liu, Xuehang Song, Xingyuan Chen, Jim K. Fredrickson, John M. Zachara, and Timothy D. Scheibe. 2017. “Regulation-Structured Dynamic Metabolic Model Provides a Potential Mechanism for Delayed Enzyme Response in Denitrification Process.” *Frontiers in Microbiology* 8. <https://doi.org/10.3389/fmicb.2017.01866>.
- Sonthiphand, Puntipar, and Josh D. Neufeld. 2014. “Nitrifying Bacteria Mediate Aerobic Ammonia Oxidation and Urea Hydrolysis within the Grand River.” *Aquatic Microbial Ecology* 73 (2): 151–62. <https://doi.org/10.3354/ame01712>.
- Staley, C., T. Unno, T. J. Gould, B. Jarvis, J. Phillips, J. B. Cotner, and M. J. Sadowsky. 2013. “Application of Illumina Next-Generation Sequencing to Characterize the Bacterial Community of the Upper Mississippi River.” *Journal of Applied Microbiology* 115 (5). <https://doi.org/10.1111/jam.12323>.
- Starry, Olyssa S., H. Maurice Valett, and Madeline E. Schreiber. 2005. “Nitrification Rates in a Headwater Stream: Influences of Seasonal Variation in C and N Supply.” *Journal of the North American Benthological Society* 24 (4): 753–68. <https://doi.org/10.1899/05-015.1>.
- Stegen, James C., James K. Fredrickson, Michael J. Wilkins, Allan E. Konopka, William C. Nelson, Evan V. Arntzen, William B. Chrisler, et al. 2016. “Groundwater-Surface Water Mixing Shifts Ecological Assembly Processes and Stimulates Organic Carbon Turnover.” *Nature Communications* 7. <https://doi.org/10.1038/ncomms11237>.
- Stegen, James C., Tim Johnson, James K. Fredrickson, Michael J. Wilkins, Allan E. Konopka, William C. Nelson, Evan V. Arntzen, et al. 2018. “Influences of Organic Carbon Speciation on Hyporheic Corridor Biogeochemistry and Microbial Ecology.” *Nature Communications* 9 (1): 1–11. <https://doi.org/10.1038/s41467-018-02922-9>.
- Stegen, James C., Xueju Lin, Jim K. Fredrickson, Xingyuan Chen, David W. Kennedy, Christopher J. Murray, Mark L. Rockhold, and Allan Konopka. 2013. “Quantifying Community Assembly Processes and Identifying Features That Impose Them.” *ISME Journal* 7 (11): 2069–79. <https://doi.org/10.1038/ismej.2013.93>.
- Stegen, James C., Xueju Lin, Jim K. Fredrickson, and Allan E. Konopka. 2015. “Estimating and Mapping Ecological Processes Influencing Microbial Community Assembly.” *Frontiers in Microbiology* 6 (MAY): 1–15. <https://doi.org/10.3389/fmicb.2015.00370>.
- Stegen, James C., Xueju Lin, Allan E. Konopka, and James K. Fredrickson. 2012. “Stochastic and Deterministic Assembly Processes in Subsurface Microbial Communities.” *ISME Journal* 6 (9): 1653–64. <https://doi.org/10.1038/ismej.2012.22>.

- Stein, Lisa Y. 2014. "Heterotrophic Nitrification and Nitrifier Denitrification." In *Nitrification*, 95–114. <https://doi.org/10.1128/9781555817145.ch5>.
- Sterngren, Anna E., Sara Hallin, and Per Bengtson. 2015. "Archaeal Ammonia Oxidizers Dominate in Numbers, but Bacteria Drive Gross Nitrification in n-Amended Grassland Soil." *Frontiers in Microbiology* 6 (NOV). <https://doi.org/10.3389/fmicb.2015.01350>.
- Storey, Richard G., D. Dudley Williams, and Roberta R. Fulthorpe. 2004. "Nitrogen Processing in the Hyporheic Zone of a Pastoral Stream." *Biogeochemistry* 69 (3): 285–313. <https://doi.org/10.1023/B:BIOG.0000031049.95805.ec>.
- Straub, Daniel, Nia Blackwell, Adrian Langarica-Fuentes, Alexander Peltzer, Sven Nahnsen, and Sara Kleindienst. 2020. "Interpretations of Environmental Microbial Community Studies Are Biased by the Selected 16S rRNA (Gene) Amplicon Sequencing Pipeline." *Frontiers in Microbiology* 11. <https://doi.org/10.3389/fmicb.2020.550420>.
- Strauss, Eric A., and Gary A. Lamberti. 2002. "Effect of Dissolved Organic Carbon Quality on Microbial Decomposition and Nitrification Rates in Stream Sediments." *Freshwater Biology* 47 (1): 65–74. <https://doi.org/10.1046/j.1365-2427.2002.00776.x>.
- Stuart, Maureen A., Fredrick J. Rich, and Gale A. Bishop. 1995. "Survey of Nitrate Contamination in Shallow Domestic Drinking Water Wells of the Inner Coastal Plain of Georgia." *Groundwater* 33 (2): 284–90. <https://doi.org/10.1111/j.1745-6584.1995.tb00283.x>.
- Sutton, Mark, Raghuram Nandula, and Tapan Kumar Adhya. 2019. "UNEP (2019). Frontiers 2018/19 Emerging Issues of Environmental Concern. United Nations Environment Programme, Nairobi." *Frontiers 2018/19: Emerging Issues of Environmental Concern*, 2019. <http://wedocs.unep.org/handle/20.500.11822/27543>.
- Taberlet, Pierre, Eric Coissac, François Pompanon, Christian Brochmann, and Eske Willerslev. 2012. "Towards Next-Generation Biodiversity Assessment Using DNA Metabarcoding." *Molecular Ecology* 21 (8): 2045–50. <https://doi.org/10.1111/j.1365-294X.2012.05470.x>.
- Tang, Shuangyu, Yin hao Liao, Yichan Xu, Zhengzhu Dang, Xianfang Zhu, and Guodong Ji. 2020. "Microbial Coupling Mechanisms of Nitrogen Removal in Constructed Wetlands: A Review." *Bioresour ce Technology*. <https://doi.org/10.1016/j.biortech.2020.123759>.
- Tarhriz, Vahideh, Vera Thiel, Ghorbanali Nematzadeh, Mohammad Amin Hejazi, Johannes F. Imhoff, and Mohammad Saeid Hejazi. 2013. "Tabrizicola Aquatica Gen. Nov. Sp. Nov., a Novel Alphaproteobacterium Isolated from Qurugöl Lake Nearby Tabriz City, Iran." *Antonie van Leeuwenhoek, International Journal of General and Molecular Microbiology* 104 (6): 1205–15. <https://doi.org/10.1007/s10482-013-0042-y>.
- Tatusov, Roman L, Natalie D Fedorova, John D Jackson, Aviva R Jacobs, Boris Kiryutin, Eugene V Koonin, Dmitri M Krylov, et al. 2003. "The COG Database: An Updated Version Includes Eukaryotes." *BMC Bioinformatics* 4 (1): 41. <https://doi.org/10.1186/1471-2105-4-41>.
- Taylor, Anne E., Neeraja Vajrала, Andrew T. Giguere, Alix I. Gitelman, Daniel J. Arp, David D. Myrold, Luis Sayavedra-Soto, and Peter J. Bottomley. 2013. "Use of Aliphatic N-Alkynes to Discriminate Soil Nitrification Activities of Ammonia-Oxidizing Thaumarchaea and Bacteria." *Applied and Environmental Microbiology* 79 (21): 6544–

51. <https://doi.org/10.1128/AEM.01928-13>.
- Tekedar, Hasan C., Attila Karsi, Joseph S. Reddy, Seong W. Nho, Safak Kalindamar, and Mark L. Lawrence. 2017. "Comparative Genomics and Transcriptional Analysis of *Flavobacterium Columnare* Strain ATCC 49512." *Frontiers in Microbiology* 8 (APR). <https://doi.org/10.3389/fmicb.2017.00588>.
- Temkin, Alexis, Sydney Evans, Tatiana Manidis, Chris Campbell, and Olga V. Naidenko. 2019. "Exposure-Based Assessment and Economic Valuation of Adverse Birth Outcomes and Cancer Risk Due to Nitrate in United States Drinking Water." *Environmental Research* 176. <https://doi.org/10.1016/j.envres.2019.04.009>.
- Thomas, François, Anne E. Giblin, Zoe G. Cardon, and Stefan M. Sievert. 2014. "Rhizosphere Heterogeneity Shapes Abundance and Activity of Sulfur-Oxidizing Bacteria in Vegetated Salt Marsh Sediments." *Frontiers in Microbiology* 5 (JUN). <https://doi.org/10.3389/fmicb.2014.00309>.
- Throbäck, Ingela Noredal, Karin Enwall, Åsa Jarvis, and Sara Hallin. 2004. "Reassessing PCR Primers Targeting NirS, NirK and NosZ Genes for Community Surveys of Denitrifying Bacteria with DGGE." *FEMS Microbiology Ecology* 49 (3): 401–17. <https://doi.org/10.1016/j.femsec.2004.04.011>.
- Tian, Renmao, Daliang Ning, Zhili He, Ping Zhang, Sarah J. Spencer, Shuhong Gao, Weiling Shi, et al. 2020. "Small and Mighty: Adaptation of Superphylum Patescibacteria to Groundwater Environment Drives Their Genome Simplicity." *Microbiome* 8 (1). <https://doi.org/10.1186/s40168-020-00825-w>.
- Tiedje, James M. 1988. "Ecology of Denitrification and Dissimilatory Nitrate Reduction to Ammonium." *Environmental Microbiology of Anaerobes*, no. April: 179–244.
- Tiedje, James M., Alan J. Sexstone, David D. Myrold, and Joseph A. Robinson. 1983. "Denitrification: Ecological Niches, Competition and Survival." *Antonie van Leeuwenhoek* 48 (6). <https://doi.org/10.1007/BF00399542>.
- Tikhonova, Tamara V., Alvira Slutsky, Alexey N. Antipov, Konstantin M. Boyko, Konstantin M. Polyakov, Dimitry Y. Sorokin, Renata A. Zvyagilskaya, and Vladimir O. Popov. 2006. "Molecular and Catalytic Properties of a Novel Cytochrome c Nitrite Reductase from Nitrate-Reducing Haloalkaliphilic Sulfur-Oxidizing Bacterium *Thioalkalivibrio Nitratireducens*." *Biochimica et Biophysica Acta - Proteins and Proteomics* 1764 (4): 715–23. <https://doi.org/10.1016/j.bbapap.2005.12.021>.
- Tittonell, Pablo, and Ken E. Giller. 2013. "When Yield Gaps Are Poverty Traps: The Paradigm of Ecological Intensification in African Smallholder Agriculture." *Field Crops Research* 143. <https://doi.org/10.1016/j.fcr.2012.10.007>.
- Tommaso, Paolo DI, Maria Chatzou, Evan W. Floden, Pablo Prieto Barja, Emilio Palumbo, and Cedric Notredame. 2017. "Nextflow Enables Reproducible Computational Workflows." *Nature Biotechnology*. <https://doi.org/10.1038/nbt.3820>.
- Tosques, Ivan E., Adam V. Kwiatkowski, Jiarong Shi, and James P. Shapleigh. 1997. "Characterization and Regulation of the Gene Encoding Nitrite Reductase in *Rhodobacter Sphaeroides* 2.4.3." *Journal of Bacteriology* 179 (4): 1090–95. <https://doi.org/10.1128/jb.179.4.1090-1095.1997>.

- Tourna, Maria, Michaela Stieglmeier, Anja Spang, Martin Könneke, Arno Schintlmeister, Tim Urich, Marion Engel, et al. 2011. “Nitrososphaera Viennensis, an Ammonia Oxidizing Archaeon from Soil.” *Proceedings of the National Academy of Sciences of the United States of America* 108 (20): 8420–25. <https://doi.org/10.1073/pnas.1013488108>.
- Trauth, Nico, Andreas Musolff, Kay Knöller, Ute S. Kaden, Toralf Keller, Ulrike Werban, and Jan H. Fleckenstein. 2018. “River Water Infiltration Enhances Denitrification Efficiency in Riparian Groundwater.” *Water Research* 130: 185–99. <https://doi.org/10.1016/j.watres.2017.11.058>.
- Tsallagov, Stanislav I., Dimitry Y. Sorokin, Tamara V. Tikhonova, Vladimir O. Popov, and Gerard Muyzer. 2019. “Comparative Genomics of Thiohalobacter Thiocyanaticus HRh1T and Guyparkeriasp. SCN-R1, Halophilic Chemolithoautotrophic Sulfur-Oxidizing Gammaproteobacteria Capable of Using Thiocyanate as Energy Source.” *Frontiers in Microbiology* 10 (MAY). <https://doi.org/10.3389/fmicb.2019.00898>.
- Veraart, Annelies J., Maurício R. Dimitrov, Arina P. Schrier-Uijl, Hauke Smidt, and Jeroen J.M. de Klein. 2017. “Abundance, Activity and Community Structure of Denitrifiers in Drainage Ditches in Relation to Sediment Characteristics, Vegetation and Land-Use.” *Ecosystems* 20 (5): 928–43. <https://doi.org/10.1007/s10021-016-0083-y>.
- Verhamme, Daniel T., James I. Prosser, and Graeme W. Nicol. 2011. “Ammonia Concentration Determines Differential Growth of Ammonia-Oxidising Archaea and Bacteria in Soil Microcosms.” *ISME Journal* 5 (6): 1067–71. <https://doi.org/10.1038/ismej.2010.191>.
- Vetriani, Costantino, James W. Voordeckers, Melitza Crespo-Medina, Charles E. O’Brien, Donato Giovannelli, and Richard A. Lutz. 2014. “Deep-Sea Hydrothermal Vent Epsilonproteobacteria Encode a Conserved and Widespread Nitrate Reduction Pathway (Nap).” *ISME Journal* 8 (7). <https://doi.org/10.1038/ismej.2013.246>.
- Vos, Michiel, Alexandra B. Wolf, Sarah J. Jennings, and George A. Kowalchuk. 2013. “Micro-Scale Determinants of Bacterial Diversity in Soil.” *FEMS Microbiology Reviews*. <https://doi.org/10.1111/1574-6976.12023>.
- Wagner, Michael, Gabriele Rath, Hans Peter Koops, Janine Flood, and Rudolf Amann. 1996. “In Situ Analysis of Nitrifying Bacteria in Sewage Treatment Plants.” In *Water Science and Technology*, 34:237–44. [https://doi.org/10.1016/0273-1223\(96\)00514-8](https://doi.org/10.1016/0273-1223(96)00514-8).
- Waite, David W., Maria Chuvochina, Claus Pelikan, Donovan H. Parks, Pelin Yilmaz, Michael Wagner, Alexander Loy, et al. 2020. “Proposal to Reclassify the Proteobacterial Classes Deltaproteobacteria and Oligoflexia, and the Phylum Thermodesulfobacteria into Four Phyla Reflecting Major Functional Capabilities.” *International Journal of Systematic and Evolutionary Microbiology* 70 (11): 5972–6016. <https://doi.org/10.1099/ijsem.0.004213>.
- Waite, David W., Inka Vanwonterghem, Christian Rinke, Donovan H. Parks, Ying Zhang, Ken Takai, Stefan M. Sievert, et al. 2017. “Comparative Genomic Analysis of the Class Epsilonproteobacteria and Proposed Reclassification to Epsilonbacteraeota (Phyl. Nov.)” *Frontiers in Microbiology* 8 (APR). <https://doi.org/10.3389/fmicb.2017.00682>.
- Wang, Jianlong, and Libing Chu. 2016. “Biological Nitrate Removal from Water and Wastewater by Solid-Phase Denitrification Process.” *Biotechnology Advances* 34 (6):

1103–12. <https://doi.org/10.1016/j.biotechadv.2016.07.001>.

- Wang, Zhe, Oscar Jimenez-Fernandez, Karsten Osenbrück, Marc Schwientek, Michael Schloter, Jan H. Fleckenstein, and Tillmann Lueders. 2022. “Streambed Microbial Communities in the Transition Zone between Groundwater and a First-Order Stream as Impacted by Bidirectional Water Exchange.” *Water Research* 217: 118334. <https://doi.org/10.1016/j.watres.2022.118334>.
- Ward, Adam S., Jay P. Zarnetske, Viktor Baranov, Phillip J. Blaen, Nicolai Brekenfeld, Rosalie Chu, Romain Derelle, et al. 2019. “Co-Located Contemporaneous Mapping of Morphological, Hydrological, Chemical, and Biological Conditions in a 5th-Order Mountain Stream Network, Oregon, USA.” *Earth System Science Data* 11 (4). <https://doi.org/10.5194/essd-11-1567-2019>.
- Waterhouse, Robert M., Mathieu Seppey, Felipe A. Simao, Mosè Manni, Panagiotis Ioannidis, Guennadi Klioutchnikov, Evgenia V. Kriventseva, and Evgeny M. Zdobnov. 2018. “BUSCO Applications from Quality Assessments to Gene Prediction and Phylogenomics.” *Molecular Biology and Evolution* 35 (3). <https://doi.org/10.1093/molbev/msx319>.
- Wegner, Carl Eric, and Werner Liesack. 2016. “Microbial Community Dynamics during the Early Stages of Plant Polymer Breakdown in Paddy Soil.” *Environmental Microbiology* 18 (9). <https://doi.org/10.1111/1462-2920.12815>.
- WHO. 2016. “Nitrate and Nitrite in Drinking Water: Background Document for Development of WHO Guidelines for Drinking Water Quality.” *Geneva: World Health Organization*, 31. http://www.who.int/publications/guidelines/%0Ahttp://www.who.int/water_sanitation_health/dwq/chemicals/nitratenitrite2ndadd.pdf.
- Wickham, Hadley. 2016. *Ggplot2: Elegant Graphics for Data Analysis*. Springer-Verlag New York. <https://ggplot2.tidyverse.org>.
- Wickham, Hadley, Mara Averick, Jennifer Bryan, Winston Chang, Lucy McGowan, Romain François, Garrett Golemund, et al. 2019. “Welcome to the Tidyverse.” *Journal of Open Source Software* 4 (43): 1686. <https://doi.org/10.21105/joss.01686>.
- Winter, Christian, Thomas Hein, Gerhard Kavka, Robert L. Mach, and Andreas H. Farnleitner. 2007. “Longitudinal Changes in the Bacterial Community Composition of the Danube River: A Whole-River Approach.” *Applied and Environmental Microbiology* 73 (2): 421–31. <https://doi.org/10.1128/AEM.01849-06>.
- Wittke, Rauni, Wolfgang Ludwig, Stefan Peiffer, and Diethelm Kleiner. 1997. “Isolation and Characterization of Burkholderia Norimbergensis Sp. Nov., A Mildly Alkaliphilic Sulfur Oxidizer.” *Systematic and Applied Microbiology* 20 (4). [https://doi.org/10.1016/S0723-2020\(97\)80025-2](https://doi.org/10.1016/S0723-2020(97)80025-2).
- Wright, Erik S. 2016. “Using DECIPHER v2.0 to Analyze Big Biological Sequence Data in R.” *R Journal* 8 (1): 352–59. <https://doi.org/10.32614/rj-2016-025>.
- . 2020. “RNAcontest: Comparing Tools for Noncoding RNA Multiple Sequence Alignment Based on Structural Consistency.” *RNA* 26 (5). <https://doi.org/10.1261/rna.073015.119>.

- Wu, Bo, Feifei Liu, Wenwen Fang, Tony Yang, Guang Hao Chen, Zhili He, and Shanquan Wang. 2021. "Microbial Sulfur Metabolism and Environmental Implications." *Science of the Total Environment*. <https://doi.org/10.1016/j.scitotenv.2021.146085>.
- Xia, Fei, Jian Gong Wang, Ting Zhu, Bin Zou, Sung Keun Rhee, and Zhe Xue Quan. 2018. "Ubiquity and Diversity of Complete Ammonia Oxidizers (Comammox)." *Applied and Environmental Microbiology* 84 (24). <https://doi.org/10.1128/AEM.01390-18>.
- Xia, Siqing, Yan Shi, Yigang Fu, and Xingmao Ma. 2005. "DGGE Analysis of 16S rDNA of Ammonia-Oxidizing Bacteria in Chemical-Biological Flocculation and Chemical Coagulation Systems." *Applied Microbiology and Biotechnology* 69 (1): 99–105. <https://doi.org/10.1007/s00253-005-0035-5>.
- Xu, Xi Jun, Chuan Chen, Hong Liang Guo, Ai Jie Wang, Nan Qi Ren, and Duu Jong Lee. 2016. "Characterization of a Newly Isolated Strain *Pseudomonas* Sp. C27 for Sulfide Oxidation: Reaction Kinetics and Stoichiometry." *Scientific Reports* 6. <https://doi.org/10.1038/srep21032>.
- Yang, Yan, Sean Gerrity, Gavin Collins, Tianhu Chen, Ruihua Li, Sihuang Xie, and Xinmin Zhan. 2018. "Enrichment and Characterization of Autotrophic *Thiobacillus* Denitrifiers from Anaerobic Sludge for Nitrate Removal." *Process Biochemistry* 68. <https://doi.org/10.1016/j.procbio.2018.02.017>.
- Yang, Yuchun, Craig W. Herbold, Man Young Jung, Wei Qin, Mingwei Cai, Huan Du, Jih Gaw Lin, Xiaoyan Li, Meng Li, and Ji Dong Gu. 2021. "Survival Strategies of Ammonia-Oxidizing Archaea (AOA) in a Full-Scale WWTP Treating Mixed Landfill Leachate Containing Copper Ions and Operating at Low-Intensity of Aeration." *Water Research* 191: 116798. <https://doi.org/10.1016/j.watres.2020.116798>.
- Yang, Yuyin, Jingxu Zhang, Qun Zhao, Qiheng Zhou, Ningning Li, Yilin Wang, Shuguang Xie, and Yong Liu. 2016. "Sediment Ammonia-Oxidizing Microorganisms in Two Plateau Freshwater Lakes at Different Trophic States." *Microbial Ecology* 71 (2): 257–65. <https://doi.org/10.1007/s00248-015-0642-3>.
- Yao, Yuanzhi, Hanqin Tian, Hao Shi, Shufen Pan, Rongting Xu, Naiqing Pan, and Josep G. Canadell. 2020. "Increased Global Nitrous Oxide Emissions from Streams and Rivers in the Anthropocene." *Nature Climate Change*. <https://doi.org/10.1038/s41558-019-0665-8>.
- Yu, Liang, Joachim Rozemeijer, Boris M. Van Breukelen, Maarten Ouboter, Corné Van Der Vlugt, and Hans Peter Broers. 2018. "Groundwater Impacts on Surface Water Quality and Nutrient Loads in Lowland Polder Catchments: Monitoring the Greater Amsterdam Area." *Hydrology and Earth System Sciences* 22 (1): 487–508. <https://doi.org/10.5194/hess-22-487-2018>.
- Zarnetske, Jay P., Roy Haggerty, and Steven M. Wondzell. 2015. "Coupling Multiscale Observations to Evaluate Hyporheic Nitrate Removal at the Reach Scale." *Freshwater Science* 34 (1): 172–86. <https://doi.org/10.1086/680011>.
- Zarnetske, Jay P., Roy Haggerty, Steven M. Wondzell, and Michelle A. Baker. 2011. "Dynamics of Nitrate Production and Removal as a Function of Residence Time in the Hyporheic Zone." *Journal of Geophysical Research: Biogeosciences* 116 (1). <https://doi.org/10.1029/2010JG001356>.
- Zdobnov, Evgeny M., Fredrik Tegenfeldt, Dmitry Kuznetsov, Robert M. Waterhouse, Felipe

- A. Simao, Panagiotis Ioannidis, Mathieu Seppey, Alexis Loetscher, and Evgenia V. Kriventseva. 2017. "OrthoDB v9.1: Cataloging Evolutionary and Functional Annotations for Animal, Fungal, Plant, Archaeal, Bacterial and Viral Orthologs." *Nucleic Acids Research* 45 (D1). <https://doi.org/10.1093/nar/gkw1119>.
- Zhang, Lixun, Yuntao Guan, and Sunny C. Jiang. 2021. "Investigations of Soil Autotrophic Ammonia Oxidizers in Farmlands through Genetics and Big Data Analysis." *Science of the Total Environment* 777. <https://doi.org/10.1016/j.scitotenv.2021.146091>.
- Zhang, Sibao, Wei Qin, Xinghui Xia, Lingzi Xia, Siling Li, Liwei Zhang, Yubei Bai, and Gongqin Wang. 2020. "Ammonia Oxidizers in River Sediments of the Qinghai-Tibet Plateau and Their Adaptations to High-Elevation Conditions." *Water Research* 173. <https://doi.org/10.1016/j.watres.2020.115589>.
- Zhang, Y., X. Xie, N. Jiao, S. S.Y. Hsiao, and S. J. Kao. 2014. "Diversity and Distribution of AmoA-Type Nitrifying and NirS-Type Denitrifying Microbial Communities in the Yangtze River Estuary." *Biogeosciences* 11 (8): 2131–45. <https://doi.org/10.5194/bg-11-2131-2014>.
- Zhang, Zhi-Yuan, Christian Schmidt, Erik Nixdorf, Xingxing Kuang, and Jan H Fleckenstein. 2021. "Effects of Heterogeneous Stream-Groundwater Exchange on the Source Composition of Stream Discharge and Solute Load." *Water Resources Research* 57 (8): e2020WR029079. <https://doi.org/https://doi.org/10.1029/2020WR029079>.
- Zhao, Z., W. Qiu, A. Koenig, X. Fan, and J. D. Gu. 2004. "Nitrate Removal from Saline Water Using Autotrophic Denitrification by the Bacterium Thiobacillus Denitrificans MP-1." *Environmental Technology* 25 (10). <https://doi.org/10.1080/09593332508618387>.
- Zhou, Jizhong, and Daliang Ning. 2017. "Stochastic Community Assembly: Does It Matter in Microbial Ecology?" *Microbiology and Molecular Biology Reviews* 81 (4). <https://doi.org/10.1128/membr.00002-17>.
- Zhu, Baoli, Zhe Wang, Dheeraj Kanaparthi, Susanne Kublik, Tida Ge, Peter Casper, Michael Schlöter, and Tillmann Lueders. 2020. "Long-Read Amplicon Sequencing of Nitric Oxide Dismutase (Nod) Genes Reveal Diverse Oxygenic Denitrifiers in Agricultural Soils and Lake Sediments." *Microbial Ecology* 80 (1): 243–47. <https://doi.org/10.1007/s00248-020-01482-0>.
- Zhu, Tongbin, Tianzhu Meng, Jinbo Zhang, Wenhui Zhong, Christoph Müller, and Zucong Cai. 2015. "Fungi-Dominant Heterotrophic Nitrification in a Subtropical Forest Soil of China." *Journal of Soils and Sediments* 15 (3): 705–9. <https://doi.org/10.1007/s11368-014-1048-4>.

PUBLICATIONS AND AUTHORSHIP CLARIFICATION

List of publications

Publications:

- Zhe Wang, Daniel Straub, Dan Thomas, Óscar Jiménez Fernández, Tillmann Lueders et al. "Deciphering microbial nitrogen and sulfur cycling in lower-order agricultural stream sediments using genome-resolved long-read metagenomics." (2023) (*in prep*)
- Zhe Wang, Anna Störiko, Aileen Jakobs, Daniel Straub, Holger Pagel, Adrian Mellage, Olaf Cirpka, Tillmann Lueders et al. "Linking abundance and activity of ammonia-oxidizing bacteria and archaea in an agriculturally impacted first-order stream." (2023) (*Under Review*)
- Zhe Wang, Oscar Jimenez-Fernandez, Karsten Osenbrück, Marc Schwientek, Michael Schloter, Jan H. Fleckenstein, and Tillmann Lueders. "Streambed microbial communities in the transition zone between groundwater and a first-order stream as impacted by bidirectional water exchange." *Water Research* (2022): 118334.
- Fengchao Sun, Adrian Mellage, Zhe Wang, Rani Bakkour, Christian Griebler, Martin Thullner, Martin Elsner et al. "Response of BAM-degradation activity to concentration and flow changes in a bench-scale sediment tank." *Environmental Science & Technology* (2022)
- Natalia Jakus, Nia Blackwell, Karsten Osenbrück, Daniel Straub, James M. Byrne, Zhe Wang, David Glöckler, Martin Elsner, Andreas Kappler et al. "Nitrate removal by a novel lithoautotrophic nitrate-reducing iron (II)-oxidizing culture enriched from a pyrite-rich limestone aquifer." *Applied and Environmental Microbiology* (2021): AEM-00460.
- Zhu, Baoli, Sebastian Friedrich, Zhe Wang, András Tánácsics, and Tillmann Lueders. "Availability of Nitrite and Nitrate as Electron Acceptors Modulates Anaerobic Toluene-Degrading Communities in Aquifer Sediments." *Frontiers in Microbiology* 11 (2020).
- Zhu, Baoli, Zhe Wang, Dheeraj Kanaparthi, Susanne Kublik, Tida Ge, Peter Casper, Michael Schloter, and Tillmann Lueders. "Long-read amplicon sequencing of nitric oxide dismutase (nod) genes reveal diverse oxygenic denitrifiers in agricultural soils and lake sediments." *Microbial ecology* 80, no. 1 (2020): 243-247.

Studies featured in this dissertation

Sections 2.1, 3.1, 4.1: The study was conceptualized and designed by Zhe Wang and Tillmann Lueders. Sediment sampling at the Schönbrunnen stream was performed in July, 2017 by Gabriele Barthel and Tillmann Lueders. Sample preparation, DNA extraction, qPCR, amplicons generation were all done by Zhe Wang. Sequencing library preparation and PacBio sequencing were conducted by Susanne Kublik and Silvia Gschwendtner, with technical support from Michael Schloter. Bioinformatics and data analysis were performed by Zhe Wang. Hydrology and water chemistry data showed in this study were collected by CAMPOS project collaborators Oscar Jimenez-Fernandez, Karsten Osenbrück, Marc Schwientek. Analyzation and visualization of hydrology and water chemistry data were conducted by Zhe Wang and Oscar Jimenez-Fernandez. The manuscript was written by Zhe Wang with feedback from Tillmann Lueders, and other co-authors. This study has been published.

Wang, Zhe, Oscar Jimenez-Fernandez, Karsten Osenbrück, Marc Schwientek, Michael Schloter, Jan H. Fleckenstein, and Tillmann Lueders. "Streambed microbial communities in the transition zone between groundwater and a first-order stream as impacted by bidirectional water exchange." Water Research 217 (2022): 118334. <https://doi.org/10.1016/j.watres.2022.118334>

Sections 2.2, 3.2, 4.2: The study was conceptualized and designed by Zhe Wang, Tillmann Lueders, and Aileen Jakobs. Field sampling campaigns for this study were in June 2020, conducted by Zhe Wang, Aileen Jakobs and Tillmann Lueders. Microcosms were set up by Zhe Wang and Aileen Jakobs. Ammonium and nitrate measurement were performed by Aileen Jakobs with analytical support from Martin Obst and the BayCEER Keylab for Experimental Biogeochemistry. DNA extraction and qPCR measurement were conducted by Zhe Wang and Aileen Jakobs. Amplicons generation were performed by Zhe Wang. Library preparation and Illumina sequencing were executed by Microsynth AG, Switzerland. 16S rRNA amplicon sequences were processed and analyzed by Zhe Wang. *amoA* gene amplicon sequences were processed by Daniel Straub at the Quantitative Biology Center, University of Tübingen, and analyzed by Zhe Wang. The manuscript was written by Zhe Wang and Anna

Störiko with feedback from Tillmann Lueders, Holger Pagel, Olaf Cirpka and other co-authors. The Model was conceived and calibrated by CAMPOS project collaborators Anna Störiko and Holger Pagel of the University of Tübingen and University of Hohenheim, respectively, using the experimental data generated in this study.

Zhe Wang, Anna Störiko, Aileen Jakobs, Daniel Straub, Holger Pagel, Adrian Mellage, Olaf Cirpka, Tillmann Lueders et al. "Linking abundance and activity of ammonia-oxidizing bacteria and archaea in an agriculturally impacted first-order stream." (2023) (Under Review)

Sections 2.3, 3.3, 4.3: Sample collection was in September, 2019, conducted by Zhe Wang and Tillmann Lueders. Sample preparation and DNA extraction were done by Zhe Wang. Microsensor measurement was done by Zhe Wang with the aid of Corinna Sachs. 16S rRNA amplicons and PacBio Library construction were conducted by Zhe Wang. PacBio sequencing was performed by Susanne Kublik at the Research Unit for Comparative Microbiome Analyses at the Helmholtz Zentrum München. Oxford Nanopore sequencing was performed by GenXone in Poland. Illumina shotgun metagenomic sequencing was performed by CeGaT gmbH in Germany. Both PacBio amplicon sequencing data and metagenomics data were processed by Daniel Straub at the Quantitative Biology Center, University of Tübingen, and analyzed by Zhe Wang.

